



**PALACKÝ UNIVERSITY**

**FACULTY OF MEDICINE AND DENTISTRY**

Programme DSP: Pediatrics

**NOVEL ROLE OF HEATR1 IN RIBOSOME  
BIOGENESIS AND DNA DAMAGE SIGNALING**

**Zsófia Turi, M.Sc.**

**Supervising department:**

Institute of Molecular and Translational Medicine, Faculty of Medicine and  
Dentistry, Palacký University and University Hospital in Olomouc

**Supervisor:**

Pavel Moudry, PhD

**Olomouc 2019**

**Statement:**

I hereby declare that I wrote this dissertation entitled: “Novel Role of HEATR1 in ribosome biogenesis and DNA damage signaling.” by myself. The research was carried out at the Institute of Molecular and Translational Medicine, Laboratory of Genome Integrity, Olomouc.

**Acknowledgement:**

First, I would like to thank my supervisor, Pavel Moudry, PhD for his leadership, help and support throughout my PhD study. Secondly, to Prof. Jiri Bartek and Martin Mistrik PhD for giving me a chance to participate in many exciting projects and to work in a highly motivating atmosphere in both Olomouc and Copenhagen. I am grateful to all my colleagues at Laboratory of Genome Integrity in Olomouc for all their help and patience during my development as a researcher.

Finally, I would like to thank my family, for all their support and love. My special thanks go to my fiancé for his love, support and his faith in me.

Olomouc .....

April 2019 Zsófia Turi M.Sc.

**Bibliographical identification:**

Author's name and surname: Zsófia Turi

Title: Novel Role of HEATR1 in ribosome biogenesis and DNA damage signaling

Type of thesis: Dissertation

Department: Institute of Molecular and Translational Medicine, Faculty of Medicine and Dentistry, Palacký University Olomouc

Supervisor: Pavel Moudry, PhD

The year of defence: 2019

Keywords: Ribosome biogenesis, nucleolus, HEATR1, p53, cancer, DNA damage response

Language: English

## **ABSTRACT**

Ribosome biogenesis is an energy consuming process that occurs mainly in the nucleolus. This membrane-less organelle is located in the nucleus, and its structural organization is dependent on active ribosome biogenesis. The process itself includes the transcription and maturation of ribosomal RNAs, their assembly with ribosomal proteins, their export to the cytoplasm and ribosomal subunit assembly. The synthesis of ribosomes requires a huge energy investment of the cells; therefore it is tightly synchronized with nutrient availability, cell growth, cell cycle and stress signals reaching the cells. Impaired ribosome biogenesis triggers the activation of the tumor suppressor p53, that promotes cell cycle arrest, apoptosis or senescence. Collectively, this cellular response is termed as ribosome biogenesis stress. Perturbation of ribosome biosynthesis is also a hallmark of multiple diseases, characterized mainly by the altered structure of the nucleolus. According to a recently emerged concept, the nucleolus and factors of ribosome biogenesis are also involved in the coordination of multiple signaling pathways, such as DNA damage response.

In this work, we identified a nucleolar protein, HEATR1 as an important player of ribosome biogenesis. In the absence of this protein, ribosome biogenesis stress is activated, characterized by the elevated level of p53, cell cycle arrest and structural changes of the nucleolus. Furthermore, HEATR1 seems to be involved in the early steps of ribosome biogenesis, since it possesses similar localization signal to Pol I and its ablation completely abolishes rRNA transcription. Besides its function in ribosome biosynthesis, HEATR1 may be required for DNA damage signaling as well, evidenced by DNA damage-dependent phosphorylation of this protein. Overall, our work presents HEATR1, a novel player in ribosome biogenesis and DNA damage response.

**Keywords:** Ribosome biogenesis, nucleolus, HEATR1, p53, cancer, DNA damage response

## TABLE OF CONTENTS

1. INTRODUCTION.....	7
1.1. THE NUCLEOLUS .....	8
1.1.1. RRNA ENCODING GENES.....	8
1.1.2. THE STRUCTURE OF THE NUCLEOLUS.....	9
1.2. RIBOSOME BIOGENESIS.....	11
1.2.1. RRNA SYNTHESIS .....	11
1.2.2. RRNA PROCESSING .....	15
1.2.3. IMPORT AND ASSEMBLY OF RPS .....	17
1.2.4. EXPORT OF PRE-40S AND PRE-60S SUBUNITS AND FINAL ASSEMBLY OF THE RIBOSOME.....	19
1.3. RIBOSOME BIOGENESIS STRESS .....	20
1.3.1. THE 5S RNP/MDM2/P53 PATHWAY .....	21
1.3.2. NON-CANONICAL RIBOSOME BIOGENESIS STRESS PATHWAYS .....	25
1.3.3. IMPAIRED RIBOSOME BIOGENESIS CHECKPOINT AND THE ASSOCIATED DISEASES .....	28
1.3.4. RIBOSOME BIOGENESIS AND CANCER .....	36
1.4. EXTRA-RIBOSOMAL FUNCTIONS OF THE NUCLEOLUS .....	42
1.4.1. THE NUCLEOLUS AS THE MAIN STRESS SENSOR OF THE CELLS.....	43
1.4.2. THE NUCLEOLUS IN GENOME MAINTENANCE .....	47
1.5. HEATR1, A NEW PLAYER IN RIBOSOME BIOGENESIS .....	48
2. AIMS OF THE THESIS .....	50
3. MATERIAL AND METHODS .....	51
3.1. CELL CULTURE, TREATMENTS AND GENERATION OF DSBS.....	51
3.2. RNA INTERFERENCE.....	52
3.3. CELL CYCLE ANALYSIS.....	52
3.4. WESTERN BLOTTING.....	52
3.5. IMMUNOFLUORESCENCE.....	54
3.6. EDU AND EU STAINING .....	55

3.7. IMMUNOPRECIPITATION.....	55
4. RESULTS AND DISCUSSION .....	56
4.1. IDENTIFICATION OF HEATR1 IN A HIGH-RESOLUTION MICROSCOPY SCREEN .....	56
4.2. DEPLETION OF HEATR1 LEADS TO THE STABILIZATION OF P53 AND INITIATES P53-DEPENDENT CELL CYCLE ARREST ...	57
4.3. HEATR1 IS LOCALIZED INTO THE NUCLEOLUS .....	61
4.4. DOWNREGULATION OF HEATR1 INDUCES RIBOSOME BIOGENESIS STRESS .....	63
4.4.1. NUCLEOLAR STRUCTURE ALTERATIONS .....	64
4.4.2. ACTIVATION OF THE CANONICAL 5S RNP/MDM2/P53 PATHWAY .....	65
4.5. HEATR1 IS INVOLVED IN RRNA SYNTHESIS .....	68
4.6. UPREGULATION OF HEATR1 IN CANCER.....	71
4.7. INVOLVEMENT OF HEATR1 IN DNA DAMAGE RESPONSE	73
4.7.1. PHOSPHORYLATION OF HEATR1 BY ATM.....	73
4.7.2. DEPLETION OF HEATR1 LEADS TO ATTENUATED $\gamma$ H2AX FORMATION .....	74
5. SUMMARY .....	77
6. REFERENCES.....	78
7. ABBREVIATIONS.....	103
8. BIBLIOGRAPHY .....	107
8.1. ORIGINAL ARTICLES AND REVIEWS.....	107
8.2. CONFERENCE LECTURES AND POSTER PRESENTATIONS .....	107
8.2.2. ORAL TALKS.....	107
8.2.3. POSTER PRESENTATIONS.....	108
8.3. APPENDIX – FULL TEXT PUBLICATIONS RELATED TO THE THESIS .....	109
8.3.1. APPENDIX A .....	109
8.3.2. APPENDIX B .....	110
8.3.3. APPENDIX C .....	111
8.3.4. APPENDIX D .....	112

# 1. INTRODUCTION

Ribosomes are large protein-RNA complexes, composed of a small subunit (40S or SSU) and a large subunit (60S or LSU) (Klinge et al. 2012; Wilson and Doudna Cate 2012; Yusupova and Yusupov 2014). Ribosomes are present in the cytoplasm and engaged in protein translation, however their biosynthesis is mainly tied to a sub-nuclear organelle, called nucleolus. The main steps of ribosome biogenesis occurring in the nucleolus include ribosomal RNA (rRNA) synthesis, processing and assembly with ribosomal proteins (RPs). During their maturation, the ribosomal subunits are moving towards the nucleus followed by transport to the cytoplasm where late steps of processing and assembly take place (Fig. 1) (Henras et al. 2008; Henras et al. 2015). The fully assembled 80S ribosomes contain four rRNAs and 80 RPs (Yusupova and Yusupov 2014).

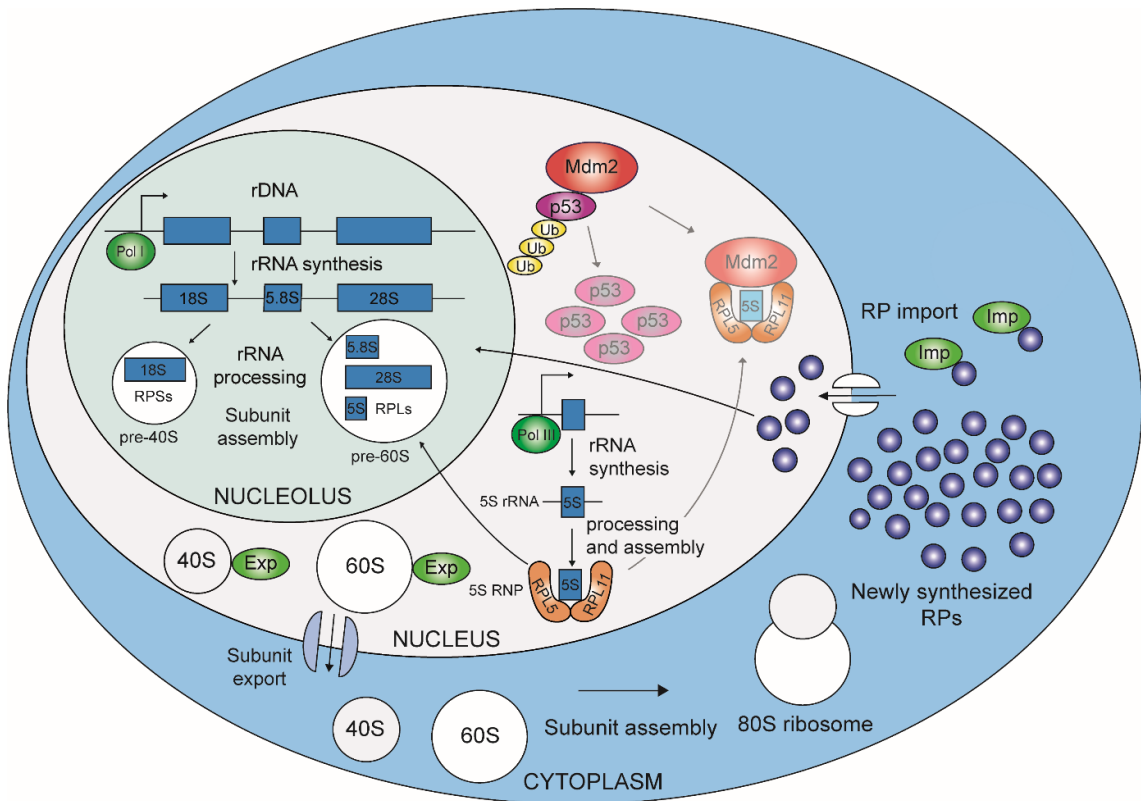


**Figure 1. Ribosome biogenesis.** Ribosome biogenesis is initiated in the nucleolus by the rRNA synthesis, followed by rRNA processing and subunit assembly. The premature ribosomal subunits are moving through the nucleus and transported into the cytoplasm. In the cytoplasm, the 40S and 60S subunits unite to formulate the 80S ribosome during translation. Under normal conditions 5S RNP is incorporated into the 60S ribosomal subunit and p53 is sequestered and ubiquitinated by Mdm2, followed by proteasomal degradation of p53. The newly synthesized ribosomal proteins are transported into the nucleolus in order to be incorporated into the ribosome. Exp: exportin; Imp: importin; RP: ribosomal protein; RPS: ribosomal protein of the small subunit; RPL: ribosomal protein of the large subunit.

## 1.1. The nucleolus

### 1.1.1. rRNA encoding genes

The nucleolus is a specialized membrane-less organelle, organized around nucleolar organizer regions (NORs) found on the short arms of acrocentric chromosomes, i.e. chromosome 13, 14, 15, 21 and 22 (Fig. 2). NORs are highly repetitive regions of the genome, containing clusters of rRNA encoding genes (McStay 2016). The individual ribosomal DNA (rDNA) genes are separated by intergenic spacers (IGS) (Fig. 3), which contain the rDNA promoter and enhancer elements that regulate rDNA transcription; replication origins; replication fork barriers, which inhibit collision of replication and transcription machineries; and spacer promoters that are involved in the transcription of other non-coding RNAs (Goodfellow and Zomerdijk 2013; Akamatsu and Kobayashi 2015). Because of the repetitive nature of this genomic region, rDNA is exposed to

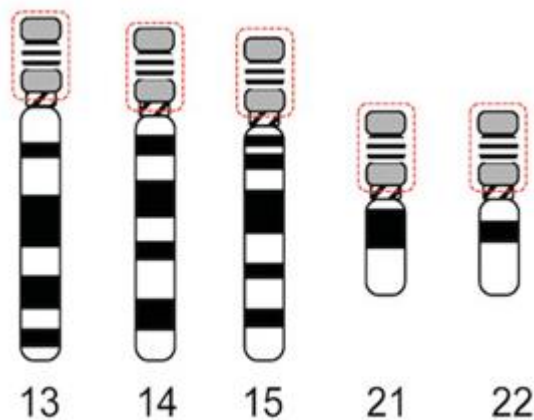


**Figure 2. Human acrocentric chromosomes.** Short arms of the chromosomes containing the NORs are marked with red circles. (Adopted from McStay et al., 2016.)

recombination events, which renders it highly unstable. Therefore, it is not surprising that

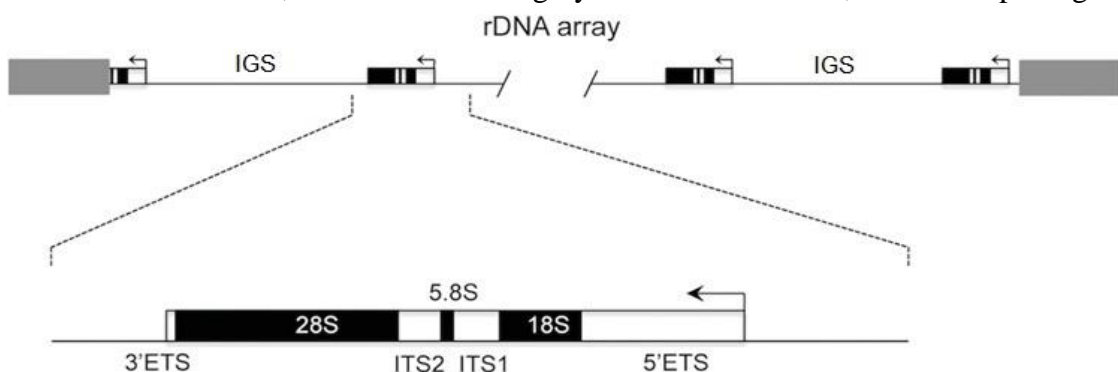


**Figure 3. Organization of the human rDNA array.** rDNA genes are separated by intergenic spacers (IGS). 5'ETS – 5' external transcribed spacer; ITS1 – internal transcribed spacer; ITS2 – internal transcribed spacer; 3'ETS – 3' external transcribed spacer. (Adopted from McStay, 2016.)

the amount of rDNA repeats can vary between individuals of the same species and even



between cells of the same individual (McStay 2016). Moreover, it was also shown that the instability of this genomic region contributes to decreased lifespan and altered rDNA clusters are often seen in solid cancers (Qu et al. 1999; Powell et al. 2002; Chan et al. 2005; Stults et al. 2009; Kobayashi 2014).

In mammalian cells, only half of the rDNA genes are involved in active transcription at any given time. Transcriptionally active rDNA genes are associated with promoter CpG hypomethylation and euchromatic histone modifications such as acetylation of histone 4 (H4ac) and trimethylation of histone 3 lysine 4 (H3K4me3). In contrast, silent rDNA genes exhibit promoter hypermethylation and heterochromatic histone marks, such as di- or trimethylation of histone 3 lysine 9 (H3K9me2/3), trimethylation of histone 4 lysine 20 (H4K20me3) and trimethylation of histone 3 lysine 27 (H3K27me3) (Guettg and Santoro 2012; Grummt and Langst 2013). Under normal conditions, silent rDNA genes are maintained in a transcriptionally repressed state which contributes to genome stability, as these regions counteract unequal recombination events and govern the formation of nuclear heterochromatic regions as well (Guettg and Santoro 2012; Grummt and Langst 2013). Therefore, rRNA synthesis is mainly regulated via alterations in the transcription rate of already active rDNA genes (Orsolich et al. 2016).

### 1.1.2. The structure of the nucleolus

The nucleolus is assembled in the early G1 phase of the cell cycle and disassembled during the beginning of mitosis. In interphase, silent rDNA genes are located in extra-nucleolar regions surrounding the nucleolus, while actively transcribed rDNA genes are dispersed within this organelle, encompassed by the primary rRNA transcript and other protein and RNA factors involved in ribosome biogenesis (Sirri et al. 2008; Guettg and Santoro 2012). Consequently, the amount of global nucleolar DNA is very low, therefore nucleoli are DAPI excluded structures, seen as dark areas when stained with this fluorescent dye (Fig. 4) (Sirri et al. 2008). In mammalian cells the structure of the nucleolus can be further divided into three main components, observed by electron microscopy (Fig. 5).

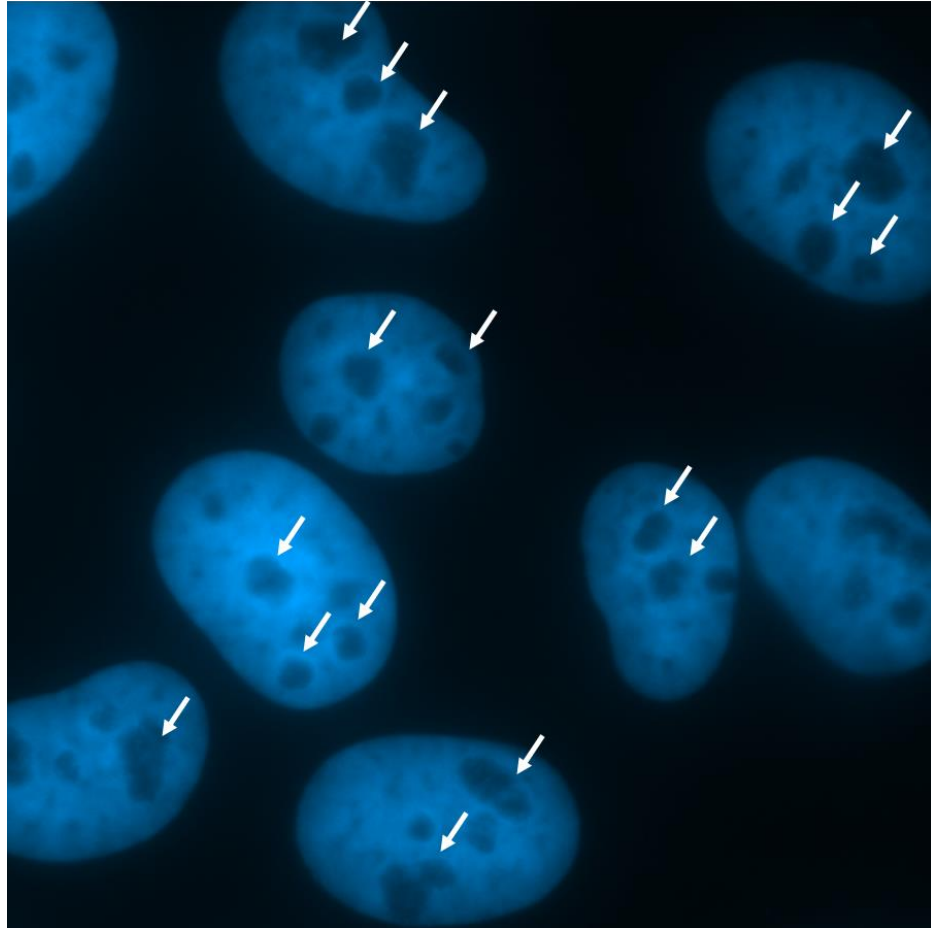


**Figure 4. Nucleoli are DAPI excluded structures.** Nuclei of U2OS cells were visualized by DAPI staining. Dark areas represent nucleoli. Prominent nucleoli are marked with white arrows.

Fibrillar centers (FC) are clear areas, containing the rDNA and the components of the rRNA transcription machinery which are not engaged in transcription at the moment. FCs are surrounded by the highly contrasted dense fibrillar component (DFC). The transcription of rRNA occurs at the interface between FC and DFC, and the primary rRNA transcript accumulates in the DFC. Early processing factors are also localized to the DFC to promote rRNA maturation. The FC-DFC compartments are embedded into the granular component (GC) of the nucleolus. The GC contains late rRNA processing factors, and RPs are localized here as well (Fig. 5) (Sirri et al. 2008; Hernandez-Verdun et al. 2010). Tripartite organization of the nucleolus is the characteristic of higher eukaryotes and is dependent on active ribosome biogenesis. Repression of ribosome biosynthesis by low doses of actinomycin D (ActD), which is known to specifically, leads to the reorganization of the nucleolar structure. Under these circumstances, the components of FC and DFC migrate to the periphery of the nucleolus to form so-called ‘nucleolar caps’ in a juxtaposed position, while GC proteins remain in the central body (Shav-Tal et al. 2005). Furthermore, similar nucleolar segregation can be observed, when

rRNA processing is inhibited (Sirri et al. 2008), which further supports the notion that nucleolar organization is directly related to the activity of ribosome biogenesis.

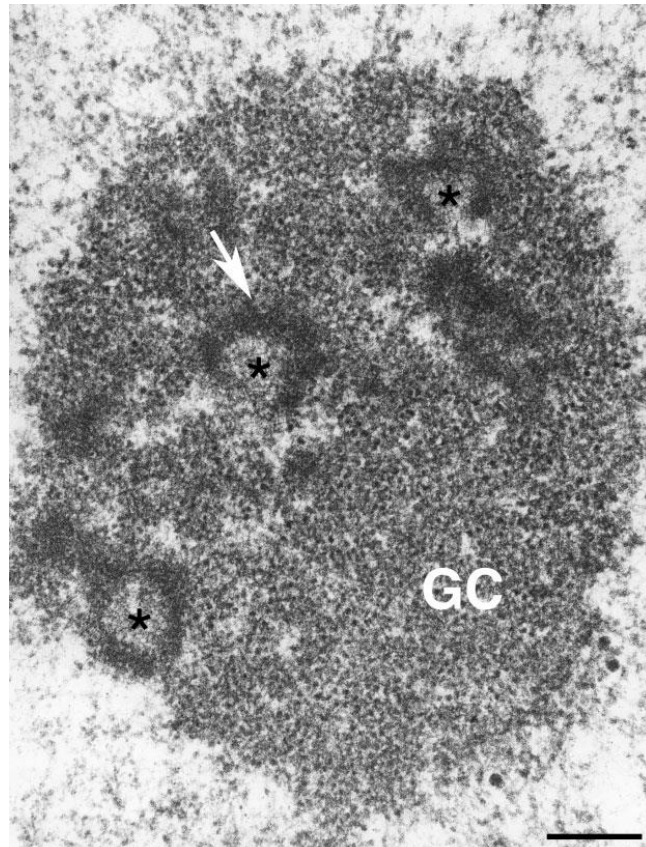


**Figure 5. Tripartite structure of the nucleolus of HeLa cells visualized by electron microscopy.** The three nucleolar components are: fibrillar center (asteriks); dense fibrillar component (white arrow); granular component (GC). (Adopted from Hernandez-Verdun et al., 2010.)

## 1.2. Ribosome Biogenesis

### 1.2.1. rRNA synthesis

The first step of ribosome biogenesis, rRNA synthesis is carried out by the RNA polymerase I (Pol I) (Fig. 1). Pol I is assembled with the upstream binding factor (UBF), the selectivity factor (SL1 or TIF1-B) and the transcription initiation factor 1A (TIF1-A in mice and hRRN3 in human) to form the pre-initiation complex (PIC) at the rDNA promoters. Mechanistically, PIC assembly is initiated by UBF homodimer formation; thus it gains an ability to bind distinct sequences in the promoter region. One subunit of the homodimer is associated with the core promoter region, whereas the other is bound to the upstream core element (UCE), thereby UBF creates a DNA stem-loop structure, which promotes the enhancement of transcription. SL1 is recruited to this structure to

interact with both UBF and the rDNA promoter. Meanwhile Pol I associated with hRRN3 is also recruited to the promoter via multiple interactions to form the PIC. The successful formation of the PIC enables promoter opening and transcription initiation. After the first couple of ribonucleotides are formed, Pol I is released from the complex to proceed to the transcription elongation phase. Promoter escape leads to the dissociation of hRRN3 from the promoter region as well, whereas UBF and SL1 remain to be bound and able to initiate another cycle of PIC formation. Surprisingly, UBF is associated with the whole length of the rDNA gene, suggesting a role for this protein in transcription elongation as well. Finally, transcription termination is facilitated by several factors, such as the transcription termination factor 1 (TTF-1) and the Pol I and transcript-release factor 1 (PTRF1). Dissociation of Pol I from the rDNA transcript unit can be immediately followed by the recycling of the Pol I complex and the initiation of the next cycle of transcription (Fig. 6) (Russell and Zomerdijk 2005; Albert et al. 2012).

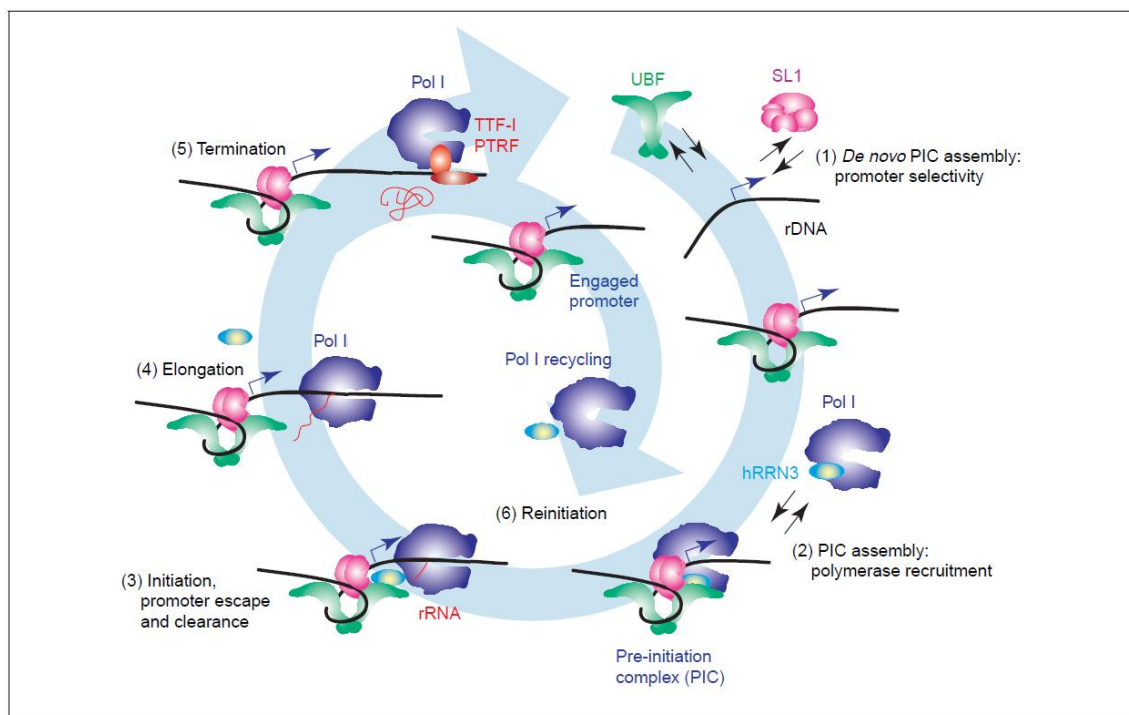


**Figure 6. The transcription cycle of the Pol I machinery.** See text for detailed description. (Adopted from Russell and Zomerdijk, 2005.)

rDNA transcription by Pol I machinery results in the synthesis of a single, polycistronic primary transcript, called 47S pre-rRNA. The 47S pre-rRNA contains rRNA components of the SSU: 18S and the LSU: 5.8S and 28S. These individual rRNAs are separated from each other by internal transcribed spacers (ITS1 and ITS2), and the whole transcript is flanked by external transcribed spacers at the 5'- and 3'-end (5'-ETS and 3'-ETS, respectively) (Fig. 1; Fig. 3 and Fig. 7) (Henras et al. 2015). The mature

rRNAs arise after subsequent processing steps, which occur either co- or post-transcriptionally (see below).

Ribosome biogenesis is mainly regulated by alteration of the rRNA synthesis. Multiple pathways involved in cell growth, proliferation or stress signaling converge on the activation or repression of the Pol I transcription machinery. Mitogenic signals, the presence of growth factors and nutrient availability activate mitogen-activated protein kinase/extracellular-signal regulated kinase (MAPK/ERK) and phosphatidylinositol 3-kinase/protein kinase B alpha/mammalian target of rapamycin (PI3K/AKT/mTOR) signaling cascades which upregulate rRNA synthesis (Grummt 2010; Hannan et al. 2011). For instance, ERK is capable of phosphorylating both hRRN3 and UBF, increasing transcription initiation and elongation rate, respectively (Zhao et al. 2003; Stefanovsky et al. 2006; Stefanovsky and Moss 2008). The PI3K/AKT/mTOR pathway also affects Pol I transcription machinery at multiple levels. Through the activation of ribosomal protein S6 kinase (S6K) this pathway also upregulates the phosphorylation of UBF and hRRN3, promoting PIC assembly (Hannan et al. 2003; Mayer et al. 2004). MAPK/ERK and PI3K/AKT/mTOR signaling are interconnected, and both can activate the transcription factor c-Myc (Mendoza et al. 2011). It has been suggested that c-Myc is the master regulator of ribosome biogenesis since it can increase rRNA synthesis, through multiple mechanisms. For instance, it enhances the transcription of Pol I machinery components (Poortinga et al. 2004; Grewal et al. 2005; Poortinga et al. 2011) interacts with SL1 to promote UBF-SL1 complex formation and it also binds to the rDNA to facilitate PIC formation (Arabi et al. 2005; Grandori et al. 2005; Shiue et al. 2009; van Riggelen et al. 2010). Opposing these signaling cascades, specific tumor suppressors act to decrease the rate of rRNA synthesis. The most common example is the tumor suppressor protein p53, which can downregulate ribosome biogenesis directly by forming a complex with SL1, preventing its association with UBF (Zhai and Comai 2000) or indirectly by the activation of the retinoblastoma protein (pRB). pRB binds to UBF and inhibits its function to recruit SL1 to the rDNA promoter (Cavanaugh et al. 1995; Hannan et al. 2000). Moreover, the negative regulator of PI3K/AKT/mTOR pathway, PTEN tumor suppressor protein is involved in quenching rRNA synthesis directly by inducing the dissociation of the subunits of SL1 (Zhang et al. 2005a). Besides these central regulators, a multitude of other factors contributes to the control and alteration of the rRNA synthesis rate via posttranslational modifications (PTMs) or by altering the expression level or the accessibility of Pol I transcription machinery proteins (Grummt 2010).

It has been suggested that the rate of rRNA synthesis, thus ribosome biogenesis is mainly regulated by altering the activity of Pol I transcription machinery at transcriptionally active genes (Grummt and Langst 2013). However, several studies implicated that it can be modulated by changing the ratio between eu- and heterochromatic rDNA as well. Although the presence of stable, silent rDNA genes is indispensable for genome stability, certain shift between eu- and heterochromatic state (which correlates with rRNA synthesis rate) is observed under physiological conditions, such as cellular differentiation and changes in energy status of the cell (Murayama et al. 2008; Poortinga et al. 2011). The maintenance of the heterochromatic rDNA is established by the nucleolar remodeling complex (NoRC) that promotes transcription repression by recruiting factors involved in DNA methylation and histone modification (Grummt 2010).

rRNA synthesis by Pol I occurs in the nucleolus and leads to the emergence of 3 rRNAs: SSU 18S rRNA and LSU 5.8S and 28S rRNAs (Henras et al. 2015). The third LSU component, 5S rRNA is an exception, in a manner that 5S rRNA genes are located outside of the NORs, on chromosome 1 (Fig. 7), where similarly to 47S rRNA genes, they are also organized into tandem repeated units (Sørensen and Frederiksen 1991). These genes are transcribed by RNA Polymerase III (Pol III) in the nucleus (Fig. 1). Besides 5S rRNA, Pol III is also involved in the production of other small, non-coding RNAs, such as all transfer RNAs (tRNAs), U6 spliceosomal RNA and signal recognition particle 7SL RNA (Paule and White 2000). Transcription initiation at the promoter region of the 5S rRNA gene is facilitated by several transcription factors: transcription factor IIIA, IIIB and IIIC (TFIIIA, TFIIB and TFIIC). Initiation is followed by promoter opening and escape, elongation and termination of transcription. In contrast to Pol I, Pol III is able to recognize terminator sequences and does not require other factors (such as TTF-1 in the case of Pol I) to terminate transcription. Moreover, after releasing the nascent primary transcript, Pol III might remain bound to the template, which facilitates rapid re-initiation of the transcription cycle (Paule and White 2000).

Regulation of the 5S rRNA transcription is governed by the same pathways involved in the control of Pol I transcription machinery. For instance, MAPK/ERK signaling and c-Myc both activate TFIIB (Felton-Edkins et al. 2003; Gomez-Roman et al. 2006), while mTOR also stimulates TFIIB (Woiwode et al. 2008), as well as TFIIC to upregulate Pol III-mediated 5S rRNA transcription (Kantidakis et al. 2010). In contrast, p53 and pRB counteract Pol III activity by directly targeting TFIIB (Scott et al. 2001;

Crighton et al. 2003). Thus, regardless of the differences between the synthesis of 47S and 5S rRNAs, rRNA transcription is controlled by these mitogenic and tumor suppressive signaling pathways via the up- or downregulation of all rRNA transcription, respectively.

### 1.2.2. rRNA processing

Maturation of the 47S pre-rRNA is a complex and highly hierarchic process, which includes endo- and exonucleolytic cleavages and posttranscriptional modifications of the transcript. rRNA processing is initiated co-transcriptionally, as some processing factors are recruited to the 5' end of nascent rRNA already during transcription. These earliest factors are involved in the processing of the 18S rRNA, thus this complex is often referred to as SSU processome. Later on, the SSU and LSU processing pathways are separated by a cleavage introduced in the ITS1 region (Fig. 7). For a detailed description of 47S pre-rRNA processing steps see Figure 7 and reviews in the topic (Mullineux and Lafontaine 2012; Henras et al. 2015).

Posttranscriptional modifications of the rRNA include pseudouridylation and 2'-*O*-methylation. These chemical reactions are carried out by box H/ACA and box C/D small nucleolar ribonucleoprotein (snoRNP) complexes, respectively. Both of these complexes are named after the unique motif present in the RNA component. The components of box H/ACA snoRNP are the pseudouridine synthase dyskerin, auxiliary proteins Nhp2, Nop10, Gar1 and the box H/ACA snoRNA. Box C/D snoRNP consists of the methyltransferase fibrillarin (FBL), accessory proteins Nop56, Nop58, 15.5 K/NHPX and the box C/D snoRNA. In both snoRNP complexes, the RNA component is responsible for site-specificity, as it hybridizes to the rRNA which allows the accessibility of the complex as well as the chemical modification to occur at defined sites of the rRNA. Furthermore, by binding and changing its conformation, both box H/ACA and box C/D snoRNP complexes are involved in directing endo- and exonucleolytic cleavage of the rRNAs (Watkins and Bohnsack 2012).

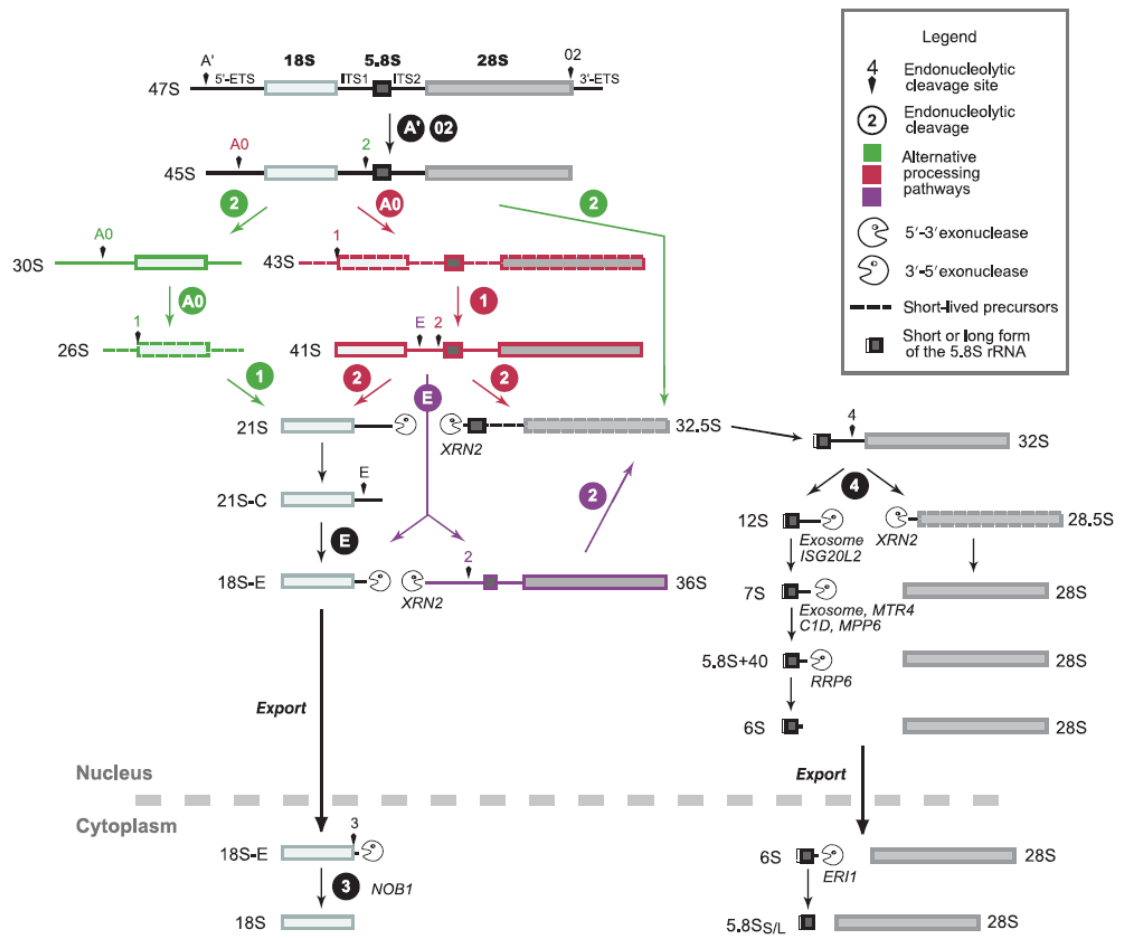


**Figure 7. rRNA processing steps in mammalian cells.** A very early cleavage of the 47 S pre-rRNA in the 5' – ETS (A' site) and in the 3' – ETS (O2 site) result in the emergence of 45 S rRNA. Subsequently, 45 S rRNA is cleaved either in 5' – ETS (red) or in ITS1 (green). If the first cleavage of the 45 S rRNA occurs in the 5' – ETS (A0 site), the resulting 41 S rRNA can be processed either at E or at 2 cleavage sites of the ITS1. By the cleavage at site 2 of ITS1, 21 S rRNA of the SSU pathway and the LSU 32 S rRNA are separated. Resection of the 3' end of 21 S rRNA leads to the formation of 21 S-C intermediate, which is cleaved at E site to produce 18 S-E pre-rRNA. Finally, 18 S rRNA is formed by exonucleolytic processing of 3' end by NOB1 in the cytoplasm. Alternatively, 41 S pre-rRNA can be cleaved at site E (purple), which leads to the immediate formation of 18 S-E rRNA and a 36 S LSU precursor, which is converted into 32 S rRNA by ITS1 resection. However, if the first cleavage of 45 S rRNA occurs in the ITS1 at site 2, the SSU pathway is initiated by the formation of the 30 S precursor, which is cleaved at A0 site in 5' – ETS subsequently, leading to the formation of 21 S rRNA and the following steps occur as described before. In all cases, cleavage of ITS1 leads to the formation of the 32 S LSU precursor. ITS2 is processed by an endonucleolytic cleavage at site 4, followed by exonucleolytic resections leading to the emergence of mature 28 S rRNA in the nucleus and mature 5.8 S rRNA in the cytoplasm. (Adopted from Henras et al., 2015.)

To ensure ongoing ribosome biogenesis, other proteins or protein complexes, such as RNA helicases, kinases, ATPases and GTPases are involved in altering the conformation of the rRNA, removal of processing factors from the rRNA and facilitating assembly of RPs (Henras et al. 2008; Henras et al. 2015). It is worth to highlight the importance of two multifunctional proteins: nucleophosmin (NPM) and nucleolin (NCL),



both of which have a crucial role at multiple stages of ribosome biogenesis (Tajrishi et al. 2011; Durut and Saez-Vasquez 2015; Box et al. 2016). Both these proteins possess histone chaperone activity to facilitate remodeling and dissociation of histones around the rDNA genes, thus promoting rRNA synthesis (Swaminathan et al. 2005; Angelov et al. 2006; Murano et al. 2008). Furthermore, NCL was also found to be associated with the rDNA genes at promoter and coding regions, thereby aiding Pol I mediated transcription elongation (Cong et al. 2012). Both NPM and NCL have a role in rRNA processing as well, however while NPM is involved in LSU maturation via assisting ITS2 cleavage of the pre-rRNA, NCL is required for 5'-ETS processing, thus for SSU maturation (Ginisty et al. 1998; Savkur and Olson 1998; Ginisty et al. 2000; Itahana et al. 2003). Moreover, NPM regulates the nuclear export of RPL5 and pre-ribosomal subunits, whereas NCL coordinates diverse steps of pre-ribosomal assembly (Bouvet et al. 1998; Roger et al. 2003; Yu et al. 2006; Maggi et al. 2008). In addition, NPM, as well as NCL, have extra-ribosomal functions (e.g. regulation of cell cycle and genome maintenance) which provides a possible regulatory connection between ribosome biogenesis and other cellular processes (Box et al. 2016; Scott and Oeffinger 2016; Jia et al. 2017).

The maturation of the 5S rRNA mainly occurs in the nucleus, however, this complex process –especially in mammalian cells – is poorly understood. After its transcription, the precursor of 5S rRNA is associated with the La protein. La protein is involved in chaperoning and stabilizing Pol III transcripts, including 5S rRNA (Wolin and Cedervall 2002). Furthermore, several exonucleases have been shown to be involved in the processing of the 3'end of 5S rRNA in *Saccharomyces cerevisiae* (Ciganda and Williams 2011). Human homologs of these yeast exonucleases exist, however, are not characterized to date. Furthermore, pseudouridylation of 5S rRNA has been demonstrated to require Pus7 pseudouridine synthase independently of box H/ACA snoRNPs in yeast (Decatur and Schnare 2008). Importantly, 5S rRNA forms a complex with several RPs which is required for its subsequent transport into the nucleolus and incorporation into the pre-60S subunit (Fig. 1; see below).

### 1.2.3. Import and assembly of RPs

Mature ribosomes are composed of the 18S rRNA and 33 SSU RPs (RPSs), which form the 40S and the 5S, 5.8S, 28S rRNAs and 47 LSU RPs (RPLs), which form the 60S subunit (Yusupova and Yusupov 2014). RP genes are located at both sex chromosomes

and all autosomal chromosomes, except for chromosome 7 and 21 (Fig. 8) (Uechi et al. 2001). The genes encoding RPs are transcribed by the RNA Polymerase II (Pol II) in the

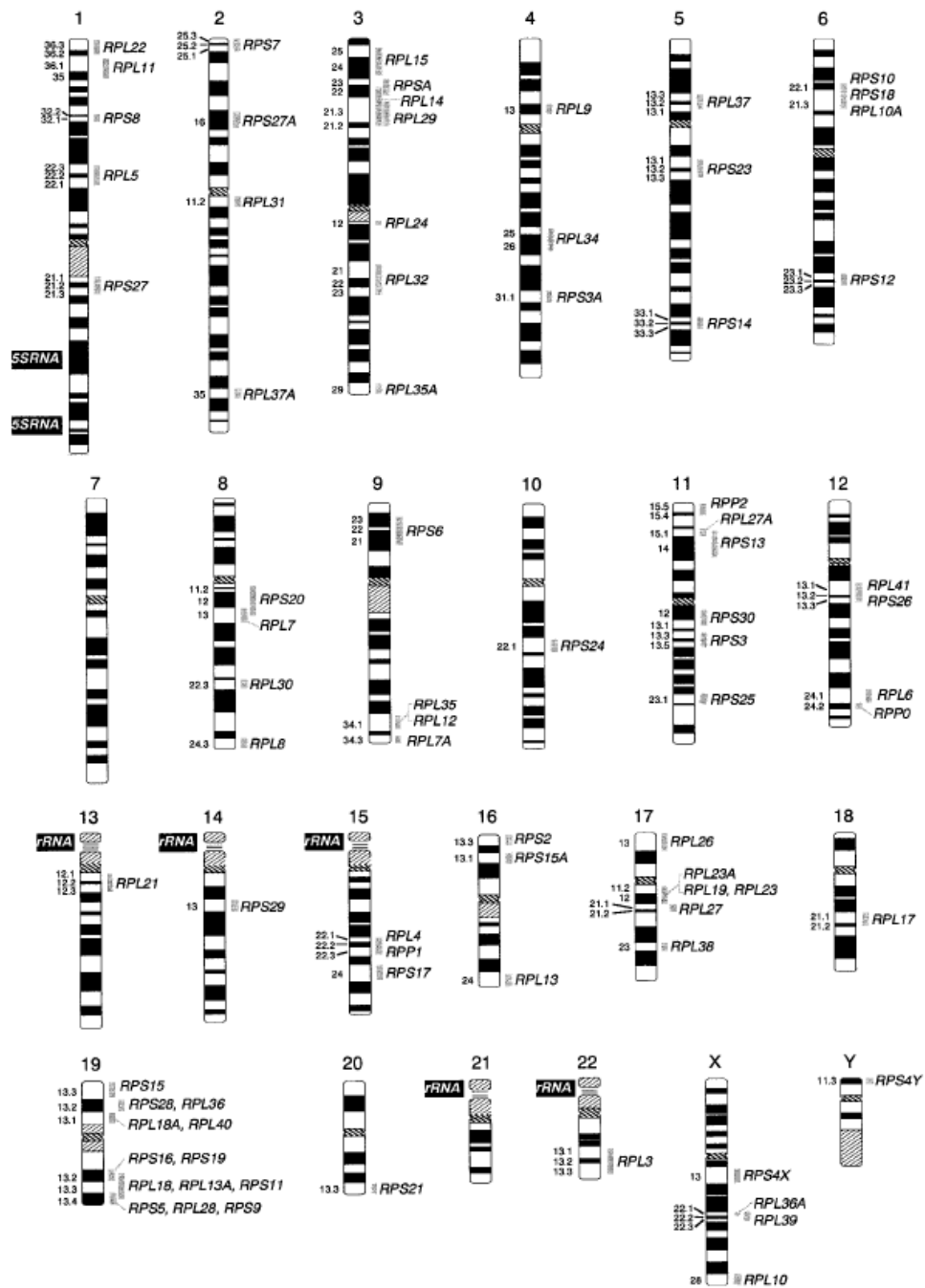


**Figure 8. Human ribosomal protein encoding genes are located on all chromosomes, with the exceptions of chromosome 7 and 21.** The localization of 47 s rRNA and 5 S rRNA encoding genes are represented here as well. (Adopted from Uechi et al., 2001.)

nucleus, and RP mRNAs are translated in the cytoplasm. However, most of these RPs accumulate in the nucleolus immediately after their synthesis to be incorporated into the ribosomal subunits, otherwise free RPs are rapidly degraded by the proteasome (Warner et al. 1985; Lam et al. 2007). In order to be imported into the nucleolus, the RPs must

pass the nuclear membrane through the nuclear pore complex (NPC). RPs cannot directly diffuse through the NPC; their transport is an energy-dependent process, facilitated by several nuclear receptor proteins of the  $\beta$ -karyopherin family, called importins (Fig. 1) (Rout et al. 1997; Jäkel and Görlich 1998; Jäkel et al. 2002). For instance, importin- $\beta$ , transportin, RanBP5 and RanBP7 have been suggested to be involved in the import of RPL23A, RPS7 and RPL5 (Jäkel and Görlich 1998), importin-11 has been shown to participate in RPL12 import (Plafker and Macara 2002), while importin-7 seems to be required for the nuclear import of RPL4, RPL6 and RPL23A (Jäkel et al. 2002). However, the detailed mechanism of nuclear import of many RPs still remains to be elucidated.

The incorporation of RPs into the ribosome and rRNA processing occur simultaneously. RPs are assembled with the rRNAs during their maturation in a highly hierarchic order, and it has been reported that these proteins contribute to the rRNA processing as well, possibly by chaperoning rRNAs. Assembly of the RPs can occur early or late in ribosome biogenesis, which determines their position in the mature ribosome. Some of the RPs that are located on the outer surface of the ribosome, associate with the pre-ribosome only in the cytoplasm (Henras et al. 2015).

In contrast to other RPs, LSU components RPL5 and RPL11 have been reported to have different incorporation mechanism. RPL5 and RPL11 associate with the 5S rRNA to form the 5S RNP complex in the nucleus (Fig. 1) (Zhang et al. 2007; Sloan et al. 2013). Incorporation of the 5S RNP into the pre-ribosome is facilitated by two assembly factors, called Bxdc1 and Rrs1 in yeast (Zhang et al. 2007; Donati et al. 2013; Sloan et al. 2013). Furthermore, the formation of the ternary complex of 5S RNP might provide mutual protection of its components from proteasomal degradation, and indeed, 5S RNP has been reported to be stably present in ribosome-free fraction and to be involved in another process (see chapter 1.3.).

#### 1.2.4. Export of pre-40S and pre-60S subunits and final assembly of the ribosome

At later steps of ribosome biogenesis, the premature SSU and LSU are transported into the cytoplasm. The energy-dependent nuclear export is promoted mainly by another  $\beta$ -karyopherin family member protein, exportin-1 (Fig. 1) (Thomas and Kutay 2003), followed by the association of last RPs and the dissociation of processing factors (Henras et al. 2008). Final assembly of the 80 S ribosome occurs only during the initiation of protein synthesis by the release of eukaryotic translation initiation factor 6 (eIF6) from

LSU mediated by the elongation factor like-1 (EFL1) GTPase enzyme (Jackson et al. 2010; Weis et al. 2015).

### 1.3. Ribosome biogenesis stress

Ribosome biogenesis is a complex process and requires the coordinated action of numerous factors in the cell, including all three RNA Pols, for the synthesis of rRNAs and RP mRNAs; more than 200 auxiliary factors, for rRNA maturation and subunit assembly; protein translation apparatus, for the synthesis of RPs; and ATP-dependent nuclear transport of RPs and ribosomal subunits (Golomb et al. 2014). Thus, ribosome biosynthesis means a vast energy investment for the cell, and it has been suggested that ca. 80% of the cell's energy is consumed in this process (James et al. 2014). Furthermore, the rate of ribosome biogenesis directly determines the rate of translation, which ultimately drives cellular growth and proliferation (Grummt 2003; Ruggero and Pandolfi 2003; Moss 2004; Rudra and Warner 2004). Accordingly, ribosome biogenesis must be tightly regulated by numerous pathways and strictly dependent on the nutrient availability, cell cycle and stress level of the cell. Vice versa, ribosome biosynthesis also affects numerous cellular pathways (Fig. 9) (Grummt 2003; Boulon et al. 2010; Grummt

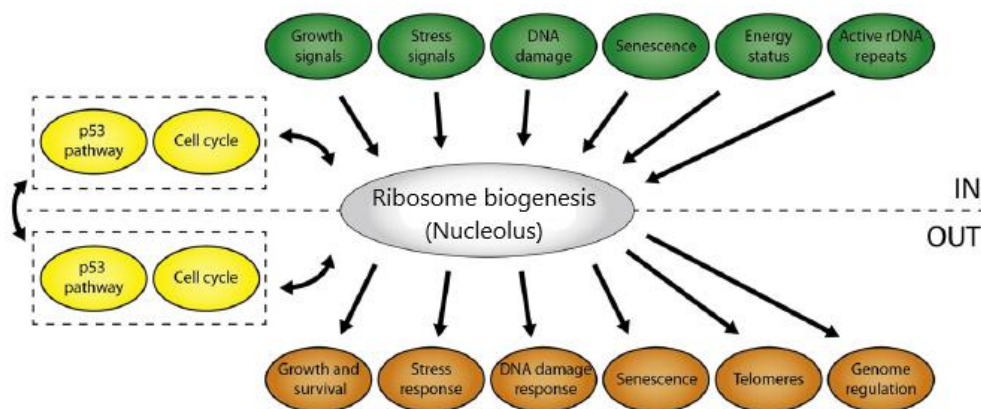


**Figure 9. The in- and outputs of ribosome biogenesis.** Examples of cellular pathways that affect the rate of ribosome biogenesis. On the other hand, ribosome biogenesis is also involved in the regulation of numerous pathways. (Adopted from Quin et al., 2014.)

2010; Quin et al. 2014; Sanchez et al. 2016). This complex relationship of ribosome biogenesis and other cellular processes can be best investigated when the production of ribosomes is perturbed. Impairment of ribosome biogenesis can be achieved by the deficiency or overexpression and overstimulation of ribosome biogenesis factors, by the perturbation of nutrient signaling pathways or by cellular stressors (Boulon et al. 2010;

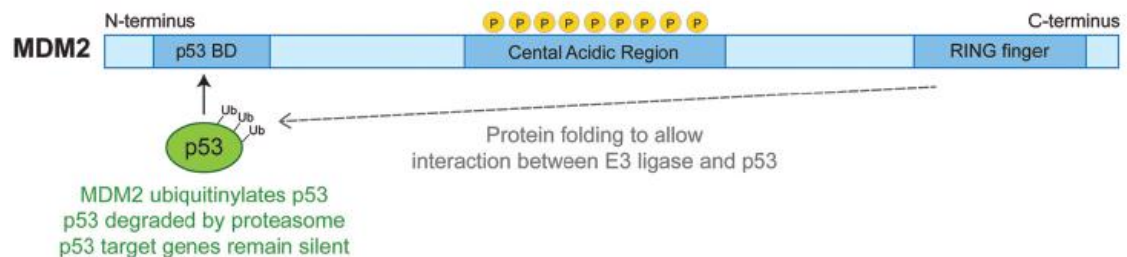
Grummt 2010; Quin et al. 2014). Collectively, the dysregulation of ribosome biogenesis is often referred to as ribosome biogenesis stress, ribosomal stress or nucleolar stress (Bursac et al. 2014; Golomb et al. 2014; James et al. 2014; Quin et al. 2014). Specifically, gross alteration of ribosome biogenesis can result in severe consequences, such as cell cycle arrest, apoptosis or senescence. In majority of these cases activation of the p53 protein is responsible for the onset of such stress responses. Ribosome biogenesis stress is also one of the main characteristics of a diverse group of human diseases, such as ribosomopathies, cancer and neurodegenerative diseases (Narla and Ebert 2010; Hetman and Pietrzak 2012; Armistead and Triggs-Raine 2014; Parlato and Liss 2014; Orsolich et al. 2016).

### 1.3.1. The 5S RNP/Mdm2/p53 pathway

p53 is often referred to as ‘the guardian of the genome’ and is considered to be the main tumor suppressor protein in the cells (Lane 1992; Efeyan and Serrano 2007). p53 is activated in response to numerous cellular stresses, and as a transcription factor it is able to stimulate or repress the expression of its target genes; moreover it possesses transcription-independent functions, as well (Vousden and Prives 2009; Zilfou and Lowe 2009; Brady and Attardi 2010). The fate of the stressed cells defined by p53 activation is determined by the cell type, the genetic and environmental background and the nature of the cellular stress. Lower levels of stress will activate p53-dependent temporary cell cycle arrest, which allows the cells to repair the damage before proceeding to replication or mitosis. On the contrary, persistent or severe stress activates p53-mediated programmed cell death or apoptosis; or cellular senescence, the metabolically inactive state of the cells (Murray-Zmijewski et al. 2008; Zilfou and Lowe 2009; Brady and Attardi 2010). Under normal conditions the level of p53 is kept low, to ensure proper growth and division and to avoid pathological activation of the processes mentioned above. This is assured by a heterodimeric protein complex, called Mdm2-MdmX by binding to p53 (Fig. 1; Fig. 10) (Haupt et al. 1997; Honda et al. 1998; Gu et al. 2002; Michael and Oren 2003). The active enzyme of this complex is Mdm2, an E3 ubiquitin ligase that is responsible for attaching mono- and polyubiquitin moieties to p53, thus triggering its nuclear export and proteasomal degradation, respectively (Fig. 1) (Hock and Vousden 2014). MdmX is the inactive paralogue of Mdm2, which renders the protein complex more stable, ensuring the activity of Mdm2 towards its substrate, p53 (Gu et al. 2002). Furthermore, by binding

to p53, the Mdm2-MdmX complex also inhibits p53's transactivating activity, the ability of p53 to induce the expression of its target genes (Toledo and Wahl 2006).

## A Regulation of p53 by MDM2



## B Lack of p53 regulation by MDM2

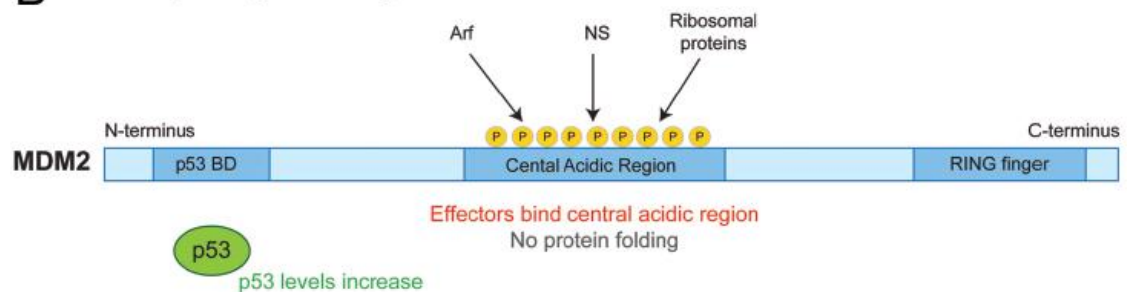


**Figure 10. Schematic structure and regulation of Mdm2.** A. Under normal conditions p53 is bound to the p53 binding domain (p53 BD) of Mdm2. The protein folding of Mdm2 allows the interaction between p53 and the E3 ubiquitin ligase activity possessing RING finger domain of Mdm2. As a result p53 is ubiquitylated by Mdm2 and degraded by the proteasome. B. Under diverse conditions ARF, NS and RPs bind to the central acidic domain of Mdm2 at distinct sites. These interactions disrupt the protein folding of Mdm2. Consequently, p53 is released from its interaction with Mdm2 and it can be stabilized to fulfil its effector functions. (Adopted from James et al., 2014.)

The stress-induced activation of p53 can occur through two diverse processes: via PTMs of Mdm2 and/or p53 (e.g. DNA damage-dependent phosphorylation of p53) or sequestration of Mdm2 by several factors. Both mechanisms result in the disruption of the interaction between Mdm2 and p53, followed by the stabilization of p53, so it can fulfil its effector functions to trigger stress responses (Caspari 2000; Sherr 2006; Zhang and Lu 2009; Brady and Attardi 2010; Cheng and Chen 2010). However, in response to cellular stress p53 is often stabilized through both PTMs and Mdm2 sequestration that ensures the full transactivation potential of p53 (Murray-Zmijewski et al. 2008). Stabilized p53 binds to DNA to transcriptionally activate p53-responsive genes. Some of the main target genes involve p21 protein and 14-3-3 complex which are promoting cell cycle arrest; Bax, Noxa and Puma which are factors that activate apoptosis and p53, which is involved in cellular senescence (Murray-Zmijewski et al. 2008; Vousden and

Prives 2009). p53 is also responsible for the transactivation of Mdm2, thus providing a negative feedback loop to quench its own activity after the activating stress has been overcome (Picksley and Lane 1993; Murray-Zmijewski et al. 2008). Additionally, p53 possesses transcription independent effector functions as well. For instance, upon stress conditions, it can bind to some of the anti-apoptotic Bcl-2 family proteins to counteract their function and promote apoptotic response (Moll et al. 2005; Zilfou and Lowe 2009).

Under ribosome biogenesis stress conditions, a subset of RPs bind to the central acidic domain of Mdm2 (Fig. 10), thereby disrupting its interaction with p53 and the stabilized tumor suppressor protein can trigger cell cycle arrest, apoptosis or senescence subsequently, depending on the nature of the stress (Zhang and Lu 2009; Golomb et al. 2014). Multiple RPs (e.g. RPL23, RPL26, RPS3, RPS7, RPS14) have been described to bind Mdm2 and also to promote p53 activation, when they are overexpressed in cells (Dai and Lu 2004; Dai et al. 2004; Jin et al. 2004; Chen et al. 2007; Yadavilli et al. 2009; Zhu et al. 2009; Zhang et al. 2010; Zhou et al. 2013). Although, given the fact, that RPs are highly basic proteins that can easily interact with the acidic domain of Mdm2 non-specifically when in excess amount, data with overexpressed RPs must be handled with caution (Bursac et al. 2014). On the contrary, the interaction of two LSU components RPL5 and RPL11 with Mdm2 has been suggested to promote p53-mediated stress responses upon ribosome biogenesis stress exclusively. The central role of RPL5 and RPL11 in this pathway is widely accepted and is supported by several observations. First, the depletion of RPL5 and/or RPL11 leads to the impairment of ribosome biogenesis, similarly to other RP deficiencies. However, unlike depletion of other RPs, ablation of RPL5 and/or RPL11 cannot activate p53, suggesting that these RPs are central mediators of p53 induction (Bursac et al. 2012; Fumagalli et al. 2012). Second, Pol I inhibition by low dose ActD treatment generally induces ribosome biogenesis stress and a p53 response; however, in the absence of RPL5 and/or RPL11 this p53 induction is totally inhibited, while concomitant depletion of most other RPs cannot abolish p53 activation in this manner (Bursac et al. 2012; Fumagalli et al. 2012). Furthermore, despite RPs are being continuously synthesized upon perturbed ribosome biogenesis, most free RPs are rapidly degraded by the proteasome (Warner 1977; Lam et al. 2007; Bursac et al. 2012). However, under these same conditions, RPL5 and RPL11 are able to accumulate in a ribosome-free fraction, as a result of their mutual protection from proteasomal degradation, further supporting the central function of these proteins in p53 induction (Bursac et al. 2012). As it was described before, during unperturbed ribosome biogenesis,

RPL5 and RPL11 are assembled with the 5S rRNA to form the 5S RNP complex, which is then incorporated into the ribosome as a unit (Fig. 1) (Zhang et al. 2007; Sloan et al. 2013). 5S RNP has been shown to accumulate in the ribosome-free fraction; therefore it has been suggested that RPL5 and RPL11 are needed to be also assembled in this complex in order to interact with Mdm2 under ribosome biogenesis stress conditions (Donati et al. 2013). Indeed, the requirement of the 5S RNP for the activation of p53 has been reported by several research groups. For instance, depletion of the *POLR3A* gene that encodes the catalytic subunit of Pol III abolished 5S rRNA synthesis and induced a p53-independent cell cycle arrest (Onofrillo 2013). Similarly, the deficiency of TFIIIA transcription factor, which is involved exclusively in 5S rRNA transcription (Engelke et al., 1980; Shastry et al., 1984), induced cell cycle arrest in a p53-independent manner and could also reverse the activation of p53, induced by Pol I inhibition (Donati et al. 2013; Sloan et al. 2013). These data further supported the essence of the 5S RNP complex in this process.

Traditionally, ribosome biogenesis stress has been associated with the morphological alterations of the nucleolus. The disintegration of the nucleolar structure is often described upon perturbed ribosome biogenesis, which led to the assumption that nucleolar RPs and other nucleolar proteins are released to the nucleoplasm passively, where some of them can interact with Mdm2 to activate p53 response (Zhang and Lu 2009). More recently, however, several studies have reported an alternative source of RPs involved in p53 regulation. Fumagalli *et al.* have presented that impairment of the SSU biogenesis does not lead to the disruption of the nucleolar structure; however, still triggers p53 activation. In this case, the authors observed that the translation of 5' terminal oligopyrimidine tract containing messenger RNAs (5'-TOP mRNAs), including RPL11 mRNA, is upregulated (Fumagalli et al. 2009). The nascent RPL11 protein produced in this process can be transported into the nucleus subsequently, and along with freshly synthesized RPL5, it could be the source of Mdm2 sequestration, which promotes the activation of p53 (Fumagalli et al. 2009; Fumagalli et al. 2012). However, it can be argued that the upregulation of RPL11 translation might be only a unique consequence of the impaired SSU biogenesis since biosynthesis of the LSU is still intact and RPL11 is consumed in the assembly of the 60S subunit as well as in the p53 response to SSU impairment. Under these conditions, there is an increased need for RPL11 protein synthesis. Surprisingly, simultaneous defects of both LSU and SSU biogenesis still causes translational upregulation of RPL11, however, in this case, the more significant amount of freshly synthesized RPL11 elicits stronger induction of p53 (Fumagalli et al. 2012).



Nonetheless, Bursac *et al.* have demonstrated that even under conditions when the nucleolar structure is disrupted, induction of p53 relies rather on the presence of freshly synthesized RPL5 and RPL11 (Bursac et al. 2012). Thus, it seems that disintegration of the nucleolus is preferably a passive consequence of ribosome biogenesis stress, although it is still unknown why only certain conditions can induce such morphological alterations. Additionally, the sensing and signaling of ribosome biogenesis stress is also a matter of debate. Some suggest that the 5S RNP complex might have a function in monitoring ribosome biogenesis. The rationale behind this theory is that this complex stably exists in the ribosome-free fraction and can be quickly mobilized to interact with Mdm2 to turn on the p53 response when it is needed (Sloan et al. 2013). However, details of this mechanism remain mostly unexplored.

### 1.3.2. Non-canonical ribosome biogenesis stress pathways

#### *Alternative activation of p53*

Besides the 5S RNP complex, there are several other factors which are involved in p53 activation upon ribosome biogenesis stress. The nucleolar factor, alternative reading frame protein (ARF) is such an example. The gene encoding ARF is located at the *INK4A* locus, which also encodes a cyclin-dependent kinase (CDK) inhibitor protein, p16 under alternative reading frame (Quelle et al. 1995; Sherr 2006). Under normal growth conditions, ARF is expressed at low levels and found in a complex with NPM in the nucleolus. The expression of ARF is typically upregulated by increased mitogenic signaling, which promotes excessive growth, therefore the elevation in the rate of ribosome biogenesis. Under these conditions, ARF is moved towards the nucleoplasm, where it can interact with the central acidic domain of Mdm2, at a site distinct from the 5S RNP binding site (Fig. 10) (Midgley et al. 2000; Korgaonkar et al. 2005; Sherr 2006; Sherr 2012). Similarly to Mdm2 binding by the 5S RNP, this interaction also promotes the stabilization and activation of p53 (Midgley et al. 2000; Sherr 2006; Sherr 2012). Additionally, ARF possesses several p53-independent effector functions to inhibit ribosome biogenesis. For instance, this protein directly suppresses Pol I-mediated transcription, by counteracting the phosphorylation of UBF, and the nucleolar import of TTF-1 (Ayrault et al. 2006; Lessard et al. 2010). Furthermore, ARF also constrains the activity of DDX5, an RNA helicase involved in both rRNA transcription and maturation (Saporita et al. 2011). By exerting an inhibitory effect on multiple levels of ribosome biogenesis, thus strongly inhibiting ribosome biosynthesis, ARF also promotes the

emergence of the 5S RNP mediated canonical ribosome biogenesis stress pathway (Bursac et al. 2014).

The nucleolar protein NPM is involved in the regulation of ARF. Most studies suggest that by interacting with ARF, NPM protects it from being degraded and also sequesters ARF to the nucleolus, preventing its interaction with Mdm2 in the nucleoplasm under normal conditions (Kuo et al. 2004; Korgaonkar et al. 2005). Surprisingly, one study demonstrated that NPM is also capable of interacting with Mdm2, thereby promoting the activation of p53 (Kurki et al. 2004). However, the involvement of NPM in the regulation of p53 is rather context-dependent, as it can either promote or inhibit both the activation and the effector functions of p53 (Lim and Wang 2006; Colombo et al. 2011; Box et al. 2016).

Another nucleolar factor, nucleostemin (NS) has been suggested to be required for p53 activation under certain conditions (Dai et al. 2008). The expression of NS is high in stem and cancer cells; however in normal differentiated cells its level is decreased (Tsai and McKay 2002). When overexpressed, NS also interacts with the central acidic domain of Mdm2, disrupts its complex with p53, thus promotes the stabilization and activation of p53 (Fig. 10) (Dai et al. 2008). While this mechanism has been clearly demonstrated under artificial conditions, the involvement of NS in p53 regulation under physiological conditions remains to be elucidated.

Besides RPL5 and RPL11, there are several RPs which can contribute to the activation of p53 through different mechanisms. For instance, under certain stress conditions (e.g. genotoxic stress) RPL26 can bind to the 5' and 3' UTR regions of the p53 mRNA, thereby stabilizing it and promoting its translation (Takagi et al. 2005; Ofir-Rosenfeld et al. 2008). Furthermore, RPS15, RPS20 and RPL37 have been reported to downregulate the level of MdmX, which then promotes the degradation of Mdm2, thus the stabilization and activation of p53 (Daftuar et al. 2013).

It is now generally accepted that the activation of p53 is promoted predominantly by the canonical 5S RNP/Mdm2/p53 pathway when ribosome biogenesis is perturbed. Although these and maybe more, yet undiscovered alternative processes exist which might have a rather fine-tuning effect on p53 activation, under specialized circumstances.

#### *p53-independent ribosome biogenesis stress response*

Recently, several studies have been reported that ribosome biogenesis stress response can also be activated in the absence of p53. Cells which have defective p53 expression are still capable of inducing cell cycle arrest in response to ribosome

biogenesis perturbing conditions. This p53-independent cell cycle arrest can occur through several mechanisms. Donati *et al.* have reported that in cells lacking p53 RPL11 is responsible for inducing cell cycle arrest, by promoting the degradation of E2F-1 when ribosome biogenesis is impaired (Donati et al. 2011b). E2F-1 is a transcription factor involved in cell cycle progression, and it is often found upregulated in cancer cells (Crosby and Almasan 2014). Mechanistically, E2F-1 forms a complex with Mdm2, and this interaction protects it for proteasomal degradation (Zhang et al. 2005b). However, impaired ribosome biogenesis promotes the association of RPL11 with Mdm2, which in turn releases E2F-1 from the complex. As a result, E2F-1 is degraded, and cell cycle progression is inhibited in a p53 independent manner (Donati et al. 2011b).

Additionally, RPL11 has also been shown to counteract mitogenic signaling induced upregulation of ribosome biogenesis, independently of p53. As described earlier, the elevated expression of the oncogene c-Myc increases the rate of ribosome biogenesis at multiple levels: it upregulates both rRNA and RP synthesis (van Riggelen et al. 2010). Therefore, as other RPs, RPL11 is in excess amount upon c-Myc activation. Consequently, when overexpressed, RPL11 is capable of binding to both the oncoprotein cMyc and its mRNA, leading to the degradation of c-Myc (Dai et al. 2007). Thus, RPL11 is involved in an autoregulatory negative feedback loop, which serves as a p53-independent protection against increased ribosome biogenesis in response to mitogenic stress.

Besides RPL11, another RP has been suggested to be required for the induction of p53-independent ribosome biogenesis stress checkpoint. Russo *et al.* have noted that RPL3, when overexpressed, can promote the expression of p21 (Russo et al. 2013). p21 is one of the main transcriptional targets of p53, and as being a CDK inhibitor, it can trigger cell cycle arrest (Abbas and Dutta 2009; El-Deiry 2016). In this case, RPL3, in complex with other factors accumulates at the promoter of p21 and activates its expression, independently of p53 (Russo et al. 2013). Although this study is based on the artificial overexpression of RPL3, which might not represent physiological conditions in the cells, upregulation of RP synthesis is often seen in response to mitogenic signaling. Although, since most RPs are degraded rapidly by the proteasome when not consumed in ribosome biogenesis until the physiological upregulation of RPL3 has been unambiguously shown, the validity of such a model remains questionable.

In addition to RPs, another, somewhat surprising factor has also been presented to be involved in p53-independent cell cycle arrest upon impaired ribosome biogenesis. The

proto-oncogene serine/threonine-protein kinase 1 (PIM1) has been reported to have such a function. Under normal conditions, PIM1 binds to the SSU through its interaction with RPS19 (Chiocchetti et al. 2005). Moreover, PIM1 is also responsible for the phosphorylation of a cell cycle inhibitor, p27<sup>Kip1</sup>. By this PTM, p27<sup>Kip1</sup> is marked for further ubiquitylation and proteasomal degradation (Larrea et al. 2009). However, impaired ribosome biogenesis causes the proteasomal degradation of PIM1 through an unknown mechanism, which in turn stabilizes p27<sup>Kip1</sup>, followed by a p27<sup>Kip1</sup>-dependent cell cycle arrest (Iadevaia et al. 2010).

Ribosome biogenesis stress pathways, which operate independently of p53 gained prominent attention throughout the past couple of years. Because the knowledge withdrawn from these studies is extremely relevant for the clinics, especially in cancer therapy (see chapter 1.3.4.), understanding details of these processes or discovering similar pathways are central issues in this research field.

### 1.3.3. Impaired Ribosome Biogenesis Checkpoint and the associated diseases

#### *Impaired Ribosome Biogenesis Checkpoint*

Ribosome biogenesis is consuming most of the cells' energy, therefore it is interconnected with all signaling pathways in the cell. Mitogenic or stress signals all affect this process and are capable of causing ribosome biogenesis stress, as it was described earlier. Deficiency of the components and factors of ribosome biogenesis or direct inhibition of the process elicit a strong response in terms of ribosome biosynthesis perturbation and activation of p53-dependent and -independent stress responses. Recently, this subtype of ribosome biogenesis stress response was named Impaired Ribosome Biogenesis Checkpoint (IRBC) (Gentilella et al. 2017). The earliest observation of IRBC originates from a study performed by Volarevic *et al.* These authors reported that the conditional knockout of *RPS6* leads to cell cycle arrest in mouse liver cells (Volarević et al. 2000). In the past two decades, a myriad of studies has reported that disruption of ribosome biogenesis at virtually any level can activate the canonical 5S RNP/Mdm2/p53 pathway, followed by cell cycle arrest, apoptosis or senescence.

Perturbation of the Pol I mediated rRNA synthesis by depletion of the PIC components (Rubbi and Milner 2003; Yuan et al. 2005; Donati et al. 2011a) or by chemical inhibition of rRNA transcription (Rubbi and Milner 2003; Peltonen et al. 2010; Bywater et al. 2012; Holmberg Olausson et al. 2012; Peltonen et al. 2014); impaired rRNA processing by decreased expression of maturation factors (Takagi et al. 2005;

Angelov et al. 2006; Qin et al. 2011; Carrillo et al. 2014; Watanabe-Susaki et al. 2014); impaired subunit assembly by deficient RPs (Jin et al. 2004; Barkic et al. 2009; Fumagalli et al. 2009; Lindström and Nistér 2010; Llanos and Serrano 2010; Sun et al. 2010; Dutt et al. 2011; Bursac et al. 2012; Fumagalli et al. 2012; Daftuar et al. 2013; Zhou et al. 2013); impaired nuclear import of the RPs and impaired nuclear export of the ribosomal subunits by depleted  $\beta$ -kariopherins (Golomb et al. 2012) all result in the strong activation of p53 mediated mainly by the 5S RNP complex (Fig. 11).

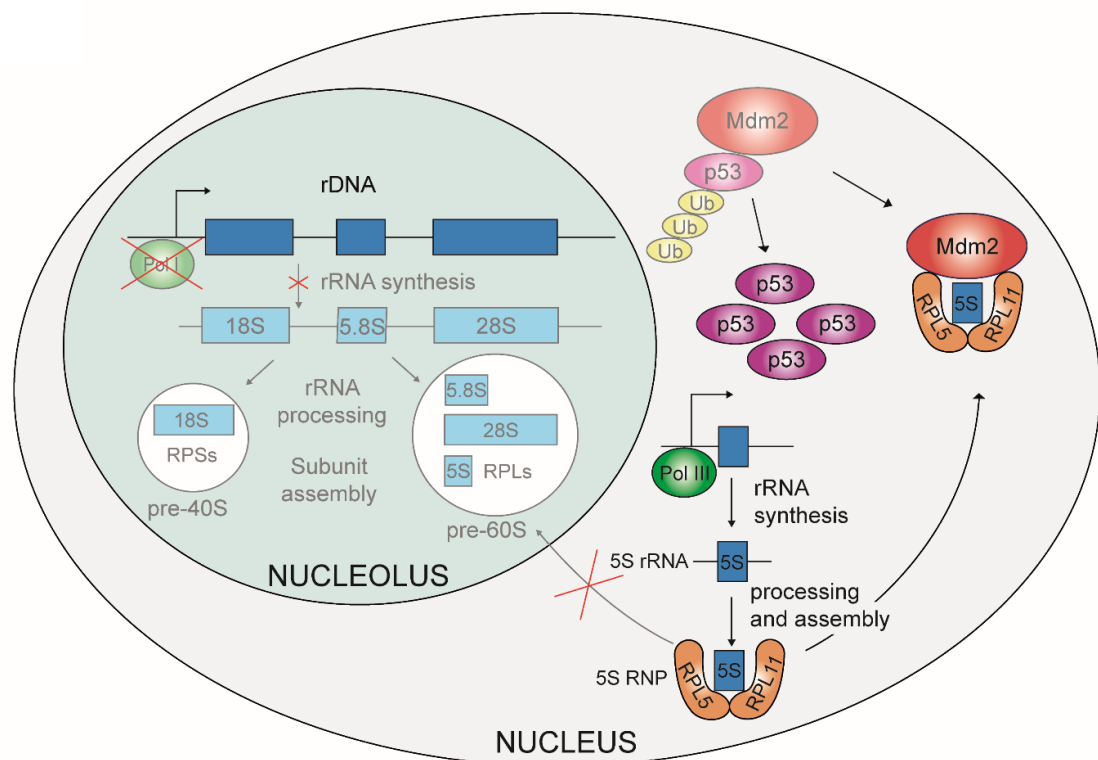


**Figure 11. The activation of the IRBC response in response to perturbation of the rRNA synthesis.** Impaired 47S pre-rRNA synthesis results in the stabilization and activation of p53 that initiates cell cycle arrest, apoptosis or senescence.

### *Ribosomopathies*

IRBC is clinically well-represented by a group of diseases, called ribosomopathies. Ribosomopathies are characterized by natural mutations in RP or ribosome biogenesis factor genes (Table 1; Fig 12). Since cells rely on ribosome biogenesis for their growth and proliferation, one could easily imagine that complete abrogation of this fundamental process is incompatible with life. However, the mutations associated with ribosomopathies rather affect the availability of mutated proteins that cause a decrease in the rate of ribosome biogenesis. Thus, such conditions lead to growth

arrest, due to the insufficient translation and/or the continuous activation of the IRBC pathway. Although the impairment of such ubiquitous process would suggest a global effect on the affected individual, symptoms of patients suffering from ribosomopathies are tissue-specific. Although the affected tissue also varies among the different ribosomopathy conditions, several standard features can be characterized, i.e. hematological defects, short stature and predisposition to cancer (Narla and Ebert 2010; Armistead and Triggs-Raine 2014; Nakhoul et al. 2014; Danilova and Gazda 2015). Tremendous effort was made to discover what causes the tissue-specific phenotypes of these disorders at the molecular level. It is generally accepted that these specific phenotypes featuring each disease add up from the combined effect of insufficient translation, constant activation of p53 due to activated IRBC and impaired extra-ribosomal function of the deficient factor (Armistead and Triggs-Raine 2014). Ribosomopathies include rare genetic disorders, such as Treacher-Collins syndrome, Dyskeratosis congenita, Diamond-Blackfan anemia, 5q- syndrome, Shwachman-Diamond syndrome and other even less frequent syndromes (Table 1).

**Table 1. Ribosomopathies**

<b><i>Ribosomopathy</i></b>	<b><i>Inheritance</i></b>	<b><i>Main clinical symptoms</i></b>	<b><i>Affected gene(s)</i></b>	<b><i>Role in ribosome biogenesis</i></b>
<i>5q- syndrome</i>	somatically acquired	macrocytic anemia, AML	<i>RPS14</i>	SSU biogenesis
<i>Bowen-Conradi syndrome</i>	autosomal recessive	prenatal growth delay, craniofacial, limb, kidney, brain, heart abnormalities	<i>EMG1</i>	SSU biogenesis
<i>Cartilage hair hypoplasia</i>	autosomal recessive	skeletal abnormalities, hypoplastic anemia, immunodeficiency, cancer	<i>RMRP</i>	rRNA maturation
<i>Diamond-Blackfan anemia</i>	autosomal dominant	craniofacial, limb, cardiac, urogenital abnormalities, cancer	<i>RPS19, RPL5, RPL11, RPL15, RPL36, RPL35A, RPS7, RPS10, RPS17, RPS24, RPS26, RPS27A</i>	SSU/LSU biogenesis
<i>Dyskeratosis congenita</i>	X-linked/autosomal dominant/autosomal recessive	mucocutaneous abnormalities, immunodeficiency, growth retardation, neurological	<i>DKC1, TERC, TERT, NHP2, NOP10</i>	rRNA maturation

<i>Isolated congenital asplenia</i>	abnormalities, pulmonary fibrosis			
	cancer			
	autosomal dominant	asplenia, primary immunodeficiency	<i>RPSA</i>	SSU biogenesis
<i>North American Childhood cirrhosis</i>	autosomal recessive	neonatal jaundice, biliary cirrhosis	<i>UTP4</i>	rRNA synthesis and early processing
<i>Shwachman-Diamond syndrome</i>	autosomal recessive	pancreatic insufficiency, gastrointestinal, skeletal, immune system abnormalities, AML	<i>SBDS</i>	LSU biogenesis, ribosome assembly
<i>Treacher-Collins syndrome</i>	autosomal dominant/	craniofacial abnormalities	<i>TCOF1</i>	rRNA synthesis and early processing
	autosomal recessive		<i>POLR1C</i> <i>POLR1D</i>	

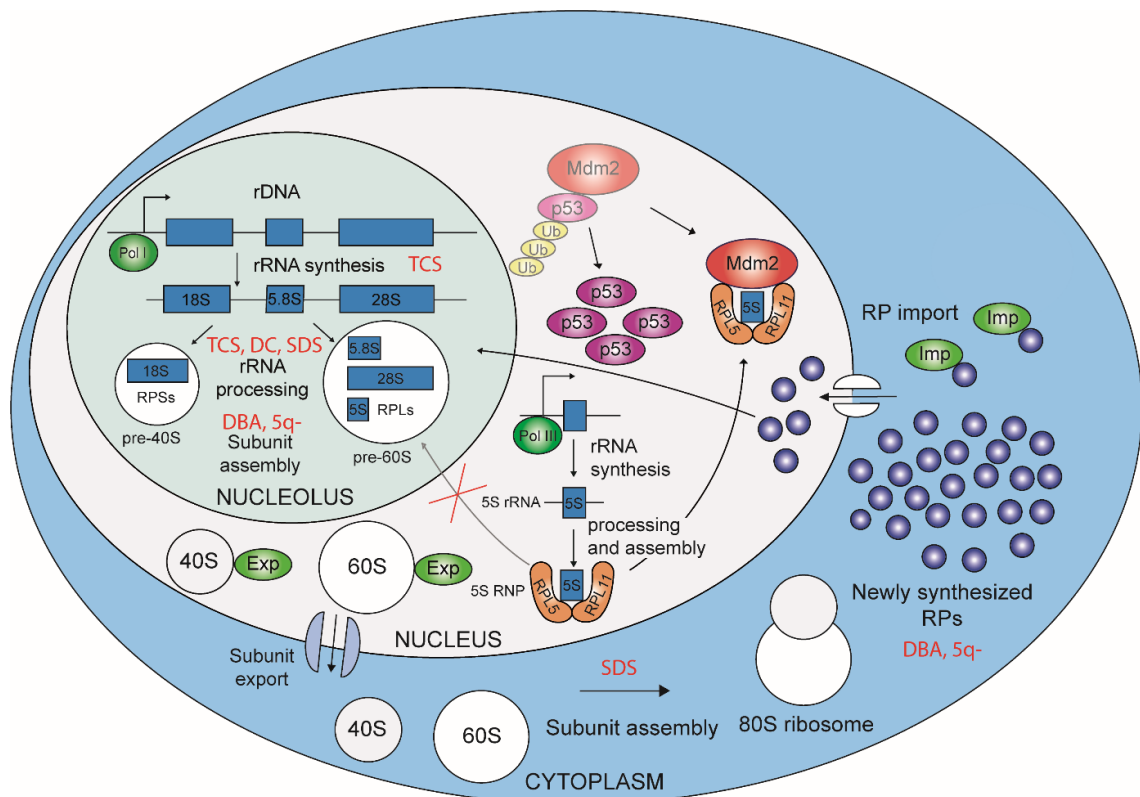


**Figure 12. Human ribosomopathies impair ribosome biogenesis at diverse steps.** TCS: Treacher-Collins syndrome, DC: Dyskeratosis congenita, SDS: Shwachman-Diamond syndrome, DBA: Diamond-Blackfan anemia, 5q-: 5q- syndrome.

Treacher-Collins syndrome (TCS) is a severe craniofacial disorder, inherited mainly in an autosomal dominant fashion., TCS is most frequently associated with mutations in the *TCOF1* gene, which encodes a protein named Treacle. Treacle has involvement in rRNA transcription and early pre-rRNA processing steps (Fig 12) (Valdez et al. 2004; Gonzales et al. 2005; Kadakia et al. 2014). In a minor group (ca. 8%) of TCS patients mutations occur in the *POLR1C* and *POLR1D* genes that encode RPAC1 and RPAC2 proteins, respectively. Both proteins are subunit components of Pol I and Pol III complexes (Kadakia et al. 2014; Ahmed et al. 2016). Mutations in the *TCOF1* gene lead to haploinsufficiency of Treacle, which impairs ribosome biogenesis, followed by the activation of the IRBC pathway. As a consequence, p53 is stabilized, and it mediates apoptosis, specifically in neural crest cells during early embryogenesis (Dixon et al. 2006; Sakai and Trainor 2009). This population of stem cells are responsible for the formation of most of the bone, connective, cartilage and peripheral neuron tissues of the head (Graham et al. 1996). In TCS extensive apoptosis of neural crest cells causes the severe craniofacial abnormalities, including underdevelopment of the lower jaw and the zygomatic bone, external ear deformities, eye problems due to the drooping of the eyelids or absence of the eyelashes, dental and nasal abnormalities (Chang and Steinbacher 2012; Posnick 2014). TCS is an excellent example of IRBC activation and pathological effects of constitutively active p53. Mouse TCS models are further promoting the importance of p53 in the development of this disease. Treacle haploinsufficient mice display similar craniofacial abnormalities, which phenotype could be easily reversed by chemical inhibition or genetic inactivation of p53 (Jones et al. 2008). Although in neural crest cells abnormal activation of p53 seems to mediate the pathological effects, it remains mostly unknown why other cells are not affected by these mutations. Some suggest that Treacle may have several extra-ribosomal functions which could be more critical in the affected cell type (Sakai et al. 2012). Indeed, Treacle has been presented to be required for mitotic progression (Sakai et al. 2012), translational regulation (Werner et al. 2015) and DNA damage signaling (see chapter 1.4.1.) (Ciccia et al. 2014; Larsen et al. 2014; Sakai et al. 2016). Most importantly, the function of Treacle in DNA damage response has emerged as a reasonable explanation for the tissue-specific penetrance of this disease. Specifically, it has been reported that neuroepithelial cells exhibit a higher level of reactive oxygen species (ROS), compared to other cell types (Sakai et al. 2016). ROS are potent inducers of DNA damage (Jena 2012; Cadet and Wagner 2013); thus proficient DNA damage response, mediated by Treacle, may be extremely crucial in neuroepithelial cells (Sakai



et al. 2016). Additionally, a recent study proposed that another protein, namely DDX21 is responsible for the tissue-specific pathology of TCS (Calo et al. 2018). DDX21 is an RNA helicase, required for rRNA synthesis and processing; furthermore it is also involved in the Pol II-mediated transcription of RP genes (Calo et al. 2014). It has been noted that Treacle ablation or suppression of rRNA transcription induces the redistribution of DDX21, as it relocates from the nucleolus and chromatin fraction to the nucleoplasm, resulting in the inhibition of ribosome biogenesis. Importantly, this redistribution occurs in cranial neural crest cells, but not in other cell types. Thus, the authors suggest that Treacle haploinsufficiency induces faulty rRNA transcription, rDNA damage, p53 activation and DDX21 redistribution as a consequence that results in apoptosis in neural crest cells, which are hypersensitive to the increased level of p53 (Calo et al. 2018). Although precise mechanism through which DDX21 may mediate the pathology of TCS is still missing, recent developments in this field may hold a great promise for therapy of TCS patients.

Dyskeratosis congenita (DC) is another disease, traditionally called ribosomopathy and usually diagnosed by a classical triad of mucocutaneous symptoms: hyper- or hypopigmentation of the skin, nail dystrophy and leukoplakia of the oral mucosa. Additionally, patients might also show a variety of the following symptoms: telangiectasia, alopecia or premature greying of the hair, neurological abnormalities, cancer predisposition and pulmonary fibrosis. Most commonly the cause of death is bone marrow failure (Kirwan and Dokal 2008; Wilson et al. 2014). DC is caused mainly by mutations in the *DKC1* gene. *DKC1* is located on the X chromosome and encodes dyskerin protein, which is a component of the box H/ACA snoRNP. As box H/ACA snoRNP is required for the pseudouridylation of the pre-rRNA, mutations of *DKC1* have been suggested to impair ribosome biogenesis (Fig. 12; Table 1) (Angrisani et al. 2014). However, in addition to its function in rRNA maturation, as a part of the telomerase complex, dyskerin is also involved in the maintenance of telomeres (Kirwan and Dokal 2008; Angrisani et al. 2014). Indeed, patients suffering from DC show accelerated telomere shortening which is more pronounced in the rapidly dividing stem and progenitor cell populations, explaining the majority of the symptoms and affected tissues in this disease (Angrisani et al. 2014). Furthermore, instead of disrupting the catalytic activity or the expression level of dyskerin, mutations occurring in the *DKC1* gene rather impair the RNA binding domain of the protein, which associates with the telomerase complex, through an interaction with the telomerase RNA component (TERC) (Kirwan

and Dokal 2008; Mason and Bessler 2011). Moreover, a minority of DC patients show mutations in the telomerase reverse transcriptase (TERT) and TERC encoding genes, in these cases, DC is inherited in an autosomal dominant manner (Table 1) (Kirwan and Dokal 2008; Angrisani et al. 2014; Fok et al. 2017). Additionally, in several cases, other telomerase components have been observed to carry the mutation causing the pathology of DC, which are inherited in an autosomal recessive fashion (Table 1) (Walne et al. 2007; Vulliamy et al. 2008). All these pieces of evidence show that symptoms of DC arise instead from the dysfunction of the telomerase complex and not from impaired ribosome biogenesis. However, it has also been reported that in the X-linked form of DC (X-DC), when dyskerin is mutated, pseudouridylation of the rRNA is also affected. This impaired rRNA maturation causes qualitative alterations in translation, which might promote tumorigenesis, contributing to the cancer susceptibility seen in X-DC patients (see chapter 1.3.4.) (Yoon et al. 2006; Bellodi et al. 2010). The activation of p53 can be also observed in cells derived from DC patients; however it seems to be rather a consequence of telomere dysfunction than activated IRBC (Carrillo et al. 2014; Fok et al. 2017). Thus, although it might contribute to the complex pathogenesis of the disease, ribosome biogenesis stress is presumably not the primary cause of DC.

Diamond-Blackfan anemia (DBA) and 5q- syndrome are classic examples of ribosomopathies, as both of these diseases are characterized by mutations of the RP genes (Table 1; Fig. 12) (Nakhoul et al. 2014). DBA is a bone marrow failure syndrome inherited in an autosomal dominant fashion. Symptoms of DBA patients also include macrocytic anemia, short stature, craniofacial, limb and urogenital abnormalities and cardiac defects (Lipton and Ellis 2009; Wilson et al. 2014). In nearly half of the cases, DBA is caused by mutations in small or large subunit RP genes, while the genetic background in the other half remains mostly unknown. The known DBA causing mutations occur in the following RP genes: *RPS19*, *RPL5*, *RPL11*, *RPL15*, *RPL36*, *RPL35A*, *RPS7*, *RPS10*, *RPS17*, *RPS24*, *RPS26* and *RPS27A*, however, the mutation of *RPS19* is most commonly observed. These mutations cause haploinsufficiency of RP proteins, which lead to both activation of IRBC and insufficient translation (Table 1) (Narla and Ebert 2010; Ellis and Gleizes 2011). Consequently, increased apoptosis of the erythroid progenitor cells can be observed in the bone marrow of DBA patients, causing severe anemia (Ellis 2014; Danilova and Gazda 2015). However, the exact mechanism that leads to impaired erythropoiesis is a matter of debate. Reduced expression of RPs is known to induce IRBC and p53-mediated apoptosis that could explain increased

apoptosis of erythroid progenitors (Lipton and Ellis 2009; Narla and Ebert 2010; Dutt et al. 2011). Indeed, activation of p53 has been observed in bone marrow samples derived from DBA patients (Dutt et al. 2011). However, several reports suggest that RP haploinsufficiency also reduces the rate of global translation that might be crucial for erythroid progenitors, which express hemoglobin at a lower level in this case. Consequently, the amount of free heme is increased that leads to oxidative stress, which induces p53-independent apoptosis in these cells (Chiabrando and Tolosano 2010; Narla and Ebert 2010; Ellis 2014). This theory also provides an appealing explanation for the tissue-specific cell death observed in DBA, although the involvement of IRBC in the pathology of the disease cannot be entirely excluded. Furthermore, it is also worth to mention that many RPs also possess extra-ribosomal function, which could also be affected, when expressed at a lower level, therefore could contribute to the pathological appearance of DBA (Warner and McIntosh 2009; Zhou et al. 2015). For instance, haploinsufficiency of RPL5 and RPL11, the primary mediators of IRBC, are known to cause a more severe form of the disease, as phenotypes like cleft palate/cleft lip and thumb malformations can be seen only when these proteins are mutated (Gazda et al. 2008).

5q- syndrome is a somatically acquired condition, characterized by the deletion of the long arm of chromosome 5. Patients suffering from the 5q- syndrome show macrocytic anemia and predisposition to acute myeloid leukemia (AML) due to impaired erythropoiesis (Padron et al. 2011; Pellagatti and Boulwood 2015). Among the ca. 40 genes encoded by the lost chromosomal fragment, *RPS14* seems to be the most important for the pathology of this disease (Table 1; Fig. 12) (Padron et al. 2011; Pellagatti and Boulwood 2015). Supporting this theory, haploinsufficiency of RPS14 in mouse models is capable of inducing the same phenotype, observed in 5q- patients (Barlow et al. 2010). Furthermore, activation of p53 as a consequence of IRBC can be detected in both the mouse models and in cells derived from 5q- patients (Barlow et al. 2010; Pellagatti et al. 2010). Thus, active IRBC and p53-dependent apoptosis have been suggested to mediate impaired erythropoiesis (Armistead and Triggs-Raine 2014; Nakhoul et al. 2014), however, similarly to DBA, oxidative stress induced by heme overload cannot be excluded as a positive contributor to 5q- syndrome.

Shwachman-Diamond syndrome (SDS) is another ribosomopathy, inherited in an autosomal recessive manner (Table 1). SDS is also characterized as a bone marrow failure syndrome, and additional symptoms of SDS include mainly: exocrine pancreatic insufficiency, gastrointestinal, skeletal and immune system abnormalities with

susceptibility to AML (Burroughs et al. 2009; Nakhoul et al. 2014; Nelson and Myers 2018). Majority of the SDS patients carry biallelic mutations of the *SBDS* gene, which encodes a protein presumably involved in multiple steps of ribosome biogenesis. *SBDS* has been reported to participate in the final assembly of the ribosomal subunits during translation initiation, by promoting the EFL1-mediated removal of eIF6 from the LSU (Fig. 12) (Finch et al. 2011; Wong et al. 2011; Burwick et al. 2012). Furthermore, several studies have suggested that *SBDS* might also be involved in rRNA maturation, due to its localization to the nucleolus and interactions with NPM and the 28S rRNA (Fig. 12) (Austin et al. 2005; Ganapathi et al. 2007). Activation of IRBC has been suggested to be the primary cause of this disease, supported by upregulation of p53 observed in cells derived from SDS patients (Dror 2002; Elghetany and Alter 2002). However, less is known about the mechanism, through which *SBDS* mutations affect only specific tissues. Thus, similarly to other ribosomopathies, the molecular background of SDS needs to be further evaluated to understand better the role and contribution of ribosome biogenesis and IRBC to these and other related diseases, such as cancer (see chapter 1.3.4.).

#### 1.3.4. Ribosome biogenesis and cancer

Altered nucleolar structure can be seen in many human diseases, and it usually reflects altered ribosome biogenesis. For instance, the increased size and/or number of the nucleoli are recognized as traits of many tumor types (Zink et al. 2004). It is widely accepted that upregulation of ribosome biogenesis drives the excessive growth and proliferation of cancer cells, which are gaining a competitive advantage over normal cells as a result (Orsolich et al. 2016). Proto-oncogenic mitogen signaling pathways, such as MAPK/ERK and PI3K/AKT/mTOR signaling cascades, upregulate ribosome biogenesis on the level of rRNA synthesis, affecting mainly the Pol I transcription machinery. Furthermore, c-Myc promotes ribosome biogenesis on multiple levels: it triggers PIC formation and rRNA synthesis; and increases the synthesis of RPs and factors involved in diverse steps of ribosome biogenesis (see chapter 1.2.) (Felton-Edkins et al. 2003; Hannan et al. 2003; Zhao et al. 2003; Mayer et al. 2004; Gomez-Roman et al. 2006; Stefanovsky et al. 2006; Stefanovsky and Moss 2008; Woiwode et al. 2008; Grummt 2010; Kantidakis et al. 2010; van Riggelen et al. 2010; Hannan et al. 2011).

Although in the majority of the cases upregulation of rRNA synthesis in cancer is achieved through positive regulation of the Pol I transcription machinery, many tumors show altered epigenetic features of the rDNA as well. These alterations include the

decrease of the CpG methylation of rDNA promoters and the increased amount of euchromatin histone modifications of rRNA genes (Qu et al. 1999; Powell et al. 2002; Ghoshal et al. 2004). These epigenetic alterations promote rRNA synthesis, as well as induce changes in the extra-nucleolar chromatin structure, leading to genome instability (Guettg et al. 2010; Orsolich et al. 2016).

Recent studies suggest that upregulation of ribosome biogenesis is a crucial step in the tumorigenic program, thus instead of being a passive consequence it rather promotes the initiation and progression of tumors (Yoon et al. 2006; Barna et al. 2008; Belin et al. 2009; Bywater et al. 2012). For instance, in their pioneer study Barna *et al.* have used a transgenic mouse model that is overexpressing c-Myc (E $\mu$ -Myc mice), which make these animals prone to develop B-cell lymphomas. However, when intercrossed with mice heterozygous for *RPL24* and showing haploinsufficiency of this protein, the onset of B-cell lymphoma was delayed. The authors have suggested that this outcome was the consequence of normalized translation, decreased growth rate and re-established genome stability (Barna et al. 2008). Although the results of this study indeed suggest that upregulation of ribosome biogenesis is an essential step in tumorigenesis, several other factors might also contribute to this process. First, *RPL24* haploinsufficiency might lead to the activation of p53 via the IRBC pathway, which is resulting in growth arrest. Therefore, increased ribosome biogenesis might only constrain the activation of p53. On the other hand, *RPL24*-deficient ribosomes might not promote the translation of specific mRNAs, which are required for excessive growth following c-Myc upregulation (Orsolich et al. 2016).

Nonetheless, more and more studies report that not only the upregulation in the rate of ribosome biogenesis but also the selective overexpression of diverse factors in ribosome biogenesis may have tumorigenic potential. For instance, the expression of the key rRNA processing factor, box C/D snoRNP component FBL has been shown to be upregulated in some malignancies (Choi et al. 2007; Belin et al. 2009; Koh et al. 2011; Su et al. 2013). Overexpression of FBL changes the 2'-*O*-methylation pattern of the rRNA, and as a consequence, structurally altered ribosomes can be formed that severely affect the quality of translation. These non-conventional ribosomes have been termed as 'cancer ribosomes' by Marcel *et al.*, who have also demonstrated that the overexpression of FBL leads to alterations in the internal ribosome entry site (IRES)-dependent translation of several mRNAs (Marcel et al. 2013). Importantly, upregulation of the IRES-dependent translation of proto-oncogenic mRNAs, such as IGF1R, MYC, FGF1/2 and

VEGFA (Marcel et al. 2013); and downregulation of the IRES-dependent translation of p53 (Belin et al. 2009) occur under these conditions. Collectively, this differential translation caused by FBL overexpression and thus altered 2-*O*-methylation of rRNA seems to contribute to tumorigenesis.

Similarly to FBL, overexpression of other rRNA processing factors have been observed in cancer. For instance, the box H/ACA snoRNP component dyskerin has been shown to be upregulated in several tumor types (Sieron et al. 2009; Liu et al. 2012a). Dyskerin governs pseudouridylation of rRNA, thus analogously to FBL upregulation, dyskerin overexpression might also lead to the formation of structurally altered ‘cancer ribosomes’, by changing the pseudouridylation pattern of rRNA. However, such data has not been reported to date.

Upregulation of NCL and NPM multifunctional ribosome biogenesis factors have also been reported in many cancers (Tsui et al. 2004; Leotoing et al. 2008; Coutinho-Camillo et al. 2010; Pianta et al. 2010; Liu et al. 2012b; Kalra and Bapat 2013; Wong et al. 2013; Kim et al. 2014; Sekhar et al. 2014; Zhou et al. 2014; Holmberg Olausson et al. 2015; Jia et al. 2017). Their tumorigenic potential is commonly associated with their positive impact on ribosome biogenesis, however since both factors are involved in several extra-ribosomal cellular processes (Tajrishi et al. 2011; Abdelmohsen and Gorospe 2012; Box et al. 2016; Jia et al. 2017), other effects might add up to induce tumor transformation in NCL or NPM overexpressing cells.

Furthermore, selective overexpression of RPs has also been observed to promote tumor progression in some cancers (Shi et al. 2004; Guo et al. 2011; Du et al. 2014; Sulima et al. 2017). Theoretically, the excess amount of an RP leads to a change in the stoichiometry of RPs, which might result in the formation of structurally altered ribosomes, which again promote proto-oncogenic mRNA translation or suppress tumor suppressor mRNA translation. An example of such selective upregulation of RPs has been reported in gastric cancer. In this case, selective upregulation of RPS13 and RPL23 have been shown to contribute to the multidrug resistance of these cells (Shi et al. 2004). However, it is also worth to mention that RPs have also been reported to possess several extra-ribosomal functions (Warner and McIntosh 2009; Zhou et al. 2015), which might also contribute to tumorigenesis and/or tumor progression.

The main consequence of upregulated ribosome biogenesis is the upregulation of global protein synthesis. The higher rate of translation increases the number of proteins in the cells and might also result in the decrease of translation fidelity, that leads to the

appearance of damaged or misfolded proteins (Conn and Qian 2013; Galbiati et al. 2017; Sulima et al. 2017). Furthermore, selective upregulation of several ribosome biogenesis factors or RPs may also alter the physiological balance of proteins, proteostasis in cells. Collectively, these pathological changes in global protein homeostasis are termed as proteotoxic stress and often occur in cancer cells (Bastola et al. 2018; Madden et al. 2019). Consequently, abundant and/or damaged proteins accumulate in the endoplasmic reticulum (ER), which in turn initiates the unfolded protein response (UPR). UPR aims to restore proteostasis, by enhancing protein folding processes, proteasomal degradation of misfolded and damaged proteins and slowing down translation (Moon et al. 2018; Madden et al. 2019). Upregulated UPR provides an advantage for cancer cells to avoid proteotoxic stress but still obtain a high proliferation rate (Bastola et al. 2018; Madden et al. 2019). Proteasomes are essential elements of the UPR pathway; therefore in various malignancies, the primary therapeutic approach includes proteasome inhibition (Bastola et al. 2018; Moon et al. 2018). We have recently discovered that a commercially available drug, called Antabuse, has a similar mechanism of action and it could be beneficial for cancer therapy. Antabuse is an alcohol-aversion drug, which has been used to treat alcoholism for decades. The active compound of Antabuse is disulfiram, the main metabolite of which is a ditiocarb-copper complex (CuET) that has potent anti-tumor effects (Skrott et al. 2017). CuET inhibits the activity of the p97/VCP segregase, which is involved in the removal of membrane-embedded ubiquitylated proteins for further proteasomal degradation, thereby contributing to UPR and maintenance of global proteostasis (Skrott et al. 2017; van den Boom and Meyer 2018). CuET binds to and immobilizes NPL4 protein, which is an important cofactor of p97. By this mechanism, CuET treatment leads to the accumulation of polyubiquitylated proteins in the cells, which cannot be degraded and form insoluble protein aggregates. Consequently, cell death is induced. Furthermore, cancer cells seem to be hypersensitive for CuET treatment, and CuET also seems to preferentially accumulate in cancer cells of mouse xenograft models (Skrott et al. 2017). This pre-clinical study is encouraging and promotes the initiation of clinical trials based on CuET treatment. Since there is a direct connection between intensive ribosome biogenesis, a higher rate of translation and UPR in cancer cells, the indication of upregulated ribosome biosynthesis, such as altered nucleolar structure, could be a useful marker for the successful treatment with CuET in cancer therapy.

Targeting the upregulated ribosome biogenesis directly is also an emerging approach in cancer therapy. Small molecule inhibitors of rRNA synthesis have been proved to have very potent anti-cancer effects. Such a promising compound, called CX-5461, exerts its inhibitory effect on rRNA transcription through the suppression of SL1 recruitment to rDNA promoters (Drygin et al. 2011). Additionally, CX-5461 has also been shown to induce DNA damage via the stabilization of four-stranded DNA structures, so-called G-quadruplexes (Xu et al. 2017). Importantly, CX-5461 has been reported to preferentially target cancer cells, leading to apoptosis, senescence or autophagy, whereas normal cells remain mostly unaffected by this drug (Drygin et al. 2011; Bywater et al. 2012). These encouraging results show the potential of targeting ribosome biogenesis in cancer therapy. Consequently, CX-5461 is now being tested in phase I clinical trials (<https://www.anzctr.org.au/Trial/Registration/TrialReview.aspx?id=364713>; <https://ClinicalTrials.gov/show/NCT02719977>). ActD is another rRNA synthesis inhibitor, which is being used for the therapy of multiple cancers (Sikora et al. 1999; Kroon et al. 2014; Bhavana et al. 2017). ActD is a DNA intercalator, and it preferentially intercalates into the DNA at guanosine-cytosine (GC) rich regions, which are enriched in rDNA genes. This, in turn, inhibits the progression of the Pol I transcription machinery, however at higher concentration it also suppresses RNA synthesis by Pol II or Pol III. As a result, ActD interferes with many processes in the cells and exerts its cytotoxic effects in cancer as well as in normal cells. Consequently, severe adverse effects can be observed in patients treated with ActD (Chun et al. 2007; Burger et al. 2010; Hernandez-Verdun et al. 2010). Another newly identified drug, BMH-21 is also a DNA intercalating compound, which, similarly to ActD, intercalates into GC-rich rDNA genes. In addition to its inhibitory effect on rRNA synthesis, it also promotes proteasomal degradation of Pol I (Peltonen et al. 2010; Peltonen et al. 2014). This additional effect of BMH-21 on Pol I degradation might increase its specificity towards rRNA synthesis inhibition, thus could improve cancer therapy when compared to ActD treatment. Clinical trials with BMH-21 have not been initiated to date.

Small molecules, which are targeting other selectively upregulated ribosome biogenesis factors might be also beneficial for cancer therapy. For instance, an aptameric compound AS1411 interferes with NCL's RNA binding activity, thus inhibits its function in ribosome biogenesis (Soundararajan et al. 2008; Bates et al. 2009). This compound has been tested in phase I/II clinical trials, where its therapeutic potential has been presented



(Laber et al. 2004; Laber et al. 2006; Stuart et al. 2009; Rosenberg et al. 2014). Another promising compound is NSC348884, which by binding to NPM induces cytotoxicity in several cancers (Qi et al. 2008; Balusu et al. 2011; Zhang et al. 2012).

The high cytotoxic efficiency of these ribosome biogenesis inhibitors in cancer cells is mainly explained by their effect to induce IRBC. As most cancer cells have upregulated ribosome biogenesis and rely on this process for their growth and proliferation, impairment of this process strikes these cells and induces a more robust activation of p53, when compared to normal non-transformed cells. Consequently, this therapeutic approach is selective enough to be extremely beneficial for cancer treatment. Furthermore, although half of the human cancers gain diverse p53 mutations, which render p53 ineffective in tumor suppression, drug-induced IRBC can promote several p53-independent pathways leading to growth arrest and/or cell death (see chapter 1.3.2) (Bursac et al. 2014; James et al. 2014; Orsolich et al. 2016). Selective cancer targeting and promotion of both p53-dependent and -independent IRBC have been reported for CX-5461 in pre-clinical studies. While CX-5461 induces p53-dependent apoptosis in E $\mu$ -Myc lymphoma cells (Bywater et al. 2012), it promotes p53-independent senescence and autophagy in solid tumor cell lines (Drygin et al. 2011). In both cases the cytotoxic effect of CX-5461 on normal primary cells is negligible (Drygin et al. 2011; Bywater et al. 2012). Although these examples show that targeting upregulated ribosome biogenesis is an advantageous approach in cancer therapy, it is also worth to mention, that other highly proliferative cells, such as stem cells have upregulated ribosome biosynthesis (Yang et al. 2011; Qu and Bishop 2012; Le Bouteiller et al. 2013; Watanabe-Susaki et al. 2014). Thus, the usage of these compounds must be considered cautiously, since it can lead to severe consequences in patients, emerging from stem cell depletion.

As the previous examples show, cancer cells often obtain upregulated ribosome biogenesis via various mechanisms, which is believed to be associated with their elevated growth potential. However, several recent studies have reported that the decreased rate of ribosome biosynthesis can also contribute to tumorigenesis (Bursac et al. 2014; Orsolich et al. 2016). The best examples are ribosomopathies where, despite the perturbation of ribosome biogenesis, the appearance of various types of tumors is relatively common (Narla and Ebert 2010; Armistead and Triggs-Raine 2014; Nakhoul et al. 2014; Danilova and Gazda 2015). There are several mechanisms through which a decreased rate of ribosome biogenesis is believed to promote tumorigenesis. For instance, the reduction in the rate of ribosome biogenesis results in the limited amount of available ribosomes,

which leads to a global drop in protein synthesis. Thus, translation of those mRNAs, which have a lower affinity towards the ribosomes is lost, due to competition with other high-affinity mRNAs. Since these low-affinity mRNAs usually encode tumor suppressor proteins, decreased ribosome biogenesis and thus the reduced number of ribosomes can be accounted for tumor progression (Lodish 1974; Ruggero 2013). Moreover, in ribosomopathies the decreased rate or defective components of ribosome biogenesis promote IRBC response, resulting in the activation of p53. Thus, there is a selection pressure for inactivating mutations of p53, and indeed, p53 is often found mutated in ribosomopathies, such as 5q- syndrome (Jädersten et al. 2011; Bursac et al. 2014).

Another mechanism by which impaired ribosome biogenesis can promote tumorigenesis is specifically characterized in DC. In addition to the pathological impact on telomere maintenance, mutations of *DKC1* also alter the pattern of rRNA pseudouridylation, which leads to several qualitative changes in the translation. Altered rRNA pseudouridylation, as well as altered rRNA methylation, due to FBL overexpression are hypothesized to lead to the formation of differential ‘cancer ribosomes’. In X-DC, mutations in the *DKC1* gene seem to alter the IRES-dependent translation of several mRNAs. Specifically, downregulation of IRES-dependent translation of p53 and p27 tumor suppressor and XIAP and BCL-X<sub>L</sub> anti-apoptotic proteins have been observed (Yoon et al. 2006; Bellodi et al. 2010).

Furthermore, similarly to the selective overexpression, selective downregulation of RPs, seen in DBA and 5q- diseases, can also alter the stoichiometry of RPs in the ribosome. As it was described earlier, this could result in the production of structurally altered ribosomes, which might promote tumorigenesis.

In conclusion, alterations, such as upregulation or impairment of ribosome biogenesis both have the potential to promote tumorigenesis; thus tight regulation of ribosome biogenesis is indispensable to avoid such pathological consequences.

#### 1.4. Extra-ribosomal functions of the nucleolus

According to the new, emerging concept, besides governing ribosome biogenesis, the nucleolus possesses several extra-ribosomal functions and is involved in various cellular processes. As a proteomic study revealed, more than 4500 proteins localize to the nucleolus and only a minority of these proteins (about 30%) are actively required for ribosome biogenesis (Ahmad et al. 2009). The rest of these nucleolar proteins are linked

to various unrelated cellular processes, such as cell cycle regulation, DNA damage signaling and repair, telomere maintenance, global gene expression, and others (Diesch et al. 2014; Orsolic et al. 2016). Furthermore, since the nucleolus is a membrane-less organelle, instead of having a stationary proteome, soluble proteins efficiently shuttle between the nucleolus and the nucleoplasm, mostly depending on the physiological state of the cell. Additionally, several ribosome biogenesis factors also have recognized extra-ribosomal functions (Yang et al. 2018). These observations indicate that the nucleolus is a multifunctional organelle.

#### 1.4.1. The nucleolus as the main stress sensor of the cells

Numerous external and internal stress stimuli have been shown to alter the protein composition of the nucleolus, also leading to alterations in the nucleolar morphology and/or impairment of ribosome biogenesis. Virtually any cell stressing conditions, including but not limited to: hypoxia, heat shock, DNA damage, nutrient starvation and nucleotide depletion are able to induce ribosome biogenesis stress, leading mainly to the activation of p53 (Fig. 8) (Boulon et al. 2010; Quin et al. 2014). In this manner, the nucleolus acts as a stress sensor, in response to various insults it shuts down the energy consuming process of ribosome biogenesis and initiates growth arrest to avoid further damage to the cells and re-sort the energy supplies to be used for repair mechanisms. The molecular mechanism by which the nucleolus senses stress stimuli differs among diverse stress insults and best characterized in the case of DNA damage.

##### *Ribosome biogenesis stress as a consequence of DNA damage*

Various forms of DNA damage may arise from endogenous or exogenous sources. For instance, ROS originating from cellular metabolism, or DNA mismatches as a result of faulty DNA replication are examples of the former and ionizing radiation (IR), and ultraviolet light (UV) are examples of the latter sources of DNA damage (Jackson and Bartek 2009). DNA damaging agents induce the formation of various DNA lesions, including DNA base damages, base mismatches, DNA helix distortions due to the incorporation of bulky adducts, DNA strand crosslinks, DNA strand breaks (Hoeijmakers 2001). The pathway responsible for DNA damage sensing and the following extensive signaling and DNA damage repair is termed DNA damage response (DDR) (Jackson and Bartek 2009; Ciccia and Elledge 2010). Besides facilitating the repair of DNA lesions, DDR also promotes cell cycle arrest, in order to avoid replication of damaged DNA, which would lead to the occurrence of mutations in the genome. Furthermore, in case of

severe, persistent and irreparable damage, DDR rather triggers apoptosis or senescence (Rich et al. 2000; Bartek et al. 2007). DNA damage signaling events are governed by two major kinases of the phosphatidylinositol 3-kinase-related kinase (PIKK) family, namely: ataxia telangiectasia mutated (ATM) and ataxia telangiectasia and Rad3-related protein (ATR) kinases. While ATM mainly responds to DNA double strand breaks (DSBs), ATR is activated following recognition of diverse DNA damage types (Marechal and Zou 2013). Once activated, these kinases phosphorylate hundreds of substrates, involved in DNA repair, cell cycle regulation, apoptosis and other cellular processes (Fig 13) (Matsuoka et al. 2007). The DDR kinases phosphorylate these substrates at specific sites composed of a serine or threonine, followed by glutamine residue (S/TQ site) (Kim et al. 1999; O'Neill et al. 2000; Matsuoka et al. 2007). Although ATM and ATR are involved in the signaling initiated by distinct DNA damage types, the two kinases phosphorylate almost the same subset of substrates and often trigger the activation of each other (Marechal and Zou 2013). One of the main target proteins of ATM and ATR is the tumor suppressor p53. In response to DNA damage, DDR kinases phosphorylate the serine 15 residue on p53 (pSer15-p53). This PTM, along with the phosphorylation of Mdm2 by ATM/ATR stimulates the dissociation of p53 and Mdm2, resulting in the stabilization and activation of p53, followed by the initiation of p53-dependent cell cycle arrest, apoptosis or senescence (Caspari 2000).

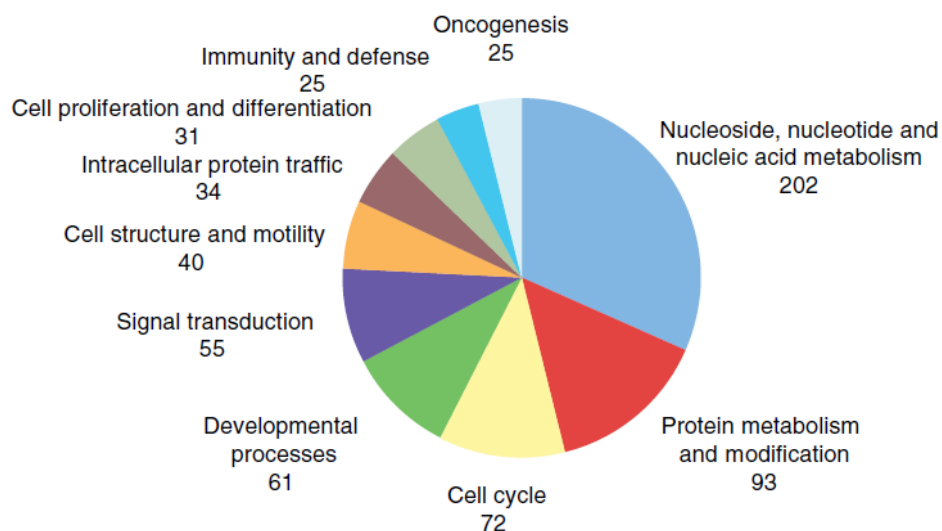


**Figure 13. Substrates of ATM/ATR are involved in numerous cellular processes.** By a proteomic screen numerous substrates of ATM/ATR could be identified and classified to several groups according to their cellular function (Adopted from Matsuoka et al., 2007).

In their pioneer study, Rubbi and Milner proposed that the nucleolus acts as a stress sensor in response to DNA damage, as stabilization and activation of p53 under these conditions only occur when the nucleolar structure is also disrupted (Rubbi and Milner 2003). This suggests that in case of severe DNA damage, the DDR signaling and/or DNA damage itself must reach the nucleolus, to induce its disruption. Consequently, ribosome biogenesis is also disrupted, which promotes activation of IRBC and the stabilization and activation of p53. Several research groups have demonstrated that the DDR signaling indeed reaches the nucleolus, however instead of inducing its disruption directly, it rather triggers the shutdown of rRNA synthesis, thereby triggering IRBC and p53 activation (Kruhlak et al. 2007; Larsen et al. 2014; Harding et al. 2015; van Sluis and McStay 2015). Kruhlak and colleagues were the first to report the connection between the nucleolus and DDR. The authors have used laser micro-irradiation to introduce DSBs in the nucleolar DNA and observed that rRNA transcription by Pol I was transiently inhibited. This rRNA transcription inhibition did not spread to the surrounding nucleoli, nor affected the rate of global transcription (Kruhlak et al. 2007). Kruhlak *et al.* also showed that this local inhibition of Pol I is mediated by the DDR kinase, ATM. Mechanistically, when DSBs are introduced in the rDNA, ATM in complex with two DDR adaptor proteins, Nijmegen breakage syndrome 1 (NBS1) and mediator of DNA damage checkpoint (MDC1) interferes with PIC formation and promotes the dissociation of the elongating Pol I (Fig. 14) (Kruhlak et al. 2007). DSBs in the rDNA induce the formation of nucleolar caps, where proteins involved in DDR and DNA repair are recruited and bind to rDNA (Harding et al. 2015; van Sluis and McStay 2015). Repression of rRNA transcription also occurs as a result of globally introduced DSBs. Severe DNA damage in the non-nucleolar chromatin triggers the transcriptional shutdown in all nucleoli of the cells and this global Pol I inhibition is also mediated by ATM. Larsen *et al.* reported that in this case an ATM-dependent accumulation of NBS1 on nucleolar chromatin is facilitated, where NBS1 forms a complex with the Treacle protein, which results in the inhibition of rRNA synthesis (Fig. 14) (Larsen et al. 2014). Surprisingly, ATM is also localized to the nucleoli under normal conditions, suggesting that it has a primary role in the protection of rDNA against damage (van Sluis and McStay 2015). Compared to non-nucleolar chromatin, due to the high transcription rate and its repetitive nature, rDNA is extremely fragile (Durkin and Glover 2007; McStay 2016), which might explain the basal localization of ATM to the nucleoli and its rapid response to rDNA damage. Furthermore, other nucleolar proteins may be targeted by ATM

(Matsuoka et al. 2007; Larsen and Stucki 2016). Additionally, while in the case of locally introduced DSBs DDR signaling inhibits Pol I to trigger a fast response of repair mechanisms in rDNA, in the case of globally introduced DSBs rRNA transcription repression rather serves as a signal to turn on IRBC, leading to p53-dependent cell cycle arrest. Similarly, other stress signaling pathways also converge on the inhibition of Pol I and or other nucleolar factors (Boulon et al. 2010), indicating a significant role for ribosome biogenesis in general stress response.

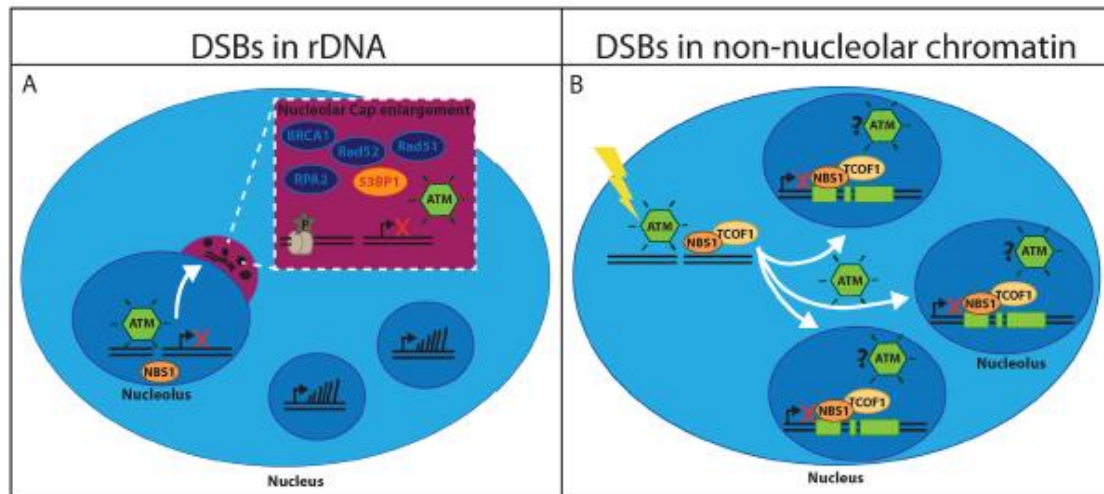


**Figure 14. rRNA transcription shutdown in response to DSBs.** A. DSBs induced in an individual rDNA promote local rRNA transcription shutdown. Furthermore, a nucleolar cap is formed which facilitates rapid DNA damage repair. B. DSBs formed in the non-nucleolar chromatin induce a global Pol I transcription shutdown (Adopted from Larsen and Stucki., 2016).

Further supporting the importance of the nucleolus in stress sensing, Burger et al. have recently reported that a subset of common chemotherapeutic drugs has a substantial effect on ribosome biogenesis. Alkylating agents, e.g. cisplatin and oxaliplatin; intercalating agents, e.g. doxorubicin and mitomycin C; and antimetabolites, e.g. methotrexate strongly impair rRNA synthesis, while other antimetabolites, e.g. 5-fluorouracil; topoisomerase inhibitors, e.g. camptothecin; kinase inhibitors, e.g. flavopiridol; and translation inhibitors, e.g. cycloheximide perturb early or late rRNA processing steps. Although these agents cause severe damage to the cells by inducing DNA damage or by impairing other prominent cellular pathways, their inhibitory effect on ribosome biogenesis also contributes to cytotoxicity (Burger et al. 2010). Targeting ribosome biogenesis has been shown to be beneficial in cancer therapy, as it promotes both p53-dependent and -independent responses. However, these chemotherapeutic compounds have other cytotoxic effects, which may be toxic for non-transformed cells,

as well. In contrast, drugs that solely target ribosome biogenesis could be more selective to cancer cells.

#### 1.4.2. The nucleolus in genome maintenance

There are several features of the rDNA genes, which render them extremely vulnerable to DNA damage, and thus genome instability. These characteristics include the highly repetitive nature and the elevated transcription rate of rDNA genes. On the one hand, the repetitive nature of rDNA genes promotes the occurrence of intra- and interchromosomal recombination, which might lead to gross chromosomal deletions or translocations. On the other hand, the high rate of rRNA transcription might either facilitate collisions between the transcriptional and replicational machineries, or inhibit replication by the appearance of R-loops (DNA:RNA hybrids) formed during transcription. Ultimately, both of these mechanisms trigger genome instability (Tsekrekou et al. 2017; Lindstrom et al. 2018).

Recent proteomic studies have reported that besides of ATM, numerous other DDR proteins and DNA repair components are also localized to the nucleolus (Ahmad et al. 2009; Ogawa and Baserga 2017). Under normal conditions, these proteins accumulate in a sub-nucleolar structure, called the intranucleolar body (INB) and are quickly re-localized into nucleolar caps, in case of nucleolar DNA damage (Fig. 14) (Hutten et al. 2011). Although these DDR and DNA repair factors do not seem to have a function in ribosome biogenesis, their nucleolar localization probably serves as a protection against rDNA damage, promoting a fast sensing, signaling and repairing system to avoid genome instability. Additionally, several nucleolar proteins which have a prominent function in ribosome biogenesis have been shown to be involved in DDR as well (Ogawa and Baserga 2017). For instance, NCL has been reported to accumulate at DNA damage sites, where it facilitates DNA repair (Kobayashi et al. 2012). Moreover, numerous ribosome biogenesis factors carry the S/TQ phosphorylation site and are phosphorylated by ATM and/or ATR DDR kinases following  $\gamma$ -irradiation, which assumes a novel role for these proteins, in genome maintenance processes (Matsuoka et al. 2007).

Besides being involved in DDR and DNA damage repair, the nucleolus presumably promotes genome maintenance through other mechanisms as well. For instance, it has critical importance in the regulation of cell cycle, telomere maintenance, chromatin and genome organization (Tsekrekou et al. 2017; Lindstrom et al. 2018; Yuan and Tong 2018). The key function of the nucleolus in extra-ribosomal processes might be

interconnected with its primary function in the synthesis of ribosomes. Since ribosome biogenesis is an energy consuming process, which is directly proportional to the rate of translation that drives growth and proliferation, it has a strong effect on genome stability. Accordingly, genome maintenance and ribosome biogenesis must operate in agreement and be tightly controlled to avoid pathological consequences. This may also provide an explanation, why the nucleolus governs numerous processes and behaves as a hub for a myriad of proteins.

### 1.5. HEATR1, a new player in ribosome biogenesis

The human HEAT repeat containing 1 (HEATR1) is a mostly uncharacterized protein. Although it has been suggested to play a role in ribosome biogenesis and other cellular pathways, its detailed function in these processes remains largely unknown. The yeast homolog of HEATR1, UTP10 is classified as a transcriptional U three protein (t-UTP) (Gallagher et al. 2004; Krogan et al. 2004; Dez et al. 2007). t-UTPs are components of the SSU processome and are amongst the earliest factors recruited to the 5' end of the nascent 47S pre-rRNA. These proteins are required for early 18S rRNA processing steps, which are occurring co-transcriptionally and seem to promote Pol I mediated transcription as well (Gallagher et al. 2004; Prieto and McStay 2007). Supporting their function in rRNA synthesis, t-UTPs form bead-like structures during active transcription and re-localize to nucleolar caps upon transcription inhibition and are strictly co-localized with Pol I transcription complex under both conditions (Prieto and McStay 2007). Due to their dual functions in both transcription and processing, it was suggested that t-UTPs might facilitate interactions between the Pol I transcription machinery and subsequent processing factors (Gallagher et al. 2004; Prieto and McStay 2007). In addition to the yeast UTP10, zebrafish BAP28 and *Trypanosoma brucei* UTP10 homologs of HEATR1 have also been identified in rRNA synthesis and/or early SSU processing (Azuma et al. 2006; Faktorová et al. 2018).

The human *HEATR1* gene is located at chromosome 1q43 and encodes a large (236 kDa) protein consisting of 2144 amino acids. This protein contains one HEAT repeat on its C-terminus (Fig 15) (<http://www.uniprot.org/uniprot/Q9H583>). HEAT repeats have been suggested to provide a platform for protein-protein interactions and can be found in numerous other proteins, such as huntingtin, elongation factor 3 or protein phosphatase 2A, ATM, ATR and mTOR (Perry and Kleckner 2003; Yoshimura and Hirano 2016).



Although the function of human HEATR1 remains largely uncharacterized, it has been implicated in cancer. One study has presented that HEATR1 is often overexpressed in glioblastomas and thus it may serve as an excellent target for cytotoxic T lymphocytes (Wu et al. 2014). Another research group has reported that the frequent downregulation of HEATR1 observed in pancreatic ductal adenocarcinomas (PDAC) accounts for reduced sensitivity towards gemcitabine chemotherapeutic drug. Mechanistically, HEATR1 promotes the dephosphorylation of AKT by acting as a scaffold and bringing AKT in close proximity with the inactivating protein phosphatase 2A (PP2A). Therefore, in the absence of HEATR1, the PI3K/AKT/mTOR pathway is upregulated, assuring resistance against gemcitabine treatment in PDAC cells. Furthermore, the authors of this study proposed that HEATR1 primary localized to the cytoplasm, where it can interact with AKT and PP2A (Liu et al. 2016).

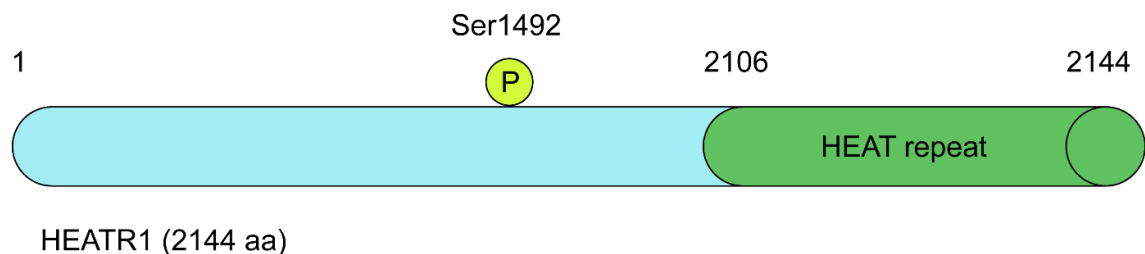


**Figure 15. The schematic structure of HEATR1 protein.** The HEATR1 protein consist of 2144 amino acids and contains a HEAT repeat domain at its C terminus. HEATR1 is phosphorylated by ATM/ATR, putatively on the Ser 1492 residue.

Several proteomic studies revealed that HEATR1 might also be a component of DDR signaling pathway. For instance, it seems to be recruited to the DNA damage site in response to UV irradiation (Chou et al. 2010). Additionally, HEATR1 might be a substrate of the ATM/ATR DDR kinases, and its putative phosphorylation site is located on the serine 1942 residue (Ser1492) (Fig 15) (Matsuoka et al. 2007).

In the following experimental part, we investigated the function of human HEATR1 in ribosome biogenesis.

## **2. AIMS OF THE THESIS**

1. Validating the role of a newly identified protein, HEATR1 in the stabilization and activation of p53.

2. Characterization of HEATR1 and elucidation of its function in ribosome biogenesis.

3. Elucidation of the possible involvement and function of HEATR1 in DDR.

### 3. MATERIAL AND METHODS

#### 3.1. Cell culture, treatments and generation of DSBs

All cell lines used in this study were cultured in Dulbecco's modified Eagle's medium (DMEM) (Table 2), supplemented with 10% fetal bovine serum (Life Technologies) and penicillin/streptomycin (Sigma-Aldrich) in a humidified atmosphere of 5% CO<sub>2</sub> at 37 °C. In the case of human primary fibroblasts (BJ and MRC-5 cells), DMEM was supplemented with 1% MEM Non-essential amino acids (Life Technologies).

**Table 2. The list of cell lines used in this study.** Cell lines were obtained from either ATCC or the collection of Danish Cancer Society

<i>Cell line</i>	<i>Origin</i>	<i>Growth mode</i>	<i>Cell culture media</i>
<i>BJ (ATCC)</i>	Human skin fibroblast	Adherent	DMEM
<i>HeLa (DCS)</i>	Human cervix carcinoma	Adherent	DMEM
<i>MRC-5 (ATCC)</i>	Human lung fibroblast	Adherent	DMEM
<i>U2OS (DCS)</i>	Human bone osteosarcoma	Adherent	DMEM

Treatments of the cells were done as indicated in the 'Results and discussion' section. Chemical compounds are listed in Table 3.

**Table 3. The list of chemical compounds used in this study.**

<i>Chemical compound</i>	<i>Used concentration</i>	<i>Treatment period</i>
<i>Cycloheximide (CHX, Sigma-Aldrich)</i>	50 µg/ml	0-2 hours
<i>Actinomycin D (ActD, Sigma-Aldrich)</i>	5 nM	O/N
<i>BMH-21 (Selleckchem)</i>	0.5 µM	3 hours

X-ray irradiation was carried out using the XYLON.SMART 160E/1.5 device (XYLON, Horsens, Denmark) at the following settings: 150 kV, 6 mA, 11mGy/s.

### 3.2. RNA interference

siRNA transfections were done using the Lipofectamin RNAiMAX (Invitrogen) transfection reagent, according to the manufacturer's instructions. All siRNA duplexes were purchased from Thermo Fisher Scientific, Ambion (Table 4).

**Table 4. The list of siRNAs used in this study.**

<i>siRNA</i>	<i>Sequence</i>
siCON (negative control, AM4635)	5'-AGUACUGCUUACGAUACGGTT-3'
siHEATR1#1 (s30230)	5'-CCACUUUCCAUUUGCGAUATT-3'
siHEATR1#2 (s30231)	5'-GAUGUUGUUUUGUCGGCUATT-3'
siHEATR1#3 (s30232)	5'-CACUUCCAUUUGCGAUAAATT-3'
sip53 (s605)	5'-GUAAUCUACUGGGACGGAATT-3'
siRPL5 (s56733)	5'-CAGUUCUCUCAAUACAUAATT-3'
siRPL11 (s12169)	5'-CAACUUCUCAGAUACUGGATT -3'

### 3.3. Cell cycle analysis.

Cells were fixed in 70% ice-cold ethanol and stained with propidium iodide for flow cytometric analysis. Fixed cells were analyzed on a FACS Verse instrument (BD Biosciences), and cell cycle distribution was measured using the FACSuite software (BD Biosciences).

### 3.4. Western blotting

Whole cell lysates were prepared in Laemmli sample buffer (LSB; 50 mM Tris, pH 6.8; 100 mM DTT, 2% SDS, 0.1% bromophenol blue, 10% glycerol). Cells from a confluent 60 mm Petri dish were lysed in 300  $\mu$ l LSB, followed by an incubation at 95 °C for 5 minutes with shaking at 1250 rpm. Whole-cell lysates were subsequently separated by SDS-PAGE, using 3-8% or 4-12% gradient, pre-cast electrophoresis gels (Thermo Fisher Scientific) and transferred to nitrocellulose membranes (GE Healthcare). The membranes were blocked in 5% (wt/vol) skim milk in 0.1% (vol/vol) Tween-20 in PBS and probed with the primary antibodies (see Table 5 for the dilutions of specific antibodies), followed by the HRP-labeled secondary antibodies (in 1:1000 dilution) GE

Healthcare), and visualized by ECL detection reagents (GE Healthcare) and the Chemidoc system. Band intensities were measured and quantified by the ImageJ system (<http://imagej.nih.gov/ij/>).

**Table 5. The list of antibodies used in this study.**

<b><i>Antibody</i></b>	<b><i>Origin</i></b>	<b><i>Clonality</i></b>	<b><i>Dilution</i></b>	<b><i>Method</i></b>
<i>β-actin</i> (Santa Cruz)	Mouse	Monoclonal	1:2000	Western blot
<i>Fibrillarin</i> (Abcam)	Rabbit	Polyclonal	1:500	Immunofluorescence
<i>HEATR1</i> (Sigma-Aldrich)	Rabbit	Polyclonal	1:250 1:50	Western blot Immunofluorescence
<i>Importin β (3E9)</i> (Abcam)	Mouse	Monoclonal	1:1000	Western blot
<i>MDM2 (2A10)</i> (Abcam)	Mouse	Monoclonal	1:500	Western blot
<i>Nucleolin</i> (Abcam)	Rabbit	Polyclonal	1:500 1:1000	Immunofluorescence Western blot
<i>Nucleophosmin</i> (FC82291) (Abcam)	Mouse	Monoclonal	1:500 1:1000	Immunofluorescence Western blot
<i>Nucleostemin</i> (Abcam)	Rabbit	Polyclonal	1:2000	Western blot
<i>p21 (12D1)</i> (Cell Signaling)	Rabbit	Monoclonal	1:500	Western blot
<i>p53 (DO-1)</i> (Santa Cruz)	Mouse	Monoclonal	1:250 1:500	Immunofluorescence Western blot
<i>phospho-Histone H2AX (pSer139)</i> (JBW301) (Millipore/Merck)	Mouse	Monoclonal	1:1000	Immunofluorescence

<i>phospho-Histone H2AX (pSer139) (EP854(2)Y) (Novus Biologicals)</i>	Rabbit	Monoclonal	1:500	Western blotting
<i>Phospho-(Ser/Thr) ATM/ATR substrate (Cell Signaling)</i>	Rabbit	Polyclonal	1:20	Immunoprecipitation
<i>RPA194 (C-1) (Santa Cruz)</i>	Mouse	Monoclonal	1:1000	Immunofluorescence
<i>RPL5 (Abcam)</i>	Rabbit	Polyclonal	1:2000 1 µg/mg of lysate	Western blot Immunoprecipitation
<i>SMC1</i>	Rabbit	Polyclonal	1:1000	Western blot

### 3.5. Immunofluorescence

Cells were grown on 12-mm coverslips and were fixed with 4% paraformaldehyde in phosphate buffered saline (PBS) for 15 minutes at 4 °C. Permeabilization was carried out with PBS containing 0.2% (vol/vol) Triton X-100 for 5 minutes at room temperature. The fixed cells were blocked in 5% (vol/vol) fetal bovine serum in PBS for 30 minutes, then incubated with primary antibodies (see Table 5 for the dilutions of specific antibodies) diluted in 5% (wt/vol) bovine serum albumin in PBS for 1 hour at room temperature. Coverslips were washed 3 times in PBS supplemented with 0.1% (vol/vol) Tween 20, once with PBS, then incubated with an appropriate secondary goat anti-rabbit or goat anti-mouse Alexa Fluor 488 or Alexa Fluor 568 conjugated (Invitrogen) secondary antibody (1:1000 dilution), diluted in 5% (wt/vol) bovine serum albumin in PBS for 1 hour at room temperature. Coverslips were washed 3 times in PBS supplemented with 0.1% (vol/vol) Tween 20, once with PBS, then mounted onto slides using the DAPI containing Vectashield mounting reagent (Vector Laboratories). Slides were visualized by the Axio Observer.Z1/Cell Observer Spinning Disc microscopic system (Yokogawa and Zeiss) equipped with an Evolve 512 Photometrix) EMCCD camera. Zeiss Plan Apochromat 100x/1.40 NA objective was used.

### 3.6. EdU and EU staining

Cells were grown on 12-mm coverslips and labelled either with 10  $\mu$ M EdU or with 1 mM EU (Sigma-Aldrich) for 30 minutes, then fixed with 4 % paraformaldehyde in PBS for 15 minutes and permeabilized with 0.2 % Triton X-100 for 5 minutes, followed by incubation with the staining solution (100 mM Tris-HCl, pH=8.5, 1 mM CuSO<sub>4</sub>, 1  $\mu$ M azide conjugated Alexa Fluor 488, 100 mM ascorbic acid) for 30 minutes. Coverslips were washed 3 times in PBS supplemented with 0.1% (vol/vol) Tween 20, once with PBS, then mounted onto slides using the DAPI containing Vectashield mounting reagent (Vector Laboratories). Image acquisition and analysis were performed using Scan R acquisition and analysis software (Olympus).

### 3.7. Immunoprecipitation

Cells on a confluent 100-mm Petri dish were washed 3 times in PBS and lysed in an ice-cold TNE buffer (150 mM NaCl, 50 mM Tris-HCl, pH 8.0, 1 mM EDTA, 0.5% NP-40) supplemented with cComplete and PhosSTOP tablets (Roche). Lysates were homogenized by a 20G needle and incubated on ice for 30 minutes, then cleared by centrifugation. Where appropriate, primary antibodies (see Table 5 for the dilutions of specific antibodies) were added to the supernatant of the lysate and incubated for 16 hours at 4°C. Lysates were then incubated with 25  $\mu$ l of Dynabeads M-280 Sheep anti-Rabbit IgG (Novex) for 1 hour at 4°C. IgG–antigen complexes were washed extensively, then eluted in 2 $\times$  LSB before SDS-PAGE.

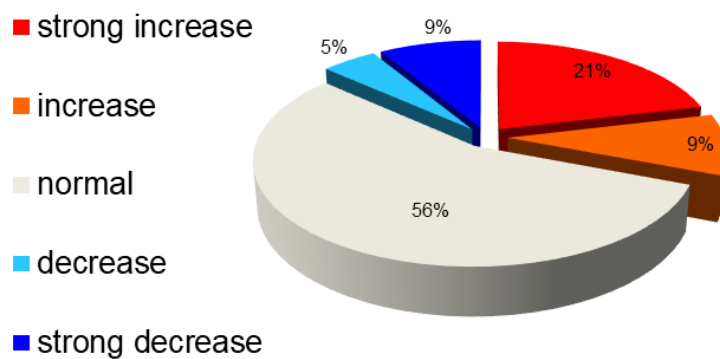
## 4. RESULTS AND DISCUSSION

### 4.1. Identification of HEATR1 in a high-resolution microscopy screen

To investigate the regulation of p53 stabilization and activation, a high content RNA interference (RNAi) screen was performed in our laboratory (Moudry et al., unpublished data). In this screen, 175 unique human genes were targeted, each with three independent siRNAs. A part of these genes was previously identified as ribosome biogenesis factors in yeast, while the other half of them was suggested to have a role in ribosome biosynthesis and related processes (Wild et al. 2010). Importantly, the RNAi screen was performed in the human osteosarcoma (U2OS) cell line, which is expressing wild-type p53. Following the genetic knockdown of these target genes, the activation of p53 was visualized by immunofluorescence.

The investigated genes were divided into five categories: inactivation of whose resulted in no changes in the level of p53 (normal); gene knockdowns that caused a decrease in p53 expression (decrease and strong decrease); and depletion of whose, which induced the increase of p53 (increase and strong increase). Among 21% of siRNAs, which strongly induced the expression of p53, we identified those that are targeting HEATR1 protein. Following HEATR1 depletion the fluorescence intensity of p53 increased from the normal range around 150 to 497, 498 and 410 for each siRNA targeting HEATR1 (Fig. 16).





	Color	P53 intensity	siRNA count	Percentage
strong increase	<span style="color: red;">■</span>	> 300	161	21,3%
increase	<span style="color: orange;">■</span>	299 - 250	72	9,5%
normal	<span style="color: lightgrey;">■</span>	249 - 110	422	55,7%
decrease	<span style="color: lightblue;">■</span>	109 - 80	36	4,8%
strong decrease	<span style="color: darkblue;">■</span>	79 - 0	66	8,7%

HEATR1 knockdown – p53 intensity: 497, 498, 410

**Figure 16. The expression level of p53 measured in the RNAi screen.** 175 unique genes were targeted, each by three independent siRNAs. Depletion of 56% of these genes did not alter, 5% and 9% of them decreased and strongly decreased the expression of p53, respectively. Impaired expression of 9% of the investigated genes led to the increase of p53 level, while 21% caused strong increase in the expression of p53. Depletion of HEATR1 led to the strong increase of p53 level, as the fluorescence intensities of p53 were 497, 498 and 410 in the case of the 3 siRNAs specific to HEATR1.

#### 4.2. Depletion of HEATR1 leads to the stabilization of p53 and initiates p53-dependent cell cycle arrest

To validate our observation from the RNAi screen that HEATR1 depletion leads to an elevated level of p53, we transfected U2OS cells with the three independent siRNAs against HEATR1. All three siRNAs led to a reduction in the endogenous level of HEATR1 to the same extent, while they indeed increased the expression of p53 and its transcriptional target, p21 (Fig. 17A). Furthermore, to reduce potential off-target effects of the individual siRNAs (Jackson et al. 2003), we used a pool of these siRNAs in this (Fig 17A) and all following experiments. Depletion of HEATR1 was also efficient in diploid human fibroblast (BJ) cells, where, similarly to U2OS impaired HEATR1 expression led to the increased expression of both p53 and p21 (Fig. 17B).

Increased expression of p53 is usually achieved by the stabilization of the protein through several mechanisms (see chapter 1.3.1.). To confirm that p53 stabilization occurs when HEATR1 is depleted, we inhibited global protein synthesis by applying cycloheximide (CHX) to U2OS cells, to investigate protein turnover of p53. Indeed, the half-life of p53 increased in HEATR1-depleted cells from about 1 hour to nearly 2 hours (Fig. 17C), suggesting that protein stabilization is contributing to the increased expression of p53 in the absence of HEATR1.

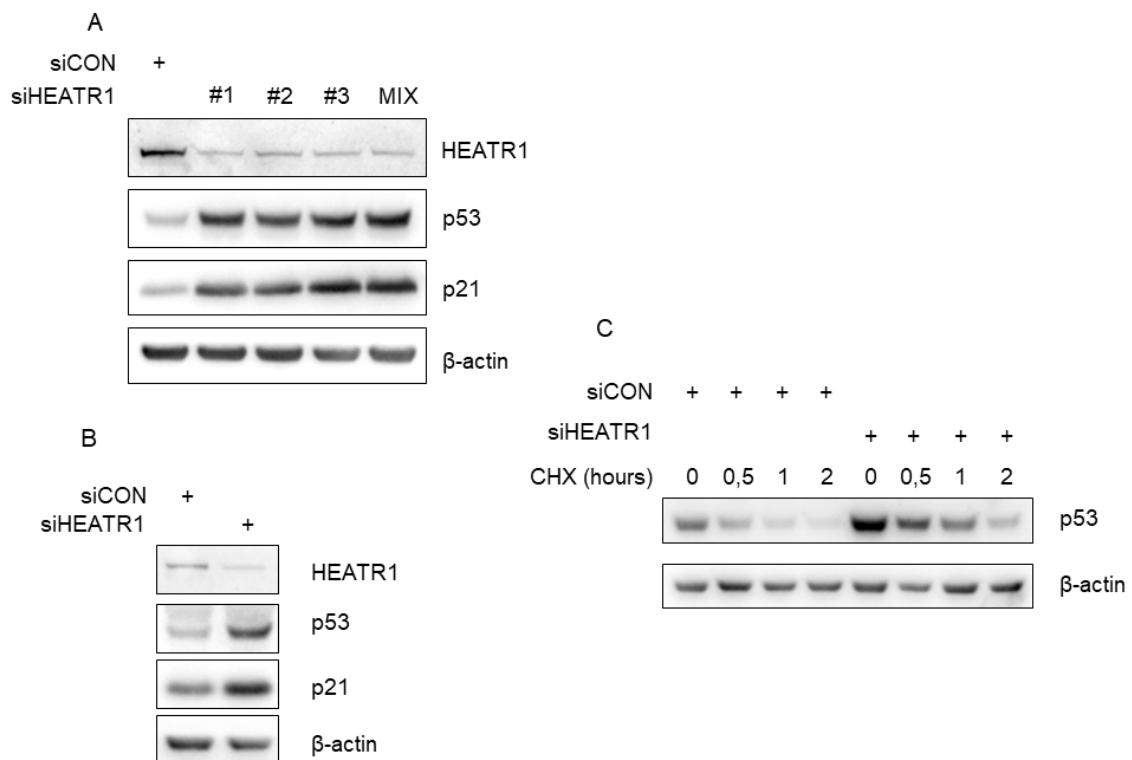


**Figure 17. Depletion of HEATR1 leads to the stabilization of p53.** A. U2OS cells were transfected with control and HEATR1 siRNAs and 72 hours later whole cell lysates were prepared and immunoblotted with the indicated antibodies. B. BJ cells were transfected with control and HEATR1 siRNAs and 72 hours after the transfection whole cell lysates were prepared and immunoblotted with the indicated antibodies. C. U2OS cells were transfected with control and HEATR1 siRNAs and treated with 50 µg/ml cycloheximide (CHX) 72 hours after transfection. Whole cell lysates were prepared at indicated time points and immunoblotted with p53 and β-actin antibodies.

Next, we wondered whether stabilization of p53 following HEATR1 depletion has an observable effect on the cells. In order to obtain more information about the cell cycle progression of control *versus* HEATR1 deficient cells, we first studied the proliferation rate of these cells. Total cell counts, assessed at 2, 4 and 6 days after siRNA transfection showed that decreased expression of HEATR1 impairs proliferation in U2OS cells (Fig.

18A). Furthermore, a similar impairment of the proliferation rate could be seen in the case of HEATR1 depleted BJ cells, indicating that the observed proliferation arrest was not cell-type restricted (Fig. 18B).

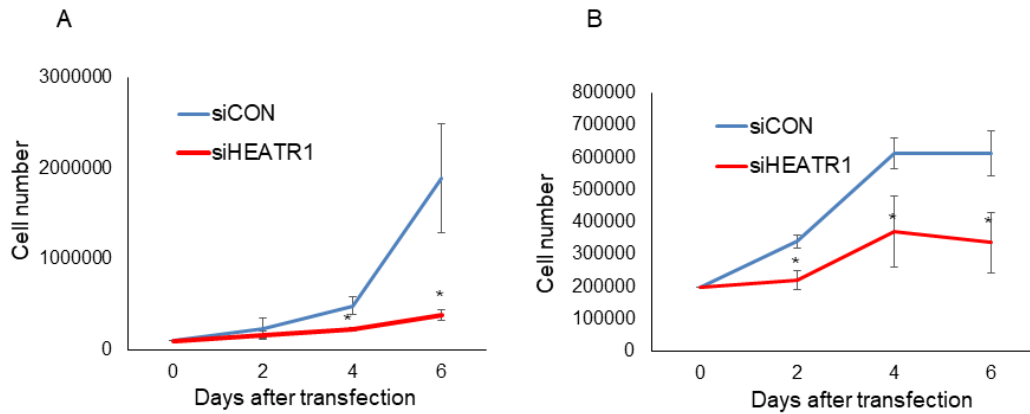


**Figure 18. Deficiency of HEATR1 leads to growth and/or proliferation arrest.** A. U2OS cells were transfected with control and HEATR1 siRNAs and 100000 cells were seeded. Cell number was determined 2, 4 and 6 days after transfection. Error bars indicate standard deviations (SDs), n=3. Significance was determined by a two-tailed student test: \* p<0.05. B. BJ cells were transfected with control and HEATR1 siRNAs and 200000 cells were seeded. Cell number was determined 2, 4 and 6 days after transfection. Error bars indicate SDs, n=3. Significance was determined by a two-tailed student test: \* p<0.05.

In further experiments, we compared the cell cycle profile of control *versus* HEATR1 deficient cells. U2OS cells transfected with a control siRNA showed a normal cell cycle profile, where a larger cell population (42% of the cells) was in G1 phase, while 38% of the cells progressed through S phase and 20% of them were in G2 phase (Fig. 19A). HEATR1 ablation largely altered the standard cell cycle profile, since the amount of cell in S phase was reduced to 19%, while the subpopulation of cells in G1 was increased to 59% (Fig. 19A). To investigate whether this cell cycle arrest seen in HEATR1 depleted cells is mediated by p53, we performed co-depletion of HEATR1 and p53. Interestingly, the cell cycle progression of HEATR1 and p53-deficient cells was restored entirely (Fig 19A). It is also worth to mention that RNAi-mediated depletion of p53 alone did not induce any significant changes in the cell cycle profile (Fig. 20A). In contrast to U2OS cells, in human cervical carcinoma (HeLa) cell line, which has a defective p53 expression, the ablation of HEATR1 did not result in cell cycle arrest or the alteration of the cell cycle profile (Fig. 19B).

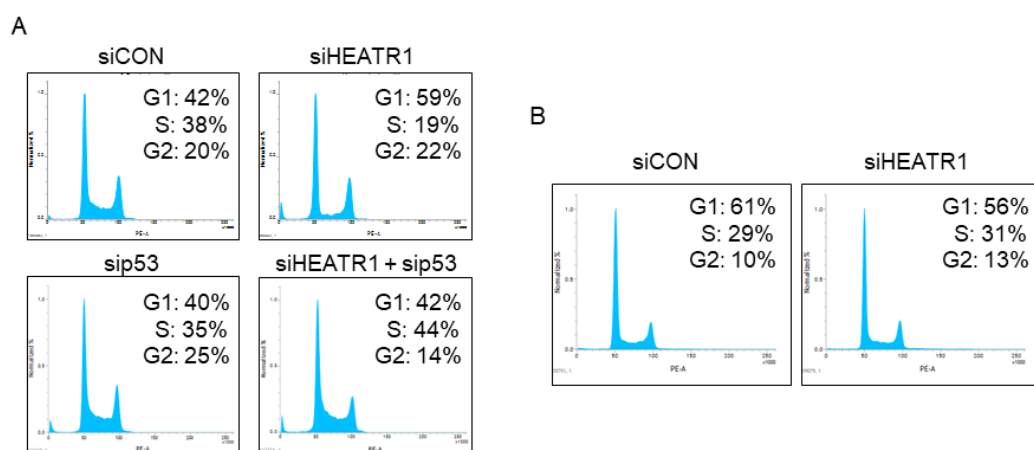


**Figure 19. Ablation of HEATR1 alters the cell cycle profile.** A. U2OS cells were transfected with the indicated siRNAs and 72 hours after the transfection cell cycle profiles were obtained by flow cytometry. Cell cycle profiles are representative of three independent experiments. B. HeLa cells were transfected with control or HEATR1 siRNAs. The cell cycle profiles were assessed by flow cytometry 72 hours after the transfection. Results are representative of three independent experiments.

To provide more evidence on the impairment of proliferation and cell cycle progression in HEATR1 deficient cells, we performed a 5-ethynyl-2'-deoxyuridine (EdU) incorporation assay, to follow the replicating population of control and HEATR1 depleted cells. The nucleotide analog EdU incorporates into the newly synthesized DNA strand and with a simple click chemistry EdU can be visualized by fluorescence (see Material and methods). Indeed, the subpopulation of replicating cells was reduced from 54% to 26% in the case of HEATR1 depleted cells (Fig. 20A). Importantly, similarly to the cell cycle profile, the reduced rate of replication measured by EdU incorporation could be rescued by the concomitant depletion of HEATR1 and p53 (Fig. 20A). Moreover, we also confirmed that RNAi-mediated knockdown of p53 efficiently reduced the endogenous level of the protein, without affecting HEATR1 protein abundance (Fig. 20B).

In conclusion, we confirmed our observations from the RNAi screen that impaired expression of HEATR1 results in the elevated expression of the tumor suppressor protein, p53. Following HEATR1 silencing, p53 seems to be stabilized on the protein level and activated, documented by the increased expression of its transcriptional target, p21. Furthermore, HEATR1 depletion resulted in prominent proliferation and cell cycle arrest in the G1 phase. Importantly, this cell cycle arrest could be reversed by concomitant depletion of p53, indicating that the observed proliferation and cell cycle arrest is mediated by p53. Additionally, we show here that activation of p53 and impaired

proliferation due to HEATR1 depletion are not restricted to one cell type, as these phenomena could be observed in both U2OS and BJ cell lines. Notably, we could not observe cell cycle arrest in HeLa cells following HEATR1 knockdown. However, in the human papilloma virus (HPV) positive HeLa cells the expression of p53 is completely abrogated by the HPV-encoded E6 oncoprotein (Scheffner et al. 1990; Werness et al. 1990). Thus, the absence of p53 could be accounted for failed cell cycle arrest in HeLa cells, which is further supporting the central role of p53 in proliferation and cell cycle arrest following HEATR1 depletion.

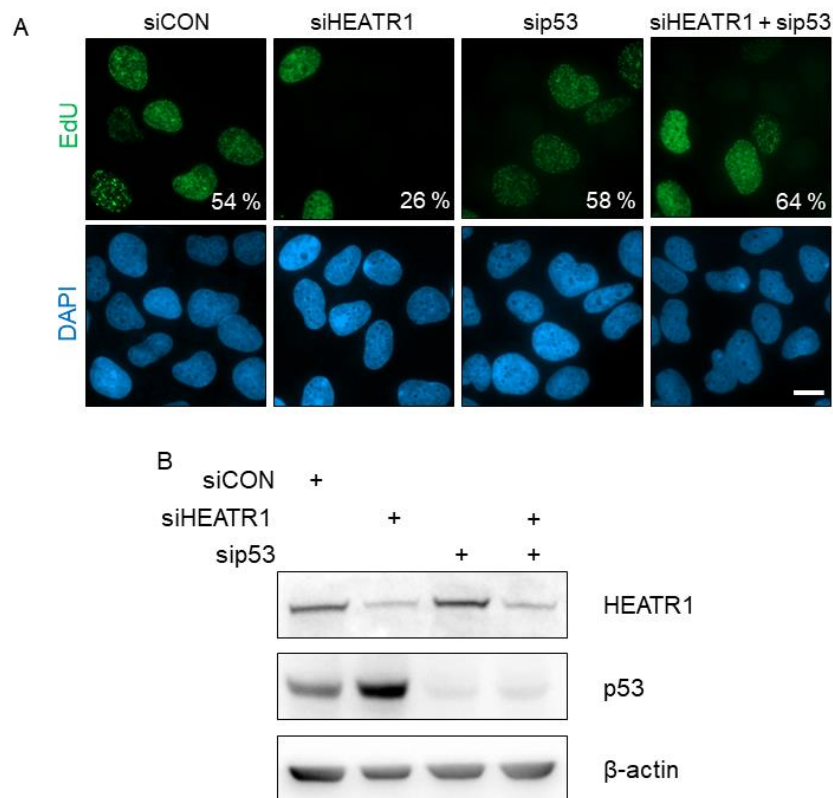


**Figure 20. Depletion of HEATR1 reduces the amount of replicating cells.** A. U2OS cells were transfected with the indicated siRNAs and 72 hours later cells were labeled with 10  $\mu$ M 5-ethynyl-2'-deoxyuridine (EdU) for 30 minutes. Cells were fixed on coverslips, EdU was visualized by click chemistry and nuclei were visualized by DAPI staining. Results are representatives of three independent experiments. Bar, 10  $\mu$ m. B. U2OS cells were transfected with the indicated siRNAs and 72 hours after transfection whole cell lysates were prepared and immunoblotted with HEATR1, p53 and  $\beta$ -actin antibodies.

#### 4.3. HEATR1 is localized into the nucleolus

HEATR1 protein homologs in diverse species, such as yeast UTP10 (Dez et al. 2007) and *Trypanosoma brucei* TbUTP10 (Faktorová et al. 2018) have been described as

nucleolar proteins, whereas Zebrafish BAP28 has also been suggested to reside in the nucleolus (Azuma et al. 2006). Although human HEATR1 was also shown to localize to the nucleolus (Prieto and McStay 2007), one recent study described HEATR1 as a cytoplasmic protein (Liu et al. 2016). The authors identified HEATR1 as a member of PI3K/AKT/mTOR signaling, being responsible for the deactivation of AKT by binding both AKT and its phosphatase enzyme PP2A (Liu et al. 2016) (see chapter 1.5). Apparently, the interaction of the three proteins must occur in the cytoplasm, where AKT and PP2A are predominantly located to. Indeed, Liu and colleagues also suggested that HEATR1 is rather a cytoplasmic protein and its localization is required for its interactions with AKT and PP2A (Liu et al. 2016).

In order to reveal the subcellular localization of HEATR1 in our cultured human cells, we applied immunostaining of endogenous HEATR1. According to our immunofluorescence experiments, HEATR1 was localized almost exclusively in the nucleus, where it was rather accumulated in nucleolar regions in U2OS cells (Fig. 21A). Similar localization of HEATR1 was observed in primary human fibroblast cells BJ and MRC-5 (Fig. 21A). Importantly, the nucleolar areas were validated by co-immunofluorescence of NPM and DAPI staining for all three cell lines (Fig. 21A). However, in the case of the two fibroblast cell lines, endogenous HEATR1 could also be visualized in the cytoplasmic fraction, indicating that HEATR1 might be present there, as well (Fig. 21A). Furthermore, to test the specificity of this immunofluorescence signal we depleted HEATR1 and then performed its immunostaining. In both U2OS and BJ cells knockdown of HEATR1 abolished the nucleolar signal of HEATR1, while left the weak nucleoplasmic and cytoplasmic background fluorescence signal unchanged (Fig. 21B and Fig. 21C).

From these results, we can conclude that HEATR1 is predominantly a nucleolar protein. Although a weaker fluorescence signal could be observed in the nucleus as well as in the cytoplasm following the immunostaining of HEATR1, silencing of the protein only abolished the nucleolar fluorescence signal. This indicates that HEATR1 resides mainly in the nucleolus and the weak nuclear and cytoplasmic fluorescent signal may be the result of unspecific binding of the antibody used against HEATR1. Furthermore, in four diverse cell lines we tested HEATR1 was localized to the nucleoli, further supporting our theory of HEATR1 being a nucleolar protein. Though, it is important to mention that we cannot exclude the possibility of differential localization of HEATR1 in other cell types, such as pancreatic cancer cells, used by Liu *et al.* Surprisingly, opposing our

results, Liu *et al.* have showed that HEATR1 resides mainly in the cytoplasm and is almost entirely excluded from the nucleus. However, since this study does not present the validation of the antibodies used to assess the localization of HEATR1, the cytoplasmic localization of HEATR1 remains debatable.

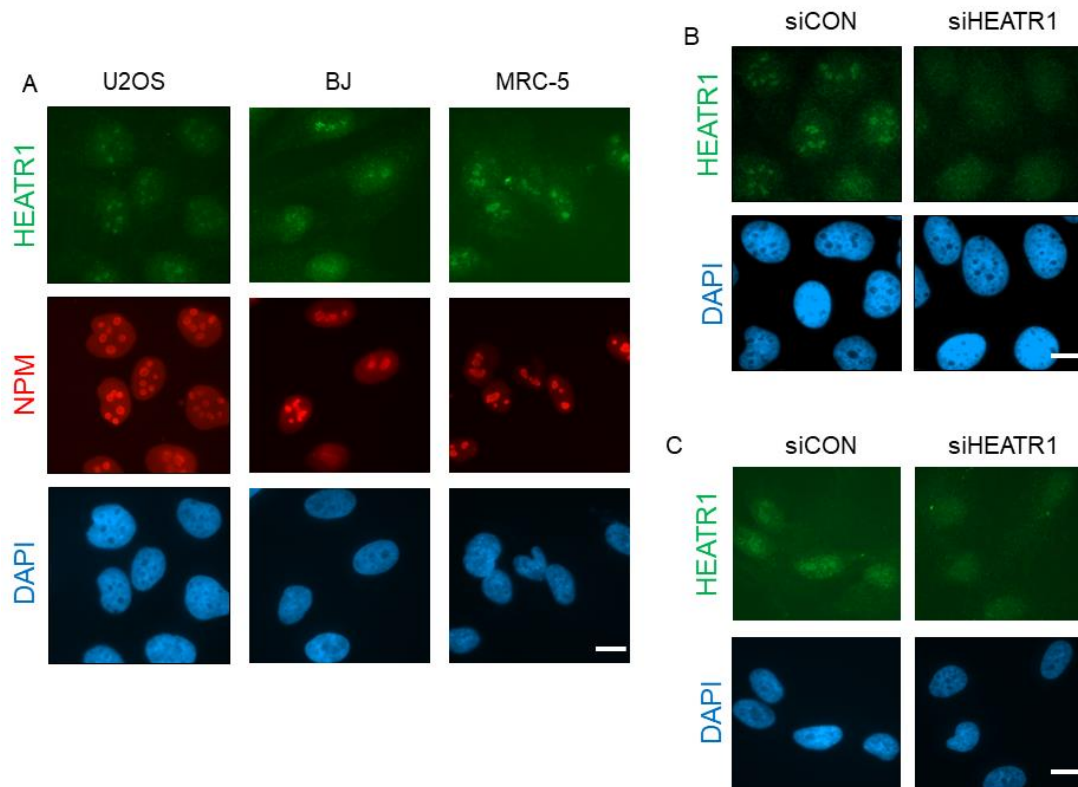


**Figure 21. HEATR1 is a nucleolar protein.** A. U2OS, BJ and MRC-5 cells were fixed and immunostained with the indicated antibodies. Nuclei of the cells were visualized by DAPI staining. Bar, 10  $\mu$ m. B. U2OS cells were transfected with control and HEATR1 siRNAs and 72 hours later cells were fixed, then immunostained with HEATR1 antibody. Nuclei were visualized by DAPI staining. Bar, 10  $\mu$ m. C. BJ cells were transfected with control and HEATR1 siRNAs and 72 hours later cells were fixed, then immunostained with HEATR1 antibody. Nuclei were visualized by DAPI staining. Bar, 10  $\mu$ m.

#### 4.4. Downregulation of HEATR1 induces ribosome biogenesis stress

The fact that HEATR1 is a predominantly nucleolar protein, whose depletion induces p53 and p53-dependent cell cycle arrest implied that HEATR1 might have an active function in ribosome biogenesis; thus abrogation its expression may induce ribosome biogenesis stress. To test this possibility, we investigated (I) the alterations of the nucleolar structure and (II) the involvement of the RPL5 and RPL11 in the activation of p53 upon HEATR1 knockdown.

#### 4.4.1. Nucleolar structure alterations

To analyze the structure of nucleoli in control *versus* HEATR1-depleted cells, we immunostained several nucleolar proteins with well-known localization. We followed the localization of FBL, NCL and NPM, all of which showed a predominant accumulation in the nucleolus under normal conditions in both U2OS and HeLa cells (Fig. 22). However, ablation of HEATR1 induced dramatic alterations in the localization of these proteins. Specifically, FBL relocated to the periphery of the nucleoli and formed nucleolar caps, while NPM and NCL staining spread into nucleoplasmic regions under these conditions (Fig. 22). Additionally, we also confirmed the activation of p53 upon HEATR1 ablation in U2OS cells by immunofluorescence staining (Fig. 22A). Furthermore, as previously discussed, HeLa cells have defective p53 expression. In agreement with this, we did not observe any induction of the protein by immunofluorescence staining following HEATR1 depletion (Fig. 22B).

Disintegration of the nucleolus described by the altered localization of nucleolar proteins is a strong indication of ribosome biogenesis stress reported by numerous studies (Rubbi and Milner 2003; Yuan et al. 2005; Boulon et al. 2010; Bursac et al. 2012) and it is an acknowledged marker of multiple diseases (Narla and Ebert 2010; Hetman and Pietrzak 2012; Armistead and Triggs-Raine 2014; Parlato and Liss 2014; Orsolich et al. 2016). For instance, FBL has been reported to form nucleolar caps in response to low dose ActD treatment (Shav-Tal et al. 2005), whereas NCL and NPM have been shown to relocate from nucleoli to nucleoplasm following diverse insults to ribosome biogenesis (Yuan et al. 2005; Llanos and Serrano 2010; Su et al. 2013). However, in some cases, ribosome biogenesis stress is not represented by the disruption of the nucleolar structure. For example, Fumagalli *et al.* reported that the depletion of RPS6 induces the stabilization of p53, which is not accompanied by morphological changes in the nucleolar structure (Fumagalli et al. 2009). To date, it is not well-understood what are the signals or processes that are leading to structural alterations of the nucleolus. Moreover, it is also not clear whether such changes could have a valuable function under some conditions. Nonetheless, it is widely accepted that disruption of the nucleolar structure means impaired ribosome biogenesis; thus our observations suggested that the absence of HEATR1 activates ribosome biogenesis stress pathways.



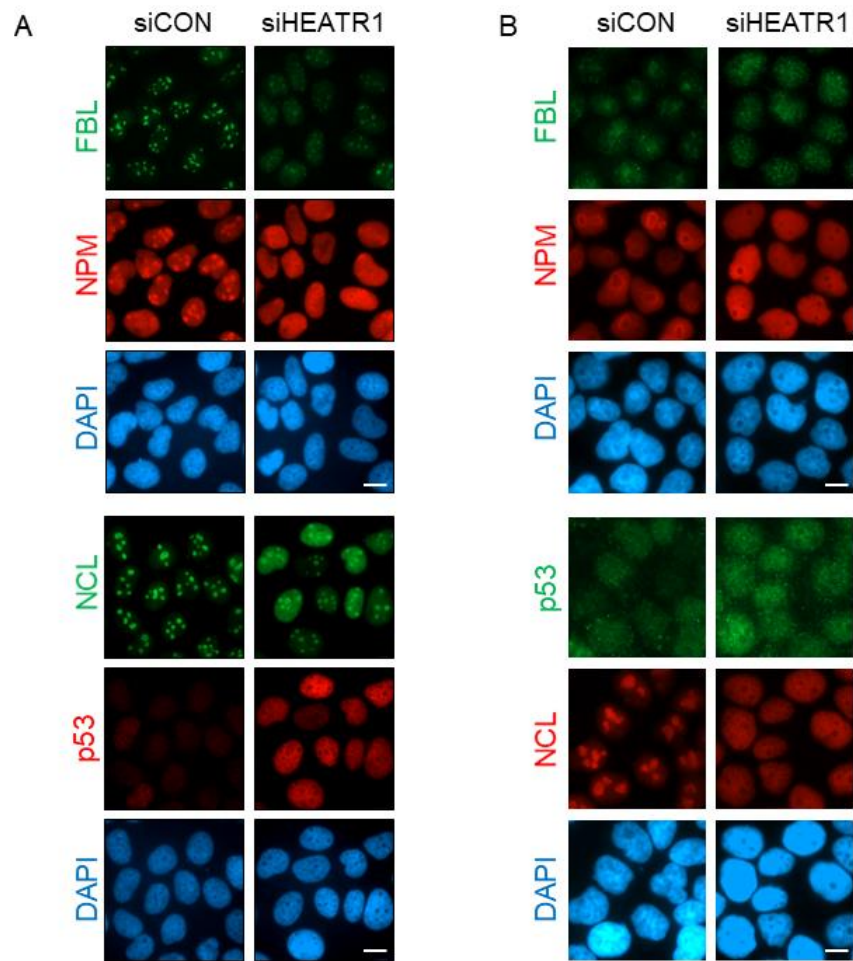


**Figure 22. Disruption of the nucleolar structure upon HEATR1 knockdown.** A. U2OS cells were transfected with control and HEATR1 siRNAs and 72 hours later the cells were fixed and immunostained with the indicated antibodies. Nuclei of the cells were visualized by DAPI staining. Bar, 10  $\mu$ m. B. HeLa cells were transfected with control and HEATR1 siRNAs and 72 hours later cells were fixed, then immunostained with the indicated antibodies. Nuclei were visualized by DAPI staining. Bar, 10  $\mu$ m.

#### 4.4.2. Activation of the canonical 5S RNP/Mdm2/p53 pathway

Next, we wondered whether the impaired expression of HEATR1 induces p53 stabilization via the canonical 5S RNP/Mdm2/p53 pathway. To test this possibility, we performed simultaneous silencing of HEATR1 and either RPL5 or RPL11 and monitored the level of p53 by immunoblotting. Co-depletion of either RPL5 or RPL11 with HEATR1 successfully quenched the activation of p53 seen in HEATR1-deficient U2OS cells (Fig. 23A). This data suggested that stabilization of p53 is indeed mediated by RPL5 and RPL11. Of note, depletion of neither RPL5 nor RPL11 could induce any changes in the expression level of HEATR1 (Fig. 23B). To further confirm the central role of these

proteins in this process, we performed immunoprecipitation of RPL5. Importantly, while in control cells RPL5 did not form a complex with Mdm2, we could detect a strong interaction between these two proteins in HEATR1-deficient U2OS cells (Fig. 23C).

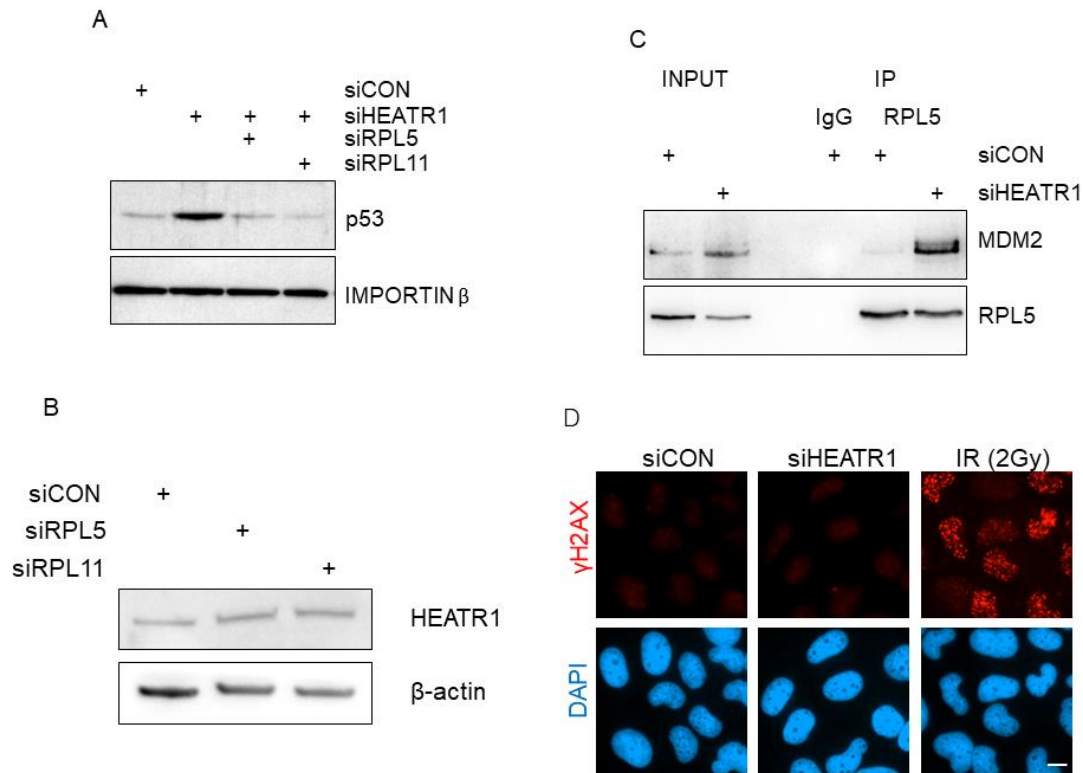


**Figure 23. HEATR1 depletion activates the canonical 5S RNP/Mdm2/p53 pathway without inducing DNA damage.** A. U2OS cells were transfected with the indicated siRNAs and 72 hours later cells were lysed and subjected for Western blot analysis with antibodies against p53 and Importin β. B. U2OS cells were transfected with control and HEATR1 siRNAs and 72 hours later cells were lysed and immunoprecipitated with control (IgG) and RPL5 antibodies, then immunoblotted with the indicated antibodies. C. U2OS cells were transfected with the indicated siRNAs and 72 hours later cells were lysed and immunoblotted with HEATR1 and β-actin antibodies. D. U2OS cells were either transfected with control or HEATR1 siRNAs or were irradiated with 2 Gy. 72 hours after transfection or 1 hour after irradiation cells were fixed and immunostained with γH2AX antibody. Nuclei were visualized by DAPI staining. Bar, 10 μm.

In the following experiment, we investigated whether RNAi-mediated knockdown of HEATR1 induces DNA damage or activation of DDR that could also lead to p53 stabilization and activation. To examine this possibility, we performed immunofluorescence staining of γH2AX, an established marker of DNA damage. Specifically, upon DNA damage, such as DSB induction ATM is activated that is responsible for the phosphorylation of the histone variant H2AX on its serine 139 residue (Rogakou et al. 1998). This key PTM is required for the recruitment of subsequent DDR

factors to the DNA lesion and its spreading around the DNA damage sustains DDR signaling (Rogakou et al. 1998; Jackson and Bartek 2009). Indeed, the introduction of DNA DSBs by  $\gamma$ -irradiation resulted in the induction of the  $\gamma$ H2AX signal, which appeared in a characteristic pattern, so-called irradiation-induced foci (IRIF) (Fig. 23D). In contrast to irradiated cells, HEATR1-depleted U2OS cells did not show the induction of  $\gamma$ H2AX (Fig. 23D); thus we could exclude DNA damage and/or active DDR as a cause of p53 stabilization in this case.

In conclusion, our experiments supported the hypothesis that ablation of HEATR1 induces p53 through the 5S RNP/Mdm2/p53 pathway. Importantly, we also excluded that stabilization of p53 is a consequence of DNA damage-dependent phosphorylation of the protein since depletion of HEATR1 did not induce DNA damage, evidenced by the absence of  $\gamma$ H2AX IRIFs. Notably, it has been reported that U2OS cells fail to induce p53-dependent cell cycle arrest in response to DNA damage due to the overexpression of a truncated, mutant form of the Wip1 phosphatase, which is responsible for the removal of the stabilizing phosphorylation mark from p53 (Kleiblova et al. 2013). This further supports our theory that HEATR1 deficiency induces p53 exclusively through the canonical 5S RNP/Mdm2/p53 pathway.

Furthermore, the absence of  $\gamma$ H2AX signal in HEATR1 deficient cells also indicates the lack of DDR activation. One study has reported that activated ATM is actively involved in the suppression of the ARF protein (Velimezi et al. 2013). Thus, under such stress conditions when ATM is non-activated, ARF might be stabilized, and by binding Mdm2 it could induce p53. Moreover, ARF has been shown to inhibit ribosome biogenesis, by suppressing the nucleolar import of the TTF-1, thereby inducing ribosome biogenesis stress (Lessard et al. 2010). This way ARF could also contribute to the activation of the 5S RNP/Mdm2/p53 pathway. Thus, since HEATR1 depletion does not induce the activation of DDR, ARF could be activated to induce the stabilization of p53 in both direct and indirect manner. However, U2OS cells, used in the majority of our experiments do not express *ARF*, due to promoter hypermethylation (Badal et al. 2008). This further supports the key importance of the 5S RNP/Mdm2/p53 pathway in the induction of p53 in HEATR1 deficient cells.

#### 4.5. HEATR1 is involved in rRNA synthesis

The nucleolar localization of HEATR1 and the fact that its depletion leads to ribosome biogenesis stress and the induction of p53-dependent cell cycle arrest via the 5S RNP/Mdm2/p53 indicated a potential role of HEATR1 in ribosome biogenesis. Since several studies reported that homologs of HEATR1 in multiple organisms are involved in rRNA synthesis (Gallagher et al. 2004; Azuma et al. 2006; Prieto and McStay 2007; Faktorová et al. 2018), first we analyzed nascent RNA synthesis in HEATR1-deficient U2OS and HeLa cells. In order to do so, we performed a 5-ethynyl uridine (EU) incorporation assay. Similarly to EdU, EU is a nucleotide analogue that incorporates into the newly synthesized RNA; thus nascent RNA synthesis can be followed by fluorescence (see Material and methods). Under normal conditions, EU incorporation was the most pronounced in the nucleoli of both U2OS and HeLa cells (Fig. 24). This is in agreement with the fact that rRNAs are the most abundant RNA species in the cell (Jao and Salic 2008). However, HEATR1 knockdown completely abolished the fluorescent signal of the nucleolus in both cell lines, suggesting that the absence of HEATR1 impaired rRNA synthesis (Fig. 24). Moreover, this inhibition of rRNA synthesis observed upon HEATR1 ablation was similar to the effect we detected upon low dose ActD treatment in U2OS cells (Fig. 24A).

Proteins, which are involved in rRNA transcription and associate with the Pol I transcription machinery, localize into the FC region of the nucleoli. Moreover, although the co-localization of these components is still retained during transcription inhibition, they are redistributed to the periphery of the nucleolus forming so-called fibrillar caps (Shav-Tal et al. 2005; Prieto and McStay 2007). Thus, in order to further confirm the involvement of HEATR1 in rRNA synthesis, we investigated the co-localization of HEATR1 with Pol I under normal conditions and upon rRNA transcription inhibition. We performed immunofluorescence staining of HEATR1 and RPA149, which is the largest subunit of Pol I. Under unperturbed growth conditions the staining pattern of HEATR1 and RPA149 was completely overlapping (Fig. 25). Furthermore, when we applied a low dose of ActD to inhibit rRNA synthesis, Pol I along with HEATR1 redistributed to overlaying fibrillar caps (Fig. 25A). To confirm our results seen upon ActD exposure, we treated the cells with another rDNA intercalator drug, BMH-21. In addition to its inhibitory effect on transcription by intercalation, the exposure to BMH-21 also induces

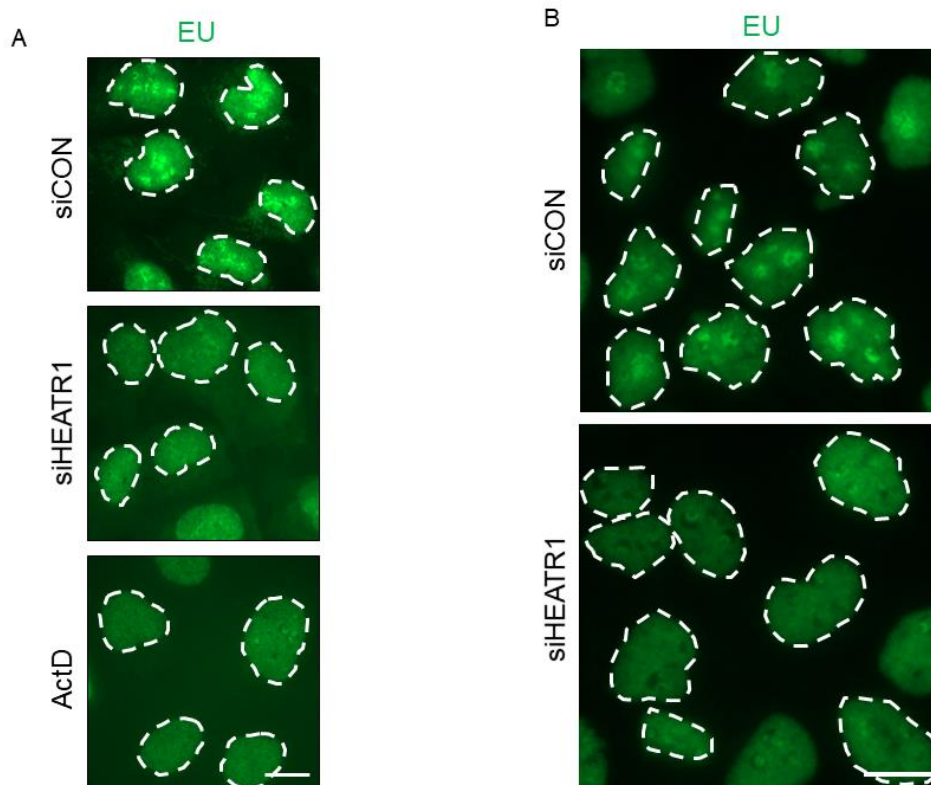


**Figure 24. HEATR1 has a role in rRNA synthesis.** A. U2OS cells were either transfected with the indicated siRNAs or treated with 5 nM ActD. 72 hours after transfection or 16 hours after treatment cells were labeled with 1 mM EU for 30 minutes. Cells were fixed and EU detection was performed by click chemistry. Nuclei are marked by white dashed lines. Bar, 10  $\mu$ m. B. HeLa cells were transfected with either control or HEATR1 siRNA and 72 hours later cells were labeled with 1 mM EU for 30 minutes. Cells were fixed and EU detection was performed by click chemistry. Nuclei are marked by white dashed lines. Bar, 10  $\mu$ m.

the degradation of Pol I (Peltonen et al. 2010; Peltonen et al. 2014). Indeed, RPA149 was almost completely degraded in response to BMH-21 treatment. Meanwhile, HEATR1 was accumulated in fibrillar caps and colocalized with the remaining, not-degraded RPA149 (Fig. 25B). Overall, these results suggested that HEATR1 is a component of the Pol I transcription machinery and supported our previous observations that it has a function in rRNA synthesis.

In conclusion, with this data, we confirmed that besides being a nucleolar protein, HEATR1 is involved in ribosome biogenesis. Specifically, we found that HEATR1, similarly to its homologs in different organisms, is a possible component of the Pol I transcription machinery and its depletion results in the potent inhibition of rRNA synthesis. Although these data represent strong evidence for HEATR1's involvement in rDNA transcription, we cannot exclude the possibility that HEATR1 participates in other steps of ribosome biogenesis as well. For instance, yeast UTP10 and Zebrafish BAP28

have been reported to be required for early SSU processing (Gallagher et al. 2004; Azuma et al. 2006); thus it is likely that HEATR1 protein has a similar function.

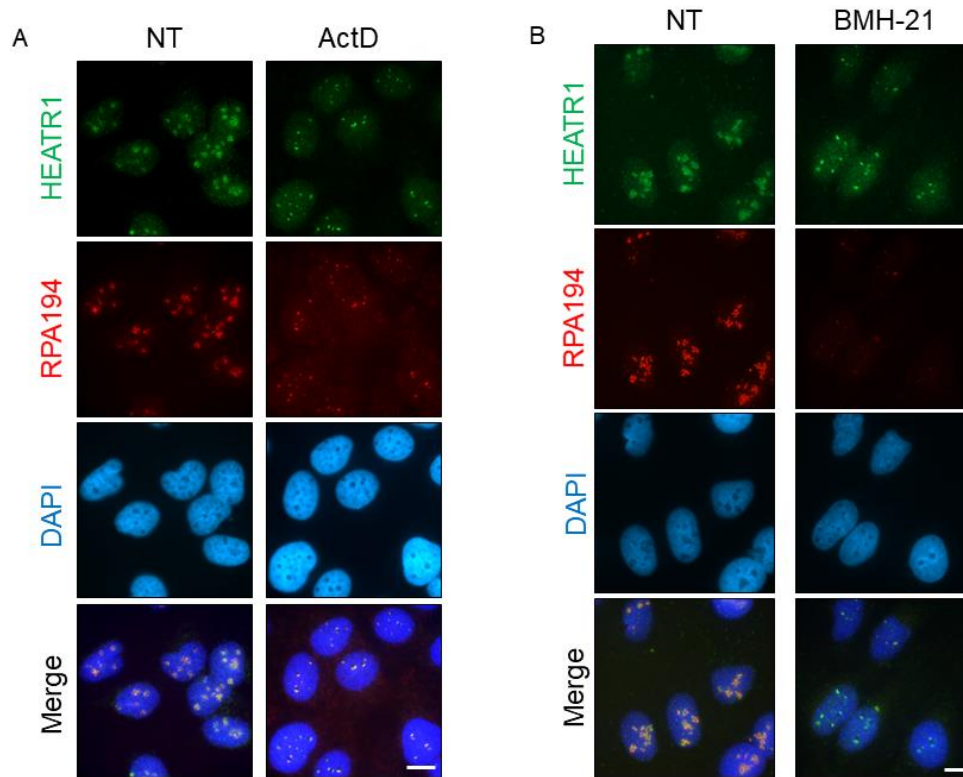


**Figure 25. HEATR1 co-localizes with Pol I.** A. U2OS cells were either mock- or ActD (5 nM)-treated overnight, then fixed and immunostained with HEATR1 and RPA149 antibodies. Nuclei were visualized by DAPI staining. Bar, 10  $\mu$ m. B. U2OS cells were either mock- or BMH-21 (0.5  $\mu$ M)-treated for 3 hours. Following the incubation cell were fixed and immunostained with HEATR1 and RPA149 antibodies. Nuclei were visualized by DAPI staining. Bar, 10  $\mu$ m.

Of note, the prominent role of HEATR1 in rRNA synthesis is not restricted to the U2OS cell line, since HEATR1 depletion impaired rDNA transcription in HeLa cells as well (Fig. 24B). Moreover, as we observed in previous experiments, the deficiency of HEATR1 also induced ribosome biogenesis stress in HeLa cells, evidenced by the altered nucleolar structure (Fig. 22B). Therefore, it is likely that similarly to U2OS cells, the 5S RNP complex binds to Mdm2 in these cells following the ablation of HEATR1. However, as it was mentioned earlier, due to the overexpression of the HPV-encoded E6 oncoprotein, the expression of p53 is downregulated in HeLa cells (Scheffner et al. 1990; Werness et al. 1990); thus the 5S RNP cannot induce p53 expression. Indeed, as we presented earlier, HEATR1 knockdown could not induce p53-dependent cell cycle arrest in HeLa cells (Fig. 22B). Interestingly, HEATR1 depletion did not induce cell cycle arrest at all (Fig. 19B). Moreover, p53 downregulation could rescue cell cycle arrest in

HEATR1-deficient U2OS cells, mimicking the conditions of the HeLa cell line. Although p53 is a central player in ribosome biogenesis stress, p53-independent cell cycle checkpoint activating pathways are also operating in response to impaired ribosome biogenesis (see chapter 1.3.2.). However, our findings did not reflect the activation of such pathways, neither in HEATR1-depleted HeLa (Fig. 19B), nor in p53- and HEATR1-ablated U2OS cells (Fig. 19A). Importantly, we cannot exclude the possibility of the induction of p53-independent processes leading to cell cycle arrest with slower kinetics.

#### 4.6. Upregulation of HEATR1 in cancer

Throughout our experiments, we observed that the protein level of HEATR1 might be lower in normal cells, compared to the cancer cell lines used in this study. To further investigate this observation, we performed a comparative Western blot analysis with exponentially growing cancer cell lines, U2OS and HeLa, and primary fibroblast cells, BJ and MRC-5. Indeed, cell lysates obtained from U2OS and HeLa contained a higher level of HEATR1, while the protein was barely detectable in BJ and MRC-5 cells (Fig. 26). The upregulation of ribosome biogenesis is a common characteristic of cancer cells, which gain a proliferative advantage over normal cells due to the increased capacity of protein production apparatus (see chapter 1.3.4.). Supporting this notion, other ribosome biogenesis factors, such as NS, NCL and NPM were also found at higher abundance in lysates of cancer cells (Fig. 26). Although the two examined cancer cell lines presented an overall upregulation of ribosome biogenesis, we cannot exclude the selective overexpression of HEATR1 in specific cancer types. For instance, a recent study reported the upregulation of HEATR1 in glioblastoma cells, where HEATR1 was demonstrated as an excellent target for T-cell mediated immunotherapy (Wu et al. 2014). However, whether there is a selective overexpression of HEATR1 or a global enhancement in ribosome biogenesis in these glioblastoma cells has not been shown.

Furthermore, selective downregulation of HEATR1 has also been reported to contribute to the increased resistance against gemcitabine of patients with PDAC (Liu et al. 2016). However, in this case, gemcitabine resistance caused by HEATR1 deficiency is ascribed to HEATR1's involvement in the Akt signaling pathway. On the other hand, our experiments show that HEATR1 depletion has severe consequences in the cells: due to its essential role in ribosome biogenesis, its absence initiates ribosome biogenesis stress, resulting in p53-dependent cell cycle arrest. Since this aspect of HEATR1

deficiency was not investigated by Liu *et al.*, we cannot exclude the possibility that defective ribosome biogenesis contributes to the phenotype of PDAC cells observed by the authors. Furthermore, one can also imagine that other nucleolar factors can compensate the absence of HEATR1, thus ribosome biogenesis can still operate sufficiently in PDAC. Nonetheless, as both these scenarios remain to be highly speculative, further studies are needed to uncover the molecular background of HEATR1 deficient cells. Moreover, the potential involvement of HEATR1 down- or upregulation in the pathogenesis of various cancer types also needs to be elucidated.

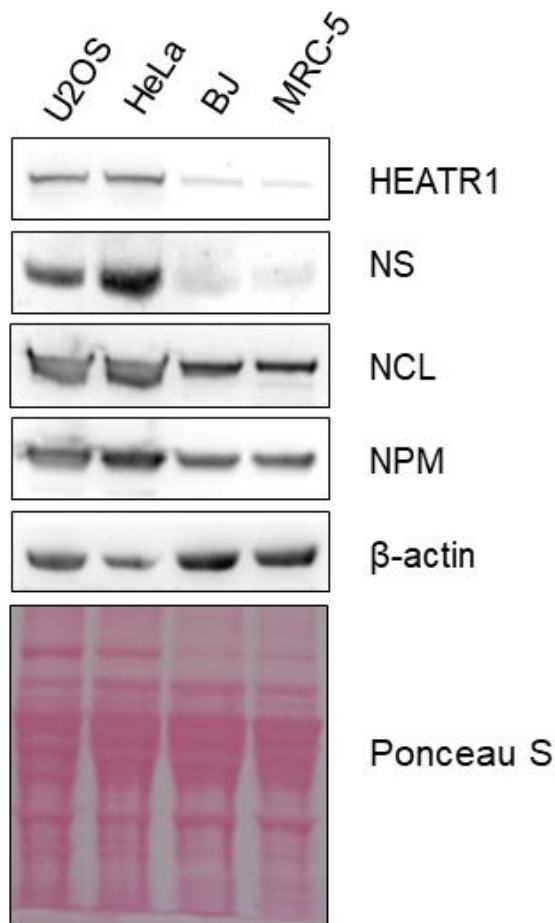


**Figure 26. HEATR1 is overexpressed in cancer cells.** Cancer cell lines U2OS and HeLa, and normal fibroblast cells BJ and MRC-5 were lysed and immunoblotted with HEATR1, NS, NCL, NPM and  $\beta$ -actin antibodies. The total protein amount is visualized by Ponceau S staining and the abundance of  $\beta$ -actin.



## 4.7. Involvement of HEATR1 in DNA damage response

Recently, numerous studies have focused on the connection between ribosome biogenesis and DDR. As described earlier, ribosome biogenesis factors have been described as essential players in DDR, several DDR factors have been shown to be located in the nucleolus and DNA damage has been reported to potently induce ribosome biogenesis stress (see chapter 1. 4.). Thus, our focus has been shifted towards the role of HEATR1 in DDR.

### 4.7.1. Phosphorylation of HEATR1 by ATM

During their effort to determine ATM/ATR substrates in response to DNA damage in HEK 293T cells, Matsuoka *et al.* identified numerous ribosome biogenesis factors in a high throughput proteomic screen, which are phosphorylated by either of these two master kinases. Along with these proteins, HEATR1 was also identified to be phosphorylated by ATM/ATR following  $\gamma$ -irradiation. Specifically, the phosphorylation site was recognized on the Ser1492 residue (Matsuoka *et al.* 2007) (Fig. 15; Fig. 27A). In order to validate their observations, we immunoprecipitated all ATM/ATR substrates with an antibody recognizing phosphorylated S/TQ sites. Notably, endogenous HEATR1 was accumulated among proteins, whose S/TQ site was phosphorylated following  $\gamma$ -irradiation, similarly to SMC1 protein, a known ATM/ATR target (Fig. 27B). These data confirmed the results seen in the screen of Matsuoka *et al.* that HEATR1 is a substrate of ATM/ATR. However, with this experiment, we could not determine the exact phosphorylation site of HEATR1. Nonetheless, these results indicated that HEATR1 might be a component of DDR signaling.

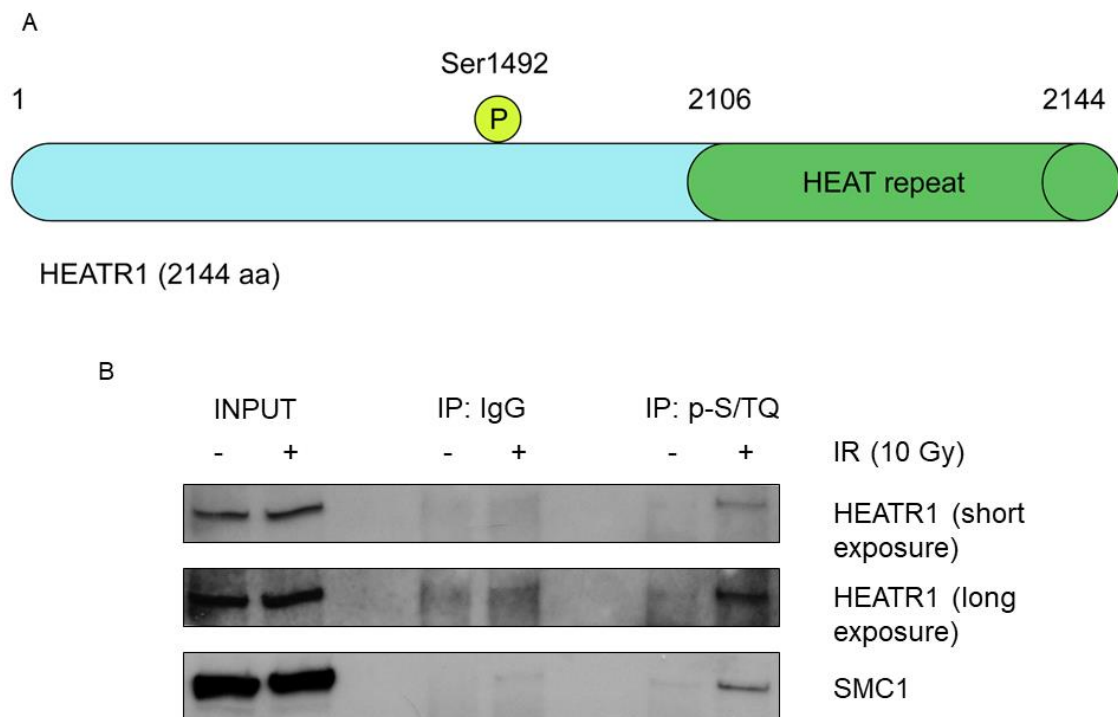


**Figure 27. HEATR1 is phosphorylated by ATM/ATR following  $\gamma$ -irradiation.** A. The schematic structure of HEATR1 protein. The HEATR1 protein consist of 2144 amino acids and contains a HEAT repeat domain at its C terminus. HEATR1 is phosphorylated by ATM/ATR, putatively on the Ser 1492 residue. B. U2OS cells were either mock-treated or irradiated with 10 Gy. 1 hour following the irradiation cells were lysed and immunoprecipitated with control (IgG) and p-S/TQ antibodies, then immunoblotted with the indicated antibodies.

#### 4.7.2. Depletion of HEATR1 leads to attenuated $\gamma$ H2AX formation

According to one proteomic study HEATR1 recruits to DNA lesions following UV irradiation (Chou et al. 2010). Therefore, we assumed that HEATR1 might have a function in the early phase of DDR. To investigate this possibility, we depleted HEATR1 in  $\gamma$ -irradiated cells and followed  $\gamma$ H2AX IRIF formation. The intensity of the  $\gamma$ H2AX fluorescence signal was indeed reduced in HEATR1-deficient cells, compared to control cells (Fig. 28A-C). This indicated that HEATR1 facilitates the DDR response, which is impaired in the absence of the protein.

Next, we aimed to confirm that this phenotype is the specific consequence of HEATR1 ablation and is independent of the ribosome biogenesis stress response. Therefore, we treated the cells with low-dose ActD and quantified  $\gamma$ H2AX fluorescence signal intensity following  $\gamma$ -irradiation. Surprisingly, we found that  $\gamma$ H2AX-formation

was attenuated, similarly to what we observed in the case of HEATR1 depletion (Fig. 28D).

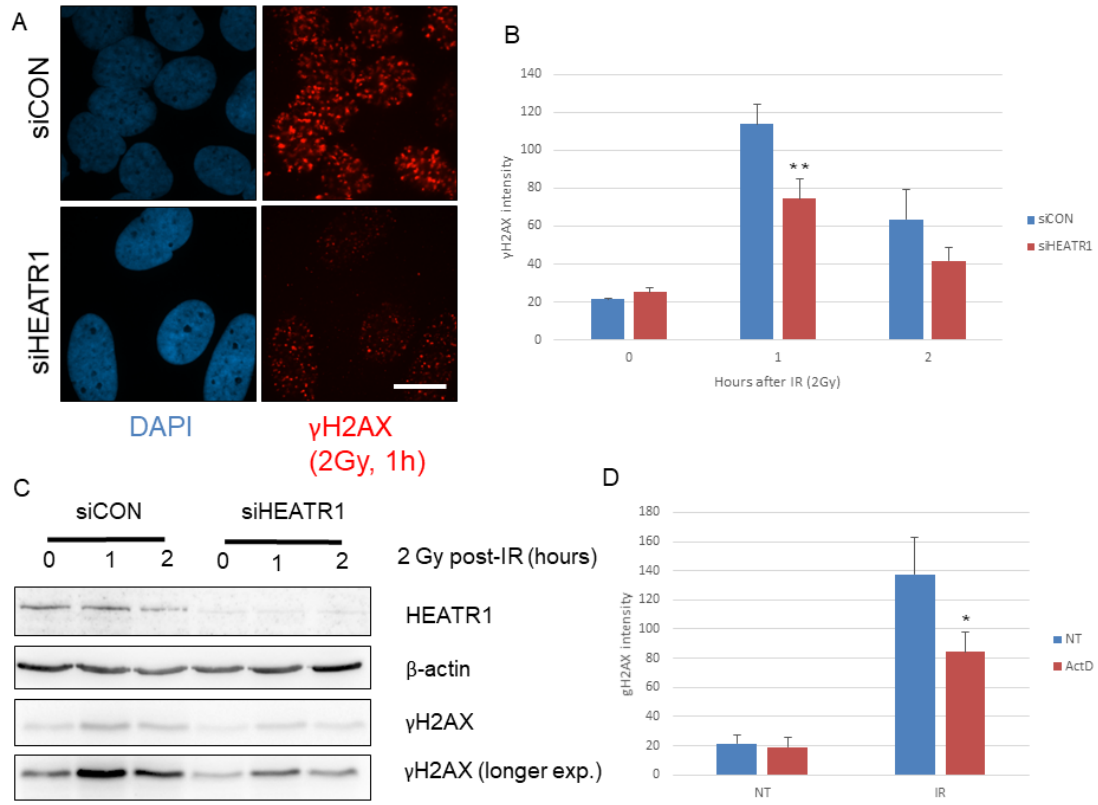


**Figure 28. HEATR1 depletion leads to reduced  $\gamma$ H2AX formation.** A. U2OS cells were transfected with either control or HEATR1 siRNA and 72 hours later cells were irradiated with 2 Gy. 1 hour following the irradiation cells were fixed and immunostained with  $\gamma$ H2AX antibody. Nuclei were visualized by DAPI staining. Bar, 10  $\mu$ m. B. U2OS cells were treated and immunostained as in A. Immunofluorescence intensity of  $\gamma$ H2AX was quantified. Error bars indicate standard deviations (SDs), n=3. Significance was determined by a two-tailed student test: \*\* p<0.01. C. U2OS cells were either mock-treated or irradiated with 2 Gy. 1 or hours later cells were lysed and immunoblotted with the indicated antibodies. D. U2OS cells were either mock- or ActD (5 nM)-treated overnight, then fixed and immunostained with  $\gamma$ H2AX antibody. Immunofluorescence intensity of  $\gamma$ H2AX was quantified. Error bars indicate standard deviations (SDs), n=3. Significance was determined by a two-tailed student test: \* p<0.05.

Overall, these data indicated that HEATR1 is a substrate of ATM/ATR when cells are challenged with  $\gamma$ -irradiation. So far, we could not validate the phosphorylation site on HEATR1, nor identify the function of this PTM.

Future studies will be required to discover the missing information regarding the role of HEATR1 in DDR. One possible approach to uncover the DNA damage responsive phosphorylation site of HEATR1 could be the introduction of an ectopically expressed and tagged form of HEATR1 to the cells. This HEATR1 construct could carry various mutations of the protein. For instance, by replacing Ser1492 with alanine, a

phosphomutant construct, while by substituting Ser1492 with aspartic acid, a phosphomimetic construct could be produced. Transfection of these constructs along with the depletion of the endogenous protein, followed by  $\gamma$ -irradiation and immunoprecipitation with the phospho-S/TQ antibody and subsequent immunoblotting with antibodies against these constructs would reveal whether Ser1492 is the site phosphorylated by ATM/ATR. Such HEATR1 constructs could also be used to monitor alterations in DDR and interactions with other DDR components, without disrupting ribosome biogenesis.

Importantly, although the reduction in the  $\gamma$ H2AX fluorescence signal intensity we observed following HEATR1 ablation can be rather attributed to the global effect of impaired ribosome biogenesis, it is not well-understood what processes cause this phenotype. One recent study has reported a similar reduction in the  $\gamma$ H2AX signal following NCL depletion. In this case, the authors explained this phenomenon by the active involvement of NCL in DDR. As a histone chaperon, NCL is required for the DNA damage-induced histone eviction, which is essential for the spreading of the  $\gamma$ H2AX signal and DDR signaling around the DNA lesion (Kobayashi et al. 2012). Although in our experiments neither HEATR1 depletion, nor ActD treatment led to the reduction in the protein level of NCL, which could explain such changes in the  $\gamma$ H2AX signal, we observed altered localization of this protein under these conditions. Typically, upon HEATR1 ablation or ActD treatment, NCL was released from nucleoli to the nucleoplasm. Thus, it is possible that such altered localization impairs the histone chaperone and DDR function of NCL. Nevertheless, the mechanism by which DDR is impaired under these scenarios needs to be further elucidated.

## 5. SUMMARY

Ribosome biogenesis is a complex process that is initiated in a subnuclear organelle, the nucleolus. The nucleolus is assembled around rDNA genes, whose transcription results in the emergence of a single transcript, the 47S pre-rRNA. The transcription is followed by the maturation of this primary transcript, resulting in the appearance of 18S, 5.8S and 28S rRNAs. Meanwhile, the forth rRNA component, 5S rRNA is transcribed and matured in the nucleus, and ribosomal proteins are synthesized in the cytoplasm. The assembly of the ribosomal components takes place in the nucleolus, nucleus and cytoplasm. Ribosome biogenesis consumes tremendous energy of the cells; therefore it is interconnected with a multitude of signaling pathways in the cell. Perturbation of this process promotes the phenomenon of ribosome biogenesis stress that is characterized mainly by the disintegration of the nucleolar structure, the activation of tumor suppressor p53 and growth arrest. Interestingly, ribosome biogenesis stress is one of the main characteristics of diverse diseases. Furthermore, the nucleolus has been described as the major stress sensor of the cells, due to impairment of ribosome biogenesis following different stress stimuli. Of these stress signals, the close connection of DNA damage and ribosome biogenesis has been best characterized.

In this work, we have identified HEATR1 as a novel nucleolar protein that is involved in the early steps of ribosome biogenesis. Supporting this notion, ablation of HEATR1 disrupts rRNA transcription, leads to the disruption of nucleolar structure and promotes the stabilization and activation of p53, which results in cell cycle arrest. Depletion of HEATR1 activates the canonical RPL5/RPL11/Mdm2/p53 pathway, evidenced by the increased interaction between RPL5 and Mdm2 under these conditions and attenuated p53 activation upon co-depletion of RPL5 and/or RPL11. Furthermore, as it was suggested by others, HEATR1 may be actively involved in the pathology of diseases, such as cancer. In addition, HEATR1 might also be involved in DNA damage signaling; however this aspect of HEATR1's function needs to be further investigated. Overall, in this study, we characterized the novel role of HEATR1 in ribosome biogenesis. Importantly, HEATR1 may also be relevant in the therapy of cancer or other diseases, where ribosome biosynthesis is impaired.

## 6. REFERENCES

- Abbas T, Dutta A. 2009. p21 in cancer: intricate networks and multiple activities. *Nature reviews Cancer* **9**: 400-414.
- Abdelmohsen K, Gorospe M. 2012. RNA-binding protein nucleolin in disease. *RNA biology* **9**: 799-808.
- Ahmad Y, Boisvert F-M, Gregor P, Cobley A, Lamond AI. 2009. NOPdb: Nucleolar Proteome Database--2008 update. *Nucleic acids research* **37**: D181-D184.
- Ahmed MK, Ye X, Taub PJ. 2016. Review of the Genetic Basis of Jaw Malformations. *Journal of pediatric genetics* **5**: 209-219.
- Akamatsu Y, Kobayashi T. 2015. The Human RNA Polymerase I Transcription Terminator Complex Acts as a Replication Fork Barrier That Coordinates the Progress of Replication with rRNA Transcription Activity. *Molecular and cellular biology* **35**: 1871-1881.
- Albert B, Perez-Fernandez J, Leger-Silvestre I, Gadal O. 2012. Regulation of ribosomal RNA production by RNA polymerase I: does elongation come first? *Genetics research international* **2012**: 13 pages.
- Angelov D, Bondarenko VA, Almagro S, Menoni H, Mongélard F, Hans F, Mietton F, Studitsky VM, Hamiche A, Dimitrov S et al. 2006. Nucleolin is a histone chaperone with FACT-like activity and assists remodeling of nucleosomes. *The EMBO journal* **25**: 1669-1679.
- Angrisani A, Vicidomini R, Turano M, Furia M. 2014. Human dyskerin: beyond telomeres. *Biological chemistry* **395**: 593-610.
- Arabi A, Wu S, Ridderstrale K, Bierhoff H, Shiue C, Fatyol K, Fahlen S, Hydbring P, Soderberg O, Grummt I et al. 2005. c-Myc associates with ribosomal DNA and activates RNA polymerase I transcription. *Nature cell biology* **7**: 303-310.
- Armistead J, Triggs-Raine B. 2014. Diverse diseases from a ubiquitous process: the ribosomopathy paradox. *FEBS letters* **588**: 1491-1500.
- Austin KM, Leary RJ, Shimamura A. 2005. The Shwachman-Diamond SBDS protein localizes to the nucleolus. *Blood* **106**: 1253-1258.
- Ayrault O, Andrique L, Fauvin D, Eymin B, Gazzeri S, Seite P. 2006. Human tumor suppressor p14ARF negatively regulates rRNA transcription and inhibits UBF1 transcription factor phosphorylation. *Oncogene* **25**: 7577-7586.
- Azuma M, Toyama R, Laver E, Dawid IB. 2006. Perturbation of rRNA synthesis in the bap28 mutation leads to apoptosis mediated by p53 in the zebrafish central nervous system. *The Journal of biological chemistry* **281**: 13309-13316.

- Badal V, Menendez S, Coomber D, Lane DP. 2008. Regulation of the p14ARF promoter by DNA methylation. *Cell cycle* **7**: 112-119.
- Balusu R, Fiskus W, Rao R, Chong DG, Nalluri S, Mudunuru U, Ma H, Chen L, Venkannagari S, Ha K et al. 2011. Targeting levels or oligomerization of nucleophosmin 1 induces differentiation and loss of survival of human AML cells with mutant NPM1. *Blood* **118**: 3096-3106.
- Barkic M, Crnomarkovic S, Grabusic K, Bogetic I, Panic L, Tamarut S, Cokaric M, Jeric I, Vidak S, Volarevic S. 2009. The p53 tumor suppressor causes congenital malformations in Rpl24-deficient mice and promotes their survival. *Molecular and cellular biology* **29**: 2489-2504.
- Barlow JL, Drynan LF, Hewett DR, Holmes LR, Lorenzo-Abalde S, Lane AL, Jolin HE, Pannell R, Middleton AJ, Wong SH et al. 2010. A p53-dependent mechanism underlies macrocytic anemia in a mouse model of human 5q- syndrome. *Nature medicine* **16**: 59-66.
- Barna M, Pusic A, Zollo O, Costa M, Kondrashov N, Rego E, Rao PH, Ruggero D. 2008. Suppression of Myc oncogenic activity by ribosomal protein haploinsufficiency. *Nature* **456**: 971-975.
- Bartek J, Bartkova J, Lukas J. 2007. DNA damage signalling guards against activated oncogenes and tumour progression. *Oncogene* **26**: 7773.
- Bastola P, Oien DB, Cooley M, Chien J. 2018. Emerging Cancer Therapeutic Targets in Protein Homeostasis. *The AAPS Journal* **20**: 94.
- Bates PJ, Laber DA, Miller DM, Thomas SD, Trent JO. 2009. Discovery and development of the G-rich oligonucleotide AS1411 as a novel treatment for cancer. *Experimental and molecular pathology* **86**: 151-164.
- Belin S, Beghin A, Solano-Gonzalez E, Bezin L, Brunet-Manquat S, Textoris J, Prats AC, Mertani HC, Dumontet C, Diaz JJ. 2009. Dysregulation of ribosome biogenesis and translational capacity is associated with tumor progression of human breast cancer cells. *PloS one* **4**: e7147.
- Bellodi C, Kopmar N, Ruggero D. 2010. Deregulation of oncogene-induced senescence and p53 translational control in X-linked dyskeratosis congenita. *The EMBO journal* **29**: 1865-1876.
- Bhavana V, Sudharshan SJS, Madhu D. 2017. Natural Anticancer Compounds and Their Derivatives in Clinical Trials. in *Anticancer Plants: Clinical Trials and Nanotechnology: Volume 3* (eds. MS Akhtar, MK Swamy), pp. 51-104. Springer Singapore, Singapore.
- Boulon S, Westman BJ, Hutten S, Boisvert FM, Lamond AI. 2010. The nucleolus under stress. *Molecular cell* **40**: 216-227.
- Bouvet P, Diaz J-J, Kindbeiter K, Madjar J-J, Amalric F. 1998. Nucleolin Interacts with Several Ribosomal Proteins through Its RGG Domain. *Journal of Biological Chemistry* **273**: 19025-19029.

- Box JK, Paquet N, Adams MN, Boucher D, Bolderson E, O'Byrne KJ, Richard DJ. 2016. Nucleophosmin: from structure and function to disease development. *BMC molecular biology* **17**: 19.
- Brady CA, Attardi LD. 2010. p53 at a glance. *Journal of cell science* **123**: 2527-2532.
- Burger K, Muhl B, Harasim T, Rohrmoser M, Malamoussi A, Orban M, Kellner M, Gruber-Eber A, Kremmer E, Holzel M et al. 2010. Chemotherapeutic drugs inhibit ribosome biogenesis at various levels. *The Journal of biological chemistry* **285**: 12416-12425.
- Burroughs L, Woolfrey A, Shimamura A. 2009. Shwachman-Diamond syndrome: a review of the clinical presentation, molecular pathogenesis, diagnosis, and treatment. *Hematology/oncology clinics of North America* **23**: 233-248.
- Bursac S, Brdovcak MC, Donati G, Volarevic S. 2014. Activation of the tumor suppressor p53 upon impairment of ribosome biogenesis. *Biochimica et biophysica acta* **1842**: 817-830.
- Bursac S, Brdovcak MC, Pfannkuchen M, Orsolich I, Golomb L, Zhu Y, Katz C, Daftuar L, Grabusic K, Vukelic I et al. 2012. Mutual protection of ribosomal proteins L5 and L11 from degradation is essential for p53 activation upon ribosomal biogenesis stress. *Proceedings of the National Academy of Sciences of the United States of America* **109**: 20467-20472.
- Burwick N, Coats SA, Nakamura T, Shimamura A. 2012. Impaired ribosomal subunit association in Shwachman-Diamond syndrome. *Blood* **120**: 5143-5152.
- Bywater MJ, Poortinga G, Sanij E, Hein N, Peck A, Cullinane C, Wall M, Cluse L, Drygin D, Anderes K et al. 2012. Inhibition of RNA polymerase I as a therapeutic strategy to promote cancer-specific activation of p53. *Cancer cell* **22**: 51-65.
- Cadet J, Wagner JR. 2013. DNA Base Damage by Reactive Oxygen Species, Oxidizing Agents, and UV Radiation. *Cold Spring Harbor perspectives in biology* **5**: a012559.
- Calo E, Flynn RA, Martin L, Spitale RC, Chang HY, Wysocka J. 2014. RNA helicase DDX21 coordinates transcription and ribosomal RNA processing. *Nature* **518**: 249.
- Calo E, Gu B, Bowen ME, Aryan F, Zalc A, Liang J, Flynn RA, Swigut T, Chang HY, Attardi LD et al. 2018. Tissue-selective effects of nucleolar stress and rDNA damage in developmental disorders. *Nature* **554**: 112-117.
- Carrillo J, Gonzalez A, Manguan-Garcia C, Pintado-Berninches L, Perona R. 2014. p53 pathway activation by telomere attrition in X-DC primary fibroblasts occurs in the absence of ribosome biogenesis failure and as a consequence of DNA damage. *Clinical & translational oncology : official publication of the Federation of Spanish Oncology Societies and of the National Cancer Institute of Mexico* **16**: 529-538.
- Caspari T. 2000. Checkpoints: How to activate p53. *Current Biology* **10**: R315-R317.



- Cavanaugh AH, Hempel WM, Taylor LJ, Rogalsky V, Todorov G, Rothblum LI. 1995. Activity of RNA polymerase I transcription factor UBF blocked by Rb gene product. *Nature* **374**: 177.
- Chan MW, Wei SH, Wen P, Wang Z, Matei DE, Liu JC, Liyanarachchi S, Brown R, Nephew KP, Yan PS et al. 2005. Hypermethylation of 18S and 28S ribosomal DNAs predicts progression-free survival in patients with ovarian cancer. *Clinical cancer research : an official journal of the American Association for Cancer Research* **11**: 7376-7383.
- Chang CC, Steinbacher DM. 2012. Treacher collins syndrome. *Seminars in plastic surgery* **26**: 83-90.
- Chen D, Zhang Z, Li M, Wang W, Li Y, Rayburn ER, Hill DL, Wang H, Zhang R. 2007. Ribosomal protein S7 as a novel modulator of p53–MDM2 interaction: binding to MDM2, stabilization of p53 protein, and activation of p53 function. *Oncogene* **26**: 5029.
- Cheng Q, Chen J. 2010. Mechanism of p53 stabilization by ATM after DNA damage. *Cell cycle (Georgetown, Tex)* **9**: 472-478.
- Chiabrando D, Tolosano E. 2010. Diamond Blackfan Anemia at the Crossroad between Ribosome Biogenesis and Heme Metabolism. *Advances in hematology* **2010**: 790632.
- Chiocchetti A, Gibello L, Carando A, Aspesi A, Secco P, Garelli E, Loreni F, Angelini M, Biava A, Dahl N et al. 2005. Interactions between RPS19, mutated in Diamond-Blackfan anemia, and the PIM-1 oncoprotein. *Haematologica* **90**: 1453.
- Choi YW, Kim YW, Bae SM, Kwak SY, Chun HJ, Tong SY, Lee HN, Shin JC, Kim KT, Kim YJ et al. 2007. Identification of Differentially Expressed Genes Using Annealing Control Primer-based GeneFishing in Human Squamous Cell Cervical Carcinoma. *Clinical Oncology* **19**: 308-318.
- Chou DM, Adamson B, Dephoure NE, Tan X, Nottke AC, Hurov KE, Gygi SP, Colaiacovo MP, Elledge SJ. 2010. A chromatin localization screen reveals poly (ADP ribose)-regulated recruitment of the repressive polycomb and NuRD complexes to sites of DNA damage. *Proceedings of the National Academy of Sciences of the United States of America* **107**: 18475-18480.
- Chun R, Garrett LD, Vail DM. 2007. Chapter 11 - Cancer Chemotherapy. in *Withrow & MacEwen's Small Animal Clinical Oncology (Fourth Edition)* (eds. SJ Withrow, DM Vail), pp. 163-192. W.B. Saunders, Saint Louis.
- Ciccia A, Elledge SJ. 2010. The DNA damage response: making it safe to play with knives. *Molecular cell* **40**: 179-204.
- Ciccia A, Huang J-W, Izhar L, Sowa ME, Harper JW, Elledge SJ. 2014. Treacher Collins syndrome TCOF1 protein cooperates with NBS1 in the DNA damage response. *Proceedings of the National Academy of Sciences* **111**: 18631–18636.

- Ciganda M, Williams N. 2011. Eukaryotic 5S rRNA biogenesis. *Wiley interdisciplinary reviews RNA* **2**: 523-533.
- Colombo E, Alcalay M, Pelicci PG. 2011. Nucleophosmin and its complex network: a possible therapeutic target in hematological diseases. *Oncogene* **30**: 2595-2609.
- Cong R, Das S, Ugrinova I, Kumar S, Mongelard F, Wong J, Bouvet P. 2012. Interaction of nucleolin with ribosomal RNA genes and its role in RNA polymerase I transcription. *Nucleic acids research* **40**: 9441-9454.
- Conn CS, Qian S-B. 2013. Nutrient signaling in protein homeostasis: an increase in quantity at the expense of quality. *Science signaling* **6**: ra24-ra24.
- Coutinho-Camillo CM, Lourenco SV, Nishimoto IN, Kowalski LP, Soares FA. 2010. Nucleophosmin, p53, and Ki-67 expression patterns on an oral squamous cell carcinoma tissue microarray. *Human pathology* **41**: 1079-1086.
- Crichton D, Woiwode A, Zhang C, Mandavia N, Morton JP, Warnock LJ, Milner J, White RJ, Johnson DL. 2003. p53 represses RNA polymerase III transcription by targeting TBP and inhibiting promoter occupancy by TFIIB. *The EMBO journal* **22**: 2810-2820.
- Crosby ME, Almasan A. 2014. Opposing roles of E2Fs in cell proliferation and death. *Cancer Biology & Therapy* **3**: 1208-1211.
- Daftuar L, Zhu Y, Jacq X, Prives C. 2013. Ribosomal proteins RPL37, RPS15 and RPS20 regulate the Mdm2-p53-MdmX network. *PLoS one* **8**: e68667.
- Dai M-S, Arnold H, Sun X-X, Sears R, Lu H. 2007. Inhibition of c-Myc activity by ribosomal protein L11. *The EMBO journal* **26**: 3332-3345.
- Dai M-S, Lu H. 2004. Inhibition of MDM2-mediated p53 Ubiquitination and Degradation by Ribosomal Protein L5. *Journal of Biological Chemistry* **279**: 44475-44482.
- Dai M-S, Sun X-X, Lu H. 2008. Aberrant expression of nucleostemin activates p53 and induces cell cycle arrest via inhibition of MDM2. *Molecular and cellular biology* **28**: 4365-4376.
- Dai M-S, Zeng SX, Jin Y, Sun X-X, David L, Lu H. 2004. Ribosomal protein L23 activates p53 by inhibiting MDM2 function in response to ribosomal perturbation but not to translation inhibition. *Molecular and cellular biology* **24**: 7654-7668.
- Danilova N, Gazda HT. 2015. Ribosomopathies: how a common root can cause a tree of pathologies. *Disease models & mechanisms* **8**: 1013-1026.
- Decatur WA, Schnare MN. 2008. Different mechanisms for pseudouridine formation in yeast 5S and 5.8S rRNAs. *Molecular and cellular biology* **28**: 3089-3100.
- Dez C, Dlakic M, Tollervey D. 2007. Roles of the HEAT repeat proteins Utp10 and Utp20 in 40S ribosome maturation. *Rna* **13**: 1516-1527.

- Diesch J, Hannan RD, Sanij E. 2014. Perturbations at the ribosomal genes loci are at the centre of cellular dysfunction and human disease. *Cell & bioscience* **4**: 43-43.
- Dixon J, Jones NC, Sandell LL, Jayasinghe SM, Crane J, Rey JP, Dixon MJ, Trainor PA. 2006. Tcof1/Treacle is required for neural crest cell formation and proliferation deficiencies that cause craniofacial abnormalities. *Proceedings of the National Academy of Sciences of the United States of America* **103**: 13403-13408.
- Donati G, Bertoni S, Brighenti E, Vici M, Trere D, Volarevic S, Montanaro L, Derenzini M. 2011a. The balance between rRNA and ribosomal protein synthesis up- and downregulates the tumour suppressor p53 in mammalian cells. *Oncogene* **30**: 3274-3288.
- Donati G, Brighenti E, Vici M, Mazzini G, Trere D, Montanaro L, Derenzini M. 2011b. Selective inhibition of rRNA transcription downregulates E2F-1: a new p53-independent mechanism linking cell growth to cell proliferation. *Journal of cell science* **124**: 3017-3028.
- Donati G, Peddigari S, Mercer CA, Thomas G. 2013. 5S ribosomal RNA is an essential component of a nascent ribosomal precursor complex that regulates the Hdm2-p53 checkpoint. *Cell reports* **4**: 87-98.
- Dror Y. 2002. p53 Protein Overexpression in Shwachman-Diamond Syndrome. *Archives of Pathology & Laboratory Medicine* **126**: 1157-1158.
- Drygin D, Lin A, Bliesath J, Ho CB, O'Brien SE, Proffitt C, Omori M, Haddach M, Schwaebe MK, Siddiqui-Jain A et al. 2011. Targeting RNA polymerase I with an oral small molecule CX-5461 inhibits ribosomal RNA synthesis and solid tumor growth. *Cancer research* **71**: 1418-1430.
- Du J, Shi Y, Pan Y, Jin X, Liu C, Liu N, Han Q, Lu Y, Qiao T, Fan D. 2014. Regulation of multidrug resistance by ribosomal protein L6 in gastric cancer cells. *Cancer Biology & Therapy* **4**: 250-255.
- Durkin SG, Glover TW. 2007. Chromosome Fragile Sites. *Annual Review of Genetics* **41**: 169-192.
- Durut N, Saez-Vasquez J. 2015. Nucleolin: dual roles in rDNA chromatin transcription. *Gene* **556**: 7-12.
- Dutt S, Narla A, Lin K, Mullally A, Abayasekara N, Megerdichian C, Wilson FH, Currie T, Khanna-Gupta A, Berliner N et al. 2011. Haploinsufficiency for ribosomal protein genes causes selective activation of p53 in human erythroid progenitor cells. *Blood* **117**: 2567-2576.
- Efeyan A, Serrano M. 2007. p53: Guardian of the Genome and Policeman of the Oncogenes. *Cell cycle* **6**: 1006-1010.
- El-Deiry WS. 2016. p21(WAF1) Mediates Cell-Cycle Inhibition, Relevant to Cancer Suppression and Therapy. *Cancer research* **76**: 5189-5191.

- Elghetany MT, Alter BP. 2002. p53 Protein Overexpression in Bone Marrow Biopsies of Patients With Shwachman-Diamond Syndrome Has a Prevalence Similar to That of Patients With Refractory Anemia. *Archives of Pathology & Laboratory Medicine* **126**: 452-455.
- Ellis SR. 2014. Nucleolar stress in Diamond Blackfan anemia pathophysiology. *Biochimica et biophysica acta* **1842**: 765-768.
- Ellis SR, Gleizes PE. 2011. Diamond Blackfan anemia: ribosomal proteins going rogue. *Seminars in hematology* **48**: 89-96.
- Faktorová D, Bär A, Hashimi H, McKenney K, Horák A, Schnauffer A, Rubio MAT, Alfonzo JD, Lukeš J. 2018. TbUTP10, a protein involved in early stages of pre-18S rRNA processing in *Trypanosoma brucei*. *Molecular and Biochemical Parasitology* **225**: 84-93.
- Felton-Edkins ZA, Fairley JA, Graham EL, Johnston IM, White RJ, Scott PH. 2003. The mitogen-activated protein (MAP) kinase ERK induces tRNA synthesis by phosphorylating TFIIB. *The EMBO journal* **22**: 2422-2432.
- Finch AJ, Hilcenko C, Basse N, Drynan LF, Goyenechea B, Menne TF, Gonzalez Fernandez A, Simpson P, D'Santos CS, Arends MJ et al. 2011. Uncoupling of GTP hydrolysis from eIF6 release on the ribosome causes Shwachman-Diamond syndrome. *Genes & development* **25**: 917-929.
- Fok WC, Niero ELO, Dege C, Brenner KA, Sturgeon CM, Batista LFZ. 2017. p53 Mediates Failure of Human Definitive Hematopoiesis in Dyskeratosis Congenita. *Stem cell reports* **9**: 409-418.
- Fumagalli S, Di Cara A, Neb-Gulati A, Natt F, Schwemberger S, Hall J, Babcock GF, Bernardi R, Pandolfi PP, Thomas G. 2009. Absence of nucleolar disruption after impairment of 40S ribosome biogenesis reveals an rpL11-translation-dependent mechanism of p53 induction. *Nature cell biology* **11**: 501-508.
- Fumagalli S, Ivanenkov VV, Teng T, Thomas G. 2012. Suprainduction of p53 by disruption of 40S and 60S ribosome biogenesis leads to the activation of a novel G2/M checkpoint. *Genes & development* **26**: 1028-1040.
- Galbiati A, Penzo M, Bacalini MG, Onofrillo C, Guerrieri AN, Garagnani P, Franceschi C, Treré D, Montanaro L. 2017. Epigenetic up-regulation of ribosome biogenesis and more aggressive phenotype triggered by the lack of the histone demethylase JHDM1B in mammary epithelial cells. *Oncotarget* **8**: 37091-37103.
- Gallagher JEG, Dunbar DA, Granneman S, Mitchell BM, Osheim Y, Beyer AL, Baserga SJ. 2004. RNA polymerase I transcription and pre-rRNA processing are linked by specific SSU processome components. *Genes & development* **18**: 2506-2517.
- Ganapathi KA, Austin KM, Lee CS, Dias A, Malsch MM, Reed R, Shimamura A. 2007. The human Shwachman-Diamond syndrome protein, SBDS, associates with ribosomal RNA. *Blood* **110**: 1458-1465.

- Gazda HT, Sheen MR, Vlachos A, Choessel V, O'Donohue M-F, Schneider H, Darras N, Hasman C, Sieff CA, Newburger PE et al. 2008. Ribosomal protein L5 and L11 mutations are associated with cleft palate and abnormal thumbs in Diamond-Blackfan anemia patients. *American journal of human genetics* **83**: 769-780.
- Gentilella A, Morón-Duran FD, Fuentes P, Zweig-Rocha G, Riaño-Canalias F, Pelletier J, Ruiz M, Turón G, Castaño J, Tauler A et al. 2017. Autogenous Control of 5'TOP mRNA Stability by 40S Ribosomes. *Molecular cell* **67**: 55-70.e54.
- Ghoshal K, Majumder S, Datta J, Motiwala T, Bai S, Sharma SM, Frankel W, Jacob ST. 2004. Role of human ribosomal RNA (rRNA) promoter methylation and of methyl-CpG-binding protein MBD2 in the suppression of rRNA gene expression. *The Journal of biological chemistry* **279**: 6783-6793.
- Ginisty H, Amalric F, Bouvet P. 1998. Nucleolin functions in the first step of ribosomal RNA processing. *The EMBO journal* **17**: 1476-1486.
- Ginisty H, Serin G, Ghisolfi-Nieto L, Roger B, Libante V, Amalric F, Bouvet P. 2000. Interaction of nucleolin with an evolutionarily conserved pre-ribosomal RNA sequence is required for the assembly of the primary processing complex. *The Journal of biological chemistry* **275**: 18845-18850.
- Golomb L, Bublik DR, Wilder S, Nevo R, Kiss V, Grabusic K, Volarevic S, Oren M. 2012. Importin 7 and exportin 1 link c-Myc and p53 to regulation of ribosomal biogenesis. *Molecular cell* **45**: 222-232.
- Golomb L, Volarevic S, Oren M. 2014. p53 and ribosome biogenesis stress: the essentials. *FEBS letters* **588**: 2571-2579.
- Gomez-Roman N, Felton-Edkins ZA, Kenneth NS, Goodfellow SJ, Athineos D, Zhang J, Ramsbottom BA, Innes F, Kantidakis T, Kerr ER et al. 2006. Activation by c-Myc of transcription by RNA polymerases I, II and III. *Biochem Soc Symp* **73**: 141-154.
- Gonzales B, Henning D, So RB, Dixon J, Dixon MJ, Valdez BC. 2005. The Treacher Collins syndrome (TCOF1) gene product is involved in pre-rRNA methylation. *Human molecular genetics* **14**: 2035-2043.
- Goodfellow SJ, Zomerdijk JC. 2013. Basic mechanisms in RNA polymerase I transcription of the ribosomal RNA genes. *Sub-cellular biochemistry* **61**: 211-236.
- Graham A, Koentges G, Lumsden A. 1996. Neural Crest Apoptosis and the Establishment of Craniofacial Pattern: An Honorable Death. *Molecular and Cellular Neuroscience* **8**: 76-83.
- Grandori C, Gomez-Roman N, Felton-Edkins ZA, Ngouenet C, Galloway DA, Eisenman RN, White RJ. 2005. c-Myc binds to human ribosomal DNA and stimulates transcription of rRNA genes by RNA polymerase I. *Nature cell biology* **7**: 311-318.

- Grewal SS, Li L, Orian A, Eisenman RN, Edgar BA. 2005. Myc-dependent regulation of ribosomal RNA synthesis during *Drosophila* development. *Nature cell biology* **7**: 295-302.
- Grummt I. 2003. Life on a planet of its own: regulation of RNA polymerase I transcription in the nucleolus. *Genes & development* **17**: 1691-1702.
- Grummt I. 2010. Wisely chosen paths--regulation of rRNA synthesis: delivered on 30 June 2010 at the 35th FEBS Congress in Gothenburg, Sweden. *The FEBS journal* **277**: 4626-4639.
- Grummt I, Langst G. 2013. Epigenetic control of RNA polymerase I transcription in mammalian cells. *Biochimica et biophysica acta* **1829**: 393-404.
- Gu J, Kawai H, Nie L, Kitao H, Wiederschain D, Jochemsen AG, Parant J, Lozano G, Yuan Z-M. 2002. Mutual Dependence of MDM2 and MDMX in Their Functional Inactivation of p53. *Journal of Biological Chemistry* **277**: 19251-19254.
- Guetg C, Lienemann P, Sirri V, Grummt I, Hernandez-Verdun D, Hottiger MO, Fussenegger M, Santoro R. 2010. The NoRC complex mediates the heterochromatin formation and stability of silent rRNA genes and centromeric repeats. *The EMBO journal* **29**: 2135-2146.
- Guetg C, Santoro R. 2012. Formation of nuclear heterochromatin: the nucleolar point of view. *Epigenetics* **7**: 811-814.
- Guo X, Shi Y, Gou Y, Li J, Han S, Zhang Y, Huo J, Ning X, Sun L, Chen Y et al. 2011. Human ribosomal protein S13 promotes gastric cancer growth through down-regulating p27(Kip1). *Journal of cellular and molecular medicine* **15**: 296-306.
- Hannan KM, Brandenburger Y, Jenkins A, Sharkey K, Cavanaugh A, Rothblum L, Moss T, Poortinga G, McArthur GA, Pearson RB et al. 2003. mTOR-Dependent Regulation of Ribosomal Gene Transcription Requires S6K1 and Is Mediated by Phosphorylation of the Carboxy-Terminal Activation Domain of the Nucleolar Transcription Factor UBF *Molecular and cellular biology* **23**: 8862-8877.
- Hannan KM, Hannan RD, Smith SD, Jefferson LS, Lun M, Rothblum LI. 2000. Rb and p130 regulate RNA polymerase I transcription: Rb disrupts the interaction between UBF and SL-1. *Oncogene* **19**: 4988.
- Hannan KM, Sanij E, Hein N, Hannan RD, Pearson RB. 2011. Signaling to the ribosome in cancer—It is more than just mTORC1. *IUBMB Life* **63**: 79-85.
- Harding SM, Boiarsky JA, Greenberg RA. 2015. ATM Dependent Silencing Links Nucleolar Chromatin Reorganization to DNA Damage Recognition. *Cell reports* **13**: 251-259.
- Haupt Y, Maya R, Kazaz A, Oren M. 1997. Mdm2 promotes the rapid degradation of p53. *Nature* **387**: 296.

- Henras AK, Plisson-Chastang C, O'Donohue MF, Chakraborty A, Gleizes PE. 2015. An overview of pre-ribosomal RNA processing in eukaryotes. *Wiley interdisciplinary reviews RNA* **6**: 225-242.
- Henras AK, Soudet J, Gerus M, Lebaron S, Caizergues-Ferrer M, Mouglin A, Henry Y. 2008. The post-transcriptional steps of eukaryotic ribosome biogenesis. *Cellular and molecular life sciences : CMLS* **65**: 2334-2359.
- Hernandez-Verdun D, Roussel P, Thiry M, Sirri V, Lafontaine DL. 2010. The nucleolus: structure/function relationship in RNA metabolism. *Wiley interdisciplinary reviews RNA* **1**: 415-431.
- Hetman M, Pietrzak M. 2012. Emerging roles of the neuronal nucleolus. *Trends in neurosciences* **35**: 305-314.
- Hock AK, Vousden KH. 2014. The role of ubiquitin modification in the regulation of p53. *Biochimica et biophysica acta* **1843**: 137-149.
- Hoeijmakers JHJ. 2001. DNA repair mechanisms. *Maturitas* **38**: 17-22.
- Holmberg Olausson K, Elsir T, Moazemi Goudarzi K, Nistér M, Lindström MS. 2015. NPM1 histone chaperone is upregulated in glioblastoma to promote cell survival and maintain nucleolar shape. *Scientific reports* **5**: 16495.
- Holmberg Olausson K, Nister M, Lindstrom MS. 2012. p53 -Dependent and -Independent Nucleolar Stress Responses. *Cells* **1**: 774-798.
- Honda R, Tanaka H, Yasuda H. 1998. Oncoprotein MDM2 is a ubiquitin ligase E3 for tumor suppressor p53. *FEBS letters* **420**: 25-27.
- Hutten S, Prescott A, James J, Riesenbergs S, Boulon S, Lam YW, Lamond AI. 2011. An intranucleolar body associated with rDNA. *Chromosoma* **120**: 481-499.
- Iadevaia V, Caldarola S, Biondini L, Gismondi A, Karlsson S, Dianzani I, Loreni F. 2010. PIM1 kinase is destabilized by ribosomal stress causing inhibition of cell cycle progression. *Oncogene* **29**: 5490.
- Itahana K, Bhat KP, Jin A, Itahana Y, Hawke D, Kobayashi R, Zhang Y. 2003. Tumor Suppressor ARF Degrades B23, a Nucleolar Protein Involved in Ribosome Biogenesis and Cell Proliferation. *Molecular cell* **12**: 1151-1164.
- Jackson AL, Bartz SR, Schelter J, Kobayashi SV, Burchard J, Mao M, Li B, Cavet G, Linsley PS. 2003. Expression profiling reveals off-target gene regulation by RNAi. *Nature Biotechnology* **21**: 635.
- Jackson RJ, Hellen CU, Pestova TV. 2010. The mechanism of eukaryotic translation initiation and principles of its regulation. *Nature reviews Molecular cell biology* **11**: 113-127.
- Jackson SP, Bartek J. 2009. The DNA-damage response in human biology and disease. *Nature* **461**: 1071-1078.

- Jädersten M, Saft L, Smith A, Kulasekararaj A, Pomplun S, Göhring G, Hedlund A, Hast R, Schlegelberger B, Porwit A et al. 2011. TP53 Mutations in Low-Risk Myelodysplastic Syndromes With del(5q) Predict Disease Progression. *Journal of Clinical Oncology* **29**: 1971-1979.
- Jäkel S, Görlich D. 1998. Importin beta, transportin, RanBP5 and RanBP7 mediate nuclear import of ribosomal proteins in mammalian cells. *The EMBO journal* **17**: 4491-4502.
- Jäkel S, Mingot J-M, Schwarzmaier P, Hartmann E, Görlich D. 2002. Importins fulfil a dual function as nuclear import receptors and cytoplasmic chaperones for exposed basic domains. *The EMBO journal* **21**: 377-386.
- James A, Wang Y, Raje H, Rosby R, DiMario P. 2014. Nucleolar stress with and without p53. *Nucleus* **5**: 402-426.
- Jao CY, Salic A. 2008. Exploring RNA transcription and turnover in vivo by using click chemistry. *Proceedings of the National Academy of Sciences of the United States of America* **105**: 15779-15784.
- Jena N. 2012. *DNA damage by reactive species: Mechanisms, mutation and repair*.
- Jia W, Yao Z, Zhao J, Guan Q, Gao L. 2017. New perspectives of physiological and pathological functions of nucleolin (NCL). *Life sciences* **186**: 1-10.
- Jin A, Itahana K, O'Keefe K, Zhang Y. 2004. Inhibition of HDM2 and activation of p53 by ribosomal protein L23. *Molecular and cellular biology* **24**: 7669-7680.
- Jones NC, Lynn ML, Gaudenz K, Sakai D, Aoto K, Rey JP, Glynn EF, Ellington L, Du C, Dixon J et al. 2008. Prevention of the neurocristopathy Treacher Collins syndrome through inhibition of p53 function. *Nature medicine* **14**: 125-133.
- Kadakia S, Helman SN, Badhey AK, Saman M, Ducic Y. 2014. Treacher Collins Syndrome: the genetics of a craniofacial disease. *International journal of pediatric otorhinolaryngology* **78**: 893-898.
- Kalra RS, Bapat SA. 2013. Enhanced levels of double-strand DNA break repair proteins protect ovarian cancer cells against genotoxic stress-induced apoptosis. *Journal of ovarian research* **6**: 66-66.
- Kantidakis T, Ramsbottom BA, Birch JL, Dowding SN, White RJ. 2010. mTOR associates with TFIIC, is found at tRNA and 5S rRNA genes, and targets their repressor Maf1. *Proceedings of the National Academy of Sciences of the United States of America* **107**: 11823-11828.
- Kim KH, Yoo BC, Kim WK, Hong JP, Kim K, Song EY, Lee JY, Cho JY, Ku JL. 2014. CD133 and CD133-regulated nucleophosmin linked to 5-fluorouracil susceptibility in human colon cancer cell line SW620. *Electrophoresis* **35**: 522-532.



- Kim S-T, Lim D-S, Canman CE, Kastan MB. 1999. Substrate Specificities and Identification of Putative Substrates of ATM Kinase Family Members. *Journal of Biological Chemistry* **274**: 37538-37543.
- Kirwan M, Dokal I. 2008. Dyskeratosis congenita: a genetic disorder of many faces. *Clinical genetics* **73**: 103-112.
- Kleiblova P, Shaltiel IA, Benada J, Sevcik J, Pechackova S, Pohlreich P, Voest EE, Dundr P, Bartek J, Kleibl Z et al. 2013. Gain-of-function mutations of PPM1D/Wip1 impair the p53-dependent G1 checkpoint. *The Journal of cell biology* **201**: 511-521.
- Klinge S, Voigts-Hoffmann F, Leibundgut M, Ban N. 2012. Atomic structures of the eukaryotic ribosome. *Trends in biochemical sciences* **37**: 189-198.
- Kobayashi J, Fujimoto H, Sato J, Hayashi I, Burma S, Matsuura S, Chen DJ, Komatsu K. 2012. Nucleolin participates in DNA double-strand break-induced damage response through MDC1-dependent pathway. *PloS one* **7**: e49245.
- Kobayashi T. 2014. Ribosomal RNA gene repeats, their stability and cellular senescence. *Proceedings of the Japan Academy, Series B* **90**: 119-129.
- Koh CM, Gurel B, Sutcliffe S, Aryee MJ, Schultz D, Iwata T, Uemura M, Zeller KI, Anele U, Zheng Q et al. 2011. Alterations in nucleolar structure and gene expression programs in prostatic neoplasia are driven by the MYC oncogene. *The American journal of pathology* **178**: 1824-1834.
- Korgaonkar C, Hagen J, Tompkins V, Frazier AA, Allamargot C, Quelle FW, Quelle DE. 2005. Nucleophosmin (B23) targets ARF to nucleoli and inhibits its function. *Molecular and cellular biology* **25**: 1258-1271.
- Krogan NJ, Peng W-T, Cagney G, Robinson MD, Haw R, Zhong G, Guo X, Zhang X, Canadien V, Richards DP et al. 2004. High-Definition Macromolecular Composition of Yeast RNA-Processing Complexes. *Molecular cell* **13**: 225-239.
- Kroon HM, Huismans AM, Kam PCA, Thompson JF. 2014. Isolated limb infusion with melphalan and actinomycin D for melanoma: A systematic review. *Journal of Surgical Oncology* **109**: 348-351.
- Kruhlak M, Crouch EE, Orlov M, Montano C, Gorski SA, Nussenzweig A, Misteli T, Phair RD, Casellas R. 2007. The ATM repair pathway inhibits RNA polymerase I transcription in response to chromosome breaks. *Nature* **447**: 730-734.
- Kuo M-L, den Besten W, Bertwistle D, Roussel MF, Sherr CJ. 2004. N-terminal polyubiquitination and degradation of the Arf tumor suppressor. *Genes & development* **18**: 1862-1874.
- Kurki S, Peltonen K, Latonen L, Kiviharju TM, Ojala PM, Meek D, Laiho M. 2004. Nucleolar protein NPM interacts with HDM2 and protects tumor suppressor protein p53 from HDM2-mediated degradation. *Cancer cell* **5**: 465-475.

- Laber DA, Choudry MA, Taft BS, Bhupalam L, Sharma VR, Hendler FJ, Barnhart KM. 2004. A phase I study of AGRO100 in advanced cancer. *Journal of Clinical Oncology* **22**: 3112-3112.
- Laber DA, Taft BS, Kloecker GH, Bates PJ, Trent JO, Miller DM. 2006. Extended phase I study of AS1411 in renal and non-small cell lung cancers. *Journal of Clinical Oncology* **24**: 13098-13098.
- Lam YW, Lamond AI, Mann M, Andersen JS. 2007. Analysis of nucleolar protein dynamics reveals the nuclear degradation of ribosomal proteins. *Current biology : CB* **17**: 749-760.
- Lane DP. 1992. p53, guardian of the genome. *Nature* **358**: 15.
- Larrea MD, Wander SA, Slingerland J. 2009. p27 as Jekyll and Hyde: Regulation of cell cycle and cell motility. *Cell cycle* **8**: 3455-3461.
- Larsen DH, Hari F, Clapperton JA, Gwerder M, Gutsche K, Altmeyer M, Jungmichel S, Toledo LI, Fink D, Rask MB et al. 2014. The NBS1-Treacle complex controls ribosomal RNA transcription in response to DNA damage. *Nature cell biology* **16**: 792-803.
- Larsen DH, Stucki M. 2016. Nucleolar responses to DNA double-strand breaks. *Nucleic acids research* **44**: 538-544.
- Le Bouteiller M, Souilhol C, Beck-Cormier S, Stedman A, Burlen-Defranoux O, Vandormael-Pournin S, Bernex F, Cumano A, Cohen-Tannoudji M. 2013. Notchless-dependent ribosome synthesis is required for the maintenance of adult hematopoietic stem cells. *The Journal of experimental medicine* **210**: 2351-2369.
- Leotoing L, Meunier L, Manin M, Mauduit C, Decaussin M, Verrijdt G, Claessens F, Benahmed M, Veyssiere G, Morel L et al. 2008. Influence of nucleophosmin/B23 on DNA binding and transcriptional activity of the androgen receptor in prostate cancer cell. *Oncogene* **27**: 2858-2867.
- Lessard F, Morin F, Ivanchuk S, Langlois F, Stefanovsky V, Rutka J, Moss T. 2010. The ARF tumor suppressor controls ribosome biogenesis by regulating the RNA polymerase I transcription factor TTF-I. *Molecular cell* **38**: 539-550.
- Lim MJ, Wang XW. 2006. Nucleophosmin and human cancer. *Cancer detection and prevention* **30**: 481-490.
- Lindstrom MS, Jurada D, Bursac S, Orsolich I, Bartek J, Volarevic S. 2018. Nucleolus as an emerging hub in maintenance of genome stability and cancer pathogenesis. *Oncogene* **37**: 2351-2366.
- Lindström MS, Nistér M. 2010. Silencing of ribosomal protein S9 elicits a multitude of cellular responses inhibiting the growth of cancer cells subsequent to p53 activation. *PloS one* **5**: e9578-e9578.

- Lipton JM, Ellis SR. 2009. Diamond-Blackfan anemia: diagnosis, treatment, and molecular pathogenesis. *Hematology/oncology clinics of North America* **23**: 261-282.
- Liu B, Zhang J, Huang C, Liu H. 2012a. Dyskerin overexpression in human hepatocellular carcinoma is associated with advanced clinical stage and poor patient prognosis. *PloS one* **7**: e43147-e43147.
- Liu T, Fang Y, Zhang H, Deng M, Gao B, Niu N, Yu J, Lee S, Kim J, Qin B et al. 2016. HEATR1 Negatively Regulates Akt to Help Sensitize Pancreatic Cancer Cells to Chemotherapy. *Cancer research* **76**: 572-581.
- Liu X, Liu D, Qian D, Dai J, An Y, Jiang S, Stanley B, Yang J, Wang B, Liu X et al. 2012b. Nucleophosmin (NPM1/B23) interacts with activating transcription factor 5 (ATF5) protein and promotes proteasome- and caspase-dependent ATF5 degradation in hepatocellular carcinoma cells. *The Journal of biological chemistry* **287**: 19599-19609.
- Llanos S, Serrano M. 2010. Depletion of ribosomal protein L37 occurs in response to DNA damage and activates p53 through the L11/MDM2 pathway. *Cell cycle* **9**: 4005-4012.
- Lodish HF. 1974. Model for the regulation of mRNA translation applied to haemoglobin synthesis. *Nature* **251**: 385-388.
- Madden E, Logue SE, Healy SJ, Manie S, Samali A. 2019. The role of the unfolded protein response in cancer progression: From oncogenesis to chemoresistance. *Biology of the Cell* **111**: 1-17.
- Maggi LB, Jr., Kuchenruether M, Dadey DY, Schwoppe RM, Grisendi S, Townsend RR, Pandolfi PP, Weber JD. 2008. Nucleophosmin serves as a rate-limiting nuclear export chaperone for the Mammalian ribosome. *Molecular and cellular biology* **28**: 7050-7065.
- Marcel V, Ghayad SE, Belin S, Therizols G, Morel AP, Solano-Gonzalez E, Vendrell JA, Hacot S, Mertani HC, Albaret MA et al. 2013. p53 acts as a safeguard of translational control by regulating fibrillarin and rRNA methylation in cancer. *Cancer cell* **24**: 318-330.
- Marechal A, Zou L. 2013. DNA damage sensing by the ATM and ATR kinases. *Cold Spring Harbor perspectives in biology* **5**.
- Mason PJ, Bessler M. 2011. The genetics of dyskeratosis congenita. *Cancer genetics* **204**: 635-645.
- Matsuoka S, Ballif BA, Smogorzewska A, McDonald ER, Hurov KE, Luo J, Bakalarski CE, Zhao Z, Solimini N, Lerenthal Y et al. 2007. ATM and ATR Substrate Analysis Reveals Extensive Protein Networks Responsive to DNA Damage. *Science* **316**: 1160.

- Mayer C, Zhao J, Yuan X, Grummt I. 2004. mTOR-dependent activation of the transcription factor TIF-IA links rRNA synthesis to nutrient availability. *Genes & development* **18**: 423-434.
- McStay B. 2016. Nucleolar organizer regions: genomic 'dark matter' requiring illumination. *Genes & development* **30**: 1598-1610.
- Mendoza MC, Er EE, Blenis J. 2011. The Ras-ERK and PI3K-mTOR pathways: cross-talk and compensation. *Trends in biochemical sciences* **36**: 320-328.
- Michael D, Oren M. 2003. The p53-Mdm2 module and the ubiquitin system. *Seminars in Cancer Biology* **13**: 49-58.
- Midgley CA, Desterro JMP, Saville MK, Howard S, Sparks A, Hay RT, Lane DP. 2000. An N-terminal p14ARF peptide blocks Mdm2-dependent ubiquitination in vitro and can activate p53 in vivo. *Oncogene* **19**: 2312.
- Moll UM, Wolff S, Speidel D, Deppert W. 2005. Transcription-independent proapoptotic functions of p53. *Current opinion in cell biology* **17**: 631-636.
- Moon HW, Han HG, Jeon YJ. 2018. Protein Quality Control in the Endoplasmic Reticulum and Cancer. *International journal of molecular sciences* **19**: 3020.
- Moss T. 2004. At the crossroads of growth control; making ribosomal RNA. *Current opinion in genetics & development* **14**: 210-217.
- Mullineux ST, Lafontaine DL. 2012. Mapping the cleavage sites on mammalian pre-rRNAs: where do we stand? *Biochimie* **94**: 1521-1532.
- Murano K, Okuwaki M, Hisaoka M, Nagata K. 2008. Transcription regulation of the rRNA gene by a multifunctional nucleolar protein, B23/nucleophosmin, through its histone chaperone activity. *Molecular and cellular biology* **28**: 3114-3126.
- Murayama A, Ohmori K, Fujimura A, Minami H, Yasuzawa-Tanaka K, Kuroda T, Oie S, Daitoku H, Okuwaki M, Nagata K et al. 2008. Epigenetic control of rDNA loci in response to intracellular energy status. *Cell* **133**: 627-639.
- Murray-Zmijewski F, Slee EA, Lu X. 2008. A complex barcode underlies the heterogeneous response of p53 to stress. *Nature reviews Molecular cell biology* **9**: 702-712.
- Nakhoul H, Ke J, Zhou X, Liao W, Zeng SX, Lu H. 2014. Ribosomopathies: mechanisms of disease. *Clinical medicine insights Blood disorders* **7**: 7-16.
- Narla A, Ebert BL. 2010. Ribosomopathies: human disorders of ribosome dysfunction. *Blood* **115**: 3196-3205.
- Nelson AS, Myers KC. 2018. Diagnosis, Treatment, and Molecular Pathology of Shwachman-Diamond Syndrome. *Hematology/oncology clinics of North America* **32**: 687-700.

- O'Neill T, Dwyer AJ, Ziv Y, Chan DW, Lees-Miller SP, Abraham RH, Lai JH, Hill D, Shiloh Y, Cantley LC et al. 2000. Utilization of Oriented Peptide Libraries to Identify Substrate Motifs Selected by ATM. *Journal of Biological Chemistry* **275**: 22719-22727.
- Ofir-Rosenfeld Y, Boggs K, Michael D, Kastan MB, Oren M. 2008. Mdm2 regulates p53 mRNA translation through inhibitory interactions with ribosomal protein L26. *Molecular cell* **32**: 180-189.
- Ogawa LM, Baserga SJ. 2017. Crosstalk between the nucleolus and the DNA damage response. *Molecular bioSystems* **13**: 443-455.
- Onofrillo C. 2013. Ribosome Biogenesis and cell cycle regulation: Effect of RNA Polymerase III inhibition [dissertation]. in *Oncologia e Patologia Sperimentale*. Università di Bologna.
- Orsolich I, Jurada D, Pullen N, Oren M, Eliopoulos AG, Volarevic S. 2016. The relationship between the nucleolus and cancer: Current evidence and emerging paradigms. *Seminars in Cancer Biology* **37-38**: 36-50.
- Padron E, Komrokji R, List AF. 2011. Biology and treatment of the 5q- syndrome. *Expert Review of Hematology* **4**: 61-69.
- Parlato R, Liss B. 2014. How Parkinson's disease meets nucleolar stress. *Biochimica et biophysica acta* **1842**: 791-797.
- Paule MR, White RJ. 2000. Survey and summary: transcription by RNA polymerases I and III. *Nucleic acids research* **28**: 1283-1298.
- Pellagatti A, Boultonwood J. 2015. Recent Advances in the 5q- Syndrome. *Mediterranean journal of hematology and infectious diseases* **7**: e2015037.
- Pellagatti A, Marafioti T, Paterson JC, Barlow JL, Drynan LF, Giagounidis A, Pileri SA, Cazzola M, McKenzie ANJ, Wainscoat JS et al. 2010. Induction of p53 and up-regulation of the p53 pathway in the human 5q- syndrome. *Blood* **115**: 2721.
- Peltonen K, Colis L, Liu H, Jaamaa S, Moore HM, Enback J, Laakkonen P, Vaahtokari A, Jones RJ, af Hallstrom TM et al. 2010. Identification of novel p53 pathway activating small-molecule compounds reveals unexpected similarities with known therapeutic agents. *PloS one* **5**: e12996.
- Peltonen K, Colis L, Liu H, Trivedi R, Moubarek MS, Moore HM, Bai B, Rudek MA, Bieberich CJ, Laiho M. 2014. A targeting modality for destruction of RNA polymerase I that possesses anticancer activity. *Cancer cell* **25**: 77-90.
- Perry J, Kleckner N. 2003. The ATRs, ATMs, and TORs Are Giant HEAT Repeat Proteins. *Cell* **112**: 151-155.
- Pianta A, Puppini C, Franzoni A, Fabbro D, Di Loreto C, Bulotta S, Deganuto M, Paron I, Tell G, Puxeddu E et al. 2010. Nucleophosmin is overexpressed in thyroid tumors. *Biochemical and biophysical research communications* **397**: 499-504.

- Picksley SM, Lane DP. 1993. What the papers say: The p53-mdm2 autoregulatory feedback loop: A paradigm for the regulation of growth control by p53? *BioEssays : news and reviews in molecular, cellular and developmental biology* **15**: 689-690.
- Plafker SM, Macara IG. 2002. Ribosomal Protein L12 Uses a Distinct Nuclear Import Pathway Mediated by Importin 11. *Molecular and cellular biology* **22**: 1266-1275.
- Poortinga G, Hannan KM, Snelling H, Walkley CR, Jenkins A, Sharkey K, Wall M, Brandenburger Y, Palatsides M, Pearson RB et al. 2004. MAD1 and c-MYC regulate UBF and rDNA transcription during granulocyte differentiation. *The EMBO journal* **23**: 3325-3335.
- Poortinga G, Wall M, Sanij E, Siwicki K, Ellul J, Brown D, Holloway TP, Hannan RD, McArthur GA. 2011. c-MYC coordinately regulates ribosomal gene chromatin remodeling and Pol I availability during granulocyte differentiation. *Nucleic acids research* **39**: 3267-3281.
- Posnick JC. 2014. Treacher Collins Syndrome. 1059-1094.
- Powell MA, Mutch DG, Rader JS, Herzog TJ, Huang TH, Goodfellow PJ. 2002. Ribosomal DNA methylation in patients with endometrial carcinoma: an independent prognostic marker. *Cancer* **94**: 2941-2952.
- Prieto JL, McStay B. 2007. Recruitment of factors linking transcription and processing of pre-rRNA to NOR chromatin is UBF-dependent and occurs independent of transcription in human cells. *Genes & development* **21**: 2041-2054.
- Qi W, Shakalya K, Stejskal A, Goldman A, Beeck S, Cooke L, Mahadevan D. 2008. NSC348884, a nucleophosmin inhibitor disrupts oligomer formation and induces apoptosis in human cancer cells. *Oncogene* **27**: 4210.
- Qin F-X, Shao H-Y, Chen X-C, Tan S, Zhang H-J, Miao Z-Y, Wang L, Hui C, Zhang L. 2011. Knockdown of NPM1 by RNA interference inhibits cells proliferation and induces apoptosis in leukemic cell line. *International journal of medical sciences* **8**: 287-294.
- Qu G-z, Grundy PE, Narayan A, Ehrlich M. 1999. Frequent Hypomethylation in Wilms Tumors of Pericentromeric DNA in Chromosomes 1 and 16. *Cancer Genetics and Cytogenetics* **109**: 34-39.
- Qu J, Bishop JM. 2012. Nucleostemin maintains self-renewal of embryonic stem cells and promotes reprogramming of somatic cells to pluripotency. *The Journal of cell biology* **197**: 731-745.
- Quelle DE, Zindy F, Ashmun RA, Sherr CJ. 1995. Alternative reading frames of the INK4a tumor suppressor gene encode two unrelated proteins capable of inducing cell cycle arrest. *Cell* **83**: 993-1000.
- Quin JE, Devlin JR, Cameron D, Hannan KM, Pearson RB, Hannan RD. 2014. Targeting the nucleolus for cancer intervention. *Biochimica et biophysica acta* **1842**: 802-816.

- Rich T, Allen RL, Wyllie AH. 2000. Defying death after DNA damage. *Nature* **407**: 777.
- Rogakou EP, Pilch DR, Orr AH, Ivanova VS, Bonner WM. 1998. DNA Double-stranded Breaks Induce Histone H2AX Phosphorylation on Serine 139. *Journal of Biological Chemistry* **273**: 5858-5868.
- Roger B, Moisan A, Amalric F, Bouvet P. 2003. Nucleolin provides a link between RNA polymerase I transcription and pre-ribosome assembly. *Chromosoma* **111**: 399-407.
- Rosenberg JE, Bambury RM, Van Allen EM, Drabkin HA, Lara PN, Jr., Harzstark AL, Wagle N, Figlin RA, Smith GW, Garraway LA et al. 2014. A phase II trial of AS1411 (a novel nucleolin-targeted DNA aptamer) in metastatic renal cell carcinoma. *Investigational new drugs* **32**: 178-187.
- Rout MP, Blobel G, Aitchison JD. 1997. A Distinct Nuclear Import Pathway Used by Ribosomal Proteins. *Cell* **89**: 715-725.
- Rubbi CP, Milner J. 2003. Disruption of the nucleolus mediates stabilization of p53 in response to DNA damage and other stresses. *The EMBO journal* **22**: 6068-6077.
- Rudra D, Warner JR. 2004. What better measure than ribosome synthesis? *Genes & development* **18**: 2431-2436.
- Ruggero D. 2013. Translational control in cancer etiology. *Cold Spring Harbor perspectives in biology* **5**.
- Ruggero D, Pandolfi PP. 2003. Does the ribosome translate cancer? *Nature reviews Cancer* **3**: 179-192.
- Russell J, Zomerdijk JC. 2005. RNA-polymerase-I-directed rDNA transcription, life and works. *Trends in biochemical sciences* **30**: 87-96.
- Russo A, Esposito D, Catillo M, Pietropaolo C, Crescenzi E, Russo G. 2013. Human rpL3 induces G<sub>1</sub>/S arrest or apoptosis by modulating p21 (waf1/cip1) levels in a p53-independent manner. *Cell cycle (Georgetown, Tex)* **12**: 76-87.
- Sakai D, Dixon J, Achilleos A, Dixon M, Trainor PA. 2016. Prevention of Treacher Collins syndrome craniofacial anomalies in mouse models via maternal antioxidant supplementation. *Nature communications* **7**: 10328-10328.
- Sakai D, Dixon J, Dixon MJ, Trainor PA. 2012. Mammalian Neurogenesis Requires Treacle-Plk1 for Precise Control of Spindle Orientation, Mitotic Progression, and Maintenance of Neural Progenitor Cells. *PLoS genetics* **8**: e1002566.
- Sakai D, Trainor PA. 2009. Treacher Collins syndrome: unmasking the role of Tcof1/treacle. *The international journal of biochemistry & cell biology* **41**: 1229-1232.
- Sanchez CG, Teixeira FK, Czech B, Preall JB, Zamparini AL, Seifert JRK, Malone CD, Hannon GJ, Lehmann R. 2016. Regulation of Ribosome Biogenesis and Protein

- Synthesis Controls Germline Stem Cell Differentiation. *Cell stem cell* **18**: 276-290.
- Saporita AJ, Chang H-C, Winkeler CL, Apicelli AJ, Kladney RD, Wang J, Townsend RR, Michel LS, Weber JD. 2011. RNA helicase DDX5 is a p53-independent target of ARF that participates in ribosome biogenesis. *Cancer research* **71**: 6708-6717.
- Savkur RS, Olson MO. 1998. Preferential cleavage in pre-ribosomal RNA by protein B23 endoribonuclease. *Nucleic acids research* **26**: 4508-4515.
- Scheffner M, Werness BA, Huibregtse JM, Levine AJ, Howley PM. 1990. The E6 oncoprotein encoded by human papillomavirus types 16 and 18 promotes the degradation of p53. *Cell* **63**: 1129-1136.
- Scott DD, Oeffinger M. 2016. Nucleolin and nucleophosmin: nucleolar proteins with multiple functions in DNA repair. *Biochemistry and Cell Biology* **94**: 419-432.
- Scott PH, Cairns CA, Sutcliffe JE, Alzuherri HM, McLees A, Winter AG, White RJ. 2001. Regulation of RNA Polymerase III Transcription during Cell Cycle Entry. *Journal of Biological Chemistry* **276**: 1005-1014.
- Sekhar KR, Benamar M, Venkateswaran A, Sasi S, Penthala NR, Crooks PA, Hann SR, Geng L, Balusu R, Abbas T et al. 2014. Targeting nucleophosmin 1 represents a rational strategy for radiation sensitization. *International journal of radiation oncology, biology, physics* **89**: 1106-1114.
- Shav-Tal Y, Blechman J, Darzacq X, Montagna C, Dye BT, Patton JG, Singer RH, Zipori D. 2005. Dynamic sorting of nuclear components into distinct nucleolar caps during transcriptional inhibition. *Molecular biology of the cell* **16**: 2395-2413.
- Sherr CJ. 2006. Divorcing ARF and p53: an unsettled case. *Nature reviews Cancer* **6**: 663-673.
- Sherr CJ. 2012. Ink4-Arf locus in cancer and aging. *Wiley interdisciplinary reviews Developmental biology* **1**: 731-741.
- Shi Y, Zhai H, Wang X, Han Z, Liu C, Lan M, Du J, Guo C, Zhang Y, Wu K et al. 2004. Ribosomal proteins S13 and L23 promote multidrug resistance in gastric cancer cells by suppressing drug-induced apoptosis. *Experimental cell research* **296**: 337-346.
- Shiue CN, Berkson RG, Wright AP. 2009. c-Myc induces changes in higher order rDNA structure on stimulation of quiescent cells. *Oncogene* **28**: 1833-1842.
- Sieron P, Hader C, Hatina J, Engers R, Wlazlinski A, Muller M, Schulz WA. 2009. DKC1 overexpression associated with prostate cancer progression. *British journal of cancer* **101**: 1410-1416.
- Sikora K, Advani S, Fau - Koroltchouk V, Koroltchouk V, Fau - Magrath I, Magrath I, Fau - Levy L, Levy L, Fau - Pinedo H, Pinedo H, Fau - Schwartzmann G, Schwartzmann G, Fau - Tattersall M, Tattersall M, Fau - Yan S, Yan S. 1999. Essential drugs for



- cancer therapy: a World Health Organization consultation. *Annals of Oncology* **10**: 385-390.
- Sirri V, Urcuqui-Inchima S, Roussel P, Hernandez-Verdun D. 2008. Nucleolus: the fascinating nuclear body. *Histochemistry and cell biology* **129**: 13-31.
- Skrott Z, Mistrik M, Andersen KK, Friis S, Majera D, Gursky J, Ozdian T, Bartkova J, Turi Z, Moudry P et al. 2017. Alcohol-abuse drug disulfiram targets cancer via p97 segregase adaptor NPL4. *Nature* **552**: 194-199.
- Sloan KE, Bohnsack MT, Watkins NJ. 2013. The 5S RNP couples p53 homeostasis to ribosome biogenesis and nucleolar stress. *Cell reports* **5**: 237-247.
- Sørensen PD, Frederiksen S. 1991. Characterization of human 5S rRNA genes. *Nucleic acids research* **19**: 4147-4151.
- Soundararajan S, Chen W, Spicer EK, Courtenay-Luck N, Fernandes DJ. 2008. The nucleolin targeting aptamer AS1411 destabilizes Bcl-2 messenger RNA in human breast cancer cells. *Cancer research* **68**: 2358-2365.
- Stefanovsky V, Langlois F, Gagnon-Kugler T, Rothblum LI, Moss T. 2006. Growth factor signaling regulates elongation of RNA polymerase I transcription in mammals via UBF phosphorylation and r-chromatin remodeling. *Molecular cell* **21**: 629-639.
- Stefanovsky VY, Moss T. 2008. The splice variants of UBF differentially regulate RNA polymerase I transcription elongation in response to ERK phosphorylation. *Nucleic acids research* **36**: 5093-5101.
- Stuart RK, Stockerl-Goldstein K, Cooper M, Devetten M, Herzig R, Medeiros B, Schiller G, Wei A, Acton G, Rizzieri D. 2009. Randomized phase II trial of the nucleolin targeting aptamer AS1411 combined with high-dose cytarabine in relapsed/refractory acute myeloid leukemia (AML). *Journal of Clinical Oncology* **27**: 7019-7019.
- Stults DM, Killen MW, Williamson EP, Hourigan JS, Vargas HD, Arnold SM, Moscow JA, Pierce AJ. 2009. Human rRNA gene clusters are recombinational hotspots in cancer. *Cancer research* **69**: 9096-9104.
- Su H, Xu T, Ganapathy S, Shadfai M, Long M, Huang THM, Thompson I, Yuan ZM. 2013. Elevated snoRNA biogenesis is essential in breast cancer. *Oncogene* **33**: 1348-1358.
- Sulima SO, Hofman IJF, De Keersmaecker K, Dinman JD. 2017. How Ribosomes Translate Cancer. *Cancer discovery* **7**: 1069-1087.
- Sun XX, Wang YG, Xirodimas DP, Dai MS. 2010. Perturbation of 60 S ribosomal biogenesis results in ribosomal protein L5- and L11-dependent p53 activation. *The Journal of biological chemistry* **285**: 25812-25821.

- Swaminathan V, Kishore AH, Febitha KK, Kundu TK. 2005. Human histone chaperone nucleophosmin enhances acetylation-dependent chromatin transcription. *Molecular and cellular biology* **25**: 7534-7545.
- Tajrishi MM, Tuteja R, Tuteja N. 2011. Nucleolin: The most abundant multifunctional phosphoprotein of nucleolus. *Communicative & integrative biology* **4**: 267-275.
- Takagi M, Absalon MJ, McLure KG, Kastan MB. 2005. Regulation of p53 translation and induction after DNA damage by ribosomal protein L26 and nucleolin. *Cell* **123**: 49-63.
- Thomas F, Kutay U. 2003. Biogenesis and nuclear export of ribosomal subunits in higher eukaryotes depend on the CRM1 export pathway. *Journal of cell science* **116**: 2409.
- Toledo F, Wahl GM. 2006. Regulating the p53 pathway: in vitro hypotheses, in vivo veritas. *Nature reviews Cancer* **6**: 909-923.
- Tsai RYL, McKay RDG. 2002. A nucleolar mechanism controlling cell proliferation in stem cells and cancer cells. *Genes & development* **16**: 2991-3003.
- Tsekrekou M, Stratigi K, Chatzinikolaou G. 2017. The Nucleolus: In Genome Maintenance and Repair. *International journal of molecular sciences* **18**.
- Tsui KH, Cheng AJ, Chang P, Pan TL, Yung BY. 2004. Association of nucleophosmin/B23 mRNA expression with clinical outcome in patients with bladder carcinoma. *Urology* **64**: 839-844.
- Uechi T, Tanaka T, Kenmochi N. 2001. A complete map of the human ribosomal protein genes: assignment of 80 genes to the cytogenetic map and implications for human disorders. *Genomics* **72**: 223-230.
- Valdez BC, Henning D, So RB, Dixon J, Dixon MJ. 2004. The Treacher Collins syndrome (TCOF1) gene product is involved in ribosomal DNA gene transcription by interacting with upstream binding factor. *Proceedings of the National Academy of Sciences of the United States of America* **101**: 10709-10714.
- van den Boom J, Meyer H. 2018. VCP/p97-Mediated Unfolding as a Principle in Protein Homeostasis and Signaling. *Molecular cell* **69**: 182-194.
- van Riggelen J, Yetil A, Felsher DW. 2010. MYC as a regulator of ribosome biogenesis and protein synthesis. *Nature reviews Cancer* **10**: 301-309.
- van Sluis M, McStay B. 2015. A localized nucleolar DNA damage response facilitates recruitment of the homology-directed repair machinery independent of cell cycle stage. *Genes & development* **29**: 1151-1163.
- Velimezi G, Lontos M, Vougas K, Roumeliotis T, Bartkova J, Sideridou M, Dereli-Oz A, Kocylowski M, Pateras IS, Evangelou K et al. 2013. Functional interplay between the DNA-damage-response kinase ATM and ARF tumour suppressor protein in human cancer. *Nature cell biology* **15**: 967.

- Volarević S, Stewart MJ, Ledermann B, Zilberman F, Terracciano L, Montini E, Grompe M, Kozma SC, Thomas G. 2000. Proliferation, But Not Growth, Blocked by Conditional Deletion of 40S Ribosomal Protein S6. *Science* **288**: 2045.
- Vousden KH, Prives C. 2009. Blinded by the Light: The Growing Complexity of p53. *Cell* **137**: 413-431.
- Vulliamy T, Beswick R, Kirwan M, Marrone A, Digweed M, Walne A, Dokal I. 2008. Mutations in the telomerase component NHP2 cause the premature ageing syndrome dyskeratosis congenita. *Proceedings of the National Academy of Sciences of the United States of America* **105**: 8073-8078.
- Walne AJ, Vulliamy T, Marrone A, Beswick R, Kirwan M, Masunari Y, Al-Qurashi F-H, Aljurf M, Dokal I. 2007. Genetic heterogeneity in autosomal recessive dyskeratosis congenita with one subtype due to mutations in the telomerase-associated protein NOP10. *Human molecular genetics* **16**: 1619-1629.
- Warner JR. 1977. In the absence of ribosomal RNA synthesis, the ribosomal proteins of HeLa Cells are synthesized normally and degraded rapidly. *Journal of molecular biology* **115**: 315-333.
- Warner JR, McIntosh KB. 2009. How common are extraribosomal functions of ribosomal proteins? *Molecular cell* **34**: 3-11.
- Warner JR, Mitra G, Schwindinger WF, Studeny M, Fried HM. 1985. *Saccharomyces cerevisiae* coordinates accumulation of yeast ribosomal proteins by modulating mRNA splicing, translational initiation, and protein turnover. *Molecular and cellular biology* **5**: 1512-1521.
- Watanabe-Susaki K, Takada H, Enomoto K, Miwata K, Ishimine H, Intoh A, Ohtaka M, Nakanishi M, Sugino H, Asashima M et al. 2014. Biosynthesis of ribosomal RNA in nucleoli regulates pluripotency and differentiation ability of pluripotent stem cells. *Stem cells* **32**: 3099-3111.
- Watkins NJ, Bohnsack MT. 2012. The box C/D and H/ACA snoRNPs: key players in the modification, processing and the dynamic folding of ribosomal RNA. *Wiley interdisciplinary reviews RNA* **3**: 397-414.
- Weis F, Giudice E, Churcher M, Jin L, Hilcenko C, Wong CC, Traynor D, Kay RR, Warren AJ. 2015. Mechanism of eIF6 release from the nascent 60S ribosomal subunit. *Nature structural & molecular biology* **22**: 914-919.
- Werner A, Iwasaki S, McGourty CA, Medina-Ruiz S, Teerikorpi N, Fedrigo I, Ingolia NT, Rape M. 2015. Cell-fate determination by ubiquitin-dependent regulation of translation. *Nature* **525**: 523-527.
- Werness BA, Levine AJ, Howley PM. 1990. Association of human papillomavirus types 16 and 18 E6 proteins with p53. *Science* **248**: 76.
- Wild T, Horvath P, Wyler E, Widmann B, Badertscher L, Zemp I, Kozak K, Csucs G, Lund E, Kutay U. 2010. A Protein Inventory of Human Ribosome Biogenesis

- Reveals an Essential Function of Exportin 5 in 60S Subunit Export. *PLOS Biology* **8**: e1000522.
- Wilson DB, Link DC, Mason PJ, Bessler M. 2014. Inherited bone marrow failure syndromes in adolescents and young adults. *Annals of medicine* **46**: 353-363.
- Wilson DN, Doudna Cate JH. 2012. The structure and function of the eukaryotic ribosome. *Cold Spring Harbor perspectives in biology* **4**.
- Woiwode A, Johnson SA, Zhong S, Zhang C, Roeder RG, Teichmann M, Johnson DL. 2008. PTEN represses RNA polymerase III-dependent transcription by targeting the TFIIB complex. *Molecular and cellular biology* **28**: 4204-4214.
- Wolin SL, Cedervall T. 2002. The La Protein. *Annual review of biochemistry* **71**: 375-403.
- Wong CC, Traynor D, Basse N, Kay RR, Warren AJ. 2011. Defective ribosome assembly in Shwachman-Diamond syndrome. *Blood* **118**: 4305-4312.
- Wong JC, Hasan MR, Rahman M, Yu AC, Chan SK, Schaeffer DF, Kennecke HF, Lim HJ, Owen D, Tai IT. 2013. Nucleophosmin 1, upregulated in adenomas and cancers of the colon, inhibits p53-mediated cellular senescence. *International journal of cancer* **133**: 1567-1577.
- Wu ZB, Qiu C, Zhang AL, Cai L, Lin SJ, Yao Y, Tang QS, Xu M, Hua W, Chu YW et al. 2014. Glioma-associated antigen HEATR1 induces functional cytotoxic T lymphocytes in patients with glioma. *Journal of immunology research* **2014**: 131494.
- Xu H, Di Antonio M, McKinney S, Mathew V, Ho B, O'Neil NJ, Santos ND, Silvester J, Wei V, Garcia J et al. 2017. CX-5461 is a DNA G-quadruplex stabilizer with selective lethality in BRCA1/2 deficient tumours. *Nature communications* **8**: 14432.
- Yadavilli S, Mayo LD, Higgins M, Lain S, Hegde V, Deutsch WA. 2009. Ribosomal protein S3: A multi-functional protein that interacts with both p53 and MDM2 through its KH domain. *DNA repair* **8**: 1215-1224.
- Yang A, Shi G, Zhou C, Lu R, Li H, Sun L, Jin Y. 2011. Nucleolin maintains embryonic stem cell self-renewal by suppression of p53 protein-dependent pathway. *The Journal of biological chemistry* **286**: 43370-43382.
- Yang K, Yang J, Yi J. 2018. Nucleolar Stress: hallmarks, sensing mechanism and diseases. *Cell Stress* **2:6**: 125 - 140.
- Yoon A, Peng G, Brandenburger Y, Zollo O, Xu W, Rego E, Ruggero D. 2006. Impaired control of IRES-mediated translation in X-linked dyskeratosis congenita. *Science* **312**: 902-906.
- Yoshimura SH, Hirano T. 2016. HEAT repeats - versatile arrays of amphiphilic helices working in crowded environments? *Journal of cell science* **129**: 3963-3970.

- Yu Y, Maggi LB, Jr., Brady SN, Apicelli AJ, Dai M-S, Lu H, Weber JD. 2006. Nucleophosmin is essential for ribosomal protein L5 nuclear export. *Molecular and cellular biology* **26**: 3798-3809.
- Yuan F, Tong T. 2018. *Nucleolus Modulates the Shuttle of Telomere Components between Nucleolus and Telomere*.
- Yuan X, Zhou Y, Casanova E, Chai M, Kiss E, Grone HJ, Schutz G, Grummt I. 2005. Genetic inactivation of the transcription factor TIF-IA leads to nucleolar disruption, cell cycle arrest, and p53-mediated apoptosis. *Molecular cell* **19**: 77-87.
- Yusupova G, Yusupov M. 2014. High-resolution structure of the eukaryotic 80S ribosome. *Annual review of biochemistry* **83**: 467-486.
- Zhai W, Comai L. 2000. Repression of RNA polymerase I transcription by the tumor suppressor p53. *Molecular and cellular biology* **20**: 5930-5938.
- Zhang C, Comai L, Johnson DL. 2005a. PTEN represses RNA Polymerase I transcription by disrupting the SL1 complex. *Molecular and cellular biology* **25**: 6899-6911.
- Zhang J, Harnpicharnchai P, Jakovljevic J, Tang L, Guo Y, Oeffinger M, Rout MP, Hiley SL, Hughes T, Woolford JL, Jr. 2007. Assembly factors Rpf2 and Rrs1 recruit 5S rRNA and ribosomal proteins rpL5 and rpL11 into nascent ribosomes. *Genes & development* **21**: 2580-2592.
- Zhang J, Zhao H-L, He J-F, Li H-Y. 2012. *Inhibitory Effect of NSC348884, a small molecular inhibitor of nucleophosmin, on the growth of hepatocellular carcinoma cell line HepG2*.
- Zhang Y, Lu H. 2009. Signaling to p53: ribosomal proteins find their way. *Cancer cell* **16**: 369-377.
- Zhang Y, Wang J, Yuan Y, Zhang W, Guan W, Wu Z, Jin C, Chen H, Zhang L, Yang X et al. 2010. Negative regulation of HDM2 to attenuate p53 degradation by ribosomal protein L26. *Nucleic acids research* **38**: 6544-6554.
- Zhang Z, Wang H, Li M, Rayburn ER, Agrawal S, Zhang R. 2005b. Stabilization of E2F1 protein by MDM2 through the E2F1 ubiquitination pathway. *Oncogene* **24**: 7238-7247.
- Zhao J, Yuan X, Frödin M, Grummt I. 2003. ERK-Dependent Phosphorylation of the Transcription Initiation Factor TIF-IA Is Required for RNA Polymerase I Transcription and Cell Growth. *Molecular cell* **11**: 405-413.
- Zhou X, Hao Q, Liao J, Zhang Q, Lu H. 2013. Ribosomal protein S14 unties the MDM2-p53 loop upon ribosomal stress. *Oncogene* **32**: 388-396.
- Zhou X, Liao WJ, Liao JM, Liao P, Lu H. 2015. Ribosomal proteins: functions beyond the ribosome. *Journal of molecular cell biology* **7**: 92-104.

- Zhou Y, Shen J, Xia L, Wang Y. 2014. Estrogen mediated expression of nucleophosmin 1 in human endometrial carcinoma clinical stages through estrogen receptor-alpha signaling. *Cancer cell international* **14**: 540.
- Zhu Y, Poyurovsky MV, Li Y, Biderman L, Stahl J, Jacq X, Prives C. 2009. Ribosomal protein S7 is both a regulator and a substrate of MDM2. *Molecular cell* **35**: 316-326.
- Zilfou JT, Lowe SW. 2009. Tumor suppressive functions of p53. *Cold Spring Harbor perspectives in biology* **1**: a001883-a001883.
- Zink D, Fischer AH, Nickerson JA. 2004. Nuclear structure in cancer cells. *Nature reviews Cancer* **4**: 677-687.

## 7. ABBREVIATIONS

3'-ETS	3'external transcribed spacer
40S or SSU	small ribosomal subunit
5'-ETS	5'external transcribed spacer
5q-	5q- syndrome
5S RNP	5S ribonucleoprotein
60S or LSU	large ribosomal subunit
ActD	actinomycin D
AKT	protein kinase B alpha
AML	acute myeloid leukemia
ARF	alternative reading frame protein
ATM	ataxia telangiectasia mutated
ATR	ataxia telangiectasia and Rad3-related protein
box C/D snoRNP	box C/D small nucleolar ribonucleoprotein
box H/ACA snoRNP	box H/ACA small nucleolar ribonucleoprotein
CDK	cyclin-dependent kinase
CHX	cycloheximide
CuET	ditiocarb-copper complex
DBA	Diamond-Blackfan anemia
DC	Dyskeratosis congenita
DDR	DNA damage response
DFC	dense fibrillar component
DMEM	Dulbecco's modified Eagle's medium
DSB	double strand break
EdU	5-ethynyl-2'-deoxyuridine
EFL1	elongation factor like-1 GTPase enzyme
eIF6	eukaryotic translation initiation factor 6
ER	endoplasmatic reticulum
ERK	extracellular-signal regulated kinase
EU	5-ethynyl uridine

FBL	fibrillar
FC	fibrillar center
GC	granular component
GC	guanosine-cytosine
H3K27me3	trimethylation of histone 3 lysine 27
H3K4me3	trimethylation of histone 3 lysine 4
H3K9me2/3	di- or trimethylation of histone 3 lysine 9
H4ac	acetylation of histone 4
H4K20me3	trimethylation of histone 4 lysine 20
HEATR1	HEAT repeat containing 1
HPV	human papilloma virus
HRP	horseradish peroxidase
IGS	intergenic spacer
INB	intranucleolar body
IR	ionizing radiation
IRBC	impaired ribosome biogenesis checkpoint
IRES	internal ribosome entry site
IRIF	irradiation-induced foci
ITS1	internal transcribed spacer 1
ITS2	internal transcribed spacer 2
LSB	Laemmli sample buffer
MAPK	mitogen-activated protein kinase
MDC1	mediator of DNA damage checkpoint
mRNA	messenger RNA
mTOR	mammalian target of rapamycin
NBS1	Nijmegen breakage syndrome 1
NCL	nucleolin
NOR	nucleolar organizer region
NoRC	nucleolar remodeling complex
NPC	nuclear pore complex
NPM	nucleophosmin



NS	nucleostemin
PBS	phosphate buffered saline
PDAC	pancreatic ductal adenocarcinoma
PI3K	phosphatidylinositol 3-kinase
PIC	pre-initiation complex
PIKK	phosphatidylinositole 3-kinase-related kinase
PIM1	proto-oncogene serine/threonine-protein kinase 1
Pol I	RNA polymerase I
Pol II	RNA Polymerase II
Pol III	RNA Polymerase III
PP2A	protein phosphatase 2A
pRB	retinoblastoma protein
pSer15-p53	p53 phosphorylated on the serine 15 residue
PTMs	posttranslational modifications
PTRF1	Pol I and transcript-release factor 1
rDNA	ribosomal DNA
RNAi	RNA interference
ROS	reactive oxygen species
RP	ribosomal protein
RPL	large subunit ribosomal protein
RPS	small subunit ribosomal protein
rRNA	ribosomal RNA
S6K	ribosomal protein S6 kinase
SDS	Shwachman-Diamond syndrome
SDS-PAGE	sodium dodecyl sulfate–polyacrylamide gel electrophoresis
Ser1492	serine 1492 residue
SL1/TIF1-B	selectivity factor
snoRNP	small nucleolar ribonucleoprotein
TCS	Treacher-Collins syndrome
TERC	telomerase RNA component
TERT	telomerase reverse transcriptase

TFIIIA	transcription factor IIIA
TFIIIB	transcription factor IIIB
TFIIIC	transcription factor IIIC
TIF1-A/hRRN3	transcription initiation factor 1A
tRNA	transfer RNA
TTF-1	transcription termination factor 1
t-UTP	transcriptional U three protein
UBF	upstream binding factor
UCE	upstream core element
UPR	unfolded protein response
UV	ultraviolet light
X-DC	X-linked form of Dyskeratosis congenita

## 8. BIBLIOGRAPHY

### 8.1. Original articles and reviews

Vesela, E.; Chroma, K.; **Turi, Z.**; Mistrik, M. Common Chemical Inductors of Replication Stress: Focus on Cell-Based Studies. *Biomolecules* **2017**, *7*, 19. IF: no IF

**Turi, Z.**; Senkyrikova, M.; Mistrik, M.; Bartek, J.; Moudry, P. Perturbation of RNA Polymerase I transcription machinery by ablation of HEATR1 triggers the RPL5/RPL11-MDM2-p53 ribosome biogenesis stress checkpoint pathway in human cells. *Cell Cycle*. **2017**. IF (2017/2018): 3.304

Skrott, Z.; Mistrik, M.; Andersen, K.; Friis, S.; Majera, D.; Gursky, J.; Ozdian, T.; Bartkova, J.; **Turi, Z.**; Moudry, P.; Kraus, M.; Medvedikova M.; Vaclavkova, J.; Dzubak, P.; Vrobel, I.; Pouckova, P.; Sedlacek, J.; Miklovicova, A.; Kutt, A.; Mattova, J.; Driessen, C.; Dou, Q.; Olsen, J.; Hajduch, M.; Cvek, B.; Deshaies, R.; Bartek, J. Alcohol-abuse drug disulfiram targets cancer via p97 segregase adaptor NPL4. *Nature*. **2017**, *552*(7684), 194-199. IF (2017/2018): 41.577

**Turi, Z.**; Lacey, M.; Mistrik, M.; Moudry, P. Impaired ribosome biogenesis: mechanisms and relevance to cancer and aging. *Aging*. In press (**2019**). IF (2019) not defined yet

### 8.2. Conference lectures and poster presentations

#### 8.2.2. Oral talks

**Turi, Z.**; Senkyrikova, M.; Mistrik, M.; Bartek, J.; Moudry, P. Downregulation of HEATR1 impairs ribosome biogenesis and activates p53 via RPL5/RPL11-MDM2 pathway. Biomania Student Scientific Meeting; October 3, 2017.

**Turi, Z.**; Senkyrikova, M.; Mistrik, M.; Bartek, J.; Moudry, P. Downregulation of HEATR1 activates p53 and induces ribosomal stress. Diagnostic, Predictive and Experimental Oncology Days; November 28-30, 2017.

### 8.2.3. Poster presentations

**Turi Z.;** Senkyrikova, M.; Yamada, M.; Bartek, J. Ubiquitin specific peptidase 7 (USP7) regulates DNA damage bypass pathway through stabilizing Cdc7 kinase and RAD18 ubiquitin ligase. Diagnostic, Predictive and Experimental Oncology Days; December 02-03, 2014.

**Turi Z.;** Senkyrikova, M.; Yamada, M.; Bartek, J. Ubiquitin specific peptidase 7 (USP7) regulates DNA damage bypass pathway through stabilizing Cdc7 kinase and RAD18 ubiquitin ligase. DNA repair & genome stability in a chromatin environment IMB Conference; June 04-07, 2015.

**Turi Z.;** Senkyrikova, M.; Yamada, M.; Bartek, J. Ubiquitin specific peptidase 7 (USP7) regulates DNA damage bypass pathway through stabilizing Cdc7 kinase and RAD18 ubiquitin ligase. The Biomania Student Scientific Meeting; September 22, 2015.

### 8.3. Appendix – Full text publications related to the thesis

#### 8.3.1. Appendix A

Vesela, E.; Chroma, K.; **Turi, Z.**; Mistrik, M. Common Chemical Inductors of Replication Stress: Focus on Cell-Based Studies. *Biomolecules* **2017**, 7, 19. IF: no IF

Review

# Common Chemical Inductors of Replication Stress: Focus on Cell-Based Studies

Eva Vesela <sup>1,2</sup>, Katarina Chroma <sup>1</sup>, Zsofia Turi <sup>1</sup> and Martin Mistrik <sup>1,\*</sup>

<sup>1</sup> Institute of Molecular and Translational Medicine, Faculty of Medicine and Dentistry, Palacky University, Hnevotinska 5, Olomouc 779 00, Czech Republic; eva.vesela@upol.cz (E.V.); katarina.chroma@upol.cz (K.C.); zsofia.turi01@upol.cz (Z.T.)

<sup>2</sup> MRC Laboratory for Molecular Cell Biology, University College London, London WC1E 6BT, UK

\* Correspondence: martin.mistrik@upol.cz; Tel.: +420-585-634-170

Academic Editor: Rob de Bruin

Received: 25 November 2016; Accepted: 10 February 2017; Published: 21 February 2017

**Abstract:** DNA replication is a highly demanding process regarding the energy and material supply and must be precisely regulated, involving multiple cellular feedbacks. The slowing down or stalling of DNA synthesis and/or replication forks is referred to as replication stress (RS). Owing to the complexity and requirements of replication, a plethora of factors may interfere and challenge the genome stability, cell survival or affect the whole organism. This review outlines chemical compounds that are known inducers of RS and commonly used in laboratory research. These compounds act on replication by direct interaction with DNA causing DNA crosslinks and bulky lesions (cisplatin), chemical interference with the metabolism of deoxyribonucleotide triphosphates (hydroxyurea), direct inhibition of the activity of replicative DNA polymerases (aphidicolin) and interference with enzymes dealing with topological DNA stress (camptothecin, etoposide). As a variety of mechanisms can induce RS, the responses of mammalian cells also vary. Here, we review the activity and mechanism of action of these compounds based on recent knowledge, accompanied by examples of induced phenotypes, cellular readouts and commonly used doses.

**Keywords:** replication stress; cisplatin; aphidicolin; hydroxyurea; camptothecin; etoposide; cancer

---

## 1. Introduction

The DNA molecule always has to keep the middle ground: it must be sufficiently rigid to maintain correct genetic information while at the same time available for ongoing processes. DNA is particularly vulnerable to insults during replication, a process where a copy of the genome is generated [1]. Replication must be tightly regulated because it is essential for genome integrity, and therefore the fate of a new cellular generation. Accurate coordination of several cellular pathways is needed to provide sufficient energy and material supply, precise timing and functional repair to overcome arising difficulties [1].

Transient slowing or disruption of replication fork (RF) progression is called replication stress (RS), which can be caused by a limitation of important factors and/or obstacles caused by intrinsic and extrinsic sources [2]. Intrinsic sources of RS involve the physiological properties of the DNA molecule, such as regions of heterochromatin structure, origin-poor regions or sites rich in some types of repetitive sequences [3–5]. Other intrinsic sources of RS are generated by deregulated pathways that cause over- and under-replication [6–8], re-replication (also known as re-duplication) [9,10], or by transcription and replication machinery collisions [9].

The most common extrinsic sources of RS are all wavelengths of ultraviolet radiation (UV) [11], ionising radiation (IR) [12] and special genotoxic chemical compounds [13] which are the main focus of this review. RS-inducing chemicals can cause a broad spectrum of DNA lesions. Alkylating agents

such as methyl-methane sulfonate (MMS) [14], temozolomide and dacarbazine [15] directly modify DNA by attaching an alkyl group that presents an obstacle to RF progression. Moreover, the bifunctional alkylating compounds (e.g., mustard gas) can cause the crosslinking of guanine nucleobases [16,17] that violate the DNA structure even further [18]. Typical crosslinking agents introduce covalent bonds between nucleotides located on the same strand (intrastrand crosslinks), like cisplatin, or opposite strands (interstrand crosslink), like mitomycin C, and psoralens [18]. Crosslinks make the strands unable to uncoil and/or separate and physically block RF progression [19]. Even a small amount of unrepaired crosslinks (approx. 100–500) is reported to be lethal to a mammalian cell [20]. Furthermore, single-strand DNA breaks (SSB) and double-strand DNA breaks (DSB) represent a specific problem for ongoing replication which is well manifested by increased sensitivity of replicating cells towards radiomimetic compounds (e.g., neocarzinostatin) [21]. Other compounds do not damage the DNA structure directly but rather interfere with replication-related enzymes. Aphidicolin, an inhibitor of replicative DNA polymerases leads to uncoupling of the replicon and generation of long stretches of single-stranded DNA (ssDNA) [22]. After hydroxyurea treatment, an inhibitor of ribonucleotide reductase (RNR), the metabolism of deoxyribonucleotide triphosphates (dNTPs) is disturbed, and subsequently, the RF progression is blocked [23]. Camptothecin and etoposide, inhibitors of topoisomerase I and topoisomerase II respectively, prevent DNA unwinding and halt relaxation of torsional stress [24,25]. The most common sources of RS are illustrated in Figure 1.

Several repair pathways are essential for rapid elimination of DNA distortions and lesions introduced by the action of RS inducing compounds [26]. Removal and replacement of single base damage (e.g., oxidised and alkylated bases), is performed by base excision repair (BER) [27]. More extensive damage affecting several adjacent bases is repaired by nucleotide excision repair pathway (NER). NER is essential for repair of UV-induced damage such as cyclobutane pyrimidine dimers, or pyrimidine-pyrimidone (6-4) photoproducts and also needed for crosslinks removal caused by for example cisplatin [28]. Single-strand break repair in higher eukaryotes rely on poly(ADP-Ribose) polymerase 1 (PARP1) and X-ray repair cross complementing 1 (XRCC1) dependent recognition of the lesion, followed by end processing and ligation [29]. Double-strand breaks (DSBs) are processed by either homologous recombination (HR), or non-homologous end-joining (NHEJ). HR is active predominantly in S and G2 phases using the sister chromatid as a template for repair with high fidelity [30]. NHEJ, considered as an error prone pathway, performs DSB repair in all cell cycle stages more rapidly by direct ligation of two unprocessed (or minimally processed) DNA ends [31].

All previously described specific structures and concomitant DNA lesions can challenge the progression of RF. If the RF encounters a lesion which the replicative polymerase is unable to process as a template, it becomes stalled [32]. Stalled RFs are vulnerable structures and may undergo spontaneous collapse which leads to DSBs and genomic instability (GI) [33,34]. To avoid the harmful consequences of stalled forks, several mechanisms—DNA damage tolerance pathways (DDT)—exist to bypass the lesions and enable fork restart. One well-described process of DDT is translesion synthesis (TLS). TLS promotes “polymerase switch” from the replicative polymerase to translesion polymerases, which are able to continue replication across the lesion. TLS polymerases possess low processivity and fidelity towards the template DNA strand. Therefore TLS is often referred to as the error-prone pathway of DDT [32,34–36]. Among the DNA lesions which block the progression of RFs, interstrand crosslinks (ICLs) belong to the most challenging to bypass [37]. Thus, a whole group of proteins called Fanconi anaemia (FA) proteins evolved to govern the bypass and the repair of ICLs. The FA network promotes the unhooking of the ICL by specific endonucleases, bypassing the lesion by TLS polymerases or the repair by HR [5–7]. Patients with a defect in the FA protein family suffer from premature ageing, show increased sensitivity to DNA crosslinking agents (e.g., cisplatin, mitomycin C) and predisposition to certain types of cancers due to increased GI [38–40]. Although the FA pathway is involved mainly in ICL repair, it contributes more generally to initial detection of RF arrest, processing and stabilisation of the forks and regulation of TLS [41,42].

DNA damage bypass can occur in an error-free manner through the activation of the other branch of DDT, called template switching (TS). The process utilises the newly synthesised strand of

the sister duplex, using it as an undamaged template. TS can be promoted either by fork regression or by strand invasion mediated by HR [34,36,43,44]. RF restart can also be achieved by firing nearby dormant replication origins or by repriming events leaving behind lesion containing single-stranded DNA (ssDNA) gaps which are subsequently processed by DTT pathways [45–50]. Altogether, these processes ensure the rapid resumption of DNA synthesis, preventing prolonged fork stalling and the potentially deleterious effects of replication fork collapse. However, upon persisting RS, or non-functional RS response, the RF may fail to restart and collapse, most probably due to destabilised, dysfunctional or displaced components of replication machinery [1,50–54]. Prolonged stalled replication forks are targeted by endonucleases followed by recombination-based restart pathways [55,56].

Among the features of RS belong accumulation of long stretches of ssDNA [46,57], resulting from the uncoupled activity of DNA polymerase and progression of DNA helicase [58,59]. The persisting ssDNA is rapidly coated by replication protein A (RPA) that in turn generates the signal triggering the checkpoint response through activation of Ataxia telangiectasia Rad3-related (ATR) checkpoint kinase [60–63]. Once activated, ATR and its downstream target checkpoint kinase 1 (CHK1) help the cell to faithfully complete DNA replication upon RS [52,53,64]. In addition, ATR as the central RS response kinase contributes to the stabilisation and restart of the stalled forks even after the stress has been removed [65]. The ATR-CHK1 pathway is responsible for cell cycle inhibition, suppression of new origin firing, DNA repair and to the overall improvement of cell survival [62,66]. The role of Ataxia telangiectasia mutated (ATM), another important checkpoint kinase, upon RS conditions is not as clear and straightforward as of ATR. ATM is preferentially activated by DSBs which are generated in later stages after RS induction, mostly after the RF collapse [67,68]. There is suggested interplay between ATM and ATR during replication stress which becomes apparent under concomitant depletion of both kinases [68]. Interplay between ATM, Werner helicase (WRN) and Bloom helicase (BLM) is needed for the resolution of replication intermediates and HR repair pathway that is important for RF restart [69,70].

Chronic replication stress conditions, particularly in the absence of proper DNA repair pathway and/or non-functional checkpoint responses might result in the transfer of RS-related DNA alterations to daughter cells, inducing mutations, GI and fuelling tumourigenesis [1].

From this point of view, the RS is a strong pro-carcinogenic factor driving selective pressure for acquisition of mutations overcoming cell cycle arrest or apoptosis [71,72]. This further leads to the progression of malignant transformation and faster selection of mutations allowing development of resistance to cancer treatment [73].

However, cells typically react on the prolonged exposure to RS by triggering mechanisms leading to permanent cell cycle arrest known as cellular senescence or apoptosis [74,75] acting as a natural barrier against tumour progression [76].

Several hereditary syndromes are linked to enhanced RS and GI. The spectrum of exhibited symptoms is broad and includes premature ageing, growth retardation, neurodegeneration, immunodeficiency, cancer predisposition and others. The disorders like Seckel syndrome (deficiency in ATR kinase) [77], Ataxia telangiectasia caused (loss of ATM kinase) [78], Xeroderma pigmentosum (XP; various defects in XP protein family group) [79] are caused by aberrations in DNA damage recognition and repair enzymes [80]. Bloom and Werner syndrome (deficiency of BLM and WRN helicase, respectively) [81,82], Fanconi anaemia (FA; mutations in FA pathway proteins) [83,84], or Rothmund-Thomson syndrome (defects in RECQ like helicase 1 protein) [85,86] are related to failure of replication fork progression and restart.

In general, RS is a potent inducer of variety of hereditary and non-hereditary diseases, including the oncogenic transformation. The knowledge and understanding of the processes during RS are crucial for choosing the most efficient therapy. The *in vitro*-based cell studies involving models of chemical induction of RS are unique source of information about molecular interactions and undergoing mechanisms. For this review five compounds were chosen, all of them are commonly used for cell-based experiments to induce RS. Several aspects are discussed in detail: mechanism of



action aimed at replication interference, proper dosing and common experimental setups. A brief overview of the medical use and important practical hints for laboratory use are also included.

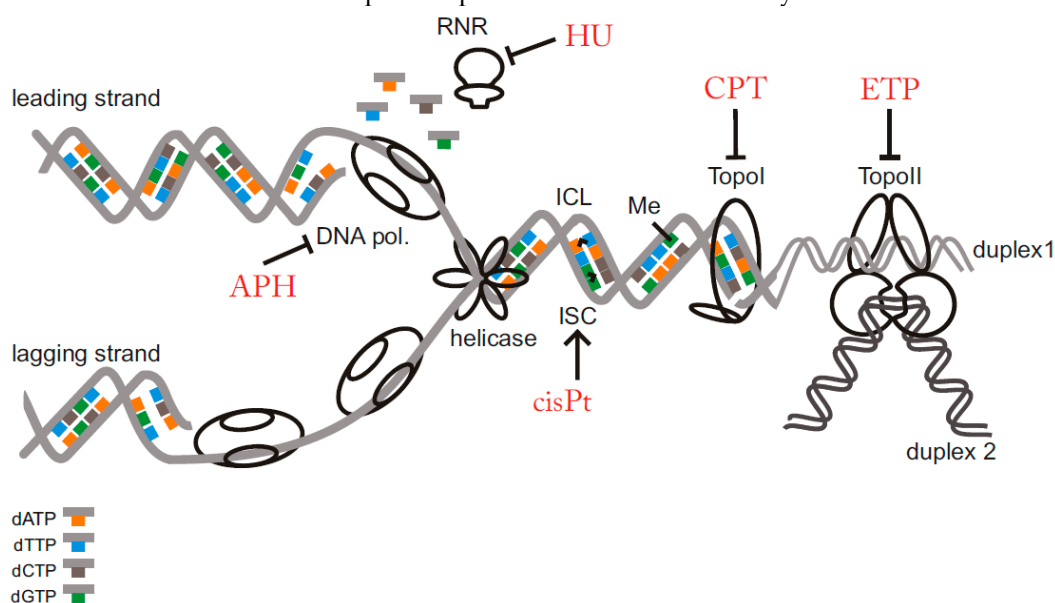


**Figure 1.** Schematic view of the most common lesions causing replication stress. In the scheme, several important replication stress (RS) inducing factors are illustrated: intra-strand crosslink (ISC), inter-strand crosslink (ICL), alkylated/modified base (Me) and inhibition of replication related enzymes. Compounds further described in the review are marked by red colour. RNR: ribonucleotide reductase; DNA pol.: DNA polymerase; TopoI: topoisomerase I; TopoII: topoisomerase II; APH: aphidicolin; HU: hydroxyurea; CPT: camptothecin; ETP: etoposide; cisPt: cisplatin; dATP: deoxyadenosine triphosphate; dTTP: deoxythymidine triphosphate; dCTP: deoxycytidine triphosphate; dGTP: deoxyguanine triphosphate.

## 2. Compounds

### 2.1. Cisplatin

Cisplatin (cisPt) is an inorganic platinum complex first synthesised by Italian chemist Michel Peyrone and originally known as ‘Peyrone’s chloride’ (Figure 2). The cytostatic activity of cisPt was first reported by Barnett Rosenberg and co-workers in 1965 following accidental discovery of *Escherichia coli* growth inhibition induced by the production of cisPt from platinum electrodes [87]. It is generally considered as a cytotoxic drug for treating cancer cells by damaging DNA and inhibiting DNA synthesis. cisPt is a neutral planar coordination complex of divalent platinum [88] with two labile chloride groups and two relatively inert amine ligands. The *cis* configuration is necessary for the antitumour activity [89], 3D structure of monofunctional cisPt bound to DNA structure can be found here [90].

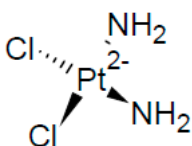


**Figure 2.** Cisplatin structure.

#### 2.1.1. Mechanism of DNA Damage Induction

The cytotoxicity of cisPt is known to be due to the formation of DNA adducts, including intrastrand (96%) and interstrand (1%) DNA crosslinks, DNA monoadduct (2%) and DNA–protein crosslinks (<1%) [91]. These structural DNA modifications block uncoiling and separation of DNA double-helix strands, events both necessary for DNA replication and transcription [92]. Inside a cell,

cisPt forms an activated platinum complex, which triggers a nucleophilic substitution reaction via an attack on nucleophilic centres on purine bases of DNA, in particular, *N7* positions of guanosine (65%) and adenosine residues (25%) [93]. The two reactive sites of cisPt enable the formation of the most critical crosslink between two adjacent guanines (1,2-d(GpG)), resulting in the formation of DNA intrastrand crosslinks [94]. Also, platinum can align to guanine bases on the opposite DNA strand, thus creating DNA interstrand crosslinks, present in lower percentage [95]. These cisPt crosslinks create severe local DNA lesions that are sensed by cellular proteins, inducing repair, replication bypass or triggering apoptosis [96]. Several protein families can recognise cisPt–DNA adducts, including nucleotide excision repair (NER) proteins [97], homology-directed repair proteins (HDR) [98], mismatch repair (MMR) proteins [99] and non-histone chromosomal high mobility group proteins 1 and 2 (HMG1 and HMG2) [100]. The intrastrand cisPt structural alteration stalls RNA polymerase II. It is recognised and efficiently repaired by global genome NER (GG-NER) or its transcription-coupled sub-pathway (TC-NER) [101]. The second DNA repair system predominantly involved in coping with cisPt–DNA adducts is error-free HDR, which removes DNA DSBs remaining after cisPt adduct removal [98]. In contrast to the previously mentioned repair pathways that increase cell viability, MMR proteins have been shown to be essential for cisPt-mediated cytotoxicity [99]. cisPt is reported to enhance interactions between MMR proteins MLH1/PMS2 (MutL homolog 1/PMS1 homolog 2, MMR component) and p73, triggering apoptosis [102]. Therefore, mutations in MMR genes are known to be associated with cisPt resistance [103]. HMG1 and HMG2 recognise intrastrand DNA adducts between adjacent guanines, affecting cell cycle events and subsequently inducing apoptosis [100].

In addition to the previously mentioned repair proteins, specialised translesion DNA polymerase eta ( $\eta$ ) can be loaded onto sites of cisPt–DNA adducts promoting TLS repair pathway [104]. cisPt also induces dose-dependent reactive oxygen species (ROS), which are responsible for the severe side effects of platinum-based therapy, including nephrotoxicity and hepatotoxicity [105]. When overwhelming the reduction capacity of the cell, cisPt-induced ROS might lead to lipid peroxidation, oxidative DNA damage, altered signal transduction pathway and calcium homeostasis failure [105]. Extensive unrepaired cisPt-induced DNA damage can proceed to apoptotic cell death mediated by various signal transduction pathways, including calcium signalling [106], death receptor signalling [107] and activation of mitochondrial pathways [108]. At least two main pathways have been proposed to mediate cisPt-induced apoptosis *in vitro*. One involves the critical tumour suppressor protein p53 directly binding to cisPt-modified DNA [109] and promoting apoptosis via several mechanisms. p53 binds and counteracts the anti-apoptotic B-cell lymphoma-extra large (Bcl-xL) [110], contributes to inactivation of nutrient sensor AMP-kinase (AMPK) [111], activates caspase-6 and -7 [112] and the pro-apoptotic Bcl-2 family member PUMA $\alpha$  in renal tubular cells [113]. However, the role of p53 in response to cisPt seems to be controversial, as it has been described to contribute to cisPt cytotoxicity [114] and also to be involved in cisPt resistance in different cancer models [115]. The other cisPt-induced apoptotic pathway is mediated via a pro-apoptotic member of the p53 family, p73. cisPt has been shown to induce p73 in several cancer cell lines [116], which cooperates with the MMR system and c-Abl tyrosine kinase, known to be involved in DNA damage-induced apoptosis [117]. In response to cisPt, c-Abl phosphorylates p73, making it stable [118], and increases its pro-apoptotic function by binding transcription coactivator p300, which triggers transcription of pro-apoptotic genes [119]. Moreover, p73 forms a complex with c-Jun N-terminal kinase/stress-activated protein kinase (JNK), leading to cisPt-induced apoptosis [120]. Intrinsic signaling pathways involved in cisPt driven apoptosis include Akt [121], protein kinase C [122,123], and mitogen activated protein kinases—MAPK (e.g., extracellular signal-regulated kinases; ERK) [124–126], JNK [127–129] and p38 [130].

### 2.1.2. Other Effects

Besides DNA, the primary target of cisPt in cells, there is some evidence for the involvement of non-DNA targets in cisPt cytotoxicity [131]. cisPt interacts with phospholipids and phosphatidylserine in membranes [132], disrupts the cytoskeleton and alters the polymerization of

actin, probably due to conformational changes resulting from the formation of Pt–S bonds [133]. MicroRNAs (miR), which play a role in posttranscriptional gene silencing, have been shown to be involved in the modulation of cisPt resistance-related pathways in different cancer models. miR-378 was shown to reverse resistance to cisPt in lung adenocarcinoma cells [134], whereas miR-27a was shown to be upregulated in a multidrug resistant ovarian cancer cell line, contributing to cisPt resistance [135]. miR-21 increases the cisPt sensitivity of osteosarcoma-derived cells [136]. For references to particular studies using cisPt, refer to Table 1.

**Table 1.** Effects of various cisplatin treatments in vitro.

Concentration	Incubation Time	Observed Effect	Cell Line	Reference
300 $\mu$ M	2 h	increase in polyADP ribosylation	O-342 rat ovarian tumour cells	[137]
100 $\mu$ M	2 h before IR	sensitization to $\gamma$ -radiation	hypoxic V-79 Chinese hamster cells	[138]
100 $\mu$ M	2 h	increase in polyADP ribosylation	CV-1 monkey cells	[139]
<20 $\mu$ g/mL (<66 $\mu$ M)	5 h	block of rRNA synthesis block of DNA replication	Hela	[140]
15 $\mu$ M	1 h	induction of SCE (sister chromatid exchange) decreased cell survival	6 primary human tumour cell culture	[141]
10–30 $\mu$ M	24 h, 48 h	induction of apoptosis	224 (melanoma cells) HCT116	[142]
10 $\mu$ M	24 h	increase in antiapoptotic Bcl-2 mRNA synthesis (regulated by PKC and Akt2)	KLE HEC-1-A Ishikawa MCF-7	[143]
2–10 $\mu$ M	72 h	induction of apoptosis	224 (melanoma cells) HCT116	[142]
5 $\mu$ M	24 h	increase in p53 stability activation of ATR increased p53(ser15) phosphorylation	A2780	[144]
5 $\mu$ M	24 h	activation of p21 activation of CHK2 increased p53(ser20) phosphorylation	HCT116	[144]
5 $\mu$ M	24 h	induction of mitochondrial reactive oxygen species (ROS) response	A549 PC3 MEF	[143]
2 $\mu$ M	24 h	G2/M arrest, subapoptotic damage	MSC	[145]
>2 $\mu$ M	24 h	decreased proliferation rate induction of apoptosis	TGCT H12.1 TGCT 2102EP	[145]
1–4 $\mu$ g/mL	2 h	block of DNA synthesis block of transcription G2 arrest apoptosis	L1210/0 cells	[146]
2 $\mu$ g/mL	48 h 144 h, 168 h	inhibition of mtDNA replication inhibition of mitochondrial genes transcription	Dorsal root ganglion (DRG) sensory neurons	[147]
1 $\mu$ g/mL	2 h	transient G2 arrest	Hela	[148]
3.0 $\mu$ M	4 h before	block of NHEJ	A2780	[138]
0.2–0.8 $\mu$ M	IR 0.5 Gy 4 h	cisPt-IR synergistic interaction	MO59J MO59K	[138]
1–2.5 $\mu$ M	24 h–48 h	block of DNA replication followed by cell apoptosis	Hela	[149]
0.3–1 $\mu$ M	overnight	inhibition of RNA polymerase II-dependent transcription	Hela XPF	[144]
0.6 $\mu$ M	2 h	90% reduction in clonogenic capacity detected after 7 days CHK1 phosphorylation causing CHK1 dependent S phase arrest	Hela	[148]
0.5 $\mu$ M	24 h 48 h	loss of telomeres (TEL), or TEL repeats cell death	Hela	[139]

ATR: Ataxia telangiectasia Rad3-related; Bcl: B-cell lymphoma; CHK1: checkpoint kinase 1; CHK2: checkpoint kinase 2; IR: ionizing radiation; mtDNA: mitochondrial DNA; NHEJ: non-homologous end-joining; PKC: protein kinase C; polyADP: poly adenosine diphosphate; rRNA: ribosomal RNA.

### 2.1.3. Solubility

cisPt (molecular weight (MW) 300.05 g/mol) is water soluble at 2530 mg/L (at 25 °C), saline solution with a high chloride concentration (approx. 154 mmol/L) is recommended. In the absence of chloride, the cisPt chloride leaving group becomes aquated, replacing the chloride ligand with water and generating a mixture of species with increased reactivity and altered cytotoxicity [150,151]. Commonly used solutions for laboratory use are aqueous-based solutions in 0.9% NaCl (0.5 mg/mL), pH 3.5–5. Dissolved cisPt may degrade over a short time, the storage of aliquots is not recommended. However, the stability at –20 °C in the dark is reported to be 14 days. Solutions (in 2 mM phosphate buffered saline buffer with chloride concentration 140 mmol/L) stored at 4 °C should be stable for 7–14 days [152]. Undiluted cisPt is stable in the dark at 2–8 °C for several months [121,153]. Dimethyl sulfoxide (DMSO) can also be used for cisPt dilution, however it is not recommended. The nucleophilic sulphur can displace cisPt ligands, affecting the stability and reducing cisPt cytotoxicity [154]. DMSO introduced in combination studies with cisPt does not affect its activity [152].

### 2.1.4. Medical Use

Following the start of clinical trials in 1971, cisPt, marketed as Platinol (Bristol-Myers Squibb, New York, USA), was approved for use in ovarian and testicular cancer by the Food and Drug Administration (FDA) in 1979 [155]. cisPt is considered one of the most commonly used chemotherapy drugs for treating a wide range of malignancies, including head and neck, bladder, oesophageal, gastric and small cell lung cancer [156,157]. Moreover, cisPt has been shown to treat Hodgkin's [158] and non-Hodgkin's lymphomas [159], neuroblastoma [160], sarcomas [161], multiple myelomas [162], melanoma [163], and mesothelioma [164]. cisPt can reach concentrations of up to 10 µg/mL in human plasma [165]. cisPt is administered either as a single agent or, in the main cases, in combination with other cytostatics (e.g., bleomycin, vinblastine, cyclophosphamide) or radiotherapy for the treatment of a variety of tumours, e.g., cervical carcinoma [153]. The most important reported side effect is nephrotoxicity, due to preferential accumulation and persistence of cisPt in the kidney [166], later ototoxicity and bone marrow depression. Pharmacokinetic and pharmacodynamic studies have shown that a maximal steady state cisPt plasma concentration of between 1.5 and 2 µg/mL has the most effective chemotherapeutic effect with minimal adverse nephrotoxicity [167]. Many cancers initially responding to cisPt treatment could become later resistant. Mechanisms involved in the development of cisPt resistance include changes in cellular uptake, drug efflux, drug inactivation by increased levels of cellular thiols, processing of cisPt-induced damage by increased NER and decreased MMR activity and inhibition of apoptosis [99,168]. To boost platinum drug cytotoxicity, overcome its resistance and achieve a synergistic effect, new platinum-based drugs, as well as their combinatorial therapy with other antineoplastic agents were developed for cancer treatment [169]. Besides of cisPt derivatives as carboplatin and oxaliplatin, are currently being used in the clinical practice, while nedaplatin, lobaplatin and nedaplatin acquired limited approval in clinical use [170,171]. Recent discoveries described the combination of cisPt with PARP inhibitor olaparib targeting DNA repair to acts synergistically in several non-small cell lung carcinoma cell lines [172]. This combinatorial therapy can be promising especially in patients with advanced breast and ovarian cancer-bearing BRCA1/2 (breast cancer 1/2) mutations [173].

### 2.1.5. Summary

cisPt is used in vitro in concentration range approx. 0.5–300 µM. The levels in human plasma can reach up to 10 µg/mL (33 µM) which should be beared in mind when interpreting in vitro data. Continuous treatment, or longer incubation time, or high cisPt concentration of 20 mg/mL lead to complete inhibition of DNA synthesis [174]. The concentration range of 15–30 µM results in a block of DNA replication and transcription and triggers DNA damage response (DDR) signalization

through ATM-CHK2, ATR-CHK1 DDR pathways resulting in p53-p21 driven cell cycle arrest or p53-mediated cell apoptosis [141–144]. However, in some cell lines also the synthesis of anti-apoptotic protein Bcl-2 was reported [143]. cisPt is in the majority of cell lines induces apoptosis above the concentration of approx. 2  $\mu\text{M}$  [139,141,142,146]. cisPt block DNA replication [139,140,146] and inhibits RNA synthesis [140,175,176] and also influences the mitochondrial DNA synthesis and metabolism [147]. As a commonly used drug in clinics, many in vitro experiments have been conducted to address problems arising during treatment. Especially, the study of mechanisms underlying drug resistance [177], causes of toxic side effects [178], enhancement of synergistic effects [179] and ways how to improve drug delivery systems [180]. cisPt massively triggers the TLS repair pathways; defective FA proteins sensitise the cells towards this compound [181], defective MMR proteins establish cisPt resistance [103,182].

## 2.2. Aphidicolin

Aphidicolin (APH) is a tetracyclin diterpenoid antibiotic isolated from *Nigrospora sphaerica* (Figure 3) which interferes with DNA replication by inhibiting DNA polymerases  $\alpha$ ,  $\epsilon$  and  $\delta$  [183]. Specifically, only cells in S phase are affected, whereas cells in other phases of the cell cycle are left to continue until the G1/S checkpoint, where they accumulate [184].

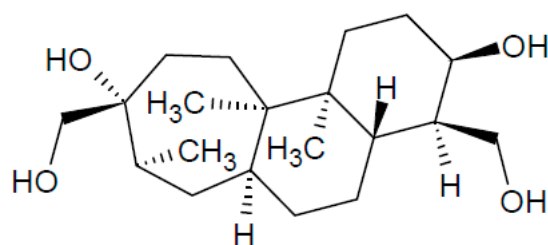


**Figure 3.** Aphidicolin structure.

### 2.2.1. Mechanism of DNA Damage Induction

APH binds to the active site of DNA polymerase  $\alpha$  and rotates the template guanine, selectively blocking deoxycytidine triphosphate (dCTP) incorporation [185]. DNA polymerase  $\alpha$  interacts with APH by its C18-binding OH group, APH forms a transient complex with polymerase and DNA [183]. The effect of APH on cell cultures is reversible if the cells are treated for no longer than 2 generations [186]. The exonuclease activity of APH-responding polymerases is only mildly affected, even at concentrations completely blocking the polymerase activity [183]. However, in the cell nucleus, the exonuclease activity is usually not retained because ternary complex APH–polymerase–DNA is formed and blocks the enzyme [183]; 3D structure of the complex can be found here [187].

Mechanistically, APH compromises the function of DNA polymerase, while helicase proceeds regularly (so called uncoupled/disconnected replicon), which leads to the generation of long stretches of single-stranded DNA [188]. The disconnected replicon is vulnerable structure prone for breakage preferentially at the so-called common fragile sites (CFSs) (also referred to as CFS expression) [189]. CFSs are specific genomic loci conserved in mammals generally prone to instability upon RS [190]. CFS expression is also common in precancerous and cancerous lesions [76]. Moreover, a causative role of CFS's in cancer development has been suggested [191]. APH reproducibly causes damage at the same sites, and thus low doses of APH are used to define APH-inducible CFSs, of which there are over 80 described in the human genome [22,192]. Other CFS inducers (hydroxyurea, camptothecin, hypoxia and folate deficiency) are not so specific, nor efficient as APH [193,194]. Importantly, APH efficiently induces CFS expression only when the rate of polymerase is slowed down but not completely blocked. The optimum concentration range usually spans 0.1–1  $\mu\text{M}$  [195] (and refer to Table 2). Apart from disconnected replicon, there might be other explanations for the extraordinary potency of APH to induce CFS-associated genomic instability. First, APH has been shown to increase the number of R-loops within certain CFSs, thus inducing replication/transcription collisions [196].

However, the mechanistic relationship between APH and increased R-loop formation is not clear. Second, re-licensing of replication origins is typical feature of oncogenic genetic backgrounds which are very prone to CFS expression. In such situations the CFS expression is explained as a result of DNA re-replication and subsequent collision of re-replicating forks within CFSs [10,197]. This phenomenon was studied in detail in yeasts at replication slow zones (analogous to CFSs in mammals) [198]. It is not clear whether the same re-licensing process is induced also by APH, however re-duplication would explain the reported APH-induced amplifications [191,199].

Prolonged treatment with low doses of APH induces cellular senescence response [74]. Interestingly, the most efficient doses were found to span the same range as doses used for CFS expression, which implies that CFSs might play a causative role in this process. Moreover, oncogene-induced senescence also displays increased CFSs-associated instability [10,197]. These phenotypical similarities between oncogenic stress and low doses of APH make this drug a good candidate for studying cellular processes in early stages of malignant transformation.

### 2.2.2. Other Effects

APH is a very specific DNA polymerase inhibitor, APH does not interact with mitochondrial DNA polymerases [186] nor proteins [201], DNA, RNA, metabolic intermediates, nor nucleic acid precursor synthesis [184]. Contradictory results have been obtained regarding the effect of APH on DNA repair synthesis (DRS). According to a radiography method, APH does not influence DRS [201], although when DRS was induced by tumor necrosis factor (TNF) or UV irradiation, APH was observed to inhibit the process [202,203]. For references to particular studies using APH, refer to Table 2.

**Table 2.** Effects of various aphidicolin treatments in vitro.

Concentration	Incubation Time	Observed Effect	Cell Line	Reference
0.2 mM	16 h, 10 h	formation of anaphase bridges and micronuclei	HeLa	[204]
30 $\mu$ M	6 h	stalled replication forks	HCT116	[205]
30 $\mu$ M	6 h	stalled replication forks	PD20 cells Bloom syndrome cells	[206]
5 $\mu$ g/mL (14.3 $\mu$ M)	4 h	DNA repair synthesis inhibition sensitization towards TNF treatment	L929 ovarian cancer cells A2780	[202]
5 $\mu$ g/mL (14.3 $\mu$ M)	2–8 h	S phase arrest kinetics and mechanism study	RKO 293T MEF	[207]
2.5 $\mu$ g/mL (7.15 $\mu$ M)	1 h	inhibition of DNA synthesis and DNA repair	Normal and XPA deficient human fibroblasts	[203]
10 $\mu$ M	15 h	cell cycle synchronisation at the G1/S boundary	REF-52 HeLa	[210]
5–25 $\mu$ M	24 h	inhibition of replicative polymerases	Werner syndrome cells Bloom syndrome cells	[209]
1 $\mu$ M	1–24 h	CFS induction	HEK293T	[210]
1 $\mu$ M	24 h	CFS induction	MEF HeLa	[211]
0.5 $\mu$ M	2 h	transient attenuation of DNA synthesis,	DT40	[212]
0.1 $\mu$ M	24 h	study of chromosome integrity and replication		
0.4 $\mu$ M	24 h	CFS induction	U-2 OS	[213]
0.1 $\mu$ M 0.2 $\mu$ M	16 h	replication stress observed on telomeres	hESC (UCSF4)	[214]
0.2 $\mu$ M	2 weeks	irreversible senescence induction	REF-52	[74]
0.2 $\mu$ M	24 h	CFS induction	BJ-hTERT	[215]
0.05 $\mu$ M 0.4 $\mu$ M	24 h	CFS induction	Werner syndrome fibroblasts AG11395 cells	[216]

0.3 $\mu\text{M}$	48 h	increased incidence of mitotic extra chromosomes replication stress	V79 hamster cell lines	[217]
0.3 $\mu\text{M}$	72 h	replication stress	Human fibroblasts HGMDFN090	[199]
2 $\mu\text{g/mL}$	not indicated	replication block	BJ BJ-tert HMEC	[197]
0.2 $\mu\text{M}$	7–24 h	cell synchronization	HeLa	[184]

CFS: common fragile site; TNF: tumour necrosis factor.

### 2.2.3. Solubility

APH (MW 338.48 g/mol) is soluble in DMSO (up to 10 mg/mL), ethanol (up to 1 mg/mL) and methanol (freely), not soluble in water. The stability of the powder is 3 years at 2–8 °C, ethanol solution for a week at 2–8 °C, DMSO solution for 6 weeks at –20 °C [218].

### 2.2.4. Medical Use

APH has limited use in clinical practice owing to its low solubility. Only APH-glycinate has so far been tested in clinical trial phase I. However, fast clearance from human plasma (no drug observed after 6–8 h of APH administration) and no anti-tumour activity was observed. Its use as a single agent or even in combination with other cytostatics is no longer being considered [219]. APH is metabolised by cytochrome P-450 dependent degradation [220]. APH and its derivatives are considered as potential therapeutics for parasitic diseases, e.g., Chagas disease [221].

### 2.2.5. Summary

APH is used for in vitro studies in concentration range approx. 0.01  $\mu\text{M}$  to 0.2 mM. APH is mainly used for cell-based experiments involving CFS expression [222], cell cycle synchronization [223], replication fork stability and restart studies [224] and for cellular senescence induction [74]. The threshold between replication fork stalling and slowing down is around 1  $\mu\text{M}$ . Upon higher concentrations (5  $\mu\text{M}$ –0.2 mM) APH was reported to stall the DNA polymerase, leading to S phase arrest. Upon lower concentrations, when the DNA polymerases are just slowed down, CFS expression can be observed. Usually, longer incubation times (approx. one population doubling) are used, so more cells within the population are affected. APH treatment causes a significant amount of DNA damage, leading to rapid ATR kinase activation. In the case of longer APH treatment also ATM is activated probably as a consequence of DSB formed within the stalled replication forks [207]. Prolonged APH incubation in the range of days up to weeks at low concentrations (0.2–1  $\mu\text{M}$ ) induces cellular senescence [74].

## 2.3. Hydroxyurea

Hydroxyurea (HU) was first synthesised in the 19th century (Figure 4) and inhibits the incorporation of nucleotides by interfering with the enzyme ribonucleotide reductase (RNR) [225]. RNR converts nucleotide di- and tri-phosphates to deoxynucleotide di- and tri-phosphates, which is the rate-limiting step in nucleotide synthesis [226]. Without proper levels of dNTPs, DNA cannot be correctly replicated nor repaired [227].

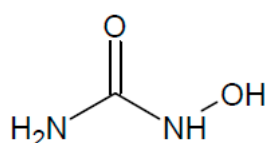


**Figure 4.** Hydroxyurea structure

### 2.3.1. Mechanism of DNA Damage Induction

RNR is a large tetrameric enzyme comprising two R1 subunits and two small regulatory subunits R2 [228]. HU scavenges the tyrosyl radical of the R2 subunit which inactivates the RNR enzymatic activity [226]. Complete inhibition of RNR has been observed within 10 min after treatment with 0.1 mM HU and within 5 min after 3 mM of HU in murine 3T6 cells [229]. Consequently DNA synthesis is inhibited, selectively stopping the cells in S phase [230]. The inhibition is caused alterations in the dNTP pools. Each type of dNTP is affected in a different way. For example, after 280–560  $\mu$ M HU treatment for 60 min, the dTTP pool was found to increase by 50%, whereas the dCTP pool is decreased by 50% [231]. HU slows down the initiation of replication and also the progression of replication forks. Moreover, after stopping the production of dNTPs, DNA repair and mitochondrial DNA synthesis are affected in all cells, regardless of the cell cycle stage [227]. HU treatment greatly affects the choice of replication origins and origin spacing in mammalian cells [232]. Although the mechanism of DNA damage induction may look similar to that for APH, HU induces a different spectrum of fragile sites, called early replicating fragile sites (ERFs) [233]. ERFs are also induced by c-Myc expression [11,12]. It was also reported that 10  $\mu$ g/mL APH [234] (concentration that stalls the replication fork progression) leads to the generation of several kilobases long unwound DNA; however, HU treatment can generate only up to 100–200 nt long ssDNA [235].

### 2.3.2. Other Effects

HU induces copy number variants (CNVs) with similar frequency and size distribution as APH [236]. It was reported for yeast cells, that HU alters Fe–S centres, enzyme cofactors catalysing oxidation-reduction reactions, which interferes with various metabolic enzymes and affects the redox balance of cells. Similar mechanism is proposed also for mammalian cells [237].

HU has been negatively tested for mutagenicity, measured by single nucleotide variation (SNV) and insertion/deletion frequency [238]. On the other hand, low doses of HU have been reported to induce DNA damage [239]. Therefore, it is possible that the compound possesses some pro-mutagenic potential (see also below). For references to particular studies using HU, refer to Table 3.

**Table 3.** Effects of various hydroxyurea treatments in vitro.

Concentration	Incubation Time	Effect	Cell Line	Reference
200 mM	2 h	replication block	yeast cells	[240]
10–200 mM	3 h	replication block replication fork (RF) restart	yeast cells	[241]
5 mM	1 h	replication block	HEK293	[242]
2 mM	3 h	replication block		
50 $\mu$ M–5 mM	40 min–2 h	replication stress	293T mouse ES cells	[243]
2 mM	1 h, 24 h	replication stress replication block	HCC1937 MCF7	[244]
2 mM	16 h	replication block	HEK293	[245]
2 mM	24 h	DNA damage induction during S phase	U-2 OS 293T	[246]
2 mM	15 h	replication block cell cycle synchronisation at the G1/S boundary	REF-52 HeLa	[208]
2 mM	5 h	dNTP depletion	REF52	[74]
2 mM	3 h	chromosomal aberrations FANCD2 pathway involvement	lymphoblastoid cell lines	[247]
1 mM	overnight	replication block	MCF7	[248]
0.5 mM	5 h–10 h	replication block		
2 mM	2 h–24 h	replication block	U-2OS	[249]
0.5 mM	90 min	nucleotides depletion stalled RF w/o DSBs formation	MEF	[250]
0.1–0.5 mM	2 h–72 h	$\gamma$ -globin gene expression	K562	[251]



0.1–0.5 mM	2 h–8 h	replication stress	PC3	[252]
0.2–0.4 mM	4 days	cell differentiation ERK signalling pathway inhibition p38 signal transduction activation	K562	[253]
0.3 mM	10 days	microsatellite instability upon FANCD2 depletion	GM08402 HeLa PD20F	[254]
0.15–0.2 mM	2 weeks	irreversible senescence induction	REF-52	[74]
0.2 mM	2 h–7 h	replication stress	MEF	[255]
0.15 mM	2 h	p53 activation	REF52	[74]
50–200 $\mu$ M	20 h	HIF1 induction eNOS induction	HUVEC	[256]
25–200 $\mu$ M	72 h	induction of apoptosis	AML cell lines (MV4-11, OCI-AML3, MOLM-13, and HL-60)	[257]
5 $\mu$ M–0.5 mM	48 h	replication stress	V79 hamster cells	[217]
2 $\mu$ M	12 h	replication stress	H1299	[258]

dNTP: deoxynucleotide triphosphate; DSBs: double-strand breaks; eNOS: endothelial nitric oxide synthase; ERK: extracellular signal-regulated kinases; FANCD2: Fanconi anaemia complementation group D2; FANCD1: Fanconi anaemia complementation group J; HIF: hypoxia induced factor 1.

### 2.3.3. Solubility

HU (MW 76.05 g/mol) is freely soluble in water at 100 mg/mL, soluble also in DMSO. The powder is stable at 4 °C for 12 months. Solutions are stable for 1 month at –20 °C (after defrosting, equilibration is recommended for 1 h at room temperature). It is recommended to prepare fresh solutions before use. HU decomposes in the presence of moisture; therefore, it is recommended that it is stored in air-tight containers in a dry atmosphere [259].

### 2.3.4. Medical Use

HU is a commonly used medicine first approved by the FDA for the treatment of neoplastic disorders in the 1960s [260]. Common plasma levels of HU range 100–200  $\mu$ M [261]. It is used for the treatment of sickle cell disease, essential thrombocytosis [262], myeloproliferative disorders and psoriasis [260] and is commonly indicated as a cytoreductive treatment in polycythemia vera [263] and others. Synergistic effects have been reported when it is used in combination with antiretroviral pills [264] and also in indicated cases with radiotherapy [265]. HU may be used as an anti-retroviral agent, especially in HIV (human immunodeficiency virus) patients. HU may cause myelofibrosis development with increased time of use and AML/MDS syndrome (acute myeloid leukaemia/myelodysplastic syndrome) [266]. Adverse side-effects have been observed, mainly myelosuppression [267]. A 17-year follow-up study of 299 patients treated with HU as a long-term therapy showed no difference in the incidence of complications such as stroke, renal disease, hepatic disease, malignancy or sepsis [268], suggesting that HU is well-tolerated. However, CNVs are generated at therapeutic doses of HU, and data from reproductive studies and studies on subsequent generations have so far been rather limited [236,268].

### 2.3.5. Summary

HU is used in vitro approx. in the range 2 mM–5 mM. The most commonly used concentrations are around 2 mM. HU is used for cell cycle synchronization [269], replication fork stability studies [249,252], studies of recovery mechanisms after the release of RS [242] and checkpoint responses [241]. Lower concentrations are used for RS induction [254], induction of senescence [74], apoptosis [257], and repair pathways induction [217]. HU reaches plasma concentrations around 0.1 mM; this should be bear in mind when interpreting the data for clinical relevance [261]. The MRN (Mre11-Rad50-Nbs1) complex members Mre11 (Meiotic recombination 11) and Nbs1 (Nijmegen breakage syndrome 1) are required for efficient recovery of replication after treatment with replication stalling agents such as hydroxyurea [12]. HU causes rapid generation of ssDNA as indicated by RPA loading

40 min after treatment [270]. Subsequently, ATR-CHK1 signalling is activated, and HR repair pathway is induced.

Cells deficient in XRCC2 or other homologous recombination components exhibit hypersensitivity to HU [271]. It was reported that for hamster V79 cells, low concentrations of HU (5–10  $\mu\text{M}$ ) mimics the replication dynamics of untreated HR deficient cells [217]. Cellular senescence after long term replication stress caused by HU is dependent on p53-p21 signalling pathway and independent of p16 [74]. HU influences multiple cellular pathways, e.g., JNK pathway, mitochondrial and peroxisome biogenesis, expression of several heat shock response proteins, autophagy pathways stimulation (beclin-1 expression), hemoglobin type F induction (in sickle cell disease,  $\beta$ -thalassemia patients), etc. [272]. There are several cell lines that respond to HU treatment in a specific manner, e.g., K562 cell line undergoes differentiation [253], T-cells activation is decreased [264], the morphology of vascular endothelial cells is affected [273].

#### 2.4. Camptothecin

Camptothecin (CPT) is a pentacyclic quinoline alkaloid first isolated from the Chinese tree *Camptotheca acuminata* (Nyssaceae) by Wall et al. [274] (Figure 5). CPT has a unique intracellular target, topoisomerase I (TopoI), a nuclear enzyme that reduces the torsional stress of supercoiled DNA [24]. This activity enables specific regions of DNA to become sufficiently exposed and relaxed to facilitate essential cellular processes, such as DNA replication, recombination and transcription [275].

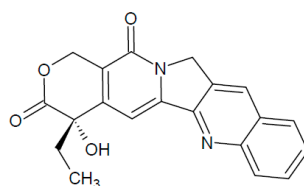


**Figure 5.** Camptothecin structure.

##### 2.4.1. Mechanism of DNA damage induction

TopoI binds covalently to double-stranded DNA through a reversible transesterification reaction, generating a SSB [276], 3D structure can be found here [277]. This so-called TopoI–DNA cleavage complex (Top1cc) facilitates the relaxation of torsional strain in supercoiled DNA, either by allowing passage of the intact single strand through the nick or by free rotation of the DNA around the uncleaved strand [278]. CPT covalently and reversibly stabilises the normally transient DNA Top1cc by inhibiting religation of the scissile strand, thereby prolonging the half-life of Top1cc and increasing the number of DNA SSBs [279,280]. Moreover, trapping of the enzyme on the DNA leads to rapid depletion of the TopoI pool [281]. The effect of CPT is readily reversible after removal of the drug. However, prolonged stabilisation of Top1cc can cause multiple problems. Firstly, failure to relieve supercoiling generated by such processes as transcription and replication can lead to RS by creating torsional strain within the DNA [279,281,282]. Furthermore, the collision of the RF with the ternary drug–enzyme–DNA complex generates DSBs with serious cellular consequences, including cell death [283,284].

Because ongoing DNA synthesis is important for CPT-induced cytotoxicity, CPT is considered an S phase-specific drug. The repair of CPT-induced DSBs involves multiple DNA damage repair proteins. Recent studies have highlighted that functional cooperation between BRCA2, FANCD2, RAD18 and RAD51 proteins are essential for repair of replication-associated DSBs through HR. Loss of any of these proteins causes disruption of HR repair, chromosomal aberrations and sensitization of cells to CPT [285]. A close link between CPT and HR has also been demonstrated in experiments measuring sister chromatid exchange events (SCEs), which are common consequence of elevated HR repair process and found to be induced by low doses of CPT [270]. CPT is applied in early S phase

cells for triggering G2 arrest accompanied by blockage of the p34cdc2/cyclin B complex, a consequence of either DNA breakage, the arrest of the replication fork or both [286]. In addition, CPT driven TopoI–DNA cleavable complex and associated strand breaks were shown to increase transcription of the c-Jun early response gene, which occurs in association with internucleosomal DNA fragmentation, a characteristic mark of apoptosis [287]. Noncytotoxic concentrations of CPT can induce the differentiation of human leukaemia cells [288], and an antiangiogenic effect is suggested [289,290]. Interestingly, when used in combined treatment with APH, CPT reduces the APH-induced RPA (an indicator of ssDNA) signal and has a rescuing effect on CFS expression [291]. For references to particular studies using CPT, refer to Table 4.

**Table 4.** Effects of various camptothecin treatments in vitro.

Concentration	Incubation Time	Observed Effect	Cell Line	Reference
20 $\mu$ M	30 min	DNA fragmentation in G1 and S phase cells	Hela	[292]
10 $\mu$ M	24 h	increase in cell sensitivity to TRAIL-mediated apoptosis	Hep3B	[293]
10 $\mu$ M	4 h	formation of replication mediated DNA DSBs	HT29	[294]
5 $\mu$ M	60 min	inhibition of RNA synthesis	CSA	[295]
1 $\mu$ M	60 min	inhibition of DNA synthesis	CSB	[296]
1 $\mu$ M	60 min	replication block DSB formation cell death	U2OS	[297]
1 $\mu$ M	60 min	formation of stabilised TopoI-cc complex DSB formation phosphorylation of CHK1 (S317) CHK2 (T68), RPA (S4/S8)	HCT116	[294]
1 $\mu$ M	60 min	inhibition of DNA replication suggested DNA DSB formation	L1210 mouse lymphoblastic leukaemic cells	[293]
200 nM–1 $\mu$ M	50 min	DSB formation	CSB	[298]
100 nM–10 nM	60 min	DSB formation	HCT116	[299]
25 nM	60 min	checkpoint activation (ATM-CHK2, ATR-CHK1) replication fork stalling replication fork reversal formation of specific DNA structures	U-2O-S	[300]
10 nM–100 nM	60 min	inhibition of EIAV (equine infectious anemia virus) replication	CF2Th	[295]
10 nM–20 nM	60 min	inhibition of HIV-1 replication block of viral protein expression	H9	[281]
6 nM	6 h	accumulation of cells in early S phase	Normal lymphocytes	[296]
	24 h	apoptosis, DNA fragmentation	MOLT-4	
6.25 nM	48 h	specific suppression of oral cancer cells growth	KB oral cancer cells	[281]
2.5 nM	48 h	increase in SCE upon depletion of Fbh1 helicase	BJ	[281]

ATM: Ataxia telangiectasia mutated; HIV: Human immunodeficiency virus; RPA: replication protein A; SCE: sister chromatid exchange; TopoI-cc: Topoisomerase I cleavage complex; TRAIL: TNF alpha related apoptosis inducing ligand, TNF: tumour necrosis factor.

#### 2.4.2. Solubility

CPT (MW 348.35 g/mol) is soluble in DMSO (up to 10 mg/mL), methanol (40 mg/mL), 0.1 N sodium hydroxide (50 mg/mL) or acetic acid, insoluble in water. At higher concentrations, heating is required to dissolve the product completely (approx. 10 min at 95 °C), but some precipitation occurs upon cooling to room temperature [301].

### 2.4.3. Medical Use

CPT cannot be used in clinical practice because of its poor solubility in aqueous solutions, instability and toxicity, but modifications at selected sites have improved the pharmacologic and activity profile [283]. Currently, three water-soluble CPT-derivates, i.e., irinotecan (CPT-11), topotecan (TPT) and belotecan (CKD-602), are available for cancer therapy. However, despite their selectivity for TopoI and unique mechanism of action, they all have critical limitations. In particular, they become inactivated against TopoI within minutes at physiological pH due to spontaneous lactone E-ring opening [302] and diffuse rapidly from the TopoI–DNA cleavage complex due to their noncovalent binding. To overcome these problems, five-membered E-ring CPT-keto non-lactone analogues S38809 and S39625 have been synthesised and selected for advanced preclinical development based on their promising activity in tumour models. Their chemical stability and ability to produce high levels of persistent Top1cc makes them useful candidates for future treatment [303].

### 2.4.4. Summary

Camptothecin is used in concentration range 2.5 nM up to 20  $\mu$ M. CPT is a potent DSBs inducer in a wide concentration range, approx. 10 nM–10  $\mu$ M. Upon higher concentration (20  $\mu$ M–10  $\mu$ M), CPT was reported to be cytotoxic, increasing cell apoptosis via DNA fragmentation predominantly in S phase cells with ongoing DNA synthesis [292,293]. The most frequently used concentration of 1  $\mu$ M CPT was shown to block DNA synthesis and induce DSBs resulting from the collision of RF due to prolonged stabilisation of TopoI DNA cleavage complex. The main implication of lower CPT concentrations is the induction of replication fork slowing and reversal, as a rapid response to TopoI inhibition is the increase in topological stress of DNA locally [300]. CPT activates predominantly ATR–CHK1 and ATM–CHK2 signalling, and leading to G2 checkpoint arrest [300]. Even at low doses of CPT HR repair pathway is triggered.

### 2.5. Etoposide

Etoposide (ETP) is a derivative of podophyllotoxin first synthesised in 1966 and approved for treatment as an antineoplastic agent in 1983 [304]. ETP structure comprises of polycyclic A–D rings, an E-ring and aglycone core (Figure 6). ETP compromises the proper function of the enzyme topoisomerase II (TopoII), 3D structure can be found here [305]. TopoII performs cleavage of both strands of a DNA duplex and enables passage of a second intact duplex through the transient break, ATP is used to power the strand transition [306]. As a result, relaxation, unknotting and decatenation of DNA are achieved enabling processes like replication and transcription [25].

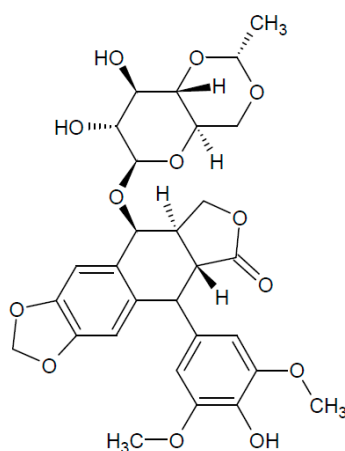


Figure 6. Etoposide structure.

### 2.5.1. Mechanism of DNA Damage Induction

Two modes of action were suggested for ETP to interfere with TopoII [25]. As a poison, it stabilises TopoII:DNA complexes, whereas as an inhibitor ETP interacts with the catalytic site of TopoII, decreasing the number of active cleavage complexes [307]. ETP acts as a poison by stabilizing the cleavage complex of TopoII via decoupling the key catalytic residues, thus preventing the religation of cleaved DNA ends [308]. As a result, the number of TopoII-associated DNA breaks are increased [309]. ETP's A, B and D-rings mediate the drug-enzyme interaction, whereas the aglycon core binds to DNA [262,308]. E-ring substituents are important for ETP activity but do not contribute to ETP-enzyme binding [310]. ETP is metabolised by cytochrome P3A4 (CYP3A4) to two metabolites, ETP-quinone and ETP-catechol. Both active against the TopoII enzyme. ETP-quinone is approx. 100× more efficient at inhibiting TopoII than ETP. ETP-quinone can block binding of the enzyme to DNA by stabilisation of the N-terminal clamp [307]. In cases where the enzyme still binds to DNA, the metabolite can stabilise the enzyme:DNA complex by inhibiting the religation step thus leading to higher levels of DSBs [307]. The ETP-catechol metabolite works similarly to the parent compound but can also be oxidised to the quinone [311]. ETP induces DSBs directly in all phases of the cell cycle, as observed by  $\gamma$ H2AX foci formation (a marker of DSBs) [312,313]. ETP does not require S-phase to induce damage, but ongoing replication enhances its cytotoxic effect [314]. ETP causes disassembly of replication factories (sites of ongoing replication), as measured by the distribution of proliferating cell nuclear antigen protein (PCNA) [315]. Moreover, the cytotoxic effect of ETP is partially reduced by inhibitors of DNA synthesis, such as APH and HU [316]. There are two isoforms of the TopoII enzyme in mammals, called TopoII $\alpha$  and TopoII $\beta$ , sharing 68% homology [317]. TopoII $\alpha$  activity is upregulated during cell cycle progression, peaks in mitosis and is essential for proliferating cells [318]. TopoII $\beta$  is needed during transcription and DNA repair, and its levels are more stable during the cell cycle [319]. ETP is not selective between these two paralogs, and the inhibition of TopoII $\beta$  is believed to be the reason for ETP therapy-related secondary malignancies [320]. TopoII $\alpha$  seems to be a better target for therapy. Therefore, new compounds and analogues of ETP have been synthesised to be selective only for TopoII $\alpha$  [321].

### 2.5.2. Other Effects

A strong mutagenic effect has been measured for ETP in mammalian cells by several assays, e.g., HPRT assay (hypoxanthine phosphoribosyl transferase), SCE and detection of mutations at the locus of the adenosine kinase gene [322]. In prokaryotic organisms (*E. coli*, *Salmonella typhimurium*), no significant genotoxic effect was observed [322]. For references to particular studies using ETP, refer to Table 5.

**Table 5.** Effects of various etoposide treatments in vitro.

Concentration	Incubation Time	Effect	Cell Line	References
up to 450 $\mu$ M	40 min	SSB and DSB formation, induction of H2AX phosphorylation with slow kinetics	SV-40 transformed human fibroblasts G361	[323]
1–100 $\mu$ M	30 min	formation of TopoII-blocked DSBs, activation of ATM-mediated repair	MEF HEK293T BJ1 AT	[324]
2–100 $\mu$ M	6 h–48 h	senescence, apoptosis induction of p53 response	HepG2 U2OS	[325]
2–100 $\mu$ M	1–3 h	disassembly of replication factories	AT1 BR AT3 BR HeLa	[315]
50–100 $\mu$ M	3–6 h/16 h	apoptosis (activation of intrinsic (mitochondrial) pathway)	Hela HCT116	[326]
50 $\mu$ M	15 h	apoptosis	BJAB Hut78	[327]

50 $\mu$ M	48 h	growth arrest (accumulation of cells at G2/M boundary) induction of p53 response	MCF-7 ZR75-1 T-47D	[328]
25 $\mu$ M	1 h	SSB and DSB formation $\gamma$ H2AX, pATM, pDNA-PKcs, MDC1 foci formation persisting DSBs cell death	HeLa HCT116	[329]
20 $\mu$ M	16 h	increase in $\gamma$ H2AX levels reduction of proliferation rate (accumulation of cells in S and G2/M boundary)	U2OS	[330]
20 $\mu$ M	1 h	repairable DSBs	HEK293T COS-7 BJ-hTERT H1299	[331,332]
	16 h	irrepairable DSBs, ATM-dependent HIC1 SUMOylation, induction of p53-dependent apoptotic response		
20 $\mu$ M	1–5 h	apoptosis	A549 HeLa, T24	[333]
10 $\mu$ M	1 h	DNA damage induction	A549	[334]
1–10 $\mu$ M	48 h	apoptosis	HCC1937 BT-549	[335]
8 $\mu$ M	1 h	induction of p53 response,	SH-SY-5Y SH-EP1	[336]
0.75–3 $\mu$ M	72 h	senescence, apoptosis	A549	[337]
0.75 $\mu$ M	24 h	cell cycle arrest in G2/M phase, DNA damage induction, induction of p53 response	MSC TGCT H12.1 TGCT 2102EP	[145]

DSBs: Double strand breaks; HIC1: Hypermethylated In Cancer 1; MDC1: Mediator of DNA Checkpoint 1; pATM: phosphorylated Ataxia telangiectasia Mutated; pDNA-PKcs: phosphorylated DNA Protein Kinase catalytic subunit; SSB: single-strand DNA break; TopoII: Topoisomerase II.

### 2.5.3. Solubility

ETP (MW 588.56 g/mol) is soluble in organic solvents (ethanol, methanol, DMSO), poorly soluble in water. It is recommended that stock solutions in organic solvents be diluted so 0.1% organic solvent is present in the final solution. The stability in aqueous solution is best at pH 4–5, but it can be improved by adding polysorbate 80 (Tween80), polyethylene glycol 300, citric acid and alcohol. ETP is unstable under oxidative conditions [338]. Under acidic conditions (pH < 4), the glycosidic linkage and lactone ring are hydrolysed, whereas, under basic conditions (pH > 6), *cis*-lactone epimers are formed [304]. Aqueous solutions are stable for several hours, depending on the concentration of the solution but irrespective of the temperature. ETP is sensitive to UV irradiation, both in solution and as a powder [338].

### 2.5.4. Medical Use

According to pharmacokinetic studies, plasma levels of ETP peak at concentrations of 20–70  $\mu$ M [339]. ETP is approved for the treatment of refractory testicular tumors and small cell lung cancer. Various chemical modifications with potential higher efficacy have also been tested for clinical use, e.g., 4'-phosphorylation or 4'-propyl carboxy derivatives [340]. In the field of so-called personalised medicine, combined subsequent treatment of ETP and cisPt has been shown to be beneficial for patients suffering from ERCC1-incompetent lung adenocarcinoma [341]. ETP is reported to cause therapy-related leukaemias [320] and specific chromosomal translocations. Chromosomal rearrangements at the 11q23 chromosome band were found in patients and seemed to be related to the CYP3A4 metabolic conversion of ETP [342]. In mouse embryonic stem cells, an increase in fusion chimeric products was observed at a 1.5 kb "hot spot" between exons 9 and 11 (analogous region to MLL (mixed lineage leukaemia) breakpoint cluster in human leukaemia) [343]. MLL gene encodes lysine (K)-specific histone methyltransferase 2A therefore influencing histone methylation and gene

expression [344]. Leukaemogenic MLL translocations lead to expression of MLL fusion proteins. Patients with such translocations exhibit poor prognosis [345]. MLL fusion proteins are efficient in transforming the hematopoietic cells into leukaemia stem cells [346]. Many studies have attempted to solve the adverse side effects of ETP treatment and understand the underlying molecular mechanisms, e.g., multi-drug resistance [347], or unwanted toxicity [348]. The search for compounds that may improve ETP treatment usually starts with cell-based experiments, e.g., protective compounds shielding healthy cells [349], compounds selectively enhancing ETP toxicity [350] or targeted delivery [351].

### 2.5.5. Summary

ETP is commonly used for the induction of apoptosis [352]. Indeed, several studies reported that higher doses of the compound (25–100  $\mu\text{M}$ ) activate apoptosis, mostly in a manner dependent on p53 [325–327,329]. Prolonged treatment at lower concentrations of ETP can also lead to induction of the p53 pathway, cell cycle arrest, senescence and apoptosis [145,325,330,335,337]. ETP induces the formation of irreversible DNA–TopoII cleavage complexes (TopoIIcc) and DNA damage regardless of concentration or incubation time [323,324, 329–332,334,353]. The initial displacement of TopoIIcc requires the coordinated action of several processes, such as cleavage by the 5'-tyrosyl DNA phosphodiesterase (TTRAP) and proteasome-dependent degradation of TopoII [354,355]. Furthermore, the MRN complex, CtIP (RBBP8 protein) and BRCA1 play a critical role in the removal of such DNA-protein adducts [356]. The remaining DNA lesions are often referred as DSBs, which are accompanied by the activation of ATM-mediated signalling or repair pathways, usually quantified by the formation of  $\gamma\text{H2AX}$  [323,324,329–332]. However, several studies argue against the ability of ETP to primarily induce DSBs, showing that majority of the DNA lesions formed upon ETP treatment are SSBs [323,329]. Despite the discrepancy, pathways engaged in DSB repair are activated after the exposure to the drug, and among them, NHEJ is seemingly predominant [329,356–358]. ETP used in relatively high concentration (20–25  $\mu\text{M}$ ) might lead to persistent or irreparable DSB formation [329, 331, 332].

## 3. Conclusions

Replication stress is a significant contributor to genomic instability, a major factor for the conservation of mutations [1], relevant promoter of tumourigenesis [8] and also one of the main features of cancer cells [76]. Owing to its complexity, replication can be disturbed by multiple mechanisms. In this review, we focused on several compounds known to be RS inducers and often used in cell-based assays. Some of the compounds have been shown to be effective in cancer treatment. Importantly, the chemicals have been primarily chosen to cover various mechanisms of action, resulting in different treatment-induced phenotypes resembling those of RS in carcinogenesis. Induction of RS in vitro, e.g., by chemicals inducing DNA damage, is a crucial research tool. Precise knowledge about the mechanism of DNA damage induction and cellular pathways involved in the RS response is particularly important for the development of appropriate cellular assays for investigating carcinogenesis and cancer treatment. The above-mentioned publications in separate compound-related tables were chosen to help with the practical aspects of such assay design. Dose and time-dependent effects related to the genetic backgrounds (i.e., dependent on the cell line used) and proper readout are important issues for experiment design. Moreover, other practical information has been included so that readers can use this review as a brief guide for choosing an appropriate model and dose scheme for cell-based studies.

**Acknowledgments:** The work was supported by Grant Agency of the Czech Republic 13-17555S, Internal Grant of Palacky University IGA-LF-2016-030, the Norwegian Financial Mechanism CZ09 (Project PHOSCAN 7F14061).

**Author Contributions:** E.V. wrote the chapter 2.3, contributed to chapters 2.2 and 2.5, prepared the figures. K.C. wrote the chapters 2.1 and 2.4, Z.T. contributed to chapter 2.5, M.M. contributed to chapter 2.2. All authors participated on the introduction part and revised the manuscript.

**Conflicts of Interest:** The authors declare no conflict of interest.

## References

1. Zeman, M.K.; Cimprich, K.A. Causes and consequences of replication stress. *Nat. Cell Biol.* **2014**, *16*, 2–9.
2. Burhans, W.C.; Weinberger, M. DNA replication stress, genome instability and aging. *Nucleic Acids Res.* **2007**, *35*, 7545–7556.
3. Huh, M.S.; Ivanochko, D.; Hashem, L.E.; Curtin, M.; Delorme, M.; Goodall, E.; Yan, K.; Picketts, D.J. Stalled replication forks within heterochromatin require ATRX for protection. *Cell Death Dis.* **2016**, *7*, e2220.
4. Gelot, C.; Magdalou, I.; Lopez, B.S. Replication stress in Mammalian cells and its consequences for mitosis. *Genes* **2015**, *6*, 267–298.
5. Krasilnikova, M.M.; Mirkin, S.M. Replication stalling at Friedreich’s ataxia (GAA)<sub>n</sub> repeats in vivo. *Mol. Cell. Biol.* **2004**, *24*, 2286–2295.
6. Neelsen, K.J.; Zanini, I.M.Y.; Mijic, S.; Herrador, R.; Zellweger, R.; Ray Chaudhuri, A.; Creavin, K.D.; Blow, J.J.; Lopes, M. Deregulated origin licensing leads to chromosomal breaks by rereplication of a gapped DNA template. *Genes Dev.* **2013**, *27*, 2537–2542.
7. Porter, A.C. Preventing DNA over-replication: A Cdk perspective. *Cell Div.* **2008**, *3*, 3.
8. Burrell, R.A.; McClelland, S.E.; Endesfelder, D.; Groth, P.; Weller, M.-C.; Shaikh, N.; Domingo, E.; Kanu, N.; Dewhurst, S.M.; Gronroos, E.; et al. Replication stress links structural and numerical cancer chromosomal instability. *Nature* **2013**, *494*, 492–496.
9. Liu, B.; Alberts, B.M. Head-on collision between a DNA replication apparatus and RNA polymerase transcription complex. *Science* **1995**, *267*, 1131–1137.
10. Bartkova, J.; Rezaei, N.; Liontos, M.; Karakaidos, P.; Kletsas, D.; Issaeva, N.; Vassiliou, L.-V.F.; Kolettas, E.; Niforou, K.; Zoumpourlis, V.C.; et al. Oncogene-induced senescence is part of the tumorigenesis barrier imposed by DNA damage checkpoints. *Nature* **2006**, *444*, 633–637.
11. Vallergera, M.B.; Mansilla, S.F.; Federico, M.B.; Bertolin, A.P.; Gottifredi, V. Rad51 recombinase prevents Mre11 nuclease-dependent degradation and excessive PrimPol-mediated elongation of nascent DNA after UV irradiation. *Proc. Natl. Acad. Sci. USA* **2015**, *112*, E6624–E6633.
12. Mazouzi, A.; Velimezi, G.; Loizou, J.I. DNA replication stress: Causes, resolution and disease. *Exp. Cell Res.* **2014**, *329*, 85–93.
13. Jekimovs, C.; Bolderson, E.; Suraweera, A.; Adams, M.; O’Byrne, K.J.; Richard, D.J. Chemotherapeutic compounds targeting the DNA double-strand break repair pathways: The good, the bad, and the promising. *Front. Oncol.* **2014**, *4*, 86.
14. Beranek, D.T. Distribution of methyl and ethyl adducts following alkylation with monofunctional alkylating agents. *Mutat. Res.* **1990**, *231*, 11–30.
15. Kondo, N.; Takahashi, A.; Mori, E.; Noda, T.; Su, X.; Ohnishi, K.; McKinnon, P.J.; Sakaki, T.; Nakase, H.; Ono, K.; et al. DNA ligase IV is a potential molecular target in ACNU sensitivity. *Cancer Sci.* **2010**, *101*, 1881–1885.
16. Brookes, P.; Lawley, P.D. The reaction of mono- and di-functional alkylating agents with nucleic acids. *Biochem. J.* **1961**, *80*, 496–503.
17. Lawley, P.D.; Brookes, P. The action of alkylating agents on deoxyribonucleic acid in relation to biological effects of the alkylating agents. *Exp. Cell Res.* **1963**, *24* (Suppl. S9), 512–520.
18. Noll, D.M.; Mason, T.M.; Miller, P.S. Formation and repair of interstrand cross-links in DNA. *Chem. Rev.* **2006**, *106*, 277–301.
19. Schärer, O.D. DNA Interstrand Crosslinks: Natural and Drug-Induced DNA Adducts that Induce Unique Cellular Responses. *ChemBioChem* **2005**, *6*, 27–32.
20. Lawley, P.D.; Phillips, D.H. DNA adducts from chemotherapeutic agents. *Mutat. Res.* **1996**, *355*, 13–40.
21. Bhuyan, B.K.; Scheidt, L.G.; Fraser, T.J. Cell cycle phase specificity of antitumor agents. *Cancer Res.* **1972**, *32*, 398–407.
22. Glover, T.W.; Arlt, M.F.; Casper, A.M.; Durkin, S.G. Mechanisms of common fragile site instability. *Hum. Mol. Genet.* **2005**, *14*, R197–R205.
23. Koç, A.; Wheeler, L.J.; Mathews, C.K.; Merrill, G.F. Hydroxyurea arrests DNA replication by a mechanism that preserves basal dNTP pools. *J. Biol. Chem.* **2004**, *279*, 223–230.
24. Hsiang, Y.H.; Lihou, M.G.; Liu, L.F. Arrest of replication forks by drug-stabilized topoisomerase I-DNA cleavable complexes as a mechanism of cell killing by camptothecin. *Cancer Res.* **1989**, *49*, 5077–5082.



25. Deweese, J.E.; Osheroff, N. The DNA cleavage reaction of topoisomerase II: Wolf in sheep's clothing. *Nucleic Acids Res.* **2009**, *37*, 738–748.
26. Helleday, T.; Petermann, E.; Lundin, C.; Hodgson, B.; Sharma, R.A. DNA repair pathways as targets for cancer therapy. *Nat. Rev. Cancer* **2008**, *8*, 193–204.
27. Krokan, H.E.; Bjørås, M. Base Excision Repair. *Cold Spring Harb. Perspect. Biol.* **2013**, *5*, a012583, doi: 10.1101/cshperspect.a012583.
28. Gillet, L.C.J.; Schärer, O.D. Molecular mechanisms of mammalian global genome nucleotide excision repair. *Chem. Rev.* **2006**, *106*, 253–276.
29. Caldecott, K.W. Protein ADP-ribosylation and the cellular response to DNA strand breaks. *DNA Repair* **2014**, *19*, 108–113.
30. Heyer, W.-D.; Ehmsen, K.T.; Liu, J. Regulation of homologous recombination in eukaryotes. *Annu. Rev. Genet.* **2010**, *44*, 113–139.
31. Davis, A.J.; Chen, D.J. DNA double strand break repair via non-homologous end-joining. *Transl. Cancer Res.* **2013**, *2*, 130–143.
32. Bi, X. Mechanism of DNA damage tolerance. *World J. Biol. Chem.* **2015**, *6*, 48–56.
33. Aguilera, A.; Gómez-González, B. Genome instability: A mechanistic view of its causes and consequences. *Nat. Rev. Genet.* **2008**, *9*, 204–217.
34. Chang, D.J.; Cimprich, K.A. DNA damage tolerance: When it's OK to make mistakes. *Nat. Chem. Biol.* **2009**, *5*, 82–90.
35. Ghosal, G.; Chen, J. DNA damage tolerance: A double-edged sword guarding the genome. *Transl. Cancer Res.* **2013**, *2*, 107–129.
36. Saugar, I.; Ortiz-Bazán, M.Á.; Tercero, J.A. Tolerating DNA damage during eukaryotic chromosome replication. *Exp. Cell Res.* **2014**, *329*, 170–177.
37. Deans, A.J.; West, S.C. DNA interstrand crosslink repair and cancer. *Nat. Rev. Cancer* **2011**, *11*, 467–480.
38. Longerich, S.; Li, J.; Xiong, Y.; Sung, P.; Kupfer, G.M. Stress and DNA repair biology of the Fanconi anemia pathway. *Blood* **2014**, *124*, 2812–2819.
39. Gaillard, H.; García-Muse, T.; Aguilera, A. Replication stress and cancer. *Nat. Rev. Cancer* **2015**, *15*, 276–289.
40. Mamrak, N.E.; Shimamura, A.; Howlett, N.G. Recent discoveries in the molecular pathogenesis of the inherited bone marrow failure syndrome Fanconi anemia. *Blood Rev.* **2016**, doi:10.1016/j.blre.2016.10.002.
41. Kennedy, R.D.; D'Andrea, A.D. The Fanconi Anemia/BRCA pathway: New faces in the crowd. *Genes Dev.* **2005**, *19*, 2925–2940.
42. Thompson, L.H.; Hinz, J.M. Cellular and molecular consequences of defective Fanconi anemia proteins in replication-coupled DNA repair: Mechanistic insights. *Mutat. Res.* **2009**, *668*, 54–72.
43. Branzei, D. Ubiquitin family modifications and template switching. *FEBS Lett.* **2011**, *585*, 2810–2817.
44. Xu, X.; Blackwell, S.; Lin, A.; Li, F.; Qin, Z.; Xiao, W. Error-free DNA-damage tolerance in *Saccharomyces cerevisiae*. *Mutat. Res. Rev. Mutat. Res.* **2015**, *764*, 43–50.
45. Ge, X.Q.; Jackson, D.A.; Blow, J.J. Dormant origins licensed by excess Mcm2–7 are required for human cells to survive replicative stress. *Genes Dev.* **2007**, *21*, 3331–3341.
46. Lopes, M.; Foiani, M.; Sogo, J.M. Multiple mechanisms control chromosome integrity after replication fork uncoupling and restart at irreparable UV lesions. *Mol. Cell* **2006**, *21*, 15–27.
47. Woodward, A.M.; Göhler, T.; Luciani, M.G.; Oehlmann, M.; Ge, X.; Gartner, A.; Jackson, D.A.; Blow, J.J. Excess Mcm2–7 license dormant origins of replication that can be used under conditions of replicative stress. *J. Cell Biol.* **2006**, *173*, 673–683.
48. Elvers, I.; Johansson, F.; Groth, P.; Erixon, K.; Helleday, T. UV stalled replication forks restart by re-priming in human fibroblasts. *Nucleic Acids Res.* **2011**, *39*, 7049–7057.
49. McIntosh, D.; Blow, J.J. Dormant origins, the licensing checkpoint, and the response to replicative stresses. *Cold Spring Harb. Perspect. Biol.* **2012**, *4*, a012955.
50. De Piccoli, G.; Katou, Y.; Itoh, T.; Nakato, R.; Shirahige, K.; Labib, K. Replisome stability at defective DNA replication forks is independent of S phase checkpoint kinases. *Mol. Cell* **2012**, *45*, 696–704.
51. Tercero, J.A.; Diffley, J.F.X. Regulation of DNA replication fork progression through damaged DNA by the Mec1/Rad53 checkpoint. *Nature* **2001**, *412*, 553–557.
52. Lopes, M.; Cotta-Ramusino, C.; Pelliccioli, A.; Liberi, G.; Plevani, P.; Muzi-Falconi, M.; Newlon, C.S.; Foiani, M. The DNA replication checkpoint response stabilizes stalled replication forks. *Nature* **2001**, *412*, 557–561.

53. Cobb, J.A.; Bjergbaek, L.; Shimada, K.; Frei, C.; Gasser, S.M. DNA polymerase stabilization at stalled replication forks requires Mec1 and the RecQ helicase Sgs1. *EMBO J.* **2003**, *22*, 4325–4336.
54. Ragland, R.L.; Patel, S.; Rivard, R.S.; Smith, K.; Peters, A.A.; Bielinsky, A.-K.; Brown, E.J. RNF4 and PLK1 are required for replication fork collapse in ATR-deficient cells. *Genes Dev.* **2013**, *27*, 2259–2273.
55. Hanada, K.; Budzowska, M.; Davies, S.L.; van Drunen, E.; Onizawa, H.; Beverloo, H.B.; Maas, A.; Essers, J.; Hickson, I.D.; Kanaar, R. The structure-specific endonuclease Mus81 contributes to replication restart by generating double-strand DNA breaks. *Nat. Struct. Mol. Biol.* **2007**, *14*, 1096–1104.
56. Forment, J.V.; Blasius, M.; Guerini, I.; Jackson, S.P. Structure-specific DNA endonuclease Mus81/Eme1 generates DNA damage caused by Chk1 inactivation. *PLoS ONE* **2011**, *6*, e23517.
57. Zellweger, R.; Dalcher, D.; Mutreja, K.; Berti, M.; Schmid, J.A.; Herrador, R.; Vindigni, A.; Lopes, M. Rad51-mediated replication fork reversal is a global response to genotoxic treatments in human cells. *J. Cell Biol.* **2015**, *208*, 563–579.
58. Pacek, M.; Walter, J.C. A requirement for MCM7 and Cdc45 in chromosome unwinding during eukaryotic DNA replication. *EMBO J.* **2004**, *23*, 3667–3676.
59. Byun, T.S.; Pacek, M.; Yee, M.; Walter, J.C.; Cimprich, K.A. Functional uncoupling of MCM helicase and DNA polymerase activities activates the ATR-dependent checkpoint. *Genes Dev.* **2005**, *19*, 1040–1052.
60. Zou, L.; Elledge, S.J. Sensing DNA damage through ATRIP recognition of RPA-ssDNA complexes. *Science* **2003**, *300*, 1542–1548.
61. MacDougall, C.A.; Byun, T.S.; Van, C.; Yee, M.; Cimprich, K.A. The structural determinants of checkpoint activation. *Genes Dev.* **2007**, *21*, 898–903.
62. Nam, E.A.; Cortez, D. ATR signalling: More than meeting at the fork. *Biochem. J.* **2011**, *436*, 527–536.
63. Maréchal, A.; Zou, L. DNA damage sensing by the ATM and ATR kinases. *Cold Spring Harb. Perspect. Biol.* **2013**, *5*, a012716.
64. Lucca, C.; Vanoli, F.; Cotta-Ramusino, C.; Pelliccioli, A.; Liberi, G.; Haber, J.; Foiani, M. Checkpoint-mediated control of replisome-fork association and signalling in response to replication pausing. *Oncogene* **2004**, *23*, 1206–1213.
65. Petermann, E.; Orta, M.L.; Issaeva, N.; Schultz, N.; Helleday, T. Hydroxyurea-stalled replication forks become progressively inactivated and require two different RAD51-mediated pathways for restart and repair. *Mol. Cell* **2010**, *37*, 492–502.
66. Labib, K.; De Piccoli, G. Surviving chromosome replication: The many roles of the S-phase checkpoint pathway. *Philos. Trans. R. Soc. Lond. B Biol. Sci.* **2011**, *366*, 3554–3561.
67. Ozeri-Galai, E.; Schwartz, M.; Rahat, A.; Kerem, B. Interplay between ATM and ATR in the regulation of common fragile site stability. *Oncogene* **2008**, *27*, 2109–2117.
68. Ciccio, A.; Elledge, S.J. The DNA damage response: Making it safe to play with knives. *Mol. Cell* **2010**, *40*, 179–204.
69. Ammazalorso, F.; Pirzio, L.M.; Bignami, M.; Franchitto, A.; Pichierri, P. ATR and ATM differently regulate WRN to prevent DSBs at stalled replication forks and promote replication fork recovery. *EMBO J.* **2010**, *29*, 3156–3169.
70. Bachrati, C.Z.; Hickson, I.D. RecQ helicases: Suppressors of tumorigenesis and premature aging. *Biochem. J.* **2003**, *374*, 577–606.
71. Hills, S.A.; Diffley, J.F.X. DNA replication and oncogene-induced replicative stress. *Curr. Biol.* **2014**, *24*, R435–R444.
72. Macheret, M.; Halazonetis, T.D. DNA replication stress as a hallmark of cancer. *Annu. Rev. Pathol.* **2015**, *10*, 425–448.
73. Murga, M.; Campaner, S.; Lopez-Contreras, A.J.; Toledo, L.I.; Soria, R.; Montaña, M.F.; D’Artista, L.; Schleker, T.; Guerra, C.; Garcia, E.; et al. Exploiting oncogene-induced replicative stress for the selective killing of Myc-driven tumors. *Nat. Struct. Mol. Biol.* **2011**, *18*, 1331–1335.
74. Marusyk, A.; Wheeler, L.J.; Mathews, C.K.; DeGregori, J. p53 mediates senescence-like arrest induced by chronic replicational stress. *Mol. Cell Biol.* **2007**, *27*, 5336–5351.
75. Bai, G.; Smolka, M.B.; Schimenti, J.C. Chronic DNA Replication Stress Reduces Replicative Lifespan of Cells by TRP53-Dependent, microRNA-Assisted MCM2–7 Downregulation. *PLoS Genet.* **2016**, *12*, e1005787.
76. Bartkova, J.; Horejsí, Z.; Koed, K.; Krämer, A.; Tort, F.; Zieger, K.; Guldborg, P.; Sehested, M.; Nesland, J.M.; Lukas, C.; et al. DNA damage response as a candidate anti-cancer barrier in early human tumorigenesis. *Nature* **2005**, *434*, 864–870.

77. O'Driscoll, M.; Ruiz-Perez, V.L.; Woods, C.G.; Jeggo, P.A.; Goodship, J.A. A splicing mutation affecting expression of ataxia-telangiectasia and Rad3-related protein (ATR) results in Seckel syndrome. *Nat. Genet.* **2003**, *33*, 497–501.
78. McKinnon, P.J. ATM and ataxia telangiectasia. *EMBO Rep.* **2004**, *5*, 772–776.
79. DiGiovanna, J.J.; Kraemer, K.H. Shining a light on xeroderma pigmentosum. *J. Investig. Dermatol.* **2012**, *132*, 785–796.
80. Callén, E.; Surrallés, J. Telomere dysfunction in genome instability syndromes. *Mutat. Res.* **2004**, *567*, 85–104.
81. Lauper, J.M.; Krause, A.; Vaughan, T.L.; Monnat, R.J. Spectrum and risk of neoplasia in Werner syndrome: A systematic review. *PLoS ONE* **2013**, *8*, e59709.
82. Bernstein, K.A.; Gangloff, S.; Rothstein, R. The RecQ DNA helicases in DNA repair. *Annu. Rev. Genet.* **2010**, *44*, 393–417.
83. Kim, H.; D'Andrea, A.D. Regulation of DNA cross-link repair by the Fanconi anemia/BRCA pathway. *Genes Dev.* **2012**, *26*, 1393–1408.
84. Joenje, H.; Patel, K.J. The emerging genetic and molecular basis of Fanconi anaemia. *Nat. Rev. Genet.* **2001**, *2*, 446–457.
85. Larizza, L.; Roversi, G.; Volpi, L. Rothmund-Thomson syndrome. *Orphanet J. Rare Dis.* **2010**, *5*, 2.
86. Lu, H.; Shamanna, R.A.; Keijzers, G.; Anand, R.; Rasmussen, L.J.; Cejka, P.; Croteau, D.L.; Bohr, V.A. RECQL4 Promotes DNA End Resection in Repair of DNA Double-Strand Breaks. *Cell Rep.* **2016**, *16*, 161–173.
87. Rosenberg, B.; Vancamp, L.; Krigas, T. Inhibition of cell division in *Escherichia coli* by electrolysis products from a platinum electrode. *Nature* **1965**, *205*, 698–699.
88. Todd, R.C.; Lippard, S.J. Inhibition of transcription by platinum antitumor compounds. *Metallomics* **2009**, *1*, 280–291.
89. Zamble, D.B.; Lippard, S.J. Cisplatin and DNA repair in cancer chemotherapy. *Trends Biochem. Sci.* **1995**, *20*, 435–439.
90. Available online: <http://www.rcsb.org/pdb/explore/explore.do?structureId=3CO3> (accessed on 23 January 2017).
91. Fichtinger-Schepman, A.M.; van der Veer, J.L.; den Hartog, J.H.; Lohman, P.H.; Reedijk, J. Adducts of the antitumor drug *cis*-diamminedichloroplatinum(II) with DNA: Formation, identification, and quantitation. *Biochemistry* **1985**, *24*, 707–713.
92. Harder, H.C.; Rosenberg, B. Inhibitory effects of anti-tumor platinum compounds on DNA, RNA and protein syntheses in mammalian cells in vitro. *Int. J. Cancer* **1970**, *6*, 207–216.
93. Eastman, A. Reevaluation of interaction of *cis*-dichloro(ethylenediamine)platinum(II) with DNA. *Biochemistry* **1986**, *25*, 3912–3915.
94. Sherman, S.E.; Gibson, D.; Wang, A.H.; Lippard, S.J. X-ray structure of the major adduct of the anticancer drug cisplatin with DNA: *cis*-[Pt(NH<sub>3</sub>)<sub>2</sub>(d(pGpG))]. *Science* **1985**, *230*, 412–417.
95. Eastman, A. Separation and characterization of products resulting from the reaction of *cis*-diamminedichloroplatinum (II) with deoxyribonucleosides. *Biochemistry* **1982**, *21*, 6732–6736.
96. Desoize, B. Cancer and metals and metal compounds: Part I—Carcinogenesis. *Crit. Rev. Oncol. Hematol.* **2002**, *42*, 1–3.
97. Köberle, B.; Masters, J.R.; Hartley, J.A.; Wood, R.D. Defective repair of cisplatin-induced DNA damage caused by reduced XPA protein in testicular germ cell tumours. *Curr. Biol.* **1999**, *9*, 273–276.
98. Borst, P.; Rottenberg, S.; Jonkers, J. How do real tumors become resistant to cisplatin? *Cell Cycle* **2008**, *7*, 1353–1359.
99. Sedletskaya, Y.; Fourrier, L.; Malinge, J.-M. Modulation of MutS ATP-dependent functional activities by DNA containing a cisplatin compound lesion (base damage and mismatch). *J. Mol. Biol.* **2007**, *369*, 27–40.
100. Brown, R.; Clugston, C.; Burns, P.; Edlin, A.; Vasey, P.; Vojtěšek, B.; Kaye, S.B. Increased accumulation of p53 protein in cisplatin-resistant ovarian cell lines. *Int. J. Cancer* **1993**, *55*, 678–684.
101. Damsma, G.E.; Alt, A.; Brueckner, F.; Carell, T.; Cramer, P. Mechanism of transcriptional stalling at cisplatin-damaged DNA. *Nat. Struct. Mol. Biol.* **2007**, *14*, 1127–1133.
102. Shimodaira, H.; Yoshioka-Yamashita, A.; Kolodner, R.D.; Wang, J.Y.J. Interaction of mismatch repair protein PMS2 and the p53-related transcription factor p73 in apoptosis response to cisplatin. *Proc. Natl. Acad. Sci. USA* **2003**, *100*, 2420–2425.

103. Aebi, S.; Kurdi-Haidar, B.; Gordon, R.; Cenni, B.; Zheng, H.; Fink, D.; Christen, R.D.; Boland, C.R.; Koi, M.; Fishel, R.; et al. Loss of DNA mismatch repair in acquired resistance to cisplatin. *Cancer Res.* **1996**, *56*, 3087–3090.
104. Alt, A.; Lammens, K.; Chiocchini, C.; Lammens, A.; Pieck, J.C.; Kuch, D.; Hopfner, K.-P.; Carell, T. Bypass of DNA lesions generated during anticancer treatment with cisplatin by DNA polymerase eta. *Science* **2007**, *318*, 967–970.
105. Brozovic, A.; Ambriović-Ristov, A.; Osmak, M. The relationship between cisplatin-induced reactive oxygen species, glutathione, and BCL-2 and resistance to cisplatin. *Crit. Rev. Toxicol.* **2010**, *40*, 347–359.
106. Spletstoeser, F.; Florea, A.-M.; Büsselberg, D. IP<sub>3</sub> receptor antagonist, 2-APB, attenuates cisplatin induced Ca<sup>2+</sup>-influx in HeLa-S3 cells and prevents activation of calpain and induction of apoptosis. *Br. J. Pharmacol.* **2007**, *151*, 1176–1186.
107. Shamimi-Noori, S.; Yeow, W.-S.; Ziauddin, M.F.; Xin, H.; Tran, T.L.N.; Xie, J.; Loehfelm, A.; Patel, P.; Yang, J.; Schrupp, D.S.; et al. Cisplatin enhances the antitumor effect of tumor necrosis factor-related apoptosis-inducing ligand gene therapy via recruitment of the mitochondria-dependent death signaling pathway. *Cancer Gene Ther.* **2008**, *15*, 356–370.
108. Qian, W.; Nishikawa, M.; Haque, A.M.; Hirose, M.; Mashimo, M.; Sato, E.; Inoue, M. Mitochondrial density determines the cellular sensitivity to cisplatin-induced cell death. *Am. J. Physiol. Cell Physiol.* **2005**, *289*, C1466–C1475.
109. Wetzels, C.C.; Berberich, S.J. p53 binds to cisplatin-damaged DNA. *Biochim. Biophys. Acta* **2001**, *1517*, 392–397.
110. Kutuk, O.; Arisan, E.D.; Tezil, T.; Shoshan, M.C.; Basaga, H. Cisplatin overcomes Bcl-2-mediated resistance to apoptosis via preferential engagement of Bak: Critical role of Noxa-mediated lipid peroxidation. *Carcinogenesis* **2009**, *30*, 1517–1527.
111. Kim, H.-S.; Hwang, J.-T.; Yun, H.; Chi, S.-G.; Lee, S.-J.; Kang, I.; Yoon, K.-S.; Choe, W.-J.; Kim, S.-S.; Ha, J. Inhibition of AMP-activated protein kinase sensitizes cancer cells to cisplatin-induced apoptosis via hyperinduction of p53. *J. Biol. Chem.* **2008**, *283*, 3731–3742.
112. Yang, C.; Kaushal, V.; Haun, R.S.; Seth, R.; Shah, S.V.; Kaushal, G.P. Transcriptional activation of caspase-6 and -7 genes by cisplatin-induced p53 and its functional significance in cisplatin nephrotoxicity. *Cell Death Differ.* **2008**, *15*, 530–544.
113. Jiang, M.; Wei, Q.; Wang, J.; Du, Q.; Yu, J.; Zhang, L.; Dong, Z. Regulation of PUMA-alpha by p53 in cisplatin-induced renal cell apoptosis. *Oncogene* **2006**, *25*, 4056–4066.
114. Righetti, S.C.; Della Torre, G.; Pilotti, S.; Ménard, S.; Ottone, F.; Colnaghi, M.I.; Pierotti, M.A.; Lavarino, C.; Cornarotti, M.; Oriana, S.; et al. A comparative study of p53 gene mutations, protein accumulation, and response to cisplatin-based chemotherapy in advanced ovarian carcinoma. *Cancer Res.* **1996**, *56*, 689–693.
115. Johnson, C.L.; Lu, D.; Huang, J.; Basu, A. Regulation of p53 stabilization by DNA damage and protein kinase C. *Mol. Cancer Ther.* **2002**, *1*, 861–867.
116. Gong, J.G.; Costanzo, A.; Yang, H.Q.; Melino, G.; Kaelin, W.G.; Levrero, M.; Wang, J.Y. The tyrosine kinase c-Abl regulates p73 in apoptotic response to cisplatin-induced DNA damage. *Nature* **1999**, *399*, 806–809.
117. Preyer, M.; Shu, C.-W.; Wang, J.Y.J. Delayed activation of Bax by DNA damage in embryonic stem cells with knock-in mutations of the Abl nuclear localization signals. *Cell Death Differ.* **2007**, *14*, 1139–1148.
118. Tsai, K.K.C.; Yuan, Z.-M. c-Abl stabilizes p73 by a phosphorylation-augmented interaction. *Cancer Res.* **2003**, *63*, 3418–3424.
119. Levy, D.; Adamovich, Y.; Reuven, N.; Shaul, Y. Yap1 phosphorylation by c-Abl is a critical step in selective activation of proapoptotic genes in response to DNA damage. *Mol. Cell* **2008**, *29*, 350–361.
120. Jones, E.V.; Dickman, M.J.; Whitmarsh, A.J. Regulation of p73-mediated apoptosis by c-Jun N-terminal kinase. *Biochem. J.* **2007**, *405*, 617–623.
121. Hayakawa, J.; Ohmichi, M.; Kurachi, H.; Kanda, Y.; Hisamoto, K.; Nishio, Y.; Adachi, K.; Tasaka, K.; Kanzaki, T.; Murata, Y. Inhibition of BAD phosphorylation either at serine 112 via extracellular signal-regulated protein kinase cascade or at serine 136 via Akt cascade sensitizes human ovarian cancer cells to cisplatin. *Cancer Res.* **2000**, *60*, 5988–5994.
122. Isonishi, S.; Andrews, P.A.; Howell, S.B. Increased sensitivity to cis-diamminedichloroplatinum(II) in human ovarian carcinoma cells in response to treatment with 12-O-tetradecanoylphorbol 13-acetate. *J. Biol. Chem.* **1990**, *265*, 3623–3627.

123. Basu, A.; Teicher, B.A.; Lazo, J.S. Involvement of protein kinase C in phorbol ester-induced sensitization of HeLa cells to *cis*-diamminedichloroplatinum(II). *J. Biol. Chem.* **1990**, *265*, 8451–8457.
124. Wang, X.; Dhalla, N.S. Modification of beta-adrenoceptor signal transduction pathway by genetic manipulation and heart failure. *Mol. Cell. Biochem.* **2000**, *214*, 131–155.
125. Basu, A.; Tu, H. Activation of ERK during DNA damage-induced apoptosis involves protein kinase Cdelta. *Biochem. Biophys. Res. Commun.* **2005**, *334*, 1068–1073.
126. Nowak, G. Protein kinase C-alpha and ERK1/2 mediate mitochondrial dysfunction, decreases in active Na<sup>+</sup> transport, and cisplatin-induced apoptosis in renal cells. *J. Biol. Chem.* **2002**, *277*, 43377–43388.
127. Sánchez-Pérez, I.; Benitah, S.A.; Martínez-Gomariz, M.; Lacal, J.C.; Perona, R. Cell stress and MEKK1-mediated c-Jun activation modulate NFκB activity and cell viability. *Mol. Biol. Cell* **2002**, *13*, 2933–2945.
128. Jones, J.A.; Stroud, R.E.; Kaplan, B.S.; Leone, A.M.; Bavaria, J.E.; Gorman, J.H.; Gorman, R.C.; Ikonomidis, J.S. Differential protein kinase C isoform abundance in ascending aortic aneurysms from patients with bicuspid versus tricuspid aortic valves. *Circulation* **2007**, *116*, I144–I149.
129. Zanke, B.W.; Boudreau, K.; Rubie, E.; Winnett, E.; Tibbles, L.A.; Zon, L.; Kyriakis, J.; Liu, F.F.; Woodgett, J.R. The stress-activated protein kinase pathway mediates cell death following injury induced by *cis*-platinum, UV irradiation or heat. *Curr. Biol.* **1996**, *6*, 606–613.
130. Hernández Losa, J.; Parada Cobo, C.; Guinea Viniegra, J.; Sánchez-Arevalo Lobo, V.J.; Ramón y Cajal, S.; Sánchez-Prieto, R. Role of the p38 MAPK pathway in cisplatin-based therapy. *Oncogene* **2003**, *22*, 3998–4006.
131. Wang, S.J.; Bourguignon, L.Y.W. Hyaluronan-CD44 promotes phospholipase C-mediated Ca<sup>2+</sup> signaling and cisplatin resistance in head and neck cancer. *Arch. Otolaryngol. Head Neck Surg.* **2006**, *132*, 19–24.
132. Speelmans, G.; Staffhorst, R.W.; Versluis, K.; Reedijk, J.; de Kruijff, B. Cisplatin complexes with phosphatidylserine in membranes. *Biochemistry* **1997**, *36*, 10545–10550.
133. Huihui, Z.; Baohuai, W.; Youming, Z.; Kui, W. Calorimetric studies on actin polymerization and a comparison of the effects of cisplatin and transplatin. *Thermochim. Acta* **1995**, *265*, 31–38.
134. Chen, X.; Jiang, Y.; Huang, Z.; Li, D.; Chen, X.; Cao, M.; Meng, Q.; Pang, H.; Sun, L.; Zhao, Y.; et al. miRNA-378 reverses chemoresistance to cisplatin in lung adenocarcinoma cells by targeting secreted clusterin. *Sci. Rep.* **2016**, *6*, 19455.
135. Zhu, H.; Wu, H.; Liu, X.; Evans, B.R.; Medina, D.J.; Liu, C.-G.; Yang, J.-M. Role of MicroRNA miR-27a and miR-451 in the regulation of MDR1/P-glycoprotein expression in human cancer cells. *Biochem. Pharmacol.* **2008**, *76*, 582–588.
136. Vanas, V.; Haigl, B.; Stockhammer, V.; Sutterlüty-Fall, H. MicroRNA-21 Increases Proliferation and Cisplatin Sensitivity of Osteosarcoma-Derived Cells. *PLoS ONE* **2016**, *11*, e0161023.
137. Double, E.B.; Richmond, R.C. Platinum complexes as radiosensitizers of hypoxic mammalian cells. *Br. J. Cancer Suppl.* **1978**, *3*, 98–102.
138. Boeckman, H.J.; Trego, K.S.; Turchi, J.J. Cisplatin sensitizes cancer cells to ionizing radiation via inhibition of nonhomologous end joining. *Mol. Cancer Res.* **2005**, *3*, 277–285.
139. Ishibashi, T.; Lippard, S.J. Telomere loss in cells treated with cisplatin. *Proc. Natl. Acad. Sci. USA* **1998**, *95*, 4219–4223.
140. Jordan, P.; Carmo-Fonseca, M. Cisplatin inhibits synthesis of ribosomal RNA in vivo. *Nucleic Acids Res.* **1998**, *26*, 2831–2836.
141. Tofilon, P.J.; Vines, C.M.; Baker, F.L.; Deen, D.F.; Brock, W.A. *cis*-Diamminedichloroplatinum(II)-induced sister chromatid exchange: An indicator of sensitivity and heterogeneity in primary human tumor cell cultures. *Cancer Res.* **1986**, *46*, 6156–6159.
142. Berndtsson, M.; Hägg, M.; Panaretakis, T.; Havelka, A.M.; Shoshan, M.C.; Linder, S. Acute apoptosis by cisplatin requires induction of reactive oxygen species but is not associated with damage to nuclear DNA. *Int. J. Cancer* **2007**, *120*, 175–180.
143. Rouette, A.; Parent, S.; Girouard, J.; Leblanc, V.; Asselin, E. Cisplatin increases B-cell-lymphoma-2 expression via activation of protein kinase C and Akt2 in endometrial cancer cells. *Int. J. Cancer* **2012**, *130*, 1755–1767.
144. Damia, G.; Filiberti, L.; Vikhanskaya, F.; Carrassa, L.; Taya, Y.; D'Incalci, M.; Broggin, M. Cisplatin and taxol induce different patterns of p53 phosphorylation. *Neoplasia* **2001**, *3*, 10–16.

145. Lützkendorf, J.; Wieduwild, E.; Nerger, K.; Lambrecht, N.; Schmoll, H.-J.; Müller-Tidow, C.; Müller, L.P. Resistance for Genotoxic Damage in Mesenchymal Stromal Cells Is Increased by Hypoxia but Not Generally Dependent on p53-Regulated Cell Cycle Arrest. *PLoS ONE* **2017**, *12*, e0169921.
146. Sorenson, C.M.; Barry, M.A.; Eastman, A. Analysis of events associated with cell cycle arrest at G2 phase and cell death induced by cisplatin. *J. Natl. Cancer Inst.* **1990**, *82*, 749–755.
147. Podratz, J.L.; Knight, A.M.; Ta, L.E.; Staff, N.P.; Gass, J.M.; Genelin, K.; Schlattau, A.; Lathroum, L.; Windebank, A.J. Cisplatin induced mitochondrial DNA damage in dorsal root ganglion neurons. *Neurobiol. Dis.* **2011**, *41*, 661–668.
148. Wagner, J.M.; Karnitz, L.M. Cisplatin-induced DNA damage activates replication checkpoint signaling components that differentially affect tumor cell survival. *Mol. Pharmacol.* **2009**, *76*, 208–214.
149. Bürkle, A.; Chen, G.; Küpper, J.H.; Grube, K.; Zeller, W.J. Increased poly(ADP-ribosyl)ation in intact cells by cisplatin treatment. *Carcinogenesis* **1993**, *14*, 559–561.
150. Jennerwein, M.; Andrews, P.A. Drug accumulation and DNA platination in cells exposed to aquated cisplatin species. *Cancer Lett.* **1994**, *81*, 215–220.
151. Shirazi, F.H.; Molepo, J.M.; Stewart, D.J.; Ng, C.E.; Raaphorst, G.P.; Goel, R. Cytotoxicity, accumulation, and efflux of cisplatin and its metabolites in human ovarian carcinoma cells. *Toxicol. Appl. Pharmacol.* **1996**, *140*, 211–218.
152. Hall, M.D.; Telma, K.A.; Chang, K.-E.; Lee, T.D.; Madigan, J.P.; Lloyd, J.R.; Goldlust, I.S.; Hoeschele, J.D.; Gottesman, M.M. Say no to DMSO: Dimethylsulfoxide inactivates cisplatin, carboplatin, and other platinum complexes. *Cancer Res.* **2014**, *74*, 3913–3922.
153. Available online: <http://www.webcitation.org/6mEemW8DM> (accessed on 23 November 2016).
154. Massart, C.; Le Tellier, C.; Gibassier, J.; Leclech, G.; Nicol, M. Modulation by dimethyl sulphoxide of the toxicity induced by *cis*-diamminedichloroplatinum in cultured thyrocytes. *Toxicol. Vitro* **1993**, *7*, 87–94.
155. Wiltshaw, E.; Subramarian, S.; Alexopoulos, C.; Barker, G.H. Cancer of the ovary: A summary of experience with *cis*-dichlorodiammineplatinum(II) at the Royal Marsden Hospital. *Cancer Treat. Rep.* **1979**, *63*, 1545–1548.
156. Galanski, M. Recent developments in the field of anticancer platinum complexes. *Recent Pat. Anticancer Drug Discov.* **2006**, *1*, 285–295.
157. Lebwahl, D.; Canetta, R. Clinical development of platinum complexes in cancer therapy: An historical perspective and an update. *Eur. J. Cancer* **1998**, *34*, 1522–1534.
158. Baetz, T.; Belch, A.; Couban, S.; Imrie, K.; Yau, J.; Myers, R.; Ding, K.; Paul, N.; Shepherd, L.; Iglesias, J.; et al. Gemcitabine, dexamethasone and cisplatin is an active and non-toxic chemotherapy regimen in relapsed or refractory Hodgkin’s disease: A phase II study by the National Cancer Institute of Canada Clinical Trials Group. *Ann. Oncol.* **2003**, *14*, 1762–1767.
159. Crump, M.; Baetz, T.; Couban, S.; Belch, A.; Marcellus, D.; Howson-Jan, K.; Imrie, K.; Myers, R.; Adams, G.; Ding, K.; et al. Gemcitabine, dexamethasone, and cisplatin in patients with recurrent or refractory aggressive histology B-cell non-Hodgkin lymphoma: A Phase II study by the National Cancer Institute of Canada Clinical Trials Group (NCIC-CTG). *Cancer* **2004**, *101*, 1835–1842.
160. Pearson, A.D.J.; Pinkerton, C.R.; Lewis, I.J.; Imeson, J.; Ellershaw, C.; Machin, D.; European Neuroblastoma Study Group; Children’s Cancer and Leukaemia Group (CCLG formerly United Kingdom Children’s Cancer Study Group) High-dose rapid and standard induction chemotherapy for patients aged over 1 year with stage 4 neuroblastoma: A randomised trial. *Lancet Oncol.* **2008**, *9*, 247–256.
161. Reichardt, P. The treatment of uterine sarcomas. *Ann. Oncol.* **2012**, *23* (Suppl. S10), x151–x157.
162. Dadacaridou, M.; Papanicolaou, X.; Maltesas, D.; Megalakaki, C.; Patos, P.; Panteli, K.; Repousis, P.; Mitsouli-Mentzikof, C. Dexamethasone, cyclophosphamide, etoposide and cisplatin (DCEP) for relapsed or refractory multiple myeloma patients. *J. BUON* **2007**, *12*, 41–44.
163. Glover, D.; Glick, J.H.; Weiler, C.; Fox, K.; Guerry, D. WR-2721 and high-dose cisplatin: An active combination in the treatment of metastatic melanoma. *J. Clin. Oncol.* **1987**, *5*, 574–578.
164. Berghmans, T.; Paesmans, M.; Lalami, Y.; Louviaux, I.; Luce, S.; Mascaux, C.; Meert, A.P.; Sculier, J.P. Activity of chemotherapy and immunotherapy on malignant mesothelioma: A systematic review of the literature with meta-analysis. *Lung Cancer* **2002**, *38*, 111–121.
165. Hanada, K.; Nishijima, K.; Ogata, H.; Atagi, S.; Kawahara, M. Population pharmacokinetic analysis of cisplatin and its metabolites in cancer patients: Possible misinterpretation of covariates for pharmacokinetic

- parameters calculated from the concentrations of unchanged cisplatin, ultrafiltered platinum and total platinum. *Jpn. J. Clin. Oncol.* **2001**, *31*, 179–184.
166. Daugaard, G.; Abildgaard, U. Cisplatin nephrotoxicity. A review. *Cancer Chemother. Pharmacol.* **1989**, *25*, 1–9.
167. Nagai, N.; Kinoshita, M.; Ogata, H.; Tsujino, D.; Wada, Y.; Someya, K.; Ohno, T.; Masuhara, K.; Tanaka, Y.; Kato, K.; et al. Relationship between pharmacokinetics of unchanged cisplatin and nephrotoxicity after intravenous infusions of cisplatin to cancer patients. *Cancer Chemother. Pharmacol.* **1996**, *39*, 131–137.
168. Kartalou, M.; Essigmann, J.M. Mechanisms of resistance to cisplatin. *Mutat. Res.* **2001**, *478*, 23–43.
169. Olszewski, U.; Hamilton, G. A better platinum-based anticancer drug yet to come? *Anticancer Agents Med. Chem.* **2010**, *10*, 293–301.
170. Dieras, V.; Girre, V.; Guilhaume, M.-N.; Laurence, V.; Mignot, L. Oxaliplatin and ovarian cancer. *Bull. Cancer* **2006**, *93* (Suppl. S1), S35–S39.
171. Ganjavi, H.; Gee, M.; Narendran, A.; Parkinson, N.; Krishnamoorthy, M.; Freedman, M.H.; Malkin, D. Adenovirus-mediated p53 gene therapy in osteosarcoma cell lines: Sensitization to cisplatin and doxorubicin. *Cancer Gene Ther.* **2006**, *13*, 415–419.
172. Michels, J.; Vitale, I.; Senovilla, L.; Enot, D.P.; Garcia, P.; Lissa, D.; Olaussen, K.A.; Brenner, C.; Soria, J.-C.; Castedo, M.; et al. Synergistic interaction between cisplatin and PARP inhibitors in non-small cell lung cancer. *Cell Cycle* **2013**, *12*, 877–883.
173. Balmaña, J.; Tung, N.M.; Isakoff, S.J.; Graña, B.; Ryan, P.D.; Saura, C.; Lowe, E.S.; Frewer, P.; Winer, E.; Baselga, J.; Garber, J.E. Phase I trial of olaparib in combination with cisplatin for the treatment of patients with advanced breast, ovarian and other solid tumors. *Ann. Oncol.* **2014**, *25*, 1656–1663.
174. Sorenson, C.M.; Eastman, A. Influence of *cis*-diamminedichloroplatinum(II) on DNA synthesis and cell cycle progression in excision repair proficient and deficient Chinese hamster ovary cells. *Cancer Res.* **1988**, *48*, 6703–6707.
175. Vichi, P.; Coin, F.; Renaud, J.P.; Vermeulen, W.; Hoeijmakers, J.H.; Moras, D.; Egly, J.M. Cisplatin- and UV-damaged DNA lure the basal transcription factor TFIID/TBP. *EMBO J.* **1997**, *16*, 7444–7456.
176. Cullinane, C.; Mazur, S.J.; Essigmann, J.M.; Phillips, D.R.; Bohr, V.A. Inhibition of RNA polymerase II transcription in human cell extracts by cisplatin DNA damage. *Biochemistry* **1999**, *38*, 6204–6212.
177. Kumar, S.; Kumar, A.; Shah, P.P.; Rai, S.N.; Panguluri, S.K.; Kakar, S.S. MicroRNA signature of *cis*-platin resistant vs. *cis*-platin sensitive ovarian cancer cell lines. *J. Ovarian Res.* **2011**, *4*, 17.
178. Ciarimboli, G.; Ludwig, T.; Lang, D.; Pavenstädt, H.; Koepsell, H.; Piechota, H.-J.; Haier, J.; Jaehde, U.; Zisowsky, J.; Schlatter, E. Cisplatin nephrotoxicity is critically mediated via the human organic cation transporter 2. *Am. J. Pathol.* **2005**, *167*, 1477–1484.
179. Gressette, M.; Verrillaud, B.; Jimenez-Pailhès, A.-S.; Lelièvre, H.; Lo, K.-W.; Ferrand, F.-R.; Gattolliat, C.-H.; Jacquet-Bescond, A.; Kraus-Berthier, L.; Depil, S.; et al. Treatment of Nasopharyngeal Carcinoma Cells with the Histone-Deacetylase Inhibitor Abexinostat: Cooperative Effects with Cis-platin and Radiotherapy on Patient-Derived Xenografts. *PLoS ONE* **2014**, *9*, e91325.
180. Rout, S.R.; Behera, B.; Maiti, T.K.; Mohapatra, S. Multifunctional magnetic calcium phosphate nanoparticles for targeted platin delivery. *Dalton Trans.* **2012**, *41*, 10777–10783.
181. Kitao, H.; Takata, M. Fanconi anemia: A disorder defective in the DNA damage response. *Int. J. Hematol.* **2011**, *93*, 417–424.
182. Sawant, A.; Kothandapani, A.; Zhitkovich, A.; Sobol, R.W.; Patrick, S.M. Role of mismatch repair proteins in the processing of cisplatin interstrand cross-links. *DNA Repair* **2015**, *35*, 126–136.
183. Cheng, C.H.; Kuchta, R.D. DNA polymerase epsilon: Aphidicolin inhibition and the relationship between polymerase and exonuclease activity. *Biochemistry* **1993**, *32*, 8568–8574.
184. Pedrali-Noy, G.; Spadari, S.; Miller-Faurès, A.; Miller, A.O.; Kruppa, J.; Koch, G. Synchronization of HeLa cell cultures by inhibition of DNA polymerase alpha with aphidicolin. *Nucleic Acids Res.* **1980**, *8*, 377–387.
185. Baranovskiy, A.G.; Babayeva, N.D.; Suwa, Y.; Gu, J.; Pavlov, Y.I.; Tahirov, T.H. Structural basis for inhibition of DNA replication by aphidicolin. *Nucleic Acids Res.* **2014**, *42*, 14013–14021.
186. Spadari, S.; Pedrali-Noy, G.; Falaschi, M.C.; Ciarrocchi, G. Control of DNA replication and cell proliferation in eukaryotes by aphidicolin. *Toxicol. Pathol.* **1984**, *12*, 143–148.
187. Available online: <http://www.rcsb.org/pdb/explore/explore.do?structureId=4Q5V> (accessed on 23 January 2017).

188. Chang, D.J.; Lupardus, P.J.; Cimprich, K.A. Monoubiquitination of proliferating cell nuclear antigen induced by stalled replication requires uncoupling of DNA polymerase and mini-chromosome maintenance helicase activities. *J. Biol. Chem.* **2006**, *281*, 32081–32088.
189. Sutherland, G.R. Chromosomal fragile sites. *Genet. Anal. Tech. Appl.* **1991**, *8*, 161–166.
190. Shiraishi, T.; Druck, T.; Mimori, K.; Flomenberg, J.; Berk, L.; Alder, H.; Miller, W.; Huebner, K.; Croce, C.M. Sequence conservation at human and mouse orthologous common fragile regions, FRA3B/FHIT and Fra14A2/Fhit. *Proc. Natl. Acad. Sci. USA* **2001**, *98*, 5722–5727.
191. Hellman, A.; Zlotorynski, E.; Scherer, S.W.; Cheung, J.; Vincent, J.B.; Smith, D.I.; Trakhtenbrot, L.; Kerem, B. A role for common fragile site induction in amplification of human oncogenes. *Cancer Cell* **2002**, *1*, 89–97.
192. Durkin, S.G.; Ragland, R.L.; Arlt, M.F.; Mulle, J.G.; Warren, S.T.; Glover, T.W. Replication stress induces tumor-like microdeletions in FHIT/FRA3B. *Proc. Natl. Acad. Sci. USA* **2008**, *105*, 246–251.
193. Bristow, R.G.; Hill, R.P. Hypoxia and metabolism. Hypoxia, DNA repair and genetic instability. *Nat. Rev. Cancer* **2008**, *8*, 180–192.
194. MacGregor, J.T.; Schlegel, R.; Wehr, C.M.; Alperin, P.; Ames, B.N. Cytogenetic damage induced by folate deficiency in mice is enhanced by caffeine. *Proc. Natl. Acad. Sci. USA* **1990**, *87*, 9962–9965.
195. Koundrioukoff, S.; Carignon, S.; Técher, H.; Letessier, A.; Brison, O.; Debatisse, M. Stepwise activation of the ATR signaling pathway upon increasing replication stress impacts fragile site integrity. *PLoS Genet.* **2013**, *9*, e1003643.
196. Helmrich, A.; Ballarino, M.; Tora, L. Collisions between replication and transcription complexes cause common fragile site instability at the longest human genes. *Mol. Cell* **2011**, *44*, 966–977.
197. Di Micco, R.; Fumagalli, M.; Cicalese, A.; Piccinin, S.; Gasparini, P.; Luise, C.; Schurra, C.; Garre', M.; Nuciforo, P.G.; Bensimon, A.; et al. Oncogene-induced senescence is a DNA damage response triggered by DNA hyper-replication. *Nature* **2006**, *444*, 638–642.
198. Cha, R.S.; Kleckner, N. ATR homolog Mec1 promotes fork progression, thus averting breaks in replication slow zones. *Science* **2002**, *297*, 602–606.
199. Arlt, M.F.; Mulle, J.G.; Schaibley, V.M.; Ragland, R.L.; Durkin, S.G.; Warren, S.T.; Glover, T.W. Replication stress induces genome-wide copy number changes in human cells that resemble polymorphic and pathogenic variants. *Am. J. Hum. Genet.* **2009**, *84*, 339–350.
200. Pedrali-Noy, G.; Belvedere, M.; Crepaldi, T.; Focher, F.; Spadari, S. Inhibition of DNA replication and growth of several human and murine neoplastic cells by aphidicolin without detectable effect upon synthesis of immunoglobulins and HLA antigens. *Cancer Res.* **1982**, *42*, 3810–3813.
201. Hardt, N.; Pedrali-Noy, G.; Focher, F.; Spadari, S. Aphidicolin does not inhibit DNA repair synthesis in ultraviolet-irradiated HeLa cells. A radioautographic study. *Biochem. J.* **1981**, *199*, 453–455.
202. Gera, J.F.; Fady, C.; Gardner, A.; Jacoby, F.J.; Briskin, K.B.; Lichtenstein, A. Inhibition of DNA repair with aphidicolin enhances sensitivity of targets to tumor necrosis factor. *J. Immunol.* **1993**, *151*, 3746–3757.
203. Waters, R. Aphidicolin: An inhibitor of DNA repair in human fibroblasts. *Carcinogenesis* **1981**, *2*, 795–797.
204. Wang, F.; Stewart, J.; Price, C.M. Human CST abundance determines recovery from diverse forms of DNA damage and replication stress. *Cell Cycle* **2014**, *13*, 3488–3498.
205. Yeo, J.E.; Lee, E.H.; Hendrickson, E.A.; Sobeck, A. CtIP mediates replication fork recovery in a FANCD2-regulated manner. *Hum. Mol. Genet.* **2014**, *23*, 3695–3705.
206. Chaudhury, I.; Stroik, D.R.; Sobeck, A. FANCD2-controlled chromatin access of the Fanconi-associated nuclease FAN1 is crucial for the recovery of stalled replication forks. *Mol. Cell. Biol.* **2014**, *34*, 3939–3954.
207. Hammond, E.M.; Green, S.L.; Giaccia, A.J. Comparison of hypoxia-induced replication arrest with hydroxyurea and aphidicolin-induced arrest. *Mutat. Res.* **2003**, *532*, 205–213.
208. Borel, F.; Lacroix, F.B.; Margolis, R.L. Prolonged arrest of mammalian cells at the G1/S boundary results in permanent S phase stasis. *J. Cell Sci.* **2002**, *115*, 2829–2838.
209. Nguyen, G.H.; Dexheimer, T.S.; Rosenthal, A.S.; Chu, W.K.; Singh, D.K.; Mosedale, G.; Bachrati, C.Z.; Schultz, L.; Sakurai, M.; Savitsky, P.; et al. A small molecule inhibitor of the BLM helicase modulates chromosome stability in human cells. *Chem. Biol.* **2013**, *20*, 55–62.
210. Basile, G.; Leuzzi, G.; Pichierri, P.; Franchitto, A. Checkpoint-dependent and independent roles of the Werner syndrome protein in preserving genome integrity in response to mild replication stress. *Nucleic Acids Res.* **2014**, *42*, 12628–12639.



211. Schmidt, L.; Wiedner, M.; Velimezi, G.; Prochazkova, J.; Owusu, M.; Bauer, S.; Loizou, J.I. ATMIN is required for the ATM-mediated signaling and recruitment of 53BP1 to DNA damage sites upon replication stress. *DNA Repair* **2014**, *24*, 122–130.
212. Fujita, M.; Sasanuma, H.; Yamamoto, K.N.; Harada, H.; Kurosawa, A.; Adachi, N.; Omura, M.; Hiraoka, M.; Takeda, S.; Hirota, K. Interference in DNA replication can cause mitotic chromosomal breakage unassociated with double-strand breaks. *PLoS ONE* **2013**, *8*, e60043.
213. Beresova, L.; Vesela, E.; Chamrad, I.; Voller, J.; Yamada, M.; Furst, T.; Lenobel, R.; Chroma, K.; Gursky, J.; Krizova, K.; et al. Role of DNA Repair Factor Xeroderma Pigmentosum Protein Group C in Response to Replication Stress As Revealed by DNA Fragile Site Affinity Chromatography and Quantitative Proteomics. *J. Proteome Res.* **2016**, *15*, 4505–4517.
214. Janson, C.; Nyhan, K.; Murnane, J.P. Replication Stress and Telomere Dysfunction Are Present in Cultured Human Embryonic Stem Cells. *Cytogenet. Genome Res.* **2015**, *146*, 251–260.
215. Miron, K.; Golan-Lev, T.; Dvir, R.; Ben-David, E.; Kerem, B. Oncogenes create a unique landscape of fragile sites. *Nat. Commun.* **2015**, *6*, 7094.
216. Murfun, I.; De Santis, A.; Federico, M.; Bignami, M.; Pichierri, P.; Franchitto, A. Perturbed replication induced genome wide or at common fragile sites is differently managed in the absence of WRN. *Carcinogenesis* **2012**, *33*, 1655–1663.
217. Wilhelm, T.; Magdalou, I.; Barascu, A.; Técher, H.; Debatisse, M.; Lopez, B.S. Spontaneous slow replication fork progression elicits mitosis alterations in homologous recombination-deficient mammalian cells. *Proc. Natl. Acad. Sci. USA* **2014**, *111*, 763–768.
218. Available online:  
[https://www.google.cz/url?sa=t&rct=j&q=&esrc=s&source=web&cd=3&cad=rja&uact=8&ved=0ahUKewibvoX5jL\\_QAhULVSwKHQfLCXwQFggsMAI&url=https%3A%2F%2Fwww.sigmaaldrich.com%2Fcontent%2Fdam%2Fsigmaaldrich%2Fdocs%2FSigma%2FDatasheet%2F6%2Fa0781dat.pdf&usq=AFQjCNEPSqAi](https://www.google.cz/url?sa=t&rct=j&q=&esrc=s&source=web&cd=3&cad=rja&uact=8&ved=0ahUKewibvoX5jL_QAhULVSwKHQfLCXwQFggsMAI&url=https%3A%2F%2Fwww.sigmaaldrich.com%2Fcontent%2Fdam%2Fsigmaaldrich%2Fdocs%2FSigma%2FDatasheet%2F6%2Fa0781dat.pdf&usq=AFQjCNEPSqAi) (accessed on 23 November 2016).
219. Sessa, C.; Zucchetti, M.; Davoli, E.; Califano, R.; Cavalli, F.; Frustaci, S.; Gumbrell, L.; Sulkes, A.; Winograd, B.; D'Incalci, M. Phase I and clinical pharmacological evaluation of aphidicolin glycinate. *J. Natl. Cancer Inst.* **1991**, *83*, 1160–1164.
220. Edelson, R.E.; Gorycki, P.D.; MacDonald, T.L. The mechanism of aphidicolin bioinactivation by rat liver in vitro systems. *Xenobiotica* **1990**, *20*, 273–287.
221. Santos, G.B.; Krogh, R.; Magalhaes, L.G.; Andricopulo, A.D.; Pupo, M.T.; Emery, F.S. Semisynthesis of new aphidicolin derivatives with high activity against *Trypanosoma cruzi*. *Bioorg. Med. Chem. Lett.* **2016**, *26*, 1205–1208.
222. Glover, T.W.; Berger, C.; Coyle, J.; Echo, B. DNA polymerase alpha inhibition by aphidicolin induces gaps and breaks at common fragile sites in human chromosomes. *Hum. Genet.* **1984**, *67*, 136–142.
223. Kurose, A.; Tanaka, T.; Huang, X.; Traganos, F.; Darzynkiewicz, Z. Synchronization in the cell cycle by inhibitors of DNA replication induces histone H2AX phosphorylation: An indication of DNA damage. *Cell Prolif.* **2006**, *39*, 231–240.
224. Trenz, K.; Smith, E.; Smith, S.; Costanzo, V. ATM and ATR promote Mre11 dependent restart of collapsed replication forks and prevent accumulation of DNA breaks. *EMBO J.* **2006**, *25*, 1764–1774.
225. Krakoff, I.H.; Brown, N.C.; Reichard, P. Inhibition of ribonucleoside diphosphate reductase by hydroxyurea. *Cancer Res.* **1968**, *28*, 1559–1565.
226. Reichard, P. Interactions between deoxyribonucleotide and DNA synthesis. *Annu. Rev. Biochem.* **1988**, *57*, 349–374.
227. Håkansson, P.; Hofer, A.; Thelander, L. Regulation of mammalian ribonucleotide reduction and dNTP pools after DNA damage and in resting cells. *J. Biol. Chem.* **2006**, *281*, 7834–7841.
228. Eriksson, M.; Uhlin, U.; Ramaswamy, S.; Ekberg, M.; Regnström, K.; Sjöberg, B.M.; Eklund, H. Binding of allosteric effectors to ribonucleotide reductase protein R1: Reduction of active-site cysteines promotes substrate binding. *Structure* **1997**, *5*, 1077–1092.
229. Bianchi, V.; Pontis, E.; Reichard, P. Changes of deoxyribonucleoside triphosphate pools induced by hydroxyurea and their relation to DNA synthesis. *J. Biol. Chem.* **1986**, *261*, 16037–16042.
230. Skog, S.; Tribukait, B.; Wallström, B.; Eriksson, S. Hydroxyurea-induced cell death as related to cell cycle in mouse and human T-lymphoma cells. *Cancer Res.* **1987**, *47*, 6490–6493.

231. Akerblom, L. Azidocytidine is incorporated into RNA of 3T6 mouse fibroblasts. *FEBS Lett.* **1985**, *193*, 203–207.
232. Anglana, M.; Apiou, F.; Bensimon, A.; Debatisse, M. Dynamics of DNA replication in mammalian somatic cells: Nucleotide pool modulates origin choice and interorigin spacing. *Cell* **2003**, *114*, 385–394.
233. Barlow, J.H.; Faryabi, R.B.; Callén, E.; Wong, N.; Malhowski, A.; Chen, H.T.; Gutierrez-Cruz, G.; Sun, H.-W.; McKinnon, P.; Wright, G.; et al. Identification of early replicating fragile sites that contribute to genome instability. *Cell* **2013**, *152*, 620–632.
234. Lönn, U.; Lönn, S. Extensive regions of single-stranded DNA in aphidicolin-treated melanoma cells. *Biochemistry* **1988**, *27*, 566–570.
235. Recolin, B.; Van der Laan, S.; Maiorano, D. Role of replication protein A as sensor in activation of the S-phase checkpoint in *Xenopus* egg extracts. *Nucleic Acids Res.* **2012**, *40*, 3431–3442.
236. Arlt, M.F.; Ozdemir, A.C.; Birkeland, S.R.; Wilson, T.E.; Glover, T.W. Hydroxyurea induces de novo copy number variants in human cells. *Proc. Natl. Acad. Sci. USA* **2011**, *108*, 17360–17365.
237. Huang, M.-E.; Facca, C.; Fatmi, Z.; Baille, D.; Bénakli, S.; Vernis, L. DNA replication inhibitor hydroxyurea alters Fe-S centers by producing reactive oxygen species in vivo. *Sci. Rep.* **2016**, *6*, 29361.
238. Szikriszt, B.; Póti, Á.; Pipek, O.; Krzystanek, M.; Kanu, N.; Molnár, J.; Ribli, D.; Szeltner, Z.; Tusnády, G.E.; Csabai, I.; et al. A comprehensive survey of the mutagenic impact of common cancer cytotoxics. *Genome Biol.* **2016**, *17*, 99.
239. Mistrik, M.; Oplustilova, L.; Lukas, J.; Bartek, J. Low-dose DNA damage and replication stress responses quantified by optimized automated single-cell image analysis. *Cell Cycle* **2009**, *8*, 2592–2599.
240. Ohouo, P.Y.; Bastos de Oliveira, F.M.; Liu, Y.; Ma, C.J.; Smolka, M.B. DNA-repair scaffolds dampen checkpoint signalling by counteracting the adaptor Rad9. *Nature* **2013**, *493*, 120–124.
241. Morafraila, E.C.; Diffley, J.F.X.; Tercero, J.A.; Segurado, M. Checkpoint-dependent RNR induction promotes fork restart after replicative stress. *Sci. Rep.* **2015**, *5*, 7886.
242. Kim, H.-S.; Kim, S.-K.; Hromas, R.; Lee, S.-H. The SET Domain Is Essential for Metnase Functions in Replication Restart and the 5' End of SS-Overhang Cleavage. *PLoS ONE* **2015**, *10*, e0139418.
243. Masuda, T.; Xu, X.; Dimitriadis, E.K.; Lahusen, T.; Deng, C.-X. “DNA Binding Region” of BRCA1 Affects Genetic Stability through modulating the Intra-S-Phase Checkpoint. *Int. J. Biol. Sci.* **2016**, *12*, 133–143.
244. Yarden, R.I.; Metsuyanin, S.; Pickholtz, I.; Shabbeer, S.; Tellio, H.; Papa, M.Z. BRCA1-dependent Chk1 phosphorylation triggers partial chromatin disassociation of phosphorylated Chk1 and facilitates S-phase cell cycle arrest. *Int. J. Biochem. Cell Biol.* **2012**, *44*, 1761–1769.
245. Awate, S.; De Benedetti, A. TLK1B mediated phosphorylation of Rad9 regulates its nuclear/cytoplasmic localization and cell cycle checkpoint. *BMC Mol. Biol.* **2016**, *17*, 3.
246. Ahlskog, J.K.; Larsen, B.D.; Achanta, K.; Sørensen, C.S. ATM/ATR-mediated phosphorylation of PALB2 promotes RAD51 function. *EMBO Rep.* **2016**, *17*, 671–681.
247. Molina, B.; Marchetti, F.; Gómez, L.; Ramos, S.; Torres, L.; Ortiz, R.; Altamirano-Lozano, M.; Carnevale, A.; Frias, S. Hydroxyurea induces chromosomal damage in G2 and enhances the clastogenic effect of mitomycin C in Fanconi anemia cells. *Environ. Mol. Mutagen.* **2015**, *56*, 457–467.
248. Croke, M.; Neumann, M.A.; Grotzky, D.A.; Kreienkamp, R.; Yaddanapudi, S.C.; Gonzalo, S. Differences in 53BP1 and BRCA1 regulation between cycling and non-cycling cells. *Cell Cycle* **2013**, *12*, 3629–3639.
249. Yamada, M.; Watanabe, K.; Mistrik, M.; Vesela, E.; Protivankova, I.; Mailand, N.; Lee, M.; Masai, H.; Lukas, J.; Bartek, J. ATR-Chk1-APC/CCdh1-dependent stabilization of Cdc7-ASK (Dbf4) kinase is required for DNA lesion bypass under replication stress. *Genes Dev.* **2013**, *27*, 2459–2472.
250. Hu, L.; Kim, T.M.; Son, M.Y.; Kim, S.-A.; Holland, C.L.; Tateishi, S.; Kim, D.H.; Yew, P.R.; Montagna, C.; Dumitrache, L.C.; et al. Two replication fork maintenance pathways fuse inverted repeats to rearrange chromosomes. *Nature* **2013**, *501*, 569–572.
251. Lou, T.-F.; Singh, M.; Mackie, A.; Li, W.; Pace, B.S. Hydroxyurea generates nitric oxide in human erythroid cells: Mechanisms for gamma-globin gene activation. *Exp. Biol. Med.* **2009**, *234*, 1374–1382.
252. Vassileva, I.; Yanakieva, I.; Peycheva, M.; Gospodinov, A.; Anachkova, B. The mammalian INO80 chromatin remodeling complex is required for replication stress recovery. *Nucleic Acids Res.* **2014**, *42*, 9074–9086.
253. Park, J.I.; Choi, H.S.; Jeong, J.S.; Han, J.Y.; Kim, I.H. Involvement of p38 kinase in hydroxyurea-induced differentiation of K562 cells. *Cell Growth Differ.* **2001**, *12*, 481–486.

254. Barthelemy, J.; Hanenberg, H.; Leffak, M. FANCI is essential to maintain microsatellite structure genome-wide during replication stress. *Nucleic Acids Res.* **2016**, *44*, 6803–6816.
255. Kunnev, D.; Rusiniak, M.E.; Kudla, A.; Freeland, A.; Cady, G.K.; Pruitt, S.C. DNA damage response and tumorigenesis in Mcm2-deficient mice. *Oncogene* **2010**, *29*, 3630–3638.
256. Da Guarda, C.C.; Santiago, R.P.; Pitanga, T.N.; Santana, S.S.; Zanette, D.L.; Borges, V.M.; Goncalves, M.S. Heme changes HIF- $\alpha$ , eNOS and nitrite production in HUVECs after simvastatin, HU, and ascorbic acid therapies. *Microvasc. Res.* **2016**, *106*, 128–136.
257. Leitch, C.; Osdal, T.; Andresen, V.; Molland, M.; Kristiansen, S.; Nguyen, X.N.; Bruserud, Ø.; Gjertsen, B.T.; McCormack, E. Hydroxyurea synergizes with valproic acid in wild-type p53 acute myeloid leukaemia. *Oncotarget* **2016**, *7*, 8105–8118.
258. Liu, K.; Graves, J.D.; Scott, J.D.; Li, R.; Lin, W.-C. Akt switches TopBP1 function from checkpoint activation to transcriptional regulation through phosphoserine binding-mediated oligomerization. *Mol. Cell. Biol.* **2013**, *33*, 4685–4700.
259. Available online: [https://www.google.cz/url?sa=t&rct=j&q=&esrc=s&source=web&cd=3&cad=rja&uact=8&ved=0ahUKEwiVt4Lulb\\_QAhUBGSwKHbcOB\\_kQFggsMAI&url=https%3A%2F%2Fwww.sigmaaldrich.com%2Fcontent%2Fdam%2Fsigma-aldrich%2Fdocs%2FSigma%2FProduct\\_Information\\_Sheet%2F2%2Fh8627pis.pdf&](https://www.google.cz/url?sa=t&rct=j&q=&esrc=s&source=web&cd=3&cad=rja&uact=8&ved=0ahUKEwiVt4Lulb_QAhUBGSwKHbcOB_kQFggsMAI&url=https%3A%2F%2Fwww.sigmaaldrich.com%2Fcontent%2Fdam%2Fsigma-aldrich%2Fdocs%2FSigma%2FProduct_Information_Sheet%2F2%2Fh8627pis.pdf&) (accessed on 23 January 2017).
260. Segal, J.B.; Strouse, J.J.; Beach, M.C.; Haywood, C.; Witkop, C.; Park, H.; Wilson, R.F.; Bass, E.B.; Lanzkron, S. *Hydroxyurea for the Treatment of Sickle Cell Disease*; Evidence Reports/Technology Assessments; Agency for Healthcare Research and Quality (US): Rockville, MD, USA, 2008; pp. 1–95.
261. Kühn, T.; Burgstaller, S.; Apfelbeck, U.; Linkesch, W.; Seewann, H.; Fridrik, M.; Michlmayr, G.; Krieger, O.; Lutz, D.; Lin, W.; et al. A randomized study comparing interferon (IFN $\alpha$ ) plus low-dose cytarabine and interferon plus hydroxyurea (HU) in early chronic-phase chronic myeloid leukemia (CML). *Leuk. Res.* **2003**, *27*, 405–411.
262. Aruch, D.; Mascarenhas, J. Contemporary approach to essential thrombocythemia and polycythemia vera. *Curr. Opin. Hematol.* **2016**, *23*, 150–160.
263. Barbui, T.; Finazzi, M.C.; Finazzi, G. Front-line therapy in polycythemia vera and essential thrombocythemia. *Blood Rev.* **2012**, *26*, 205–211.
264. Benito, J.M.; López, M.; Lozano, S.; Ballesteros, C.; González-Lahoz, J.; Soriano, V. Hydroxyurea exerts an anti-proliferative effect on T cells but has no direct impact on cellular activation. *Clin. Exp. Immunol.* **2007**, *149*, 171–177.
265. Gurberg, J.; Bouganim, N.; Shenouda, G.; Zeitouni, A. A case of recurrent anaplastic meningioma of the skull base with radiologic response to hydroxyurea. *J. Neurol. Surg. Rep.* **2014**, *75*, e52–e55.
266. Kiladjan, J.-J.; Chevret, S.; Dosquet, C.; Chomienne, C.; Rain, J.-D. Treatment of polycythemia vera with hydroxyurea and pipobroman: Final results of a randomized trial initiated in 1980. *J. Clin. Oncol.* **2011**, *29*, 3907–3913.
267. Charache, S.; Barton, F.B.; Moore, R.D.; Terrin, M.L.; Steinberg, M.H.; Dover, G.J.; Ballas, S.K.; McMahon, R.P.; Castro, O.; Orringer, E.P. Hydroxyurea and sickle cell anemia. Clinical utility of a myelosuppressive “switching” agent. The Multicenter Study of Hydroxyurea in Sickle Cell Anemia. *Medicine* **1996**, *75*, 300–326.
268. Steinberg, M.H.; McCarthy, W.F.; Castro, O.; Ballas, S.K.; Armstrong, F.D.; Smith, W.; Ataga, K.; Swerdlow, P.; Kutlar, A.; DeCastro, L.; et al. The risks and benefits of long-term use of hydroxyurea in sickle cell anemia: A 17.5 year follow-up. *Am. J. Hematol.* **2010**, *85*, 403–408.
269. Darzynkiewicz, Z.; Halicka, H.D.; Zhao, H.; Podhorecka, M. Cell synchronization by inhibitors of DNA replication induces replication stress and DNA damage response: Analysis by flow cytometry. *Methods Mol. Biol.* **2011**, *761*, 85–96.
270. Fugger, K.; Mistrik, M.; Danielsen, J.R.; Dinant, C.; Falck, J.; Bartek, J.; Lukas, J.; Mailand, N. Human Fbh1 helicase contributes to genome maintenance via pro- and anti-recombinase activities. *J. Cell Biol.* **2009**, *186*, 655–663.
271. Liu, N.; Lim, C.-S. Differential roles of XRCC2 in homologous recombinational repair of stalled replication forks. *J. Cell. Biochem.* **2005**, *95*, 942–954.

272. Brose, R.D.; Shin, G.; McGuinness, M.C.; Schneidereith, T.; Purvis, S.; Dong, G.X.; Keefer, J.; Spencer, F.; Smith, K.D. Activation of the stress proteome as a mechanism for small molecule therapeutics. *Hum. Mol. Genet.* **2012**, *21*, 4237–4252.
273. Adragna, N.C.; Fonseca, P.; Lauf, P.K. Hydroxyurea affects cell morphology, cation transport, and red blood cell adhesion in cultured vascular endothelial cells. *Blood* **1994**, *83*, 553–560.
274. Wall, M.E.; Wani, M.C.; Cook, C.E.; Palmer, K.H.; McPhail, A.T.; Sim, G.A. Plant Antitumor Agents. I. The Isolation and Structure of Camptothecin, a Novel Alkaloidal Leukemia and Tumor Inhibitor from *Camptotheca acuminata*<sup>1,2</sup>. *J. Am. Chem. Soc.* **1966**, *88*, 3888–3890.
275. Gupta, M.; Fujimori, A.; Pommier, Y. Eukaryotic DNA topoisomerases I. *Biochim. Biophys. Acta* **1995**, *1262*, 1–14.
276. Champoux, J.J. Mechanism of the reaction catalyzed by the DNA untwisting enzyme: Attachment of the enzyme to 3'-terminus of the nicked DNA. *J. Mol. Biol.* **1978**, *118*, 441–446.
277. Available online: <http://www.rcsb.org/pdb/explore/explore.do?structureId=1T8I> (accessed on 23 January 2017).
278. Stivers, J.T.; Harris, T.K.; Mildvan, A.S. Vaccinia DNA topoisomerase I: Evidence supporting a free rotation mechanism for DNA supercoil relaxation. *Biochemistry* **1997**, *36*, 5212–5222.
279. Koster, D.A.; Palle, K.; Bot, E.S.M.; Bjornsti, M.-A.; Dekker, N.H. Antitumour drugs impede DNA uncoiling by topoisomerase I. *Nature* **2007**, *448*, 213–217.
280. Staker, B.L.; Hjerrild, K.; Feese, M.D.; Behnke, C.A.; Burgin, A.B.; Stewart, L. The mechanism of topoisomerase I poisoning by a camptothecin analog. *Proc. Natl. Acad. Sci. USA* **2002**, *99*, 15387–15392.
281. Regairaz, M.; Zhang, Y.-W.; Fu, H.; Agama, K.K.; Tata, N.; Agrawal, S.; Aladjem, M.I.; Pommier, Y. Mus81-mediated DNA cleavage resolves replication forks stalled by topoisomerase I–DNA complexes. *J. Cell Biol.* **2011**, *195*, 739–749.
282. Palle, K.; Vaziri, C. Rad18 E3 ubiquitin ligase activity mediates Fanconi anemia pathway activation and cell survival following DNA Topoisomerase 1 inhibition. *Cell Cycle* **2011**, *10*, 1625–1638.
283. Pommier, Y. Topoisomerase I inhibitors: Camptothecins and beyond. *Nat. Rev. Cancer* **2006**, *6*, 789–802.
284. Tuduri, S.; Crabbé, L.; Conti, C.; Tourrière, H.; Holtgreve-Grez, H.; Jauch, A.; Pantesco, V.; De Vos, J.; Thomas, A.; Theillet, C.; et al. Topoisomerase I suppresses genomic instability by preventing interference between replication and transcription. *Nat. Cell Biol.* **2009**, *11*, 1315–1324.
285. Tripathi, K.; Mani, C.; Clark, D.W.; Palle, K. Rad18 is required for functional interactions between FANCD2, BRCA2, and Rad51 to repair DNA topoisomerase 1-poisons induced lesions and promote fork recovery. *Oncotarget* **2016**, *7*, 12537–12553.
286. Tsao, Y.P.; D'Arpa, P.; Liu, L.F. The involvement of active DNA synthesis in camptothecin-induced G2 arrest: Altered regulation of p34cdc2/cyclin B. *Cancer Res.* **1992**, *52*, 1823–1829.
287. Kharbanda, S.; Rubin, E.; Gunji, H.; Hinz, H.; Giovanella, B.; Pantazis, P.; Kufe, D. Camptothecin and its derivatives induce expression of the *c-jun* protooncogene in human myeloid leukemia cells. *Cancer Res.* **1991**, *51*, 6636–6642.
288. Aller, P.; Rius, C.; Mata, F.; Zorrilla, A.; Cabañas, C.; Bellón, T.; Bernabeu, C. Camptothecin induces differentiation and stimulates the expression of differentiation-related genes in U-937 human promonocytic leukemia cells. *Cancer Res.* **1992**, *52*, 1245–1251.
289. Clements, M.K.; Jones, C.B.; Cumming, M.; Daoud, S.S. Antiangiogenic potential of camptothecin and topotecan. *Cancer Chemother. Pharmacol.* **1999**, *44*, 411–416.
290. O'Leary, J.J.; Shapiro, R.L.; Ren, C.J.; Chuang, N.; Cohen, H.W.; Potmesil, M. Antiangiogenic effects of camptothecin analogues 9-amino-20(S)-camptothecin, topotecan, and CPT-11 studied in the mouse cornea model. *Clin. Cancer Res.* **1999**, *5*, 181–187.
291. Arlt, M.F.; Glover, T.W. Inhibition of topoisomerase I prevents chromosome breakage at common fragile sites. *DNA Repair* **2010**, *9*, 678–689.
292. Horwitz, S.B.; Horwitz, M.S. Effects of camptothecin on the breakage and repair of DNA during the cell cycle. *Cancer Res.* **1973**, *33*, 2834–2836.
293. Jayasooriya, R.G.P.T.; Choi, Y.H.; Hyun, J.W.; Kim, G.-Y. Camptothecin sensitizes human hepatoma Hep3B cells to TRAIL-mediated apoptosis via ROS-dependent death receptor 5 upregulation with the involvement of MAPKs. *Environ. Toxicol. Pharmacol.* **2014**, *38*, 959–967.

294. Strumberg, D.; Pilon, A.A.; Smith, M.; Hickey, R.; Malkas, L.; Pommier, Y. Conversion of topoisomerase I cleavage complexes on the leading strand of ribosomal DNA into 5'-phosphorylated DNA double-strand breaks by replication runoff. *Mol. Cell. Biol.* **2000**, *20*, 3977–3987.
295. Priel, E.; Showalter, S.D.; Roberts, M.; Oroszlan, S.; Blair, D.G. The topoisomerase I inhibitor, camptothecin, inhibits equine infectious anemia virus replication in chronically infected CF2Th cells. *J. Virol.* **1991**, *65*, 4137–4141.
296. Bruno, S.; Giaretti, W.; Darzynkiewicz, Z. Effect of camptothecin on mitogenic stimulation of human lymphocytes: Involvement of DNA topoisomerase I in cell transition from G0 to G1 phase of the cell cycle and in DNA replication. *J. Cell. Physiol.* **1992**, *151*, 478–486.
297. Squires, S.; Ryan, A.J.; Strutt, H.L.; Johnson, R.T. Hypersensitivity of Cockayne's syndrome cells to camptothecin is associated with the generation of abnormally high levels of double strand breaks in nascent DNA. *Cancer Res.* **1993**, *53*, 2012–2019.
298. Ding, X.; Matsuo, K.; Xu, L.; Yang, J.; Zheng, L. Optimized combinations of bortezomib, camptothecin, and doxorubicin show increased efficacy and reduced toxicity in treating oral cancer. *Anticancer Drugs* **2015**, *26*, 547–554.
299. Zhang, J.; Walter, J.C. Mechanism and regulation of incisions during DNA interstrand cross-link repair. *DNA Repair* **2014**, *19*, 135–142.
300. Ray Chaudhuri, A.; Hashimoto, Y.; Herrador, R.; Neelsen, K.J.; Fachinetti, D.; Bermejo, R.; Cocito, A.; Costanzo, V.; Lopes, M. Topoisomerase I poisoning results in PARP-mediated replication fork reversal. *Nat. Struct. Mol. Biol.* **2012**, *19*, 417–423.
301. Available online: [http://www.sigmaaldrich.com/content/dam/sigma-aldrich/docs/Sigma/Product\\_Information\\_Sheet/c9911pis.pdf](http://www.sigmaaldrich.com/content/dam/sigma-aldrich/docs/Sigma/Product_Information_Sheet/c9911pis.pdf) (accessed on 23 November 2016).
302. Jaxel, C.; Kohn, K.W.; Wani, M.C.; Wall, M.E.; Pommier, Y. Structure-activity study of the actions of camptothecin derivatives on mammalian topoisomerase I: Evidence for a specific receptor site and a relation to antitumor activity. *Cancer Res.* **1989**, *49*, 1465–1469.
303. Takagi, K.; Dexheimer, T.S.; Redon, C.; Sordet, O.; Agama, K.; Lavielle, G.; Pierré, A.; Bates, S.E.; Pommier, Y. Novel E-ring camptothecin keto analogues (S38809 and S39625) are stable, potent, and selective topoisomerase I inhibitors without being substrates of drug efflux transporters. *Mol. Cancer Ther.* **2007**, *6*, 3229–3238.
304. Hande, K.R. Etoposide: Four decades of development of a topoisomerase II inhibitor. *Eur. J. Cancer* **1998**, *34*, 1514–1521.
305. Available online: <http://www.rcsb.org/pdb/explore/explore.do?structureId=3QX3> (accessed on 23 January 2017).
306. Liu, L.F.; Rowe, T.C.; Yang, L.; Tewey, K.M.; Chen, G.L. Cleavage of DNA by mammalian DNA topoisomerase II. *J. Biol. Chem.* **1983**, *258*, 15365–15370.
307. Gibson, E.G.; King, M.M.; Mercer, S.L.; Deweese, J.E. Two-Mechanism Model for the Interaction of Etoposide Quinone with Topoisomerase II $\alpha$ . *Chem. Res. Toxicol.* **2016**, *29*, 1541–1548.
308. Wu, C.-C.; Li, T.-K.; Farh, L.; Lin, L.-Y.; Lin, T.-S.; Yu, Y.-J.; Yen, T.-J.; Chiang, C.-W.; Chan, N.-L. Structural basis of type II topoisomerase inhibition by the anticancer drug etoposide. *Science* **2011**, *333*, 459–462.
309. Bender, R.P.; Jablonksy, M.J.; Shadid, M.; Romaine, I.; Dunlap, N.; Anklin, C.; Graves, D.E.; Osheroff, N. Substituents on etoposide that interact with human topoisomerase II $\alpha$  in the binary enzyme-drug complex: Contributions to etoposide binding and activity. *Biochemistry* **2008**, *47*, 4501–4509.
310. Wilstermann, A.M.; Bender, R.P.; Godfrey, M.; Choi, S.; Anklin, C.; Berkowitz, D.B.; Osheroff, N.; Graves, D.E. Topoisomerase II—Drug interaction domains: Identification of substituents on etoposide that interact with the enzyme. *Biochemistry* **2007**, *46*, 8217–8225.
311. Jacob, D.A.; Mercer, S.L.; Osheroff, N.; Deweese, J.E. Etoposide quinone is a redox-dependent topoisomerase II poison. *Biochemistry* **2011**, *50*, 5660–5667.
312. Rogakou, E.P.; Pilch, D.R.; Orr, A.H.; Ivanova, V.S.; Bonner, W.M. DNA double-stranded breaks induce histone H2AX phosphorylation on serine 139. *J. Biol. Chem.* **1998**, *273*, 5858–5868.
313. Terasawa, M.; Shinohara, A.; Shinohara, M. Canonical non-homologous end joining in mitosis induces genome instability and is suppressed by M-phase-specific phosphorylation of XRCC4. *PLoS Genet.* **2014**, *10*, e1004563.

314. Zhao, H.; Rybak, P.; Dobrucki, J.; Traganos, F.; Darzynkiewicz, Z. Relationship of DNA damage signaling to DNA replication following treatment with DNA topoisomerase inhibitors camptothecin/topotecan, mitoxantrone, or etoposide. *Cytometry A* **2012**, *81*, 45–51.
315. Montecucco, A.; Rossi, R.; Ferrari, G.; Scovassi, A.I.; Prosperi, E.; Biamonti, G. Etoposide Induces the Dispersal of DNA Ligase I from Replication Factories. *Mol. Biol. Cell* **2001**, *12*, 2109–2118.
316. Holm, C.; Covey, J.M.; Kerrigan, D.; Pommier, Y. Differential requirement of DNA replication for the cytotoxicity of DNA topoisomerase I and II inhibitors in Chinese hamster DC3F cells. *Cancer Res.* **1989**, *49*, 6365–6368.
317. Austin, C.A.; Sng, J.H.; Patel, S.; Fisher, L.M. Novel HeLa topoisomerase II is the II beta isoform: Complete coding sequence and homology with other type II topoisomerases. *Biochim. Biophys. Acta* **1993**, *1172*, 283–291.
318. Niimi, A.; Suka, N.; Harata, M.; Kikuchi, A.; Mizuno, S. Co-localization of chicken DNA topoisomerase IIalpha, but not beta, with sites of DNA replication and possible involvement of a C-terminal region of alpha through its binding to PCNA. *Chromosoma* **2001**, *110*, 102–114.
319. Ju, B.-G.; Lunyak, V.V.; Perissi, V.; Garcia-Bassets, I.; Rose, D.W.; Glass, C.K.; Rosenfeld, M.G. A topoisomerase II $\beta$ -mediated dsDNA break required for regulated transcription. *Science* **2006**, *312*, 1798–1802.
320. Azarova, A.M.; Lyu, Y.L.; Lin, C.-P.; Tsai, Y.-C.; Lau, J.Y.-N.; Wang, J.C.; Liu, L.F. Roles of DNA topoisomerase II isozymes in chemotherapy and secondary malignancies. *Proc. Natl. Acad. Sci. USA* **2007**, *104*, 11014–11019.
321. Nitiss, J.L. DNA topoisomerase II and its growing repertoire of biological functions. *Nat. Rev. Cancer* **2009**, *9*, 327–337.
322. Gupta, R.S.; Bromke, A.; Bryant, D.W.; Gupta, R.; Singh, B.; McCalla, D.R. Etoposide (VP16) and teniposide (VM26): Novel anticancer drugs, strongly mutagenic in mammalian but not prokaryotic test systems. *Mutagenesis* **1987**, *2*, 179–186.
323. Muslimović, A.; Nyström, S.; Gao, Y.; Hammarsten, O. Numerical Analysis of Etoposide Induced DNA Breaks. *PLoS ONE* **2009**, *4*, e5859.
324. Álvarez-Quilón, A.; Serrano-Benítez, A.; Lieberman, J.A.; Quintero, C.; Sánchez-Gutiérrez, D.; Escudero, L.M.; Cortés-Ledesma, F. ATM specifically mediates repair of double-strand breaks with blocked DNA ends. *Nat. Commun.* **2014**, *5*, 3347.
325. Nagano, T.; Nakano, M.; Nakashima, A.; Onishi, K.; Yamao, S.; Enari, M.; Kikkawa, U.; Kamada, S. Identification of cellular senescence-specific genes by comparative transcriptomics. *Sci. Rep.* **2016**, *6*, 31758.
326. Brasacchio, D.; Alsop, A.E.; Noori, T.; Lufti, M.; Iyer, S.; Simpson, K.J.; Bird, P.I.; Kluck, R.M.; Johnstone, R.W.; Trapani, J.A. Epigenetic control of mitochondrial cell death through PACS1-mediated regulation of BAX/BAK oligomerization. *Cell Death Differ.* **2017**, doi:10.1038/cdd.2016.119.
327. Martin, R.; Desponds, C.; Eren, R.O.; Quadroni, M.; Thome, M.; Fasel, N. Caspase-mediated cleavage of raptor participates in the inactivation of mTORC1 during cell death. *Cell Death Discov.* **2016**, *2*, 16024.
328. Brekman, A.; Singh, K.E.; Polotskaia, A.; Kundu, N.; Bargonetti, J. A p53-independent role of Mdm2 in estrogen-mediated activation of breast cancer cell proliferation. *Breast Cancer Res.* **2011**, *13*, R3.
329. Soubeyrand, S.; Pope, L.; Haché, R.J.G. Topoisomerase II $\alpha$ -dependent induction of a persistent DNA damage response in response to transient etoposide exposure. *Mol. Oncol.* **2010**, *4*, 38–51.
330. Velma, V.; Carrero, Z.I.; Allen, C.B.; Hebert, M.D. Coilin levels modulate cell cycle progression and  $\gamma$ H2AX levels in etoposide treated U2OS cells. *FEBS Lett.* **2012**, *586*, 3404–3409.
331. Dehennaut, V.; Loison, I.; Dubuissez, M.; Nassour, J.; Abbadie, C.; Leprince, D. DNA double-strand breaks lead to activation of hypermethylated in cancer 1 (HIC1) by SUMOylation to regulate DNA repair. *J. Biol. Chem.* **2013**, *288*, 10254–10264.
332. Paget, S.; Dubuissez, M.; Dehennaut, V.; Nassour, J.; Harmon, B.T.; Spruyt, N.; Loison, I.; Abbadie, C.; Rood, B.R.; Leprince, D. HIC1 (hypermethylated in cancer 1) SUMOylation is dispensable for DNA repair but is essential for the apoptotic DNA damage response (DDR) to irreparable DNA double-strand breaks (DSBs). *Oncotarget* **2017**, *8*, 2916–2935.
333. Sypniewski, D.; Bednarek, I.; Gałka, S.; Loch, T.; Błaszczuk, D.; Softysik, D. Cytotoxicity of etoposide in cancer cell lines in vitro after BCL-2 and C-RAF gene silencing with antisense oligonucleotides. *Acta Pol. Pharm.* **2013**, *70*, 87–97.

334. Rybak, P.; Hoang, A.; Bujnowicz, L.; Bernas, T.; Berniak, K.; ZarÄ Bski, M.A.; Darzynkiewicz, Z.; Dobrucki, J. Low level phosphorylation of histone H2AX on serine 139 ( $\gamma$ H2AX) is not associated with DNA double-strand breaks. *Oncotarget* **2016**, *7*, 49574–49587.
335. Chen, L.; Cui, H.; Fang, J.; Deng, H.; Kuang, P.; Guo, H.; Wang, X.; Zhao, L. Glutamine deprivation plus BPTES alters etoposide- and cisplatin-induced apoptosis in triple negative breast cancer cells. *Oncotarget* **2016**, *7*, 54691–54701.
336. Rodriguez-Lopez, A.M.; Xenaki, D.; Eden, T.O.; Hickman, J.A.; Chresta, C.M. MDM2 mediated nuclear exclusion of p53 attenuates etoposide-induced apoptosis in neuroblastoma cells. *Mol. Pharmacol.* **2001**, *59*, 135–143.
337. Litwiniec, A.; Gackowska, L.; Helmin-Basa, A.; Żuryń, A.; Grzanka, A. Low-dose etoposide-treatment induces endoreplication and cell death accompanied by cytoskeletal alterations in A549 cells: Does the response involve senescence? The possible role of vimentin. *Cancer Cell Int.* **2013**, *13*, 9
338. Akhtar, N.; Talegaonkar, S.; Khar, R.K.; Jaggi, M. A validated stability-indicating LC method for estimation of etoposide in bulk and optimized self-nano emulsifying formulation: Kinetics and stability effects. *Saudi Pharm. J.* **2013**, *21*, 103–111.
339. Available online: [http://www.sigmaaldrich.com/content/dam/sigma-aldrich/docs/Sigma/Product\\_Information\\_Sheet/e1383pis.pdf](http://www.sigmaaldrich.com/content/dam/sigma-aldrich/docs/Sigma/Product_Information_Sheet/e1383pis.pdf) (accessed on 23 November 2016).
340. Wrasidlo, W.; Schröder, U.; Bernt, K.; Hübener, N.; Shabat, D.; Gaedicke, G.; Lode, H. Synthesis, hydrolytic activation and cytotoxicity of etoposide prodrugs. *Bioorg Med Chem Lett.* **2002**, *12*, 557–560.
341. Jokić, M.; Vlašić, I.; Rinneburger, M.; Klümper, N.; Spiro, J.; Vogel, W.; Offermann, A.; Kumpers, C.; Fritz, C.; Schmitt, A.; et al. Ercc1 Deficiency Promotes Tumorigenesis and Increases Cisplatin Sensitivity in a Tp53 Context-Specific Manner. *Mol. Cancer Res.* **2016**, *14*, 1110–1123.
342. Felix, C.A.; Walker, A.H.; Lange, B.J.; Williams, T.M.; Winick, N.J.; Cheung, N.K.; Lovett, B.D.; Nowell, P.C.; Blair, I.A.; Rebbeck, T.R. Association of CYP3A4 genotype with treatment-related leukemia. *Proc. Natl. Acad. Sci. USA* **1998**, *95*, 13176–13181.
343. Blanco, J.G.; Edick, M.J.; Relling, M.V. Etoposide induces chimeric Mll gene fusions. *FASEB J.* **2004**, *18*, 173–175.
344. Thirman, M.J.; Gill, H.J.; Burnett, R.C.; Mbangkollo, D.; McCabe, N.R.; Kobayashi, H.; Ziemer-van der Poel, S.; Kaneko, Y.; Morgan, R.; Sandberg, A.A. Rearrangement of the MLL gene in acute lymphoblastic and acute myeloid leukemias with 11q23 chromosomal translocations. *N. Engl. J. Med.* **1993**, *329*, 909–914.
345. Cerveira, N.; Lisboa, S.; Correia, C.; Bizarro, S.; Santos, J.; Torres, L.; Vieira, J.; Barros-Silva, J.D.; Pereira, D.; Moreira, C.; et al. Genetic and clinical characterization of 45 acute leukemia patients with MLL gene rearrangements from a single institution. *Mol. Oncol.* **2012**, *6*, 553–564.
346. Krivtsov, A.V.; Armstrong, S.A. MLL translocations, histone modifications and leukaemia stem-cell development. *Nat. Rev. Cancer* **2007**, *7*, 823–833.
347. Zhang, L.; Chen, F.; Zhang, Z.; Chen, Y.; Lin, Y.; Wang, J. Design, synthesis and evaluation of the multidrug resistance-reversing activity of pyridine acid esters of podophyllotoxin in human leukemia cells. *Bioorg. Med. Chem. Lett.* **2016**, *26*, 4466–4471.
348. Lee, K.-I.; Su, C.-C.; Yang, C.-Y.; Hung, D.-Z.; Lin, C.-T.; Lu, T.-H.; Liu, S.-H.; Huang, C.-F. Etoposide induces pancreatic  $\beta$ -cells cytotoxicity via the JNK/ERK/GSK-3 signaling-mediated mitochondria-dependent apoptosis pathway. *Toxicol. Vitro* **2016**, *36*, 142–152.
349. Pellegrini, G.G.; Morales, C.C.; Wallace, T.C.; Plotkin, L.I.; Bellido, T. Avenanthramides Prevent Osteoblast and Osteocyte Apoptosis and Induce Osteoclast Apoptosis in Vitro in an Nrf2-Independent Manner. *Nutrients* **2016**, *8*, 423.
350. Papież, M.A.; Krzyściak, W.; Szade, K.; Bukowska-Straková, K.; Kozakowska, M.; Hajduk, K.; Bystrowska, B.; Dulak, J.; Jozkowicz, A. Curcumin enhances the cytogenotoxic effect of etoposide in leukemia cells through induction of reactive oxygen species. *Drug Des. Dev. Ther.* **2016**, *10*, 557–570.
351. Zhang, S.; Lu, C.; Zhang, X.; Li, J.; Jiang, H. Targeted delivery of etoposide to cancer cells by folate-modified nanostructured lipid drug delivery system. *Drug Deliv.* **2016**, *23*, 1838–1845.
352. Lindsay, G.S.; Wallace, H.M. Changes in polyamine catabolism in HL-60 human promyelogenous leukaemic cells in response to etoposide-induced apoptosis. *Biochem. J.* **1999**, *337 Pt 1*, 83–87.
353. Kumar, A.; Ehrenshaft, M.; Tokar, E.J.; Mason, R.P.; Sinha, B.K. Nitric oxide inhibits topoisomerase II activity and induces resistance to topoisomerase II-poisons in human tumor cells. *Biochim. Biophys. Acta* **2016**, *1860*, 1519–1527.

354. Zhang, A.; Lyu, Y.L.; Lin, C.-P.; Zhou, N.; Azarova, A.M.; Wood, L.M.; Liu, L.F. A protease pathway for the repair of topoisomerase II–DNA covalent complexes. *J. Biol. Chem.* **2006**, *281*, 35997–36003.
355. Ledesma, F.C.; El Khamisy, S.F.; Zuma, M.C.; Osborn, K.; Caldecott, K.W. A human 5'-tyrosyl DNA phosphodiesterase that repairs topoisomerase-mediated DNA damage. *Nature* **2009**, *461*, 674–678.
356. Aparicio, T.; Baer, R.; Gottesman, M.; Gautier, J. MRN, CtIP, and BRCA1 mediate repair of topoisomerase II–DNA adducts. *J. Cell Biol.* **2016**, *212*, 399–408.
357. Quennet, V.; Beucher, A.; Barton, O.; Takeda, S.; Löbrich, M. CtIP and MRN promote non-homologous end-joining of etoposide-induced DNA double-strand breaks in G1. *Nucleic Acids Res.* **2011**, *39*, 2144–2152.
358. Adachi, N.; Suzuki, H.; Iizumi, S.; Koyama, H. Hypersensitivity of nonhomologous DNA end-joining mutants to VP-16 and ICRF-193: Implications for the repair of topoisomerase II-mediated DNA damage. *J. Biol. Chem.* **2003**, *278*, 35897–35902.

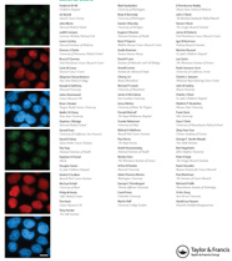


© 2017 by the authors; licensee MDPI, Basel, Switzerland. This article is an open access article distributed under the terms and conditions of the Creative Commons Attribution (CC-BY) license (<http://creativecommons.org/licenses/by/4.0/>).



### 8.3.2. Appendix B

**Turi, Z.;** Senkyrikova, M.; Mistrik, M.; Bartek, J.; Moudry, P. Perturbation of RNA Polymerase I transcription machinery by ablation of HEATR1 triggers the RPL5/RPL11-MDM2-p53 ribosome biogenesis stress checkpoint pathway in human cells. *Cell Cycle*. **2017**. IF (2017/2018): 3.304



# Perturbation of RNA Polymerase I transcription machinery by ablation of HEATR1 triggers the RPL5/RPL11-MDM2-p53 ribosome biogenesis stress checkpoint pathway in human cells

Zsofia Turi, Marketa Senkyrikova, Martin Mistrik, Jiri Bartek & Pavel Moudry

To cite this article: Zsofia Turi, Marketa Senkyrikova, Martin Mistrik, Jiri Bartek & Pavel Moudry (2018) Perturbation of RNA Polymerase I transcription machinery by ablation of HEATR1 triggers the RPL5/RPL11-MDM2-p53 ribosome biogenesis stress checkpoint pathway in human cells, *Cell Cycle*, 17:1, 92-101, DOI: [10.1080/15384101.2017.1403685](https://doi.org/10.1080/15384101.2017.1403685)

To link to this article: <https://doi.org/10.1080/15384101.2017.1403685>



View supplementary material [↗](#)



Accepted author version posted online: 16 Nov 2017.  
Published online: 10 Dec 2017.



Submit your article to this journal [↗](#)



Article views: 421



View Crossmark data [↗](#)



Citing articles: 4 View citing articles [↗](#)

REPORT



# Perturbation of RNA Polymerase I transcription machinery by ablation of HEATR1 triggers the RPL5/RPL11-MDM2-p53 ribosome biogenesis stress checkpoint pathway in human cells

Zsofia Turi<sup>a</sup>, Marketa Senkyrikova<sup>a</sup>, Martin Mistrik<sup>a</sup>, Jiri Bartek<sup>a,b,c</sup> and Pavel Moudry<sup>a</sup>

<sup>a</sup>Institute of Molecular and Translational Medicine, Faculty of Medicine and Dentistry, Palacky University, 779 00 Olomouc, Czech Republic; <sup>b</sup>Genome Integrity Unit, Danish Cancer Society Research Center, DK-2100 Copenhagen, Denmark; <sup>c</sup>Department of Medical Biochemistry and Biophysics, Division of Genome Biology, Science for Life Laboratory, Karolinska Institute, 171 65 Stockholm, Sweden

## ABSTRACT

Ribosome biogenesis is an energy consuming process which takes place mainly in the nucleolus. By producing ribosomes to fuel protein synthesis, it is tightly connected with cell growth and cell cycle control. Perturbation of ribosome biogenesis leads to the activation of p53 tumor suppressor protein promoting processes like cell cycle arrest, apoptosis or senescence. This ribosome biogenesis stress pathway activates p53 through sequestration of MDM2 by a subset of ribosomal proteins (RPs), thereby stabilizing p53. Here, we identify human HEATR1, as a nucleolar protein which positively regulates ribosomal RNA (rRNA) synthesis. Downregulation of HEATR1 resulted in cell cycle arrest in a manner dependent on p53. Moreover, depletion of HEATR1 also caused disruption of nucleolar structure and activated the ribosomal biogenesis stress pathway – RPL5 / RPL11 dependent stabilization and activation of p53. These findings reveal an important role for HEATR1 in ribosome biogenesis and further support the concept that perturbation of ribosome biosynthesis results in p53-dependent cell cycle checkpoint activation, with implications for human pathologies including cancer.

## ARTICLE HISTORY

Received 2 August 2017  
Revised 6 October 2017  
Accepted 29 October 2017

## KEYWORDS

ribosome biogenesis;  
HEATR1; p53; ribosome  
biogenesis stress; cancer

## Introduction

Protein synthesis is a fundamental feature of life that relies on specialized organelles, the ribosomes. The ribosomes are large protein-RNA complexes, formed by about 80 ribosomal proteins (RPs) and four types of ribosomal RNAs (rRNAs) to compose a platform for protein translation. In eukaryotes, each ribosome consists of a 40 S small and a 60 S large subunit [1–3]. While the matured ribosomes are localized in the cytoplasm, biosynthesis and assembly of the ribosomal subunits takes place mainly in the nucleolus. This membrane-less organelle is located within the nucleus and organized around ribosomal DNA (rDNA) genes. Ribosome biogenesis is initiated by the transcription of rDNA, performed by RNA Polymerase I (RNA Pol I). The resulting 47S pre-rRNA transcript is further processed and modified to give rise to several species of rRNAs: 18S rRNA – component of the small ribosomal subunit – 5.8S and 28S rRNAs – components of the large subunit. As an exception, transcription of another rRNA species – 5S rRNA, part of the large ribosomal subunit – occurs in the nucleus and is carried out by RNA Polymerase III. RP genes are transcribed by RNA Polymerase II in the nucleus and translated in the cytoplasm. Both the RPs and the 5S rRNA are first imported into the nucleolus where assembly of the ribosomal subunits begins. Precise maturation of the rRNAs and appropriate assembly of the ribosomal subunits requires high energy investment and

depends on the action of multiple nucleolar accessory and assembly factors – primarily non-ribosomal proteins and small nucleolar RNAs (snoRNAs) [4–6].

Due to the tremendous energy demand for ribosome biogenesis and the continuous need for protein synthesis, production of the ribosomes must be tightly regulated and synchronized with physiological conditions of the cells. Numerous studies showed that perturbation of various steps in the complex proteosynthetic process, a scenario that is commonly referred to as nucleolar or ribosome biogenesis stress [7–11] leads to cell cycle arrest and eventually to senescence or apoptosis through activation of the p53 tumor suppressor protein. Under normal growth conditions p53 is engaged in a complex with, and ubiquitinated by, the MDM2 E3 ubiquitin ligase, leading to p53's continuous proteasomal degradation [12–14]. However, impaired ribosome biogenesis triggers the release of several RPs – most notably RPL5 and RPL11 – to the nucleoplasm, where these proteins bind and sequester MDM2, resulting in p53 stabilization and activation [9,11,15].

In this study we investigated human HEAT repeat containing 1 (HEATR1) protein, its role in ribosome biogenesis and impact of its downregulation on cells. The human HEATR1 gene is located at chromosome 1q43 and encodes a large (236 kDa) protein consisting of 2144 amino acids. The HEATR1 protein contains one HEAT repeat on its C-terminal

end (<http://www.uniprot.org/uniprot/Q9H583>). HEAT repeats are found in other proteins – e.g. huntingtin, elongation factor 3 or protein phosphatase 2A – and considered to be involved in protein-protein interactions [16]. UTP10, the yeast homolog of HEATR1 also contains a HEAT repeat at its C-terminus, and was shown to be involved in rDNA transcription and small ribosomal subunit maturation [17–20]. Unlike UTP10 or human HEATR1 protein, the Zebrafish homolog Bap28 contains 8 HEAT repeats [21]. Despite the structural differences, similarly to the yeast or human protein [17,19,20,22], Bap28 was also suggested to be involved in the regulation of rRNA synthesis and maturation. Furthermore, expression of a deletion mutant of Bap28 in Zebrafish embryos severely impaired organismal development, possibly through the activation of p53-dependent apoptosis [21]. In addition, human HEATR1 has been implicated in cancer, through stimulation of cytotoxic T lymphocyte responses in gliomas [23] and promotion of AKT dephosphorylation in the mTOR signaling pathway in pancreatic ductal adenocarcinomas (PDAC) [24].

Here, we report that human HEATR1 is a nucleolar protein with a prominent role in ribosome biogenesis. Downregulation of HEATR1 leads to impaired ribosome biogenesis, thereby inducing disruption of the nucleolar structure and triggering cellular ribosome biogenesis stress response.

## Results

### Knockdown of HEATR1 activates and stabilizes p53

To identify human proteins involved in ribosome biogenesis, we performed a high-content RNA interference (RNAi) screen and found HEATR1 among prominent hits, whose depletion led to increased p53 level. To validate this observation, we used three independent siRNAs against HEATR1, all of which reduced the endogenous level of the protein and resulted in the elevation of p53 and its target, p21 to the same extent in human osteosarcoma (U2OS) cell line (Figure 1A). In order to reduce potential off-target effects [25], we also used a pool of the three siRNAs here (Figure 1A) and in all further experiments. Pooled siHEATR1 efficiently reduced the endogenous level of HEATR1, not only in U2OS but in normal diploid human fibroblast (BJ) cells, as well (Figure 1A and Figure S1A, B). Furthermore, knockdown of HEATR1 did not lead to DNA damage induction or activation of DNA damage signaling, as we did not observe any increased  $\gamma$ H2AX (an established biomarker of DNA damage) in these HEATR1-depleted samples (Figure S1C).

Next we wondered whether the observed increased abundance of the p53 protein reflects its enhanced stability. To address this issue, we applied cycloheximide – an inhibitor of protein synthesis – to examine turnover of p53 in control *versus* HEATR1-depleted cells. Indeed, absence of HEATR1 led to slower degradation of p53 protein (Figure 1B), as its half-life increased from 56 minutes to 106 minutes, suggesting that p53 upregulation upon HEATR1 knockdown might be a consequence of its elevated stability. These results demonstrated that ablation of HEATR1 leads to activation and stabilization of p53.

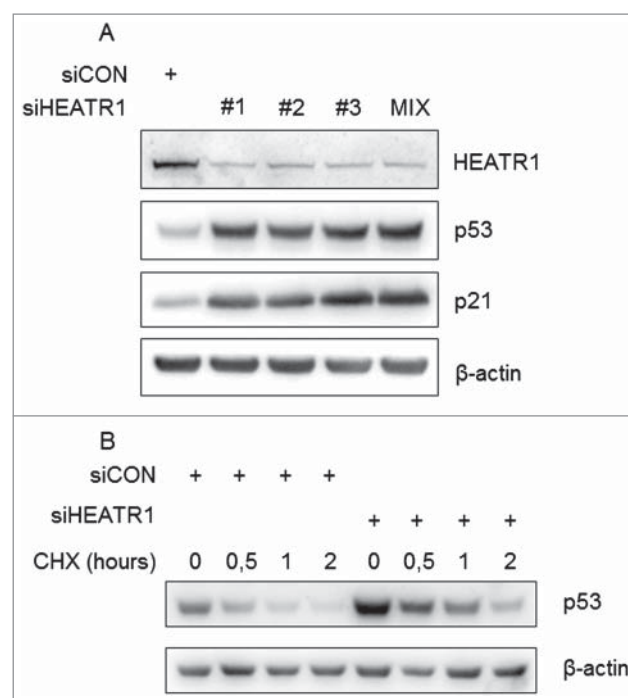


**Figure 1.** Depletion of HEATR1 stabilizes p53. A. U2OS cells were transfected with control or HEATR1 siRNAs, cell lysates were prepared 72 h after transfection and immunoblotted with indicated antibodies. B. U2OS cells were transfected with control or HEATR1 siRNAs, treated with 50  $\mu$ g/ml cycloheximide (CHX) 72 h later and harvested at indicated time points. Cell lysates were immunoblotted with indicated antibodies.

### Depletion of HEATR1 leads to impaired proliferation and induces p53-dependent cell cycle arrest

To assess any impact of HEATR1 status on cell cycle progression, we first examined proliferation rate of control and HEATR1-depleted U2OS cells. Cells deficient in HEATR1 showed impaired growth rate compared to control, as determined by total cell counts at 2, 4 and 6 days after siRNA transfection (Figure 2A). This impairment of the overall cell proliferation upon HEATR1 depletion was not cell-type restricted, as ablation of HEATR1 led to growth arrest also in normal diploid BJ cells (Figure S2A). Further analyses showed that HEATR1 knockdown led to altered cell cycle progression, documented by a dramatic decrease of cells in S phase and enhanced subpopulation of cells in G1 (Figure 2B). Notably, co-depletion of HEATR1 and p53 restored normal cell cycle profile (Figure 2B), suggesting that p53 is causally linked to the observed G1-phase accumulation of HEATR1-depleted cells. In an independent parallel set of experiments, we confirmed the reduced fraction of replicating cells upon HEATR1 knockdown by monitoring 5-ethynyl-2'-deoxyuridine (EdU) incorporation (Figure 2C). Importantly, depletion of p53 efficiently reduced the level of p53 without affecting abundance of HEATR1 protein (Figure S2B). In contrast to U2OS cells, downregulation of HEATR1 in human cervical carcinoma (HeLa) cell line did not induce cell cycle arrest, as similar fractions (29% and 31%, respectively) of the control mock-treated and HEATR1-depleted cells were present in S phase and the overall cell cycle profiles were very similar (Figure S2C). From these experiments, we concluded that the apparent lack of the p53-dependent G1 accumulation in HEATR1-depleted HeLa cells likely

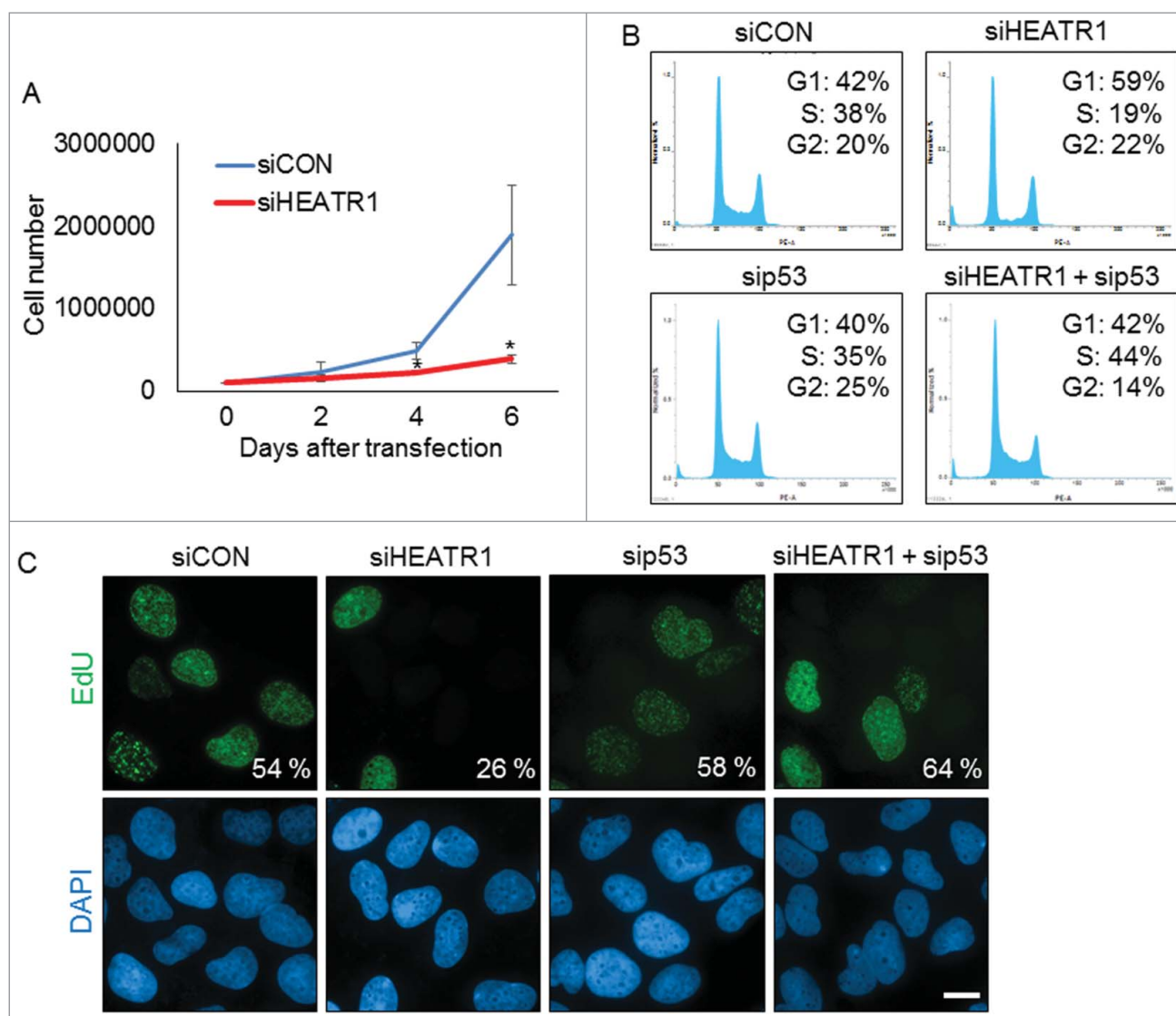


**Figure 2.** Knockdown of HEATR1 leads to impaired proliferation and induces p53-dependent cell cycle arrest. **A.** U2OS cells were transfected with control or HEATR1 siRNAs and 100000 cells were seeded. Cell counts were determined at the indicated time points after transfection. Error bars represent SDs,  $n = 3$ . Significance determined by two-tailed student's  $t$ -test: \*  $P < 0.05$ . **B.** U2OS cells were transfected with the indicated siRNAs and cell cycle profiles were assessed by flow cytometry 72 h after transfection. Results are representative of three independent experiments. **C.** U2OS cells were transfected with the indicated siRNAs and labeled with  $10 \mu\text{M}$  5-ethynyl-2'-deoxyuridine (EdU) for 30 min. The cells were fixed and incorporated EdU was visualized by click chemistry. The nuclei were stained by DAPI. Results are representative of three independent experiments. Bar,  $10 \mu\text{m}$ .

reflects the absence of functional p53 in HeLa cells, caused by the endogenous expression of the human papilloma virus E6 oncoprotein [26,27]. Overall, these data indicated that HEATR1 knockdown leads to accumulation and activation of p53 that induces cell cycle arrest and impairs cell growth in p53-proficient human normal and tumor cells.

### HEATR1 is a nucleolar protein

Next, we investigated the localization of HEATR1 in cultured human cells. Immunostaining of the endogenous HEATR1 protein in exponentially growing U2OS cells revealed that HEATR1 is localized in the nuclei, with a pronounced accumulation in the nucleoli, the latter validated by co-staining for nucleophosmin (NPM), a nuclear protein with preferential accumulation in nucleoli (Figure 3A). The nucleolar localization of HEATR1 was specific, as depletion of HEATR1 by

siRNA led to the disappearance of the staining signal from the nucleoli, while the weak nucleoplasmic background staining signal remained unchanged (Figure 3B). The observed nucleolar localization of HEATR1 was also shared by two distinct and widely used strains of human diploid fibroblasts: BJ and MRC-5 (Figure S3A and B). Transfection of siRNA targeting HEATR1 into such normal cells abolished again only the nucleolar staining signal, thereby validating the results obtained with the U2OS cells (Figure S1B and data not shown). During these experiments, we noted that the protein expression level of HEATR1 is lower in normal cells, compared to either U2OS or HeLa cells. Indeed, a comparative Western blotting analysis of total cell lysates from exponentially growing cultures confirmed higher levels of the HEATR1 protein in U2OS and HeLa cells, in contrast to very low, barely detectable levels seen in either BJ or MRC-5 cell extracts examined in parallel (Figure S3C). On the other hand, these differences may reflect distinct overall

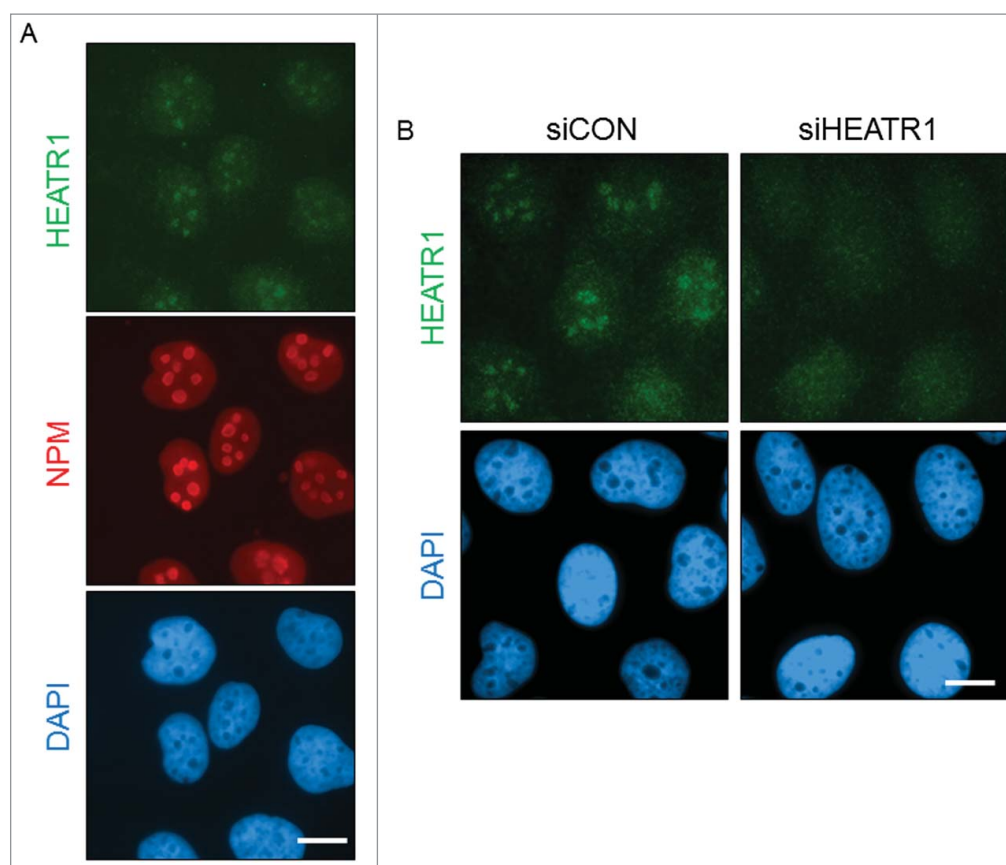


**Figure 3.** HEATR1 is localized to the nucleoli A. U2OS cells were fixed and immunostained with HEATR1 and nucleophosmin (NPM) antibodies. Nuclei were visualized by DAPI staining. Bar, 10  $\mu$ m. B. U2OS cells were transfected with indicated siRNAs and fixed and immunostained with HEATR1 antibody 72 after transfection. Nuclei were visualized by DAPI staining. Bar, 10  $\mu$ m.

size/contribution of nucleolar compartments in cancer *versus* normal cells, as we found a similar trend towards enhanced relative abundance of other nucleolar proteins in the cancer cell lines (Figure S3C).

We conclude from these analyses that human HEATR1 is a largely nucleolar protein that is overexpressed in cancerous cell lines compared to normal cells, consistent with cancer-associated over-abundance of other nucleolar proteins.

### **HEATR1 knockdown leads to disruption of nucleolar structure and induces ribosome biogenesis stress**

Nucleolar localization of HEATR1, along with induced p53 and cell-cycle arrest upon HEATR1 knockdown suggested that HEATR1 might be involved in ribosomal biogenesis. To test whether accumulation and activation of p53 upon HEATR1 knockdown is a consequence of ribosome biogenesis stress, we first analyzed the integrity of the nucleolus by immunofluorescence in control and HEATR1-depleted cells. Although disruption of nucleolar structure is not required for p53 activation upon ribosome biogenesis stress [28], perturbation of ribosome biosynthesis can result in dramatic alterations of nucleolar morphology [9,29–31]. To characterize the impact of HEATR1 depletion on nucleolar structure, we followed established markers of nucleolar disintegration. Whereas fibrillarin (FBL), NPM and nucleolin (NCL) all showed predominantly nucleolar localization in control siRNA-treated U2OS and HeLa cells

(Figure 4A, B and Figure S4A, B), parallel cultures treated with HEATR1-targeting siRNA caused redistribution of these proteins in both cell lines. Specifically, NPM and NCL became released from nucleoli into the nucleoplasm, while the FBL staining signal relocated to nucleolar caps, structures characteristic for cells with inhibited RNA Pol I-mediated transcription [32–34] (Figure 4A, B and Figure S4 A, B). In addition, we also confirmed induction of p53 in HEATR1 deficient U2OS cells by immunofluorescence staining (Figure 4B).

To test whether HEATR1 depletion triggers the canonical RPL5/RPL11-MDM2-dependent response to ribosome biogenesis stress, we performed simultaneous depletion of HEATR1 and either RPL5 or RPL11 and examined the p53 response. Indeed, knockdown of either RPL5 or RPL11 prevented the p53 accumulation seen in HEATR1-depleted U2OS cells, without affecting HEATR1 protein itself (Figure 4C and Figure S4C). Furthermore, co-immunoprecipitation experiments detected a complex of RPL5 with MDM2 in HEATR1-deficient, but not in control cells (Figure 4D). These observations supported our working hypothesis that depletion of HEATR1 leads to ribosome biogenesis stress accompanied with the disruption of the nucleolar structure. This, in turn, leads to release of some nucleolar and ribosomal proteins into the nucleoplasm, while a subset of nucleolar proteins is redistributed, forming nucleolar caps. Cells react to this stressful scenario by triggering the RPL5/RPL11-MDM2-mediated stabilization and activation of p53, leading to G1 cell cycle arrest.

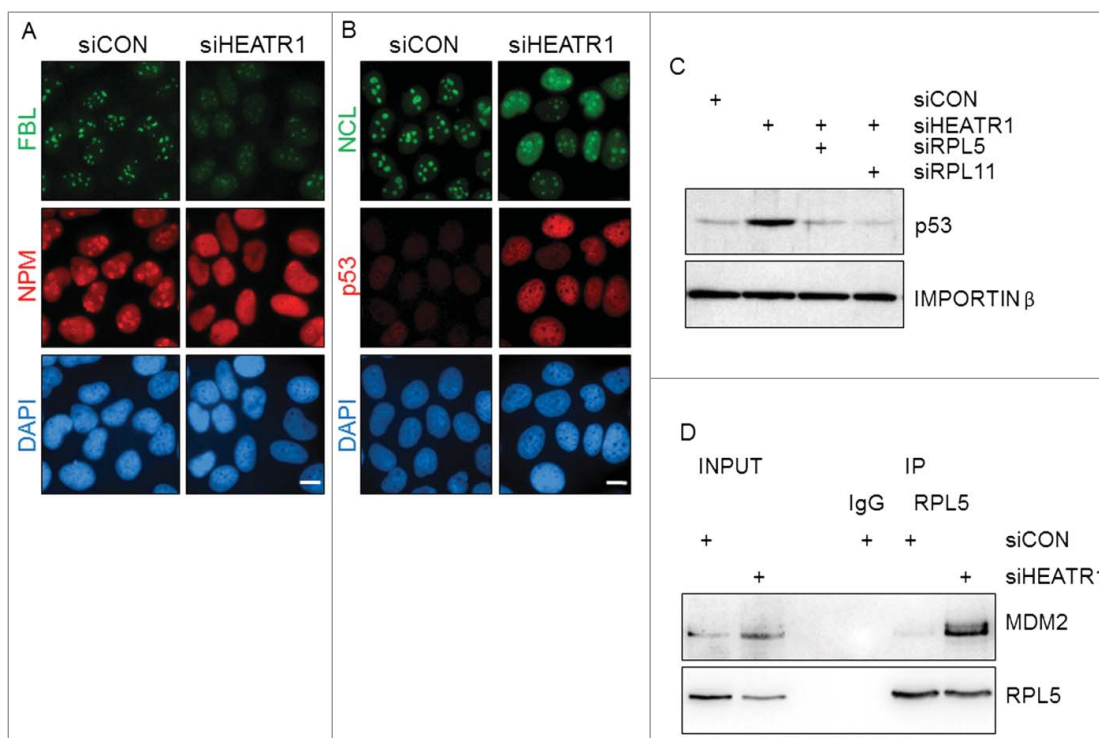


**Figure 4.** HEATR1 knockdown induces ribosomal stress A, B. U2OS cells were transfected with indicated siRNAs, fixed and immunostained with fibrillar (FBL), nucleophosmin (NPM), nucleolin (NCL) and p53 antibodies 72 h after transfection. Nuclei were visualized with DAPI staining. Bar, 10  $\mu$ m. C. U2OS cells were transfected with indicated siRNA, lysed and immunoblotted with indicated antibodies 72 h after transfection. D. U2OS cells were transfected with control or HEATR1 siRNAs. Cell lysates were immunoprecipitated 72 h after transfection with control (IgG) or RPL5 antibodies and immunoblotted with indicated antibodies.

### The role of HEATR1 in ribosome biogenesis

To provide further insights into the potential role(s) of HEATR1 in the nucleolus, we analyzed nascent RNA synthesis in control *versus* HEATR1-depleted cells. The incorporation of the nucleotide analogue, 5-ethynyl uridine (EU) into RNA was most prominent in nucleolar regions in control cells, as ribosomal RNAs are the most abundant RNA species in the cell [35] (Figure 5A and Figure S5). In contrast, siRNA-mediated depletion of HEATR1 impaired the nascent transcription in the nucleoli, evidenced by the severe depletion of the nucleolar EU signal (Figure 5A and Figure S5). The strong suppression of rRNA transcription caused by ablation of HEATR1 was comparable to effects of treatment with low concentrations of actinomycin D (ActD, Figure 5A), which is known to specifically inhibit the activity of RNA Pol I [36,37].

Proteins associated with the Pol I transcription machinery co-localize in the fibrillar center of the nucleolus and are redistributed to small, so-called fibrillar caps upon transcription inhibition [34]. Since HEATR1 seemed to be required for proper rRNA synthesis, we asked whether: i) HEATR1 co-localizes with Pol I under unperturbed growth; and ii) if yes, how is such localization pattern affected by the low-ActD treatment. To address these questions, we visualized RNA Pol I by immunostaining with antibodies against the RPA194 subunit of Pol I (Figure 5B). Under normal growth conditions, HEATR1 and RPA194 co-localized in the nucleoli, presumably in the fibrillar centers (Figure 5B). When low concentration of ActD was applied to inhibit rDNA transcription, both HEATR1 and RPA194 were redistributed to the periphery of nucleoli, forming small, overlaying nucleolar caps (Figure 5B).

Considering the emerging potential of small molecule inhibitors of ribosome biogenesis in anti-cancer treatment, we evaluated the effect of one such promising compound, BMH-21 [38,39] on HEATR1 localization. BMH-21 induces ribosome

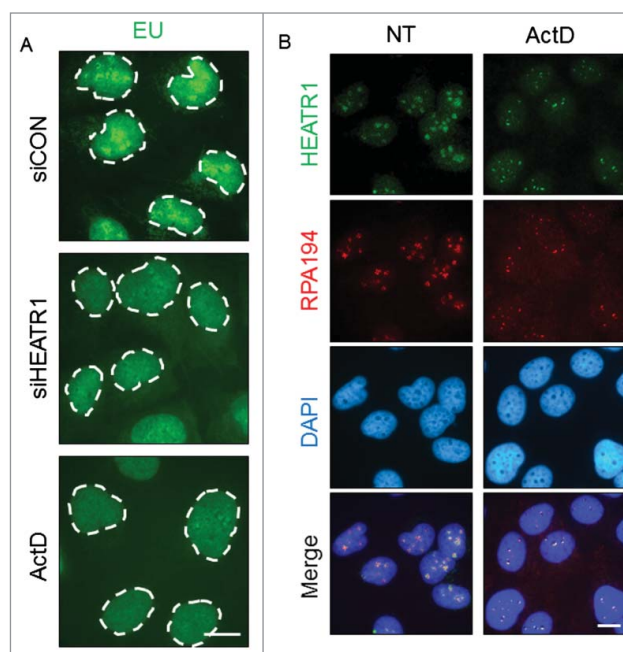


**Figure 5.** HEATR1 is involved in rRNA synthesis. A. U2OS cells were transfected with indicated siRNAs or treated with 5 nM ActD overnight and labeled with 1 mM 5-ethynyl uridine (EU) for 30 min. EU detection was performed by click chemistry. Bar, 10  $\mu$ m. B. U2OS cells were mock- or actinomycin D- (ActD, 5nM) treated overnight, then fixed and immunostained with indicated antibodies. Nuclei were visualized by DAPI staining. Bar, 10  $\mu$ m.

biogenesis stress by intercalating into GC rich region of the DNA, thereby inhibiting rRNA synthesis and promoting degradation of RPA194 [38,39]. Similarly to ActD treatment, exposure of human cells to BMH-21 induced redistribution of HEATR1 into nucleolar caps, while RPA194 was degraded (Figure S5B). These data collectively indicated that HEATR1 plays a prominent role in rRNA transcription, as knockdown of the protein led to impaired rRNA synthesis. Moreover, our results showed that HEATR1 co-localizes with Pol I under unperturbed conditions, and undergoes the same pattern of topological redistribution as Pol I upon ActD treatment, thereby further supporting HEATR1's involvement in rRNA transcription.

## Discussion

In this study, we investigated the role of human HEATR1, so far a very poorly characterized protein, which we identified as one of the prominent hits in a high-throughput siRNA screen for human proteins whose depletion leads to p53 stabilization (the complete dataset from the screen will be reported separately). Here, we showed that depletion of HEATR1 leads to activation and stabilization of the tumor suppressor protein p53. Thus, RNAi-mediated knockdown of HEATR1 caused a nearly two-fold increase of p53 protein half-life, accompanied by induced expression of p53's transcriptional target, the CDK inhibitor p21. At the cellular level, this sequence of molecular events resulted in decreased cell proliferation and cell cycle arrest in G1. Importantly, such activation of the cell cycle checkpoint was not due to the canonical DNA damage-induced phosphorylation of p53, since HEATR1 depletion did not lead to DNA damage. These results are complementary to, and consistent with, our previous report that the U2OS cells cannot induce the p53-dependent G1 checkpoint after DNA damage, despite they express wild-type p53. Such malfunction of the DNA-damage dependent p53 activation is due to the overexpression in U2OS cells of a truncated, mutant form of Wip1, a phosphatase that potently counteracts the otherwise functional phosphorylation of p53 under DNA damage conditions [40]. On the other hand, in response to HEATR1 depletion, p53 becomes stabilized via a phosphorylation-independent pathway (see below) and therefore the overexpressed mutant Wip1 does not prevent activation of the p53-p21 checkpoint under such ribosomal stress conditions. Furthermore, the absence of DNA damage signaling documented by the lack of  $\gamma$ H2AX in HEATR1-depleted cells also indicates that the DNA damage response (DDR) is not activated. ATM kinase is a key component of the DDR network and negatively regulates abundance of the alternative reading frame (ARF) tumor suppressor protein [41]. ARF is another nucleolar protein which – similarly to some RPs – is able to activate p53-dependent pathways upon stress stimuli, by disrupting MDM2's interaction with p53 [42]. ARF also inhibits ribosome biogenesis independently of p53, by preventing nucleolar import of RNA polymerase I transcription termination factor (TTF-I) [43]. Since HEATR1 ablated cells did not show DDR activation, one possibility was that ARF is induced and elicits its dual effect on p53 activation and repression of ribosome biogenesis. However, U2OS cells used in our experiments do not express ARF due to promoter

hypermethylation [44]. Thus, both the observed repression of ribosome biogenesis and activation of p53 seem to be independent of ARF, further signifying the importance of the p53 activation pathway *via* the RPL5/RPL11-MDM2 axis upon perturbation of ribosome biogenesis (see below). Additionally, we show here that the observed cell-cycle arrest induced by HEATR1 silencing could be rescued by co-depletion of p53. All these data indicated that p53 is activated through a DDR- and ARF-independent mechanism. Moreover, in the human papilloma virus (HPV) positive HeLa cells knockdown of HEATR1 did not result in cell-cycle arrest, an observation that reflects the chronically impaired function of p53 in this cell line by the HPV-encoded E6 oncoprotein [26,27]. Most relevant for our present data related to ribosomal stress responses, recent reports suggested existence of both p53-dependent, but also alternative, p53-independent checkpoint activation pathways upon impaired ribosome biogenesis (reviewed in ref. [5,45]). Perturbed ribosome biogenesis results in the release of several nucleolar RPs into the nucleoplasm where they bind MDM2. Binding of MDM2 by the RPL11 initiates not only the stabilization of p53 (through the canonical RPL5/RPL11 dimer-mediated sequestration of MDM2), but reportedly also degradation of the E2F-1 transcription factor, leading to cell-cycle arrest even in p53-deficient cells [46]. Moreover, another RP, RPL3 was reported to activate p21 independently of p53, inducing cell cycle arrest and apoptosis upon ribosome biogenesis stress [47,48]. While we cannot exclude the possibility of such alternative checkpoint activation at later time points in HeLa cells, depletion of HEATR1 in our experiments did not result in any detectable cell cycle arrest in HeLa cells, suggesting that the predominant mode of the p53 response to ribosomal stress upon HEATR1 knockdown reflects the RPL5/RPL11-MDM2 pathway.

A recent study suggested that HEATR1 is a regulator of the AKT pathway, whereby HEATR1 facilitates the interaction between AKT and its inactivating phosphatase, PP2A by acting as a scaffold. Unlike our findings presented here, this study suggested that HEATR1 is localized exclusively in the cytoplasm, a prerequisite for its co-localization and interaction with AKT [24]. In contrast, we found that HEATR1 is localized predominantly in the nucleoli of all cell types examined, both normal and cancerous, a result that is consistent with the report by Prieto and McStay [22]. Although our immunostaining of HEATR1 revealed some weaker signal also in the nucleoplasm and occasionally in the cytoplasm, our siRNA targeting HEATR1 abolished only the nucleolar staining signal, suggesting that HEATR1 mainly resides in the nucleolus. However, we cannot exclude the possibility that siRNAs used here preferentially target the 'nucleolar form' of HEATR1, or that HEATR1 may be more abundant in the cytosol of pancreatic cancer cells, the only cell type examined in the study reporting the HEATR1-AKT cytosolic interplay [24].

Perturbation of ribosome biogenesis triggers p53 activation through the RPL5/RPL11-MDM2 axis [9,11,15], often accompanied by disintegration of the nucleolus [9,29–31,34]. In our present experiments, depletion of HEATR1 disrupted the structure of the nucleolus and, consequently, the nucleolar proteins NPM and NCL were released into the nucleoplasm, while FBL redistributed to nucleolar caps. Although it is not a prerequisite



for p53 activation, nucleolar disintegration is a robust surrogate marker of ribosome biogenesis stress [9,28–31,34]. Consistently, the increased level of p53 caused by RNAi-mediated depletion of HEATR1 could be reversed by co-depletion of either RPL5 or RPL11. Moreover, ablation of HEATR1 also led to the increased interaction between RPL5 and MDM2, providing further evidence that deficiency of HEATR1 results in ribosome biogenesis stress.

HEAT repeats are expressed by a wide variety of eukaryotic proteins involved in diverse cellular processes, however protein-protein interaction is considered to represent the main function for these structures [16]. Broadly consistent with our present findings, UTP10, a yeast HEAT repeat protein was reported to localize in the nucleolus [19]. UTP10 – similarly to other UTPs (U3 small nucleolar RNA-associated proteins) – binds to U3 snoRNA and thereby contributes to maturation of 18S rRNA and assembly of the small ribosomal subunit [19,20]. Furthermore, UTP10 was also shown to regulate rDNA transcription [17]. Zebrafish Bap28 which shows 34% sequence similarity to yeast UTP10 was also characterized as a protein required for rRNA synthesis and 18S rRNA maturation [21]. Here, we showed that human HEATR1 is a positive regulator of transcription by RNA Pol I. Indeed, depletion of HEATR1 caused inhibition of rRNA synthesis to the same extent as low concentration of ActD, a widely used and selective treatment to block Pol I activity. Moreover, we found that HEATR1 was co-localized with Pol I both under normal conditions and upon inhibition of transcription by ActD. In the latter case, HEATR1 and Pol I became redistributed to the periphery of the nucleoli, into cap-like structures. Our data are also consistent with the work of Prieto and McStay who reported nucleolar co-localization of HEATR1 with the Pol I transcription machinery, in a manner independent of active transcription yet dependent on the integrity of the upstream binding factor (UBF) [22]. Last but not least, the model we propose was further supported by the responses we observed upon treatment with the ribosome biogenesis inhibitor BMH-21. While treatment with BMH-21 led to rapid degradation of RPA194, HEATR1 became redistributed to form cap-like structures, similarly to what we observed in response to ActD.

Aberrantly enlarged nucleoli and upregulation of ribosome biogenesis are common features of various types of cancer. Due to its intimate link with cell growth and cell cycle regulation, enhanced ribosomal biogenesis can impair differentiation and promote tumorigenesis [6,49–52]. Our observation that HEATR1 is elevated in cancer cell lines, compared to normal non-cancerous cells, is also consistent with the concept of the global deregulation of ribosomal biogenesis in cancer. While in the two cancer cell lines we examined, elevation of HEATR1 was accompanied by enhanced levels of other nucleolar proteins, it is possible that HEATR1 is specifically overexpressed in certain types of cancer. For instance, a recent report demonstrated that HEATR1 is overexpressed in glioblastoma cells, providing an excellent target for T-cell mediated immunotherapy [23]. In contrast, aberrantly low levels of ribosome biogenesis represent the hallmark of the so-called ribosomopathies, a group of human diseases characterized by hyperactivation of p53, reduced cell growth and protein synthesis [53–55]. Abnormal downregulation of HEATR1 seems to correlate with poor

prognosis in patients with pancreatic ductal carcinoma, however, this phenotype was attributed to the consequence of HEATR1's involvement in AKT phosphorylation (see above for the discussion of cytosolic HEATR1 in pancreatic cell lines reported in this study) and may be unrelated to its function in ribosome biogenesis [24]. Nonetheless, further studies are clearly warranted to elucidate any potential contribution of HEATR1 alteration(s) to pathogenesis of various cancer types.

Taken together, we report here that human HEATR1 is a nucleolar protein that plays a prominent positive role in regulation of rRNA synthesis. Deficiency of HEATR1 leads to perturbation of ribosome biogenesis, resulting in DNA damage-independent activation of the p53-p21 checkpoint response through the RPL5/RPL11-MDM2 axis. Our study provides fresh insights into the complex nucleolar events and the ways malfunction of ribosomal biogenesis can lead to growth and cell-cycle arrest, with implications for pathologies including cancer.

## Material and methods

### Cell culture

Cell lines used in this work were cultured in Dulbecco's modified Eagle's medium (DMEM) supplemented with 10% fetal bovine serum (Life Technologies) and penicillin/streptomycin (Sigma-Aldrich) in humidified atmosphere of 5% CO<sub>2</sub> at 37°C. For BJ and MRC-5 culturing, DMEM was supplemented with 1% MEM Non-essential amino acids (Life Technologies), as well. All cell lines were purchased from ATCC.

### Chemicals and antibodies

Actinomycin D (A1410) and cycloheximide (C4859) were purchased from Sigma-Aldrich. BMH-21 (S7718) was purchased from Selleckchem.

Antibodies used in this study included rabbit antibodies: HEATR1 (HPA046917, Sigma-Aldrich), p21 (2947, Cell Signaling), nucleolin (ab70493, Abcam), nucleostemin (ab70346, Abcam), fibrillarin (ab5821, Abcam), RPL5 (ab157099, Abcam) and mouse antibodies:  $\beta$ -actin (sc-47778, Santa Cruz), Importin- $\beta$  (ab2811, Abcam), p53 (sc-126, Santa Cruz),  $\gamma$ H2AX (05-636, Millipore), nucleophosmin (ab10530, Abcam), and MDM2 (ab16895, Abcam).

### RNA interference

All siRNA transfections were performed using Lipofectamine RNAiMAX (Invitrogen) according to the manufacturer's instructions. All siRNA duplexes were purchased from Ambion: siCON (negative control #1, AM4635, 5'-AGUACUGCUUACGAUACGGTT-3'), siHEATR1#1 (s30230, 5'-CCACUUUCCAUUUGCGAUATT-3'), siHEATR1#2 (s30231, 5'-GAUGUUGUUUUGUCGGCUATT-3'), siHEATR1#3 (s30232, 5'-CACUUUCCAUUUGCGAUATT-3'), sip53 (s605, 5'-GUAAUCUACUGGGACGGAATT-3'), siRPL5 (s56733, 5'-CAGUUCUCUCAUAUAATT-3'), and siRPL11 (s12169, 5'-CAACUUCUCAGAUACUGGATT-3').

### Cell cycle analysis

Cells were fixed in 70% ethanol and stained with propidium iodide for flow cytometric analysis. Fixed cells were analyzed on a FACS Verse instrument (BD Biosciences) and cell cycle distribution was assigned using the FACSuite software (BD Biosciences).

### Immunoblotting

Immunoblotting was performed as previously described [56]. WCLs were prepared in Laemmli sample buffer (LSB; 50 mM Tris, pH 6.8, 100 mM DTT, 2% SDS, 0.1% bromophenol blue, and 10% glycerol), separated by SDS-PAGE, and transferred to nitrocellulose membranes (GE Healthcare). The membranes were blocked with 5% (wt/vol) dry milk in 0.1% (vol/vol) Tween-20 in PBS and probed with the primary antibodies, followed by HRP-labeled secondary antibodies (GE Healthcare), and visualized using ECL detection reagents (GE Healthcare).

### Immunofluorescence

Immunofluorescence analysis was performed as previously described with minor changes [57]. Cells grown on 12-mm coverslips were fixed with 4% paraformaldehyde in PBS for 15 min and then permeabilized with PBS containing 0.2% (v/v) Triton X-100 for 5 min. Fixed cells were blocked with 5% (v/v) fetal bovine serum in PBS for 30 minutes and incubated overnight at 4 °C with primary antibodies (diluted in 5% (w/v) bovine serum albumin in PBS). Coverslips were washed 3 times in PBS supplemented with 0.1% (v/v) Tween 20, once with PBS and then incubated with an appropriate secondary goat anti-rabbit or goat anti-mouse Alexa Fluor 488 or Alexa Fluor 568 conjugated (Invitrogen) secondary antibody (diluted in 5% (w/v) bovine serum albumin in PBS) for 60 min at RT. Slips were then washed as above and mounted onto slides using the DAPI containing Vectashield mounting reagent (Vector Laboratories). Slides were visualized by the Axio Observer.Z1/Cell Observer Spinning Disc microscopic system (Yokogawa and Zeiss) equipped with an Evolve 512 Photometrix) EMCCD camera. Zeiss Plan APOCHROMAT 100x/1.40 NA objective was used.

### EdU and EU staining

Cells were labelled either with 10  $\mu$ M EdU or with 1 mM EU (Sigma-Aldrich) for 30 min, then fixed with 4% paraformaldehyde in PBS for 15 min and permeabilized with 0.2% Triton-X100 for 5 min, followed by incubation with staining solution (100 mM Tris-HCl, pH = 8.5, 1 mM CuSO<sub>4</sub>, 1  $\mu$ M azide conjugated fluorochrome, 100 mM ascorbic acid) for 30 min. Nuclei were stained with DAPI. Image acquisition and analysis was performed using ScanR system (Olympus).

### Immunoprecipitation

Immunoprecipitation was performed as previously described with minor changes [58]. Briefly, cells were washed three times in PBS and lysed in TNE buffer (150 mM NaCl, 50 mM Tris-

HCl, pH 8.0, 1 mM EDTA, 0.5% NP-40) supplemented with cComplete and PhosSTOP tablets (Roche). After 30 min incubation on ice, lysates were cleared by centrifugation. Where appropriate, antibodies were added to lysate and incubated for 16 h at 4°C. Lysates were then incubated with 25  $\mu$ l of Dynabeads M-280 Sheep anti Rabbit IgG (Novex) for 1 h at 4°C. Ig-antigen complexes were washed extensively before elution in 2  $\times$  LSB before SDS-PAGE.


### Disclosure of potential conflict of interest

No potential conflicts of interest were disclosed.

### Funding

This work was supported by the Grant Agency of the Czech Republic under grants 17-14743S and 17-25976S, the MEYS CR (CZ.02.1.01/0.0/0.0/16\_013/0001775 Czech-BioImaging), Czech National Program of Sustainability (LO1304), UP IGA\_LF\_2017\_002, the Danish Cancer Society, the Danish Council for Independent Research, the Swedish Research Council, CancerFonden, the Lundbeck Foundation, and the Danish National Research Foundation (Center of Excellence, project CARD). Czech Science Foundation (GACR) [grant number 17-14743S]

### ORCID

Pavel Moudry  <http://orcid.org/0000-0002-1479-007X>

### References

- Budkevich TV, El'skaya AV, Nierhaus KH. Features of 80S mammalian ribosome and its subunits. *Nucleic Acids Res.* 2008;36:4736-4744. doi:10.1093/nar/gkn424. PMID:18632761
- Klinge S, Voigts-Hoffmann F, Leibundgut M, et al. Atomic structures of the eukaryotic ribosome. *Trends Biochem Sci.* 2012;37:189-198. doi:10.1016/j.tibs.2012.02.007. PMID:22436288
- Wilson DN, Doudna Cate JH. The structure and function of the eukaryotic ribosome. *Cold Spring Harb Perspect Biol.* 2012;4:1-17. doi:10.1101/cshperspect.a011536. PMID:22550233
- Kressler D, Hurt E, Bassler J. A puzzle of life: crafting ribosomal subunits. *Trends Biochem Sci.* 2017;42:640-654. doi:10.1016/j.tibs.2017.05.005. PMID:28579196
- James A, Wang Y, Rajee H, et al. Nucleolar stress with and without p53. *Nucleus.* 2014;5:402-426. doi:10.4161/nucl.32235. PMID:25482194
- Derenzini M, Montanaro L, Trere D. Ribosome biogenesis and cancer. *Acta Histochem.* 2017;119:190-197. doi:10.1016/j.acthis.2017.01.009. PMID:28168996
- Yang L, Song T, Chen L, et al. Nucleolar repression facilitates initiation and maintenance of senescence. *Cell Cycle.* 2015;14:3613-3623. doi:10.1080/15384101.2015.1100777. PMID:26505814
- Morgado-Palacin L, Llanos S, Urbano-Cuadrado M, et al. Non-genotoxic activation of p53 through the RPL11-dependent ribosomal stress pathway. *Carcinogenesis.* 2014;35:2822-2830. doi:10.1093/carcin/bgu220. PMID:25344835
- Bursac S, Donati G, Brdovcak MC, et al. Activation of the tumor suppressor p53 upon impairment of ribosome biogenesis. *Biochim Biophys Acta.* 2013;1842:817-830. PMID:24514102
- Dong Z, Zhu C, Zhan Q, et al. The roles of RRP15 in nucleolar formation, ribosome biogenesis and checkpoint control in human cells. *Oncotarget.* 2017;8:13240-13252. PMID:28099941
- Fumagalli S, Ivanenkov VV, Teng T, et al. Suprainduction of p53 by disruption of 40S and 60S ribosome biogenesis leads to the activation of a novel G2/M checkpoint. *Genes Dev.* 2012;26:1028-1240. doi:10.1101/gad.189951.112. PMID:22588717

- [12] Honda R, Tanaka H, Yasuda H. Oncoprotein MDM2 is a ubiquitin ligase E3 for tumor suppressor p53. *FEBS Lett.* 1997;420:25–27. doi:10.1016/S0014-5793(97)01480-4. PMID:9450543
- [13] Michael D, Oren M. The p53-Mdm2 module and the ubiquitin system. *Semin Cancer Biol.* 2003;13:49–58. doi:10.1016/S1044-579X(02)00099-8. PMID:12507556
- [14] Haupt Y, Maya R, Kazaz A, et al. Mdm2 promotes the rapid degradation of p53. *Nature.* 1997;387:296–299. doi:10.1038/387296a0. PMID:9153395
- [15] Golomb L, Volarevic S, Oren M. p53 and ribosome biogenesis stress: the essentials. *FEBS Lett.* 2014;588:2571–2579. doi:10.1016/j.febslet.2014.04.014. PMID:24747423
- [16] Yoshimura SH, Hirano T. HEAT repeats – versatile arrays of amphiphilic helices working in crowded environments? *J Cell Sci.* 2016;129:3963–3970. PMID:27802131
- [17] Gallagher JE, Dunbar DA, Granneman S, et al. RNA polymerase I transcription and pre-rRNA processing are linked by specific SSU processome components. *Genes Dev.* 2004;18:2506–2517. doi:10.1101/gad.1226604. PMID:15489292
- [18] Oeffinger M, Dlakic M, Tollervey D. A pre-ribosome-associated HEAT-repeat protein is required for export of both ribosomal subunits. *Genes Dev.* 2004;18:196–209. doi:10.1101/gad.285604. PMID:14729571
- [19] Dez C, Dlakic M, Tollervey D. Roles of the HEAT repeat proteins Utp10 and Utp20 in 40S ribosome maturation. *Rna.* 2007;13:1516–1527. doi:10.1261/rna.609807. PMID:17652137
- [20] Krogan NJ, Peng WT, Cagney G, et al. High-definition macromolecular composition of yeast RNA-processing complexes. *Mol Cell.* 2004;13:225–239. doi:10.1016/S1097-2765(04)00003-6. PMID:14759368
- [21] Azuma M, Toyama R, Laver E, et al. Perturbation of rRNA synthesis in the bap28 mutation leads to apoptosis mediated by p53 in the zebrafish central nervous system. *J Biol Chem.* 2006;281:13309–13316. doi:10.1074/jbc.M601892200. PMID:16531401
- [22] Prieto JL, McStay B. Recruitment of factors linking transcription and processing of pre-rRNA to NOR chromatin is UBF-dependent and occurs independent of transcription in human cells. *Genes Dev.* 2007;21:2041–2054. doi:10.1101/gad.436707. PMID:17699751
- [23] Wu ZB, Qiu C, Zhang AL, et al. Glioma-associated antigen HEATR1 induces functional cytotoxic T lymphocytes in patients with glioma. *J Immunol Res.* 2014;2014:131494. doi:10.1155/2014/131494. PMID:25126583
- [24] Liu T, Fang Y, Zhang H, et al. HEATR1 negatively regulates Akt to help sensitize pancreatic cancer cells to chemotherapy. *Cancer Res.* 2016;76:572–581. doi:10.1158/0008-5472.CAN-15-0671. PMID:26676747
- [25] Jackson AL, Bartz SR, Schelter J, et al. Expression profiling reveals off-target gene regulation by RNAi. *Nat Biotechnol.* 2003;21:635–637. doi:10.1038/nbt831. PMID:12754523
- [26] Scheffner M, Werness BA, Huibregtse JM, et al. The E6 oncoprotein encoded by human papillomavirus Type-16 and Type-18 promotes the degradation of P53. *Cell.* 1990;63:1129–1136. doi:10.1016/0092-8674(90)90409-8. PMID:2175676
- [27] Werness BA, Levine AJ, Howley PM. Association of human papillomavirus types 16 and 18 E6 proteins with p53. *Science.* 1990;248:76–79. doi:10.1126/science.2157286. PMID:2157286
- [28] Fumagalli S, Di Cara A, Neb-Gulati A, et al. Absence of nucleolar disruption after impairment of 40S ribosome biogenesis reveals an rpL11-translation-dependent mechanism of p53 induction. *Nat Cell Biol.* 2009;11:501–508. doi:10.1038/ncb1858. PMID:19287375
- [29] Yuan X, Zhou Y, Casanova E, et al. Genetic inactivation of the transcription factor TIF-1A leads to nucleolar disruption, cell cycle arrest, and p53-mediated apoptosis. *Mol Cell.* 2005;19:77–87. doi:10.1016/j.molcel.2005.05.023. PMID:15989966
- [30] Boulon S, Westman BJ, Hutten S, et al. The nucleolus under stress. *Mol Cell.* 2010;40:216–227. doi:10.1016/j.molcel.2010.09.024. PMID:20965417
- [31] Rubbi CP, Milner J. Disruption of the nucleolus mediates stabilization of p53 in response to DNA damage and other stresses. *EMBO J.* 2003;22:6068–6077. doi:10.1093/emboj/cdg579. PMID:14609953
- [32] Tajrishi MM, Tuteja R, Tuteja N. Nucleolin: the most abundant multifunctional phosphoprotein of nucleolus. *Commun Integr Biol.* 2011;4:267–275. doi:10.4161/cib.4.3.14884. PMID:21980556
- [33] Colombo E, Alcalay M, Pellici PG. Nucleophosmin and its complex network: a possible therapeutic target in hematological diseases. *Oncogene.* 2011;30:2595–2609. doi:10.1038/onc.2010.646. PMID:21278791
- [34] Shav-Tal Y, Blechman J, Darzacq X, et al. Dynamic sorting of nuclear components into distinct nucleolar caps during transcriptional inhibition. *Mol Biol Cell.* 2005;16:2395–2413. doi:10.1091/mbc.E04-11-0992. PMID:15758027
- [35] Jao CY, Salic A. Exploring RNA transcription and turnover in vivo by using click chemistry. *P Natl Acad Sci USA.* 2008;105:15779–15784. doi:10.1073/pnas.0808480105.
- [36] Burger K, Muhl B, Harasim R T, et al. Chemotherapeutic drugs inhibit ribosome biogenesis at various levels. *J Biol Chem.* 2010;285:12416–12425. doi:10.1074/jbc.M109.074211. PMID:20159984
- [37] Hernandez-Verdun D, Roussel P, Thiry M, et al. The nucleolus: structure/function relationship in RNA metabolism. *Wiley Interdiscip Rev RNA.* 2010;1:415–431. doi:10.1002/wrna.39. PMID:21956940
- [38] Peltonen K, Colis L, Liu H, et al. A targeting modality for destruction of rna polymerase i that possesses anticancer activity. *Cancer Cell.* 2014;25:77–90. doi:10.1016/j.ccr.2013.12.009. PMID:24434211
- [39] Peltonen K, Colis L, Liu H, et al. Identification of novel p53 pathway activating small-molecule compounds reveals unexpected similarities with known therapeutic agents. *Plos One.* 2010;5:1–11. doi:10.1371/journal.pone.0012996.
- [40] Kleiblova P, Shaltiel IA, Benada J, et al. Gain-of-function mutations of PPM1D/Wip1 impair the p53-dependent G1 checkpoint. *J Cell Biol.* 2013;201:511–521. doi:10.1083/jcb.201210031. PMID:23649806
- [41] Velimezi G, Liontos M, Vougas K, et al. Functional interplay between the DNA-damage-response kinase ATM and ARF tumour suppressor protein in human cancer. *Nat Cell Biol.* 2013;15:967–977. doi:10.1038/ncb2795. PMID:23851489
- [42] Sherr CJ. Divorcing ARF and p53: an unsettled case. *Nat Rev Cancer.* 2006;6:663–673. doi:10.1038/nrc1954. PMID:16915296
- [43] Lessard F, Morin F, Ivanchuk S, et al. The ARF tumor suppressor controls ribosome biogenesis by regulating the RNA polymerase I transcription factor TTF-I. *Mol Cell.* 2010;38:539–550. doi:10.1016/j.molcel.2010.03.015. PMID:20513429
- [44] Badal V, Menendez S, Coomber D, et al. Regulation of the p14ARF promoter by DNA methylation. *Cell Cycle.* 2008;7:112–119. doi:10.4161/cc.7.1.5137. PMID:18196972
- [45] Russo A, Russo G. Ribosomal proteins control or bypass p53 during nucleolar stress. *Int J Mol Sci.* 2017;18:1–16. doi:10.3390/ijms18010140.
- [46] Donati G, Brighenti E, Vici M, et al. Selective inhibition of rRNA transcription downregulates E2F-1: a new p53-independent mechanism linking cell growth to cell proliferation. *J Cell Sci.* 2011;124:3017–3028. doi:10.1242/jcs.086074. PMID:21878508
- [47] Russo A, Pagliara V, Albano F, et al. Regulatory role of rpL3 in cell response to nucleolar stress induced by Act D in tumor cells lacking functional p53. *Cell Cycle.* 2016;15:41–51. doi:10.1080/15384101.2015.1120926. PMID:26636733
- [48] Russo A, Esposito D, Catillo M, et al. Human rpL3 induces G(1)/S arrest or apoptosis by modulating p21 (waf1/cip1) levels in a p53-independent manner. *Cell Cycle.* 2013;12:76–87. doi:10.4161/cc.22963. PMID:23255119
- [49] Rossetti S, Wierzbicki AJ, Sacchi N. Mammary epithelial morphogenesis and early breast cancer. Evidence of involvement of basal components of the RNA Polymerase I transcription machinery. *Cell Cycle.* 2016;15:2515–2526. doi:10.1080/15384101.2016.1215385. PMID:27485818
- [50] Boudra R, Lagrèfeuille R, Lours-Calet C, et al. mTOR transcriptionally and post-transcriptionally regulates Npm1 gene expression to contribute to enhanced proliferation in cells with Pten inactivation. *Cell Cycle.* 2016;15:1352–1362. doi:10.1080/15384101.2016.1166319. PMID:27050906
- [51] Orsolich I, Jurada D, Pullen N, et al. The relationship between the nucleolus and cancer: Current evidence and emerging paradigms. *Semin Cancer Biol.* 2016;37–38:36–50. doi:10.1016/j.semcancer.2015.12.004. PMID:26721423

- [52] Stepinski D. Nucleolus-derived mediators in oncogenic stress response and activation of p53-dependent pathways. *Histochem Cell Biol.* **2016**;146:119–139. doi:10.1007/s00418-016-1443-6. PMID:27142852
- [53] Nakhoul H, Ke J, Zhou X, et al. Ribosomopathies: mechanisms of disease. *Clin Med Insights Blood Disord.* **2014**;7:7–16. doi:10.4137/CMBD.S16952. PMID:25512719
- [54] Danilova N, Gazda HT. Ribosomopathies: how a common root can cause a tree of pathologies. *Dis Model Mech.* **2015**;8:1013–1026. doi:10.1242/dmm.020529. PMID:26398160
- [55] Koch S, Garcia Gonzalez O, Assfalg R, et al. Cockayne syndrome protein A is a transcription factor of RNA polymerase I and stimulates ribosomal biogenesis and growth. *Cell Cycle.* **2014**;13:2029–2037. doi:10.4161/cc.29018. PMID:24781187
- [56] Oplustilova L, Wolanin K, Mistrik M, et al. Evaluation of candidate biomarkers to predict cancer cell sensitivity or resistance to PARP-1 inhibitor treatment. *Cell Cycle.* **2012**;11:3837–3850. doi:10.4161/cc.22026. PMID:22983061
- [57] Moudry P, Lukas C, Macurek L, et al. Ubiquitin activating enzyme UBA1 is required for cellular response to DNA damage. *Cell Cycle.* **2012**;11:1573–1582. doi:10.4161/cc.19978. PMID:22456334
- [58] Brazina J, Svadlenka J, Macurek L, DNA damage-induced regulatory interplay between DAXX, p53, ATM kinase and Wip1 phosphatase. *Cell Cycle.* **2015**;14:375–387. doi:10.4161/15384101.2014.988019. PMID:25659035

### 8.3.3. Appendix C

Skrott, Z.; Mistrik, M.; Andersen, K.; Friis, S.; Majera, D.; Gursky, J.; Ozdian, T.; Bartkova, J.; **Turi, Z.**; Moudry, P.; Kraus, M.; Medvedikova M.; Vaclavkova, J.; Dzubak, P.; Vrobel, I.; Pouckova, P.; Sedlacek, J.; Miklovicova, A.; Kutt, A.; Mattova, J.; Driessen, C.; Dou, Q.; Olsen, J.; Hajduch, M.; Cvek, B.; Deshaies, R.; Bartek, J. Alcohol-abuse drug disulfiram targets cancer via p97 segregase adaptor NPL4. *Nature*. **2017**, 552(7684), 194-199. IF (2017/2018): 41.577

# Alcohol-abuse drug disulfiram targets cancer via p97 segregase adaptor NPL4

Zdenek Skrott<sup>1\*</sup>, Martin Mistrík<sup>1\*</sup>, Klaus Kaae Andersen<sup>2</sup>, Søren Friis<sup>2</sup>, Dusana Majera<sup>1</sup>, Jan Gursky<sup>1</sup>, Tomas Ozdian<sup>1</sup>, Jirina Bartkova<sup>2,3</sup>, Zsófia Turi<sup>1</sup>, Pavel Moudry<sup>1</sup>, Marianne Kraus<sup>4</sup>, Martina Michalova<sup>1</sup>, Jana Vaclavkova<sup>1</sup>, Petr Dzubak<sup>1</sup>, Ivo Vrobel<sup>1</sup>, Pavla Pouckova<sup>5</sup>, Jindrich Sedlacek<sup>6</sup>, Andrea Miklovicova<sup>7</sup>, Anne Kutt<sup>2</sup>, Jing Li<sup>8</sup>, Jana Mattova<sup>5</sup>, Christoph Driessen<sup>4</sup>, Q. Ping Dou<sup>9,10</sup>, Jørgen Olsen<sup>2</sup>, Marian Hajdúch<sup>1</sup>, Boris Cvek<sup>6†</sup>, Raymond J. Deshaies<sup>8,11†</sup> & Jiri Bartek<sup>2,3</sup>

**Cancer incidence is rising and this global challenge is further exacerbated by tumour resistance to available medicines. A promising approach to meet the need for improved cancer treatment is drug repurposing. Here we highlight the potential for repurposing disulfiram (also known by the trade name Antabuse), an old alcohol-aversion drug that has been shown to be effective against diverse cancer types in preclinical studies. Our nationwide epidemiological study reveals that patients who continuously used disulfiram have a lower risk of death from cancer compared to those who stopped using the drug at their diagnosis. Moreover, we identify the ditiocarb-copper complex as the metabolite of disulfiram that is responsible for its anti-cancer effects, and provide methods to detect preferential accumulation of the complex in tumours and candidate biomarkers to analyse its effect on cells and tissues. Finally, our functional and biophysical analyses reveal the molecular target of disulfiram's tumour-suppressing effects as NPL4, an adaptor of p97 (also known as VCP) segregase, which is essential for the turnover of proteins involved in multiple regulatory and stress-response pathways in cells.**

Despite advances in the understanding of cancer biology, malignant diseases have a high global toll. Furthermore, the increasing average human life expectancy is predicted to have demographic consequences, including an increase in the incidence of cancer. The high cancer-associated morbidity and mortality highlight the need for innovative treatments. Given the high costs, failure rate and long testing periods of developing new medicines, using drugs that are approved for the treatment of diverse diseases as candidate anti-cancer therapeutics represents a faster and cheaper alternative<sup>1</sup>, benefitting from available clinically suitable formulations and evidence of tolerability in patients. Among promising cancer-killing drugs<sup>2</sup> is disulfiram (tetraethylthiuram disulfide, DSF), a drug that has been used for over six decades as a treatment for alcohol dependence<sup>3</sup>, with well-established pharmacokinetics, safety and tolerance at the US Food and Drug Administration (FDA)-recommended dosage<sup>4</sup>. In the body, DSF is metabolized to ditiocarb (diethylthiocarbamate, DTC) and other metabolites, some of which inhibit liver aldehyde dehydrogenase<sup>5</sup>. Because DSF showed anti-cancer activity in preclinical models<sup>3,6–9</sup> and because adjuvant DTC was used to treat high-risk breast cancer in a clinical trial<sup>10</sup>, DSF emerges as a candidate for drug repurposing in oncology. Additional advantages of DSF include a broad spectrum of malignancies sensitive to DSF, and its ability to also target the stem-like, tumour-initiating cells<sup>11</sup>. Although the mechanism of DSF's anti-cancer activity remains unclear and it has been suggested that the drug inhibits proteasome activity<sup>6,12</sup>, it has been shown that DSF chelates bivalent metals and forms complexes with copper (Cu), which enhances its anti-tumour activity<sup>6,13</sup>. In addition to the lack of a well-defined mechanism of action in cancer cells, the main obstacles for DSF repurposing have

been: (i) uncertainty about the active metabolite(s) of DSF *in vivo*; (ii) the lack of assays to measure these active derivative(s) in tumours; (iii) missing biomarker(s) to monitor the impact of DSF in tumours and tissues; (iv) the lack of insights into the preferential toxicity towards cancer cells compared to normal tissues; and (v) the absence of a specific molecular target that could explain the potent anti-tumour activity of DSF. Here, we combine experimental approaches and epidemiology to address the important characteristics of DSF in relation to cancer, pursuing the goal of repurposing DSF for cancer therapy. We identify the active metabolite of DSF, and provide biological validation and mechanistic insights, including the discovery of a biologically attractive protein that has previously not been considered as the target for the anti-cancer activity of DSF.

## Epidemiological analyses of DSF and cancer

The relative lack of cancer-related clinical trials with DSF<sup>10,14</sup> prompted us to explore whether DSF use might reduce cancer mortality at a population level. Using the Danish nationwide demographic and health registries, we estimated hazard ratios of cancer-specific mortality associated with DSF use among patients with cancer for the first time during 2000–2013 (see Methods, Table 1 and Extended Data Fig. 1a). DSF users were categorized as (i) previous users, who were patients that were prescribed DSF for alcohol dependency only before their cancer diagnosis or (ii) continuing users, who were patients that were prescribed DSF both before and after diagnosis. As expected from the increase in cancer risk and the deleterious effect on prognosis<sup>15</sup> caused by alcohol abuse, cancer-specific mortality was higher among previous DSF users than among patients with cancer who had never

<sup>1</sup>Institute of Molecular and Translational Medicine, Faculty of Medicine and Dentistry, Palacky University, Olomouc, Czech Republic. <sup>2</sup>Danish Cancer Society Research Center, DK-2100 Copenhagen, Denmark. <sup>3</sup>Science for Life Laboratory, Division of Genome Biology, Department of Medical Biochemistry and Biophysics, Karolinska Institute, Stockholm, Sweden. <sup>4</sup>Kantonsspital St Gallen, Department Oncology/Hematology, St Gallen, Switzerland. <sup>5</sup>Institute of Biophysics and Informatics, First Faculty of Medicine, Charles University, 120 00 Prague 2, Czech Republic. <sup>6</sup>Department of Cell Biology & Genetics, Palacky University, Olomouc, Czech Republic. <sup>7</sup>Psychiatric Hospital, 785 01 Šternberk, Czech Republic. <sup>8</sup>Division of Biology and Biological Engineering, Caltech, Pasadena, California 91125, USA. <sup>9</sup>Barbara Ann Karmanos Cancer Institute and Department of Oncology, School of Medicine, Wayne State University, Detroit, Michigan, USA. <sup>10</sup>School of Basic Medical Sciences, Affiliated Tumor Hospital of Guangzhou Medical University, Guangzhou 511436, China. <sup>11</sup>Howard Hughes Medical Institute, Caltech, Pasadena, California 91125, USA. <sup>†</sup>Present addresses: Olomouc University Social Health Institute, Palacky University, Olomouc, Czech Republic (B.C.); Amgen, Thousand Oaks, California 91320, USA (R.J.D.).

\*These authors contributed equally to this work.

**Table 1 | Cancer-specific mortality associated with DSF use among Danish patients with cancer**

Cancer type	Overall				Localized stage				Non-localized stage				Unknown stage			
	Number*	HR	95% CI	P value	Number*	HR	95% CI	P value	Number*	HR	95% CI	P value	Number*	HR	95% CI	P value
<b>Any cancer†</b>																
Previous users	3,038	1.00			1,429	1.00			1,054	1.00			555	1.00		
Continuing users	1,177	0.66	0.58–0.76	0.000	602	0.69	0.64–0.74	0.000	355	0.71	0.59–0.87	0.001	220	0.65	0.57–0.75	0.000
No prescriptions	236,950	0.68	0.64–0.73	0.000	113,354	0.59	0.57–0.61	0.000	73,933	0.80	0.73–0.88	0.000	49,663	0.66	0.62–0.71	0.000

Hazard ratios (HR) and 95% confidence intervals (CI) comparing continuing and previous users of DSF, relative to the time of their cancer diagnosis. For DSF exposure categories, statistics and clinical stages, see Methods.

\*Number of patients included.

†Except cancers of the liver and kidney.

used DSF. Notably, we also found reduced cancer-specific mortality for cancer overall (Table 1), as well as for cancers of the colon, prostate and breast among continuing users compared to previous DSF users (Extended Data Fig. 1a). Stratification by clinical stage (Table 1) revealed reduced cancer-specific mortality with continuing use of DSF even among patients with metastatic disease. Although it is not possible to draw conclusions about causality, these findings supported the hypothesis that DSF may exert anti-cancer effects among patients suffering from common cancers, prompting us to perform pre-clinical analyses.

### Anti-tumour activity of the DTC–copper complex

Because DSF anti-cancer activity has been suggested to be copper-dependent<sup>6,13</sup>, we compared groups of mice injected with human MDA-MB-231 cancer cells, fed with a (i) normal diet; (ii) normal diet plus copper gluconate (CuGlu); (iii) normal diet plus DSF; or (iv) normal diet plus DSF and CuGlu (DSF/CuGlu); and tumour volume was measured over time (Fig. 1a and Extended Data Fig. 1b, c). Compared to matched controls, tumour volume in DSF- and DSF/CuGlu-treated groups at 32 days (at DSF doses equivalent to those used by alcoholics) were suppressed by 57% and 77%, respectively ( $P=0.0038$  in favour of the DSF/CuGlu treatment versus DSF alone). These results validate previous *in vitro*<sup>6,11,13</sup> and *in vivo*<sup>6–9,13,16</sup> studies, which indicated that DSF is an efficient anti-cancer agent and that copper potentiates its activity. As the reactive metabolite DTC forms complexes with metals, particularly copper<sup>17</sup>, we argued that a DTC–copper complex (bis (diethylthiocarbamate)–copper (CuET)) forms *in vivo* (Extended Data Fig. 1d), providing the anti-cancer metabolite. To test this hypothesis, we developed a high-resolution

approach based on high-performance liquid chromatography–mass spectrometry to measure CuET in tissues, and readily detected CuET after a single oral dose of DSF (Extended Data Fig. 1e, f). Extracts from plasma, liver, brain and MDA-MB-231-xenografted tumours contained CuET in samples from mice treated for five days with DSF or DSF/CuGlu. The CuET levels in plasma and liver were slightly higher after DSF/CuGlu treatment compared to DSF alone. Notably, the CuET levels in the tumour specimens were almost an order of magnitude higher compared to corresponding levels in liver and brain tissues from the same animals (Fig. 1b), suggesting preferential accumulation of CuET in tumours. Importantly, we also confirmed formation of CuET in humans undergoing DSF treatment for alcoholism (Fig. 1c).

Next, we synthesized CuET and performed comparative cell culture and animal studies. Short-term (24-h) assays and long-term (colony-forming assay, CFA) assays consistently showed higher cytotoxicity of CuET than of the primary DSF metabolite DTC in various cancer cell lines (Fig. 1d and Extended Data Fig. 1g). The half-maximal lethal dose ( $LD_{50}$ ) values of CuET in CFA experiments were  $\leq 100$  nM in three out of three tested breast cancer cell lines and similar potency was observed among cell lines derived from human lung, colon and prostate tumours (Extended Data Fig. 2a). These data were corroborated by tetrazolium dye ((2,3-bis-(2-methoxy-4-nitro-5-sulphophenyl)-2h-tetrazolium-5-carboxanilide) (XTT))-based 48-h cytotoxicity tests on a wider panel of cell types (Extended Data Fig. 2b). Unexpectedly, only the most sensitive cell lines (for example, AMO-1, Capan1) showed markers of apoptosis<sup>18</sup>, which included annexin V and activated caspases, whereas in most cell lines, for example, MDA-MB-231 and U2OS cells, CuET induced apoptosis-independent cell death (Extended Data Fig. 2c–f).

Direct therapeutic effects of CuET *in vivo* were then investigated using the MDA-MB-231 breast cancer (Fig. 1e) and AMO-1 myeloma (Fig. 1f) xenograft models treated intraperitoneally with a CuET–albumin formulation, with which the anti-tumour activity and good tolerability of this DSF metabolite was confirmed (Extended Data Fig. 1h, i).

### CuET inhibits p97-dependent protein degradation

Next, we investigated the interaction between CuET and cellular protein degradation, one of the suggested explanations for anti-tumour effects of DSF<sup>6,12</sup>. We confirmed that CuET induces phenotypic features shared with proteasome inhibitors, such as MG132 or bortezomib (BTZ), including accumulation of poly-ubiquitylated (poly-Ub) proteins (Fig. 2a and Extended Data Fig. 3a), rapid deubiquitylation of histone H2A (uH2A)<sup>19</sup> (Extended Data Fig. 3b) and accumulation of ubiquitylated proteins in the cytoplasm<sup>19</sup> (Extended Data Fig. 3c). Furthermore, TNF (also known as TNF $\alpha$ )-induced degradation of I $\kappa$ B $\alpha$  (ref. 20) was blocked after 1-h treatment with CuET or BTZ (Fig. 2b). Finally, CuET inhibited degradation of Ub(G76V)–GFP (an ubiquitin-fusion degradation substrate)<sup>21</sup> in a dose-dependent manner (Fig. 2c). However, although these data confirmed a defect in protein degradation, CuET had no effect on the CT-like, C-like or T-like activity of the 20S proteasome<sup>22</sup> (Extended Data Fig. 3d, e). This was further corroborated by the lack of a stabilizing effect of CuET on p53 tumour suppressor protein in dicoumarol-treated cells, in which

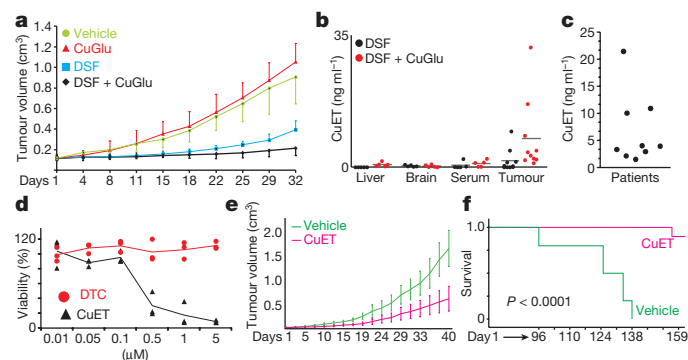


**Figure 1 | Tumour-suppressing effects of DSF and CuET.** **a**, Effects of orally administered DSF and CuGlu on subcutaneous growth of MDA-MB-231 tumours in mice.  $n=8$  mice per group. **b**, CuET levels in mouse tumours and tissues.  $n=5$  tissues,  $n=10$  tumours. **c**, CuET levels in human plasma after DSF treatment ( $n=9$  patients). **d**, Toxicity of DTC and CuET in MDA-MB-231 cells after 24 h treatment.  $n=3$  experiments. **e**, Effect of CuET on subcutaneous growth of MDA-MB-231 tumours in mice.  $n=20$  tumours. **f**, Survival of CuET- versus vehicle-treated mice with implanted AMO-1 xenografts.  $n=10$  animals per group.  $P$  value from a log-rank test. Data are mean  $\pm$  s.d. (**a**, **e**) or mean (**b**) linked means with individual values (**d**) or individual values (**c**).

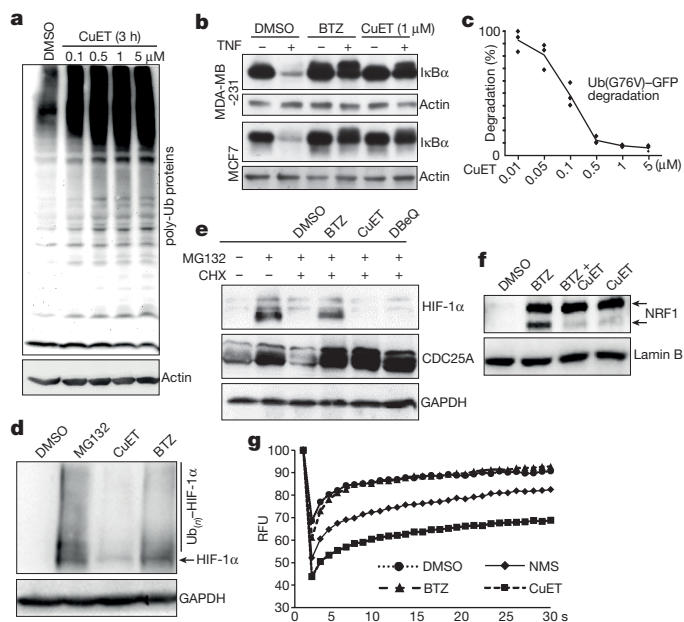


**Figure 2 | CuET inhibits p97 segregase-dependent protein degradation.** **a**, CuET causes accumulation of poly-ubiquitylated proteins in MCF7 cells. **b**, TNF-induced I $\kappa$ B $\alpha$  degradation is compromised after 1-h treatment with CuET or BTZ. **c**, Dose-dependent inhibition of Ub(G76V)-GFP degradation by CuET. HeLa cells were treated for 3 h.  $n = 3$  experiments. **d**, HIF-1 $\alpha$  levels after 2-h treatments with MG132 (5  $\mu$ M), CuET (1  $\mu$ M), BTZ (1  $\mu$ M) in HeLa cells. **e**, Differential effect of BTZ (1  $\mu$ M), CuET (1  $\mu$ M) and DBE9 (10  $\mu$ M) on CDC25A versus HIF-1 $\alpha$  in MG132-pretreated (4 h, 5  $\mu$ M), cycloheximide (CHX, 1 h, 50  $\mu$ g ml $^{-1}$ )-exposed HeLa cells. **f**, BTZ (8 h, 1  $\mu$ M) induces NRF1 120-kDa (top arrow) and 110-kDa (bottom arrow) forms; whereas CuET (8 h, 0.5  $\mu$ M) only induced the non-cleaved 120-kDa form in NIH3T3 cells. **g**, FRAP quantification in U2OS Ub-GFP cells: slower mobility of accumulated cytoplasmic GFP-Ub after a 2-h pre-treatment with NMS873 (10  $\mu$ M), CuET (1  $\mu$ M) or BTZ (1  $\mu$ M). **a**, **b**, **d**–**g**, Data are representative of two independent biological experiments. Data are linked means and individual values (**c**) and relative mean signal of the bleached region from 12 cells per treatment (**g**).

p53 turnover depends on the core 20S proteasome independently of ubiquitin<sup>23,24</sup>. In contrast to CuET, treatment with the 20S proteasome inhibitor BTZ stabilized p53 irrespective of dicoumarol (Extended Data Fig. 3f), indicating that 20S proteasome-dependent protein turnover remains operational with CuET treatment. Furthermore, CuET failed to inhibit 26S proteasome activity (Extended Data Fig. 3g), which was inferred from RPN11-dependent deubiquitylation<sup>25</sup>. Collectively, these results suggest that CuET stabilizes ubiquitylated proteins by blocking a step upstream of the proteasome.

Next we considered p97-dependent processing of poly-Ub proteins, as this pathway operates upstream of the proteasome and its malfunction resembles phenotypes of proteasome inhibition<sup>26</sup>. Unlike BTZ or MG132, CuET induced only modest accumulation (a small subfraction) of HIF-1 $\alpha$  (Fig. 2d), consistent with reported modest accumulation of HIF-1 $\alpha$  after knockdown of p97 compared to cells with inhibited proteasomes<sup>27</sup>. Next, we pre-treated cells with MG132, followed by wash-off and 1-h cycloheximide (an inhibitor of translation) treatment combined with BTZ, CuET or DBE9 (a direct inhibitor of p97 ATPase activity)<sup>28</sup>. All tested inhibitors prevented degradation of CDC25A (a known p97 target)<sup>29</sup>, whereas degradation of the mostly p97-independent target, that is, most of HIF-1 $\alpha$ <sup>27</sup>, was inhibited only by BTZ (Fig. 2e). Furthermore, consistent with cleavage of the 120-kDa species of the endoplasmic reticulum-tethered transcription factor NRF1 into an active 110-kDa form being a p97-dependent process<sup>30</sup>, appearance of the cleaved NRF1 form was inhibited by both CuET and NMS873 (another p97 ATPase inhibitor) (Fig. 2f and Extended Data Fig. 4a, b).

These results suggest that the p97 pathway is compromised in cells treated with CuET.

Next, we asked whether CuET impairs the p97 segregase activity that extracts poly-Ub proteins from cellular structures, such as the endoplasmic reticulum, Golgi apparatus or chromatin for subsequent proteasomal degradation<sup>31</sup>. Using fluorescence recovery after photobleaching (FRAP) to investigate the mobility of accumulated poly-Ub proteins, we found that whereas GFP-ubiquitin in DMSO- or BTZ-treated cells diffused rapidly into bleached areas, this diffusion was slower after treatment with CuET or NMS873 (Fig. 2g and Extended Data Fig. 4c). This suggests that after treatment with CuET or NMS873 at least a subset of the accumulated poly-Ub proteins remains immobile, probably embedded into cellular structures. Consistently, upon detergent pre-extraction of mobile proteins, we observed greater immunofluorescence signals of extraction-resistant poly-Ub(K48) proteins (destined for proteasomal degradation) in NMS873- and CuET-treated cells compared to BTZ- or DMSO-treated controls (Extended Data Fig. 4d). Western blot analysis of endoplasmic reticulum-rich microsomal fractions also revealed enrichment of poly-Ub proteins after CuET and NMS873 treatment (Extended Data Fig. 4e). Malfunction of p97 segregase is furthermore associated with a cellular unfolded protein response (UPR)<sup>32</sup>. We confirmed UPR in cells treated with CuET or NMS873 by detecting increased markers of UPR induction, including the spliced form of XBP1s, ATF4 and phosphorylated (p-) eIF2 $\alpha$ <sup>33</sup> (Extended Data Fig. 4f).

These studies are also of clinical relevance, because inhibition of p97 was suggested as an alternative treatment strategy for myeloma patients who had relapsed after therapy with BTZ (also known by the trade name Velcade)<sup>34</sup> or carfilzomib (CFZ)<sup>35</sup>. Thus, we performed cytotoxicity tests with CuET on a panel of BTZ- or CFZ-adapted and non-adapted human cell lines or on cells derived from samples of patients with myeloma before therapy and with BTZ therapy. All pairs of adapted and non-adapted cells showed similar sensitivity to CuET treatment, in contrast to BTZ (Extended Data Fig. 5a–d). These results suggest that treatment with DSF (best combined with copper) or CuET might become a feasible therapeutical option for patients with relapsed, BTZ-resistant multiple myeloma.

### CuET binds and immobilizes NPL4

To elucidate how CuET inhibits the p97 pathway, we first used an assay of p97 ATPase activity<sup>28</sup>. In contrast to treatment with NMS873, CuET had no effect on p97 ATPase activity (Extended Data Fig. 6a). Because NPL4 and UFD1 proteins are key components of the p97 segregase<sup>31</sup>, we examined whether CuET might target the pathway through these cofactors. Ectopic overexpression of NPL4-GFP, but not UFD1-GFP or p97-GFP, reduced CuET cytotoxicity, suggesting that NPL4 is a candidate target of CuET (Fig. 3a and Extended Data Fig. 6b). An analogous ‘rescue effect’ of ectopic NPL4-GFP was apparent from the reduction in accumulation of poly-Ub proteins caused by CuET (Extended Data Fig. 6c).

As shown by live-cell imaging, 2–3-h exposure to CuET induced prominent nuclear clustering of NPL4-GFP, but not of UFD1-GFP or p97-GFP (Fig. 3b). Within 2–3 h, most of cellular NPL4-GFP became immobilized in nuclear clusters and also in cytoplasmic areas, as shown by FRAP (Fig. 3c). CuET-induced immobilization of endogenous NPL4 was confirmed by accumulation, which was detectable by western blot, in the detergent-insoluble fractions from various cell lines (Fig. 3d) and by immunofluorescence on pre-extracted cells (Extended Data Fig. 6d). Notably, the immobilization of NPL4 was also detectable in pre-extracted sections of cryopreserved tumours from mice treated with DSF or DSF and CuGlu, thus providing a potential biomarker of CuET activity towards the p97 pathway *in vivo* (Fig. 3e).

NPL4 is an attractive candidate for CuET binding, because this protein contains two zinc finger domains: a C-terminal NZF (NPL4-zinc finger) and a putative zinc finger-NPL4<sup>36</sup>, which bind bivalent metals and metal complexes that might chemically resemble CuET<sup>37</sup>.



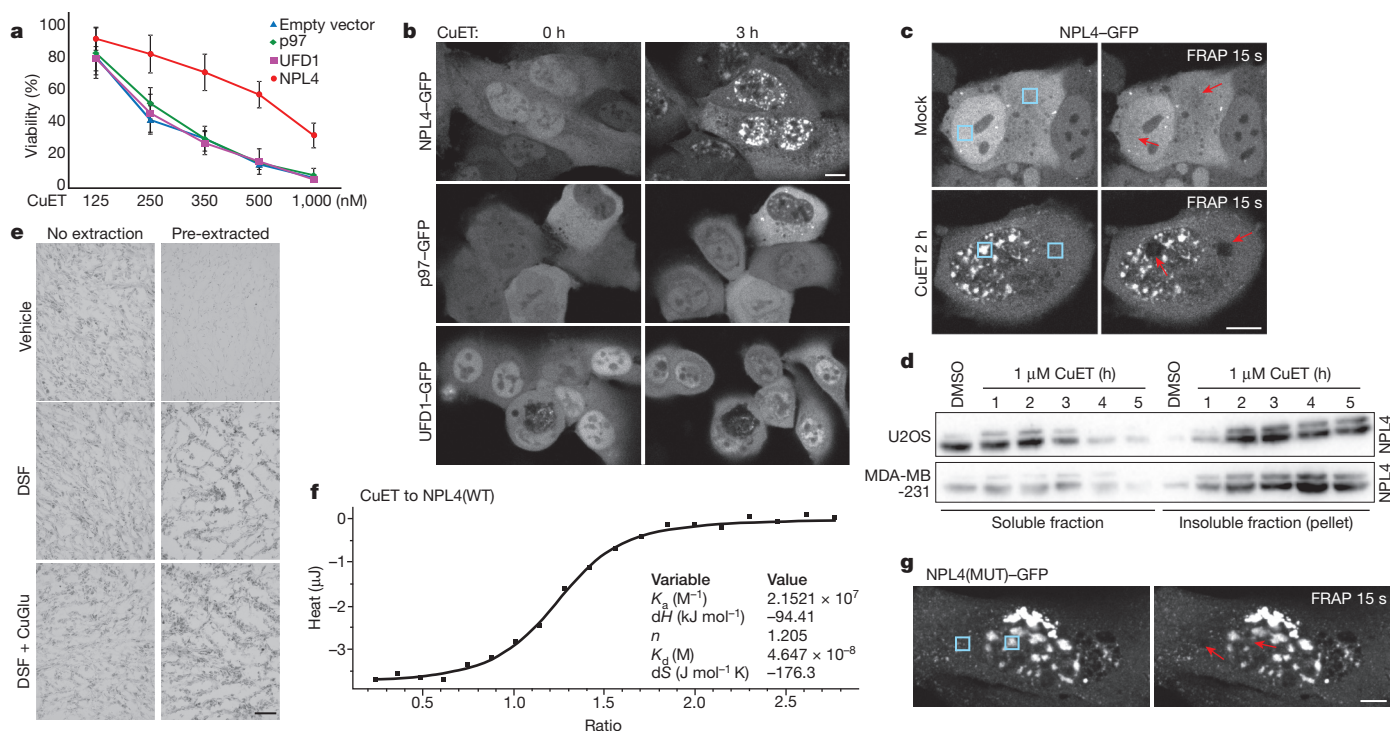


**Figure 3 | CuET binds to and immobilizes NPL4.** **a**, Ectopic NPL4–GFP, but not p97–GFP or UFD1–GFP rescues CuET toxicity in U2OS cells treated for 24 h.  $n = 3$  experiments. Data are mean  $\pm$  s.d. **b**, CuET (1  $\mu$ M) induces intranuclear clustering of NPL4–GFP, but not p97–GFP or UFD1–GFP. **c**, CuET-induced (1  $\mu$ M) immobilization of NPL4–GFP (FRAP) in U2OS cells treated for 2 h. Blue boxes, areas before bleaching; arrows, after bleaching. **d**, NPL4 enrichment in Triton X-100-insoluble fractions

after CuET (1  $\mu$ M) treatment. **e**, Immunohistochemistry demonstrates the non-extractable NPL4 in MDA-MB-231 tumours from mice treated with DSF or DSF and CuGlu. **f**, ICT shows that CuET binds to purified NPL4(WT). **g**, Spontaneous intranuclear clustering and immobilization of NPL4(MUT)–GFP using FRAP in U2OS cells. Blue boxes, areas before bleaching; arrows, after bleaching. Scale bars, 10  $\mu$ m (**b**, **c**, **g**) or 50  $\mu$ m (**e**). **b–g**. Data are representative of two independent experiments.

Using isothermal calorimetry analysis (ITC)<sup>38</sup>, we observed a standard dose–response-dependent binding curve (Fig. 3f) compatible with one binding site for CuET on wild-type NPL4 (NPL4(WT)), and a  $K_d$  in nanomolar concentrations for the NPL4–CuET interaction. Next, we used mutagenesis to test whether the putative ZF–NPL4 domain has any role in the potential NPL4–CuET interaction. The putative zinc finger domain was preferred, because an endogenous larger form of NPL4 that lacks the C-terminal NZF sequence exists in human cells. This larger NPL4 form is detectable as an upper band on western blots (Fig. 3d) and it is immobilized after CuET treatment, suggesting that the C-terminal NZF is not necessary for the interaction with CuET. No ITC interaction was found with a NPL4 mutant (NPL4(MUT)) (Extended Data Fig. 6f) in which both histidines and both cysteines in the putative zinc finger domain were substituted by alanines (Extended Data Fig. 6e). We used drug affinity responsive target stability (DARTS) as another, independent approach, which is based on altered protease susceptibility of target proteins upon drug binding<sup>39</sup>. Consistently, exposure to CuET caused a differential pronase-dependent proteolysis pattern of NPL4(WT) but not NPL4(MUT) (Extended Data Fig. 6g). These results indicate that NPL4 is directly targeted by CuET and an intact putative zinc finger domain of NPL4 is essential for this interaction.

Notably, ectopically expressed NPL4(MUT)–GFP formed immobile nuclear clusters spontaneously in untreated cells, reminiscent of events seen in cells upon CuET treatment (Fig. 3c, g). Moreover, unlike ectopic NPL4(WT)–GFP, ectopically expressed NPL4(MUT)–GFP not only did not render cells resistant to CuET but also was toxic to the acceptor cells (Extended Data Fig. 6h). We also confirmed that multiple CuET-induced cellular phenotypes were mimicked by the ectopic NPL4(MUT)–GFP model, including accumulation of poly-Ub proteins and UPR activation (Extended Data Fig. 6i).

### NPL4 aggregates trigger a heat-shock response

Although the nuclear NPL4 clusters occupied DAPI-unlabelled areas of chromatin (Extended Data Fig. 6d) co-localization with DAPI-excluded structures, such as nucleoli and nuclear speckles, were not found (Extended Data Fig. 7a). In late-G2 cells, NPL4 clusters were evidently excluded from the partially condensed chromatin (Extended Data Fig. 7b), suggesting that the NPL4 aggregates exclude chromatin rather than accumulating in specific nuclear areas. Both the nuclear clusters and the immobilized cytoplasmic NPL4 co-localized with poly-Ub proteins (confirmed by anti-Ub(K48) and FK2 antibodies), small ubiquitin-like modifiers (SUMOs) (only in nuclei) and with TDP43 protein<sup>40</sup> (Fig. 4a and Extended Data Fig. 7d), which are all features typical of aggregated defective proteins<sup>41</sup>. The same co-localization patterns were observed for spontaneous clusters formed by NPL4(MUT)–GFP showing that NPL4 aggregation is sufficient for the induction of these phenotypes even without CuET treatment (Extended Data Fig. 7c, e). Blockade of cellular ubiquitylation with a chemical inhibitor (MLN7243) of the E1 ubiquitin-activating enzyme failed to prevent either NPL4–GFP nuclear aggregation or cytoplasmic immobilization (Extended Data Fig. 7d), excluding the immobilization of NPL4 via recognition of ubiquitylated and SUMOylated substrates, but rather suggesting that immobilized NPL4 attracts ubiquitylated proteins or proteins that subsequently become ubiquitylated and/or SUMOylated. A key protein commonly associated with intracellular protein aggregates is HSP70, a chaperone implicated in aggregate processing<sup>42</sup>. Indeed, pre-extracted cells showed co-localization of HSP70 with both CuET-induced NPL4(WT)–GFP and spontaneous NPL4(MUT)–GFP aggregates (Fig. 4b, c). Both the CuET-induced NPL4(WT) aggregates and spontaneous NPL4(MUT) aggregates also co-localized with p97 (Extended Data Fig. 7f, g), as is particularly evident after pre-extraction. In the NPL4–GFP model, the amount of p97 immunoreactivity within

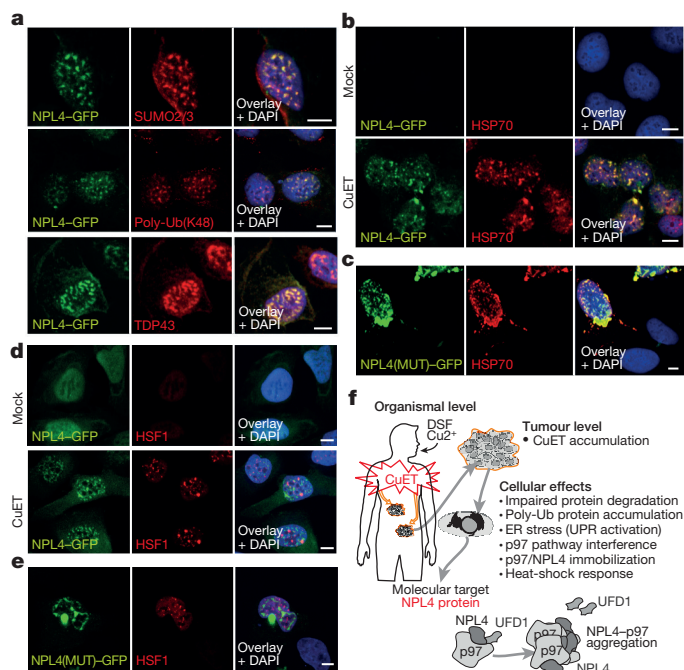


**Figure 4 | NPL4 protein aggregation triggers HSR.** **a**, NPL4–GFP co-localizes with SUMO2/3, poly-Ub(K48) and TDP43 in U2OS cells. Cells were treated with 1  $\mu$ M CuET for 3 h and pre-extracted. **b**, NPL4–GFP co-localizes with HSP70 in mock- and CuET-treated U2OS cells. Cells were treated with 1  $\mu$ M CuET for 3 h and pre-extracted. **c**, NPL4(MUT)–GFP co-localizes with HSP70 in U2OS cells after pre-extraction. **d**, CuET-induced HSF1 stress bodies. NPL4–GFP U2OS cells were treated with 1  $\mu$ M CuET for 3 h. **e**, HSF1 stress bodies in U2OS cells expressing NPL4(MUT)–GFP. **f**, Model of DSF anti-cancer activity in patients. Scale bars, 10  $\mu$ m. **a–e**, Data are representative of two independent experiments.

the NPL4–GFP clusters correlated with the GFP signal intensity, suggesting that p97 is immobilized via its interaction with NPL4. The other NPL4-binding partner, UFD1, was almost undetectable in detergent-insoluble pellets of CuET-treated or NPL4(MUT)–GFP-expressing cells despite clear p97 immobilization (Extended Data Fig. 8a, b), suggesting that UFD1 cannot bind to, or becomes only loosely attached to, the aggregated NPL4–p97 complex. Notably, non-extractable cellular p97 is detectable after CuET treatment (Extended Data Fig. 8c), including in stained tumour sections from mice treated with DSF or DSF and CuGlu, providing an additional candidate marker for CuET activity *in vivo* (Extended Data Fig. 8d).

Because aggregation of misfolded or damaged proteins triggers cellular heat-shock response (HSR) through an HSF1-dependent mechanism<sup>43</sup>, we confirmed that CuET treatment indeed triggered a robust HSR accompanied by characteristic HSF1 nuclear stress foci (Fig. 4d) that were also detectable in cells spontaneously aggregating NPL4(MUT)–GFP (Fig. 4e). HSR markers, including accumulation of heat-shock proteins and a phosphorylation shift in HSF1, were detectable by western blot (Extended Data Fig. 8e, f).

## Discussion

Our results help to explain the anti-cancer activity of the alcohol-abuse drug disulfiram. We propose a model for DSF cytotoxic activity, featuring rapid conversion of DSF into CuET, which accumulates in tumours. After entering cells, CuET binds NPL4 and induces its aggregation, consequently disabling the vital p97–NPL4–UFD1 pathway and inducing a complex cellular phenotype leading to cell death (Fig. 4f). Supporting CuET as the active metabolite is the correlation of CuET concentrations (active in the nanomolar range) with the biological effects and functional impact on the targeted pathway(s) *in vivo*. In addition, CuET is the only known metabolite of DSF containing copper ions, a metal

that enhances the anti-tumour effects of DSF; it is unlikely that another DSF metabolite could represent the major anti-cancer agent as levels of non-CuET metabolites should be lowered by copper addition. We also present a method for CuET detection in tissues and plasma, as well as data suggesting that preferential accumulation of CuET in tumours may contribute to cancer cell toxicity, consistent with the high therapeutic tolerability of DSF<sup>3</sup>, as documented even after years of daily administration at doses comparable to those we used in our mouse experiments. Considering the numerous studies on DSF and diverse opinions about the potential target of its anti-cancer effects<sup>44</sup>, identification of NPL4, a key component of the p97–NPL4–UFD1 segregase complex, as the molecular target of CuET is surprising. The CuET–NPL4 interaction leads to rapid formation of protein aggregates and immobilization of this otherwise very mobile multifunctional protein complex, resulting in a severe phenotype, induction of HSR and eventually cell death. While additional potential targets of CuET cannot be excluded, the malfunction of the p97 pathway due to the NPL4–p97 aggregate formation explains the major cell phenotypes and the consequent cell death. Our work also reconciles the controversial studies<sup>6,12</sup>, suggesting that the proteasome is the DSF target, by demonstrating that neither 20S nor 26S proteasome, but the processing of ubiquitylated proteins by the NPL4-dependent segregase, is targeted by CuET. Our results support the notion that the p97–NPL4 pathway is a promising therapeutic target in oncology<sup>45,46</sup>. Indeed, reports on p97 overabundance correlating with progression and metastasis of carcinomas of the breast, colon and prostate<sup>47–49</sup> are consistent with our present nationwide epidemiological analysis, which revealed an association between continued use of DSF and favourable prognosis, an intriguing finding that should be investigated further, particularly given the currently limited therapeutic options for patients with metastatic cancer. From a broader perspective, our study illustrates the potential of multifaceted approaches to drug repurposing, providing novel mechanistic insights, identification of new cancer-relevant targets and encouragement for further clinical trials, here with DSF, an old, safe and public domain drug<sup>4</sup> that might help to save lives of patients with cancer worldwide.

**Online Content** Methods, along with any additional Extended Data display items and Source Data, are available in the online version of the paper; references unique to these sections appear only in the online paper.

Received 1 October 2015; accepted 8 November 2017.

Published online 6 December 2017.

- Collins, F. S. Mining for therapeutic gold. *Nat. Rev. Drug Discov.* **10**, 397 (2011).
- Pantziarka, P. *et al.* The repurposing drugs in oncology (ReDO) project. *Ecantermediscience* **8**, 442 (2014).
- Ilijin, K. *et al.* High-throughput cell-based screening of 4910 known drugs and drug-like small molecules identifies disulfiram as an inhibitor of prostate cancer cell growth. *Clin. Cancer Res.* **15**, 6070–6078 (2009).
- Cvek, B. Nonprofit drugs as the salvation of the world's healthcare systems: the case of Antabuse (disulfiram). *Drug Discov. Today* **17**, 409–412 (2012).
- Shen, M. L., Johnson, K. L., Mays, D. C., Lipsky, J. J. & Naylor, S. Determination of *in vivo* adducts of disulfiram with mitochondrial aldehyde dehydrogenase. *Biochem. Pharmacol.* **61**, 537–545 (2001).
- Chen, D., Cui, Q. C., Yang, H. & Dou, Q. P. Disulfiram, a clinically used anti-alcoholism drug and copper-binding agent, induces apoptotic cell death in breast cancer cultures and xenografts via inhibition of the proteasome activity. *Cancer Res.* **66**, 10425–10433 (2006).
- Zha, J. *et al.* Disulfiram targeting lymphoid malignant cell lines via ROS–JNK activation as well as Nrf2 and NF- $\kappa$ B pathway inhibition. *J. Transl. Med.* **12**, 163 (2014).
- Safi, R. *et al.* Copper signaling axis as a target for prostate cancer therapeutics. *Cancer Res.* **74**, 5819–5831 (2014).
- Liu, P. *et al.* Liposome encapsulated disulfiram inhibits NF- $\kappa$ B pathway and targets breast cancer stem cells *in vitro* and *in vivo*. *Oncotarget* **5**, 7471–7485 (2014).
- Dufour, P. *et al.* Sodium dithiocarbamate as adjuvant immunotherapy for high risk breast cancer: a randomized study. *Biotherapy* **6**, 9–12 (1993).
- Yip, N. C. *et al.* Disulfiram modulated ROS–MAPK and NF- $\kappa$ B pathways and targeted breast cancer cells with cancer stem cell-like properties. *Br. J. Cancer* **104**, 1564–1574 (2011).

12. Lövborg, H. *et al.* Inhibition of proteasome activity, nuclear factor- $\kappa$ B translocation and cell survival by the antialcoholism drug disulfiram. *Int. J. Cancer* **118**, 1577–1580 (2006).
13. Allensworth, J. L. *et al.* Disulfiram (DSF) acts as a copper ionophore to induce copper-dependent oxidative stress and mediate anti-tumor efficacy in inflammatory breast cancer. *Mol. Oncol.* **9**, 1155–1168 (2015).
14. Nechushtan, H. *et al.* A phase IIb trial assessing the addition of disulfiram to chemotherapy for the treatment of metastatic non-small cell lung cancer. *Oncologist* **20**, 366–367 (2015).
15. Jin, M. *et al.* Alcohol drinking and all cancer mortality: a meta-analysis. *Ann. Oncol.* **24**, 807–816 (2013).
16. Li, Y. *et al.* Copper improves the anti-angiogenic activity of disulfiram through the EGFR/Src/VEGF pathway in gliomas. *Cancer Lett.* **369**, 86–96 (2015).
17. Suzuki, Y. *et al.* The origin of an EPR signal observed in dithiocarbamate-loaded tissues. Copper(II)-dithiocarbamate complexes account for the narrow hyperfine lines. *Biochim. Biophys. Acta* **1335**, 242–245 (1997).
18. Kepp, O., Galluzzi, L., Lipinski, M., Yuan, J. & Kroemer, G. Cell death assays for drug discovery. *Nat. Rev. Drug Discov.* **10**, 221–237 (2011).
19. Doil, C. *et al.* RNF168 binds and amplifies ubiquitin conjugates on damaged chromosomes to allow accumulation of repair proteins. *Cell* **136**, 435–446 (2009).
20. Li, J. M., Wu, H., Zhang, W., Blackburn, M. R. & Jin, J. The p97-UFD1L-NPL4 protein complex mediates cytokine-induced I $\kappa$ B $\alpha$  proteolysis. *Mol. Cell. Biol.* **34**, 335–347 (2014).
21. Chou, T. F. & Deshaies, R. J. Quantitative cell-based protein degradation assays to identify and classify drugs that target the ubiquitin–proteasome system. *J. Biol. Chem.* **286**, 16546–16554 (2011).
22. Kisselev, A. F. & Goldberg, A. L. Monitoring activity and inhibition of 26S proteasomes with fluorogenic peptide substrates. *Methods Enzymol.* **398**, 364–378 (2005).
23. Asher, G., Lotem, J., Cohen, B., Sachs, L. & Shaul, Y. Regulation of p53 stability and p53-dependent apoptosis by NADH quinone oxidoreductase 1. *Proc. Natl Acad. Sci. USA* **98**, 1188–1193 (2001).
24. Asher, G., Tsvetkov, P., Kahana, C. & Shaul, Y. A mechanism of ubiquitin-independent proteasomal degradation of the tumor suppressors p53 and p73. *Genes Dev.* **19**, 316–321 (2005).
25. Verma, R. *et al.* Role of Rpn11 metalloprotease in deubiquitination and degradation by the 26S proteasome. *Science* **298**, 611–615 (2002).
26. Dai, R. M. & Li, C. C. Valosin-containing protein is a multi-ubiquitin chain-targeting factor required in ubiquitin–proteasome degradation. *Nat. Cell Biol.* **3**, 740–744 (2001).
27. Alexandru, G. *et al.* UBXD7 binds multiple ubiquitin ligases and implicates p97 in HIF1 $\alpha$  turnover. *Cell* **134**, 804–816 (2008).
28. Chou, T. F. *et al.* Reversible inhibitor of p97, DBeQ, impairs both ubiquitin-dependent and autophagic protein clearance pathways. *Proc. Natl Acad. Sci. USA* **108**, 4834–4839 (2011).
29. Riemer, A. *et al.* The p97-Ufd1-Npl4 ATPase complex ensures robustness of the G2/M checkpoint by facilitating CDC25A degradation. *Cell Cycle* **13**, 919–927 (2014).
30. Radhakrishnan, S. K., den Besten, W. & Deshaies, R. J. p97-dependent retrotranslocation and proteolytic processing govern formation of active Nrf1 upon proteasome inhibition. *eLife* **3**, e01856 (2014).
31. Meyer, H., Bug, M. & Bremer, S. Emerging functions of the VCP/p97 AAA-ATPase in the ubiquitin system. *Nat. Cell Biol.* **14**, 117–123 (2012).
32. Magnaghi, P. *et al.* Covalent and allosteric inhibitors of the ATPase VCP/p97 induce cancer cell death. *Nat. Chem. Biol.* **9**, 548–556 (2013).
33. Samali, A., Fitzgerald, U., Deegan, S. & Gupta, S. Methods for monitoring endoplasmic reticulum stress and the unfolded protein response. *Int. J. Cell Biol.* **2010**, 830307 (2010).
34. Auner, H. W. *et al.* Combined inhibition of p97 and the proteasome causes lethal disruption of the secretory apparatus in multiple myeloma cells. *PLoS ONE* **8**, e74415 (2013).
35. Soriano, G. P. *et al.* Proteasome inhibitor-adapted myeloma cells are largely independent from proteasome activity and show complex proteomic changes, in particular in redox and energy metabolism. *Leukemia* **30**, 2198–2207 (2016).
36. Lass, A., McConnell, E., Fleck, K., Palamarchuk, A. & Wójcik, C. Analysis of Npl4 deletion mutants in mammalian cells unravels new Ufd1-interacting motifs and suggests a regulatory role of Npl4 in ERAD. *Exp. Cell Res.* **314**, 2715–2723 (2008).
37. Voráčková, I., Suchanová, S., Ulbrich, P., Diehl, W. E. & Ruml, T. Purification of proteins containing zinc finger domains using immobilized metal ion affinity chromatography. *Protein Expr. Purif.* **79**, 88–95 (2011).
38. Holdgate, G. *et al.* Biophysical methods in drug discovery from small molecule to pharmaceutical. *Methods Mol. Biol.* **1008**, 327–355 (2013).
39. Lomenick, B. *et al.* Target identification using drug affinity responsive target stability (DARTS). *Proc. Natl Acad. Sci. USA* **106**, 21984–21989 (2009).
40. Becker, L. A. *et al.* Therapeutic reduction of ataxin-2 extends lifespan and reduces pathology in TDP-43 mice. *Nature* **544**, 367–371 (2017).
41. Guo, L. *et al.* A cellular system that degrades misfolded proteins and protects against neurodegeneration. *Mol. Cell* **55**, 15–30 (2014).
42. Kim, Y. E., Hipp, M. S., Bracher, A., Hayer-Hartl, M. & Hartl, F. U. Molecular chaperone functions in protein folding and proteostasis. *Annu. Rev. Biochem.* **82**, 323–355 (2013).
43. Dai, C. & Sampson, S. B. HSF1: guardian of proteostasis in cancer. *Trends Cell Biol.* **26**, 17–28 (2016).
44. Cvek, B. Targeting malignancies with disulfiram (Antabuse): multidrug resistance, angiogenesis, and proteasome. *Curr. Cancer Drug Targets* **11**, 332–337 (2011).
45. Deshaies, R. J. Proteotoxic crisis, the ubiquitin–proteasome system, and cancer therapy. *BMC Biol.* **12**, 94 (2014).
46. Anderson, D. J. *et al.* Targeting the AAA ATPase p97 as an approach to treat cancer through disruption of protein homeostasis. *Cancer Cell* **28**, 653–665 (2015).
47. Cui, Y. *et al.* High expression of valosin-containing protein predicts poor prognosis in patients with breast carcinoma. *Tumour Biol.* **36**, 9919–9927 (2015).
48. Yamamoto, S. *et al.* Expression of valosin-containing protein in colorectal carcinomas as a predictor for disease recurrence and prognosis. *Clin. Cancer Res.* **10**, 651–657 (2004).
49. Tsujimoto, Y. *et al.* Elevated expression of valosin-containing protein (p97) is associated with poor prognosis of prostate cancer. *Clin. Cancer Res.* **10**, 3007–3012 (2004).

Supplementary Information is available in the online version of the paper.

**Acknowledgements** We thank J. Škvor, M. Zadinová, J. Večerka and D. Doležal for help with animal experiments, Jana Vrbkova for statistical analysis, D. Fridecky and T. Adam for help with HPLC, I. Protivankova and M. Grønng Nielsen for technical assistance. This work was supported by grants from the Kellner Family Foundation, Czech National Program of Sustainability, Grant Agency of the Czech Republic, MEYS CR project Czech-Biomed, the Czech Health Research Council, of the Danish Cancer Society, the Danish National Research Foundation (project CARD), the Danish Council for Independent Research, the Novo Nordisk Foundation, the Czech Cancer League, the Swedish Research Council, Cancerfonden of Sweden, the European Commission (EATRIS), the Czech Ministry of Education, youth and sports (OPVKCZ), Cancer Research Czech Republic and the Howard Hughes Medical Institute.

**Author Contributions** Z.S., M.Mis., B.C., R.J.D. and J.Barte. conceived the study. Z.S. and M.Mis. performed most biochemical and microscopy experiments and wrote the manuscript. D.M. established the expression cell lines and performed most cytotoxicity tests. T.O., P.D. and I.V. performed the HPLC experiments. K.K.A., S.F. and J.O. performed the epidemiological analyses. J.Bartk. performed the immunohistochemical analyses. J.V. and P.D. performed DARTS experiments. P.M. performed cell death analyses. Z.T. performed cytotoxicity tests and heat-shock response analyses. A.K. performed cytotoxicity tests. A.M. designed and performed phlebotomies of patients treated with Antabuse. M.Mic. performed the ITC. J.G. performed FACS analyses, cell death assays and cell sorting. J.S. performed 20S proteasome assays. J.L. performed 26S proteasome assays. M.K. and C.D. performed the cytotoxicity experiments on myeloid- and patient-derived cell lines. P.P., J.M. and M.H. performed mouse experiments. J.Barte., B.C., Q.P.D. and R.J.D. helped to design the experiments, interpreted the data and wrote/edited the manuscript. All authors approved the manuscript.

**Author Information** Reprints and permissions information is available at [www.nature.com/reprints](http://www.nature.com/reprints). The authors declare competing financial interests: details are available in the online version of the paper. Readers are welcome to comment on the online version of the paper. Publisher's note: Springer Nature remains neutral with regard to jurisdictional claims in published maps and institutional affiliations. Correspondence and requests for materials should be addressed to J.Barte. (jb@cancer.dk), B.C. (cvekb@seznam.cz) and R.J.D. (deshaies@caltech.edu).

**Reviewer Information** Nature thanks P. Brossart and the other anonymous reviewer(s) for their contribution to the peer review of this work.

## METHODS

The experiments were not randomized.

**Epidemiological analyses and access to health registers.** We conducted a population-based cohort study by combining Danish nationwide demographic and health registers. This study was approved by the Danish Data Protection Agency and Statistics Denmark's Scientific Board. As the epidemiological study was based solely on register data and did not involve any contact with patients, no ethical approval was required from the Danish Scientific Ethical Committee<sup>50</sup>. The cohort consisted of all Danes aged 35–85 years with a first-time diagnosis of cancer between January 2000 and December 2013. Because DSF (Antabuse) is a relative contra-indication among individuals with liver or kidney diseases, we excluded patients with cancers of the liver or kidney from the cohort. Cohort members were categorized according to use of DSF into two main groups: (i) those who filled at least one prescription of DSF within five years before the cancer diagnosis, but did not fill DSF prescription(s) during the first year after the diagnosis (previous users), that is, individuals suffering from alcoholism but taking DSF only before their cancer diagnosis; and (ii) those who used DSF before their cancer diagnosis and also filled one or more DSF prescriptions during the first year after the cancer diagnosis (continuing users), that is, individuals who underwent DSF therapy both before and after the cancer diagnosis. We also defined a category of patients with cancer who did not fill prescription(s) for DSF either before or after ( $\leq 1$  year) the cancer diagnosis (never users). In the main analyses, we calculated hazard ratios and 95% confidence intervals estimating cancer-specific mortality among continuing DSF users compared to previous DSF users based on a Cox model regressing on both propensity scores and disulfiram use. By including propensity scores in the regression, we used demographic data and comorbid conditions/diagnostic codes as well as prescription data for selected concomitant drugs, to balance baseline characteristics of previous and continuing users of DSF and to adjust estimated hazard ratios of cancer-specific mortality associated with DSF use<sup>51</sup>. The patients with cancer were followed from one year after the diagnosis until death, migration or end of study (31 December 2014). The propensity scores thus estimate the probability of being treated with DSF in the exposure window 0–1 year after the cancer diagnoses conditional on the following other covariates in the calculation of propensity scores using logistic regression: gender, age at diagnosis, calendar time, highest achieved education and disposable income; medical histories of diabetes mellitus, chronic obstructive pulmonary disease, ischaemic heart disease, congestive heart failure, cerebrovascular disease, atrial fibrillation or atrial flutter, dementia and ulcer disease; and use of non-steroidal anti-inflammatory drugs (NSAIDs; including aspirin), non-aspirin antithrombotic agents (anticoagulants), statins, antihypertensive medication, other cardiovascular drugs, anti-diabetics and psychotropic drugs. In the Cox model, the propensity score is further included as a restricted cubic spline to model possible nonlinearities, in addition to the categorical disulfiram use, which is the variable of interest. Analyses were run for cancer overall and for breast, prostate and colon cancer, separately. Furthermore, all analyses were stratified by stage (localized, non-localized or unknown). Statistical significance of DSF use was evaluated by likelihood ratio tests. We used the software R for statistical computing<sup>52</sup>.

**In vivo tumour experiments.** The human breast cancer cell line MDA-MB-231 was injected ( $10^7$  cells transplanted subcutaneously) to grow tumours in athymic NU/NU female mice (AnLab Ltd) with a body weight of 23.6–26.9 g, aged 12 weeks. Inclusion criteria were: female, appropriate age and weight (15–30 g). Exclusion criteria were: tumour size must not exceed 20 mm (volume  $4,000 \text{ mm}^3$ ) in any direction in an adult mouse, the tumour mass should not proceed to the point where it significantly interferes with normal bodily functions, or causes pain or distress owing to its location, persistent self-induced trauma, rapid or progressive weight loss of more than 25%, for seven days. In none of the experiments were these approved ethical limits exceeded. After the tumours grew to  $0.114\text{--}0.117 \text{ cm}^3$  on average, mice were randomly divided into four groups, each of eight mice, and treated as follows: (i) normal diet; (ii) normal diet plus oral administration of  $0.15 \text{ mg kg}^{-1}$  copper gluconate (CuGlu); (iii) normal diet plus oral administration of  $50 \text{ mg kg}^{-1}$  DSF; (iv) normal diet plus oral administration of  $0.15 \text{ mg kg}^{-1}$  CuGlu and  $50 \text{ mg kg}^{-1}$  DSF. Administration of compounds was carried out as a blinded experiment (all information about the expected outputs and the nature of used compounds were kept from the animal technicians). CuGlu was administered each day in the morning (08:00) and DSF each day in the evening (19:00) to mimic a clinical trial combining DSF and CuGlu in treatment of tumours involving the liver (NCT00742911). After treatment began, mice were weighed and their tumours measured twice per week. At day 32, mice were euthanized, and the tumours were removed and frozen at  $-80^\circ\text{C}$ . The experiment was evaluated by comparing growth curves of tumours in the experimental groups with those in controls. The rates of tumour growth inhibition (TGI) were calculated by the formula  $\text{TGI} = (1 - V_{\text{treated}}/V_{\text{control}})$  where  $V_{\text{treated}}$  is the mean of tumour volumes in the treated group and  $V_{\text{control}}$  is the mean of tumour volumes in the control group.

Mean tumour volume values at specific time intervals were statistically evaluated. To test directly the effect of CuET, we used MDA-MB-231 and AMO-1 models. MDA-MB-231 was injected ( $5 \times 10^6$  cells were transplanted subcutaneously) to grow tumours in SCID mice (ENVIGO) aged 10 weeks ( $\pm 2$  weeks). AMO-1 xenografts were expanded in SCID mice. Each group consisted of 10 animals, each bearing two tumours. CuET was formulated in bovine serum albumin solution (1%) to a final concentration of  $1 \text{ mg ml}^{-1}$ . CuET was applied intraperitoneally with a schedule of five days on and two days off. All aspects of the animal study met the accepted criteria for the care and experimental use of laboratory animals, and protocols were approved by the Animal Research Committee of the 1st Faculty of Medicine Charles University in Prague and Ethical Committee of Faculty of Medicine and Dentistry, Palacky University in Olomouc. For HPLC-MS and immunohistochemistry analysis, we used MDA-MB-231 xenografted mice treated with the same DSF and DSF plus copper gluconate regime as described for the anti-cancer activity assessment with the notable difference that mice were euthanized after five days of treatment.

**HPLC-MS analysis of CuET.** The HR-MRM analysis was performed on a HPLC-ESI-QTOF system consisting of HPLC chromatograph Thermo UltiMate 3000 with AB Sciex TripleTOF 5600+ mass spectrometer, using the DuoSpray ESI source operated at an ion source voltage of 5,500 V, ion source gas flow rates of 40 units, curtain gas flow rate of 30 units, declustering potential of 100 V and temperature  $400^\circ\text{C}$ . Data were acquired in product ion mode with two parent masses (358.9 and 360.9) for analysis of CuET. Chromatographic separation was done by PTFE column, which was especially designed for analysis of strong metal chelators filled by C18 sorbent (IntellMed, IM\_301). Analysis was performed at room temperature and with a flow rate of  $1,500 \mu\text{l min}^{-1}$  with isocratic chromatography. Mobile phase consisted of HPLC grade acetone (Lachner) 99.9%, HPLC water (Merck Millipore) 0.1% and 0.03% HPLC formic acid (Sigma-Aldrich). Acquired mass spectra were evaluated in software PeakView 1.2. Extracted ion chromatograms of transitions 88.0 and 116.0 (common for both parent masses) with a 0.1 mass tolerance were Gaussian smoothed with width of two points. Peak area was then recorded and recalculated to  $\text{ng ml}^{-1}$  according to the calibration curve.

**Sample preparation for HPLC-MS analysis.** Liquid nitrogen-frozen biological samples were cut into small pieces using a scalpel. Samples (30–100 mg) were immediately processed by homogenization in 100% acetone in a ratio of 1:10 sample: acetone (for plasma or serum the ratio was 1:4). Homogenization was done in a table-top homogenizer (Retsch MM301) placed in a cold room ( $4^\circ\text{C}$ ) in 2-ml Eppendorf tubes with 2 glass balls (5 mm) for 1 min at 30 Hz. The tube was immediately centrifuged at  $4^\circ\text{C}$ , 20,000g for 2 min. Supernatant was decanted into a new 1.5-ml Eppendorf tube and immediately centrifuged for 30 min using a small table-top centrifuge (BioSan FVL-2400N) placed inside a  $-80^\circ\text{C}$  freezer. Supernatant was quickly decanted into a glass HPLC vial and kept at  $-80^\circ\text{C}$  for no longer than 6 h. Just before the HPLC analysis, the vial was placed into a pre-cooled ( $4^\circ\text{C}$ ) LC-sample rack and immediately analysed. To enable an approximate quantification of analysed CuET, a calibration curve was prepared. Various amounts of CuET were spiked in plasma, frozen in liquid nitrogen, and placed at  $-80^\circ\text{C}$  to mimic sample processing. Standards were then processed as the samples described above. To measure circulating CuET concentrations, mice were given a single oral dose of DSF ( $50 \text{ mg kg}^{-1}$ ) and euthanized at different time points. Serum was collected and frozen for analysis.

**Blood collection from humans for HPLC-MS analysis of CuET.** Blood samples were collected before and 3 h after oral application of DSF (Antabuse, 400 mg) dissolved in water. Phlebotomy needles were specific for metal analysis—Sarstedt Safety Kanule 21 G  $\times 1\frac{1}{2}$  inches, 85.1162.600. Collection tubes were specific for metal analysis—Sarstedt, S-Monovette 7.5 ml LH, 01.1604.400. Immediately after blood collection samples were centrifuged in a pre-cooled centrifuge ( $4^\circ\text{C}$  at 1,300g for 10 min). After centrifugation, tubes were placed on ice and the plasma fraction was immediately aliquoted into the 1.5-ml Eppendorf tubes with approximately  $500 \mu\text{l}$  per tube. The tubes with plasma were immediately frozen on dry ice and later stored in  $-80^\circ\text{C}$ . Blood samples were collected from volunteers who gave informed consent and were undergoing Antabuse therapy because of alcohol abuse. Participants were four males (aged 34, 38, 41, 60 years) and five females (aged 37, 56, 46, 59, 63 years). All individuals were freshly diagnosed for alcohol-use disorder and were scheduled for Antabuse therapy. Blood samples were collected before and after the first use of Antabuse. All relevant ethical regulations were followed for the study. The study, including the collection of blood samples, was approved by the Ethical Committee of Faculty of Medicine and Dentistry, Palacky University in Olomouc.

**Cell lines.** Cell lines were cultured in appropriate growth medium supplemented with 10% fetal bovine serum (FBS) and penicillin–streptomycin; and maintained in a humidified, 5%  $\text{CO}_2$  atmosphere at  $37^\circ\text{C}$ . Cell lines cultured in DMEM medium were: HCT116 (ATCC), DU145 (ECACC), PC3 (ECACC), T47D (NCI60),

HS578T (NCI60), MCF7 (ECACC), MDA-MB-231 (ATCC), U2OS (ECACC), HeLa (ATCC), NIH-3T3 (ATCC), CAPAN-1 (ATCC), A253 (ATCC), FaDu (ATCC), h-TERT-RPE1 (ATCC), HeLa-Ub(G76V)-GFP-ODD-Luc<sup>21</sup>. Cell lines cultured in RPMI1640 medium were: NCI-H358 (ATCC), NCI-H52 (ATCC), HCT-15 (ATCC), AMO-1 (ATCC), MM-1S (ATCC), ARH77 (ATCC), RPMI8226 (ATCC), OVCAR-3 (NCI60), CCRF-CEM (ATCC), K562 (ATCC), 786-0 (NCI60). Cell lines cultured in EMEM medium were: U87-MG (ATCC), SiHA (ATCC). Cell line A549 (ATCC) was cultured in F12K medium, HT29 (ATCC) in McCoy's medium and LAPC4 (provided by Z. Culig, University of Innsbruck) in IMDM medium supplemented with metribolone R1881 (Sigma-Aldrich). RWPE-1 (ATCC) cells were cultured in a keratinocyte serum-free medium supplemented with bovine pituitary extract and human recombinant epidermal growth factor (Thermo Fisher Scientific). BTZ- and CFZ-resistant multiple myeloma cell lines were previously described in ref. 35. Cell lines were tested for mycoplasma contamination and authenticated by STR method. None of the cell lines used in this study is listed in the database of commonly misidentified cell lines maintained by ICLAC.

**Stable cell line construction.** For construction of all stably transfected cell lines we used the U2OS cell line (ECACC). For U2OS Ub-GFP, we used the commercial Ub-GFP EGFP-C1 vector (Addgene); for U2OS NPL4-GFP, we used the commercial NPLOC4-GFP pCMV6-AC-GFP vector (Origene); for U2OS p97-GFP, we used the commercial VCP-GFP pCMV6-AC-GFP vector (Origene); and for U2OS UFD1-GFP, we used the commercial UFD1L-GFP pCMV6-AC-GFP vector (Origene). Cells were transfected using Promega FugeneHD according to the manufacturer's instructions. Cells were further cultured in the appropriate antibiotics (geneticin, 400  $\mu\text{g ml}^{-1}$ ). Medium with geneticin was replaced every 2–3 days until the population of resistant cells was fully established. Cells were further refined by sorting for cells expressing GFP (BD FACS Aria). For preparation of inducible NPL4(MUT)-GFP cells, U2OS cells were transfected with a pcDNA6/TR plasmid (Invitrogen, V1025-20) using the FugeneHD transfection reagent (Promega, E2311) according to the manufacturer's protocol. To generate a cell line that stably expressed the Tet repressor, U2OS cells were cultured in selective medium with blasticidin (10  $\mu\text{g ml}^{-1}$ ) for 10 days. Blasticidin-resistant colonies were picked, expanded and screened for clones that exhibited the lowest basal levels and highest inducible levels of expression. Next, the most suitable clones were transfected with the PCDNA4/TO expression vector encoding the mutated NPL4-GFP protein using the Fugene transfection reagent. Cells were cultured in medium with zeocin (500  $\mu\text{g ml}^{-1}$ ) to select clones that contain pcDNA4/TO-mutated NPL4-GFP. The NPL4(MUT)-GFP-encoding plasmid was obtained from Geneti Biotech. To induce expression of protein, cells were incubated with doxycycline (Sigma-Aldrich) 1  $\mu\text{g ml}^{-1}$  for 16–48 h.

**Colony-formation assay.** Cells were seeded into six-well plates at 100–300 cells per well (depending on the cell line). The next day, cells were treated with compounds as indicated in the specific experiments and kept in culture for 7–14 days. Colonies were visualized by crystal violet and counted.

**XTT assay.** Cells were plated at a density of 10,000 per well in a 96-well plate. The next day, cells were treated as indicated. After 24 h, an XTT assay was performed according to the manufacturer's instructions (Applchem). XTT solution was added to the medium and incubated for 30–60 min, and then the dye intensity was measured at the 475 nm wavelength using a spectrometer (TECAN, Infinite M200PRO). Results are shown as mean  $\pm$  s.d. from three independent experiments, each performed in triplicate. For LD<sub>50</sub> analysis across the panel of cell lines listed in Extended Data Fig. 2b, cell lines were treated with various doses (at least five doses) for 48 h. LD<sub>50</sub> values were calculated using Graphpad Prism software based on survival curves from at least two independent experiments.

**Annexin V staining.** Cell cultures were treated as indicated and collected by trypsinization. Initial culture medium and washing buffer were collected to include detached cells. Cells were centrifuged (250g, 5 min) and re-suspended in a staining buffer (140 mM NaCl, 4 mM KCl, 0.75 mM MgCl<sub>2</sub>, 10 mM HEPES) containing 2.5 mM CaCl<sub>2</sub>, Annexin-V-APC (1:20, BD Biosciences) and 2.5  $\mu\text{g ml}^{-1}$  7-AAD (BD Biosciences) for 15 min on ice in the dark. Samples were analysed by flow cytometry using BD FACSVers (BD Biosciences) and at least 10,000 events were acquired per sample. Collected data were processed using BD FACSSuite (BD Biosciences) and exported into Microsoft Excel.

**Caspases 3/7 assay.** Activity of caspase-3 and -7 was quantified by cleavage of fluorogenic substrate CellEvent Caspase-3/7 Green Detection Reagent (Thermo Fisher Scientific). In brief, samples prepared in the same staining buffer as described for annexin V staining above, supplemented with 2% FBS, 0.5  $\mu\text{M}$  CellEvent Caspase-3/7 Green Detection Reagent and incubated for 45 min at room temperature in the dark. Subsequently, 0.5  $\mu\text{g ml}^{-1}$  DAPI was added and samples were analysed by flow cytometry using BD FACSVers (BD Biosciences) and at least 10,000 events were acquired per sample. Collected data were processed using BD FACSSuite (BD Biosciences) and exported into Microsoft Excel.

**Viability assay of multiple myeloma cells.** The CellTiter 96 MTS-assay (Promega) was used according to the manufacturer's instructions to determine the cell viability of BTZ (Janssen Cilag), CFZ and CuEt in cell lines and the absorbance of the formazan product was measured in 96-well microplates at 492 nm. The assay measures dehydrogenase enzyme activity found in metabolically active cells.

For patient cells, the more sensitive luminescent CellTiterGlo assay (Promega) was used to determine cell viability, measured by ATP production of metabolically active cells. The primary myeloma cell samples were obtained after written informed consent and approval by the independent ethics review board (St Gallen ethics committee—Ethikkommission Ostschweiz), in accordance with ICH-GCP and local regulations. Malignant plasma cells were retrieved by PBMC isolation from a patient with multiple myeloma progressing under BTZ-containing therapy, based on IMWG criteria (BTZ-resistant) and an untreated patient with multiple myeloma (BTZ-sensitive). The purity of the cell samples was >80% myeloma cells, as assessed by morphology.

**Immunoblotting and antibodies.** Equal amounts of cell lysates were separated by SDS-PAGE on hand-cast or precast tris-glycine gradient (4–20%) gels (Life Technologies), and then transferred onto a nitrocellulose membrane. The membrane was blocked with 5% bovine milk in Tris-buffered saline containing 0.1% Tween-20 for 1 h at room temperature, and then incubated overnight at 4 °C or for 1 h at room temperature, with one of the following primary antibodies (all antibodies were used in the system under study (assay and species) according to the instructions of the manufacturer): anti-ubiquitin (1:1,000; Cell Signaling, 3933), anti-H2A, acidic patch (1:1,000; Merck Millipore, 07-146), anti-monoubiquitin-H2A (1:1,000; Merck Millipore, clone E6C5), anti-I $\kappa$ B $\alpha$  (1:500; Santa Cruz Biotechnology, sc-371), anti-p53 (1:500; Santa Cruz Biotechnology, clone DO-1), anti-HIF-1 $\alpha$  (1:1,000; BD Biosciences, 610958), anti-CDC25A (1:500; Santa Cruz Biotechnology, clone DCS-120), anti-NRF1 (1:1,000; Cell Signaling, clone D5B10), anti-VCP (1:2,000; Abcam, ab11433), anti-VCP (1:1,000; Novus Bio, NBP100-1557), anti-NPLOC4 (1:1,000; Novus Bio, NBP1-82166), anti-ubiquitin lys48-specific (1:1,000; Merck Millipore, clone Apu2), anti- $\beta$ -actin (1:2,000; Santa Cruz Biotechnology, sc-1616; or 1:500, Santa Cruz Biotechnology, sc-87778), anti-GAPDH (1:1,000; GeneTex, clone 1D4), anti-lamin B (1:1,000; Santa Cruz Biotechnology, sc-6217), anti-calnexin (1:500; Santa Cruz Biotechnology, sc-11397), anti- $\alpha$ -tubulin (1:500; Santa Cruz Biotechnology, sc-5286), anti-XBP1 (1:500; Santa Cruz Biotechnology, sc-7160), UFD1 (1:500; Abcam, ab155003), cleaved PARP1 (1:500; Cell Signaling, 9544), p-eIF2 $\alpha$  (1:500; Cell Signaling, 3597), ATF4 (1:500; Merck Millipore, ABE387), HSP90 (1:500; Enzo, ADI-SPA-810), HSP70 (1:500; Enzo, ADI-SPA-830), HSF1 (1:500; Cell Signaling, 4356), p-HSP27 (1:1,000; Abcam, 155987), HSP27 (1:1,000; Abcam, 109376) followed by detection by secondary antibodies: goat anti-mouse IgG-HRP (GE Healthcare), goat anti-rabbit (GE Healthcare), donkey anti-goat IgG-HRP (Santa Cruz Biotechnology, sc-2020). Bound secondary antibodies were visualized by ELC detection reagent (Thermo Fisher Scientific) and images were recorded by imaging system equipped with CCD camera (ChemiDoc, Bio-Rad) operated by Image Laboratory software or developed on film (Amersham).

**Immunofluorescence staining.** Cells were grown in 24-well plates with a 0.170-mm glass bottom (In Vitro Scientific). Where indicated, the cells were pre-extracted before fixation with pre-extraction buffer (10 mM PIPES pH 6.8, 100 mM NaCl, 1.5 mM MgCl<sub>2</sub>, 300 mM sucrose, 0.5% Triton X-100, 1 mM DTT, 5  $\mu\text{g ml}^{-1}$  leupeptin, 2  $\mu\text{g ml}^{-1}$  aprotinin, 0.1 mM PMSF) for 20 min at 4 °C, washed by PBS and then immediately fixed with 4% formaldehyde for 15 min at room temperature. Cells were stained with primary antibodies: anti-ubiquitylated conjugated mouse FK2 antibody (1:500; Enzo, BML-PW8810), anti-VCP (1:500; Abcam; ab11433), anti-NPL4 (1:500; Novus Bio, NBP1-82166), HSP70 (1:100; Enzo, ADI-SPA-830), HSF1 (1:500; Cell Signaling, 4356), anti-ubiquitin lys48-specific (1:500; Merck Millipore, clone Apu2), SUMO2/3 (1:500; Abcam, ab37442), TDP43 (1:300; Proteintech, 10782-2-AP) and appropriate Alexa Fluor 488- and 568-conjugated secondary antibodies (Invitrogen, 1:1,000). Cytochrome *c* was stained using an Alexa Fluor 555-conjugated mouse anti-cytochrome *c* antibody according the manufacturer's protocol (BD Pharmingen, 558700).

**Microscopy, FRAP and image analysis.** Samples were analysed using a Zeiss Axioimager Z.1 platform equipped with the Elyra PS.1 super-resolution module for structured illumination (SIM) and the LSM780 module for CLSM. High resolution images were acquired in super-resolution mode using a Zeiss Pln Apo100 $\times$ /1.46 oil objective (total magnification, 1,600 $\times$ ) with appropriate oil (Immersol 518F). SR-SIM setup involved five rotations and five phases for each image layer and up to seven z-stacks (101 nm) were acquired per image. The CLSM setup for FRAP and life cells acquisition had a c-Apo 40 $\times$ /1.2 W water immersion objective. Bleaching of regions of interest (ROIs) was performed using an Argon 488 nm laser. Lower resolution images of fixed samples were acquired using a Plan Apo 63 $\times$ /1.4 oil objective (total magnification 1,008 $\times$ ). FRAP and image acquisitions were performed using Zeiss Zen 11 software. For FRAP, internal Zen's 'Bleach'

and 'Regions' modules were used. Data from FRAP analysis involving multiple bleached ROIs were exported into Microsoft Excel and plotted. Basic processing of acquired images, such as contrast and brightness settings, was done in Adobe Photoshop on images exported as TIFFs. Quantitative microscopy-based cytometry of the immunofluorescence-stained samples was performed using an automatic inverted fluorescence microscope BX71 (Olympus) using ScanR Acquisition software (Olympus) and analysed with ScanR Analysis software (Olympus).

**Cell fractionation for Triton-X100 insoluble pellets.** Cells were treated as indicated, washed in cold PBS and lysed in lysis buffer (50 mM HEPES pH 7.4, 150 mM NaCl, 2 mM MgCl<sub>2</sub>, 10% glycerol, 0.5% Triton X-100, protease inhibitor cocktail by Roche) for 10 min gently agitating at 4°C. Then, cells were scraped into Eppendorf tubes and kept for another 10 min on ice with intermittent vortexing. After that, the lysate was centrifuged at 20,000g for 10 min at 4°C. The insoluble fraction and supernatant were separately re-suspended in 1 × LSB buffer.

**Isolation of microsomal fraction.** After the desired treatment in cell culture, cells were washed with cold PBS and lysed (250 mM sucrose, 20 mM HEPES pH 7.4, 10 mM KCl, 1.5 mM MgCl<sub>2</sub>, 1 mM EDTA, 1 mM DTT, protease inhibitor cocktail). Lysates were homogenized by Potter-Elvehjem PTFE homogenizer and kept on ice for 20 min. The homogenates were subjected to serial centrifugation steps (720g and 10,000g for 5 min each, and 100,000g for 1 h). Pellets and supernatants from the last ultracentrifugation step were resuspended in the 1 × LSB buffer and used for western blot analysis.

**Immunoperoxidase staining of pre-extracted tissue sections.** Frozen sections (4–5 μm thick) from xenograft-grown, cryopreserved tumour tissues were cut on a cryostat and placed on commercial adhesion slides (SuperFrost Plus, Menzel, Germany) and air-dried for 2 h at room temperature. The dried sections were carefully covered with the cold extraction buffer: 50 mM Tris-HCl (pH 7.5), 150 mM NaCl, 1 mM MgCl<sub>2</sub>, 5% glycerol, 1 mM DTT, 1% Triton X-100, 1% IGEAL, protease inhibitor cocktail (Phos Stop Easy pack, 04906837001, Roche) or cold PBS (controls) and incubated in a cold room for 20 min. Pre-extracted and control PBS-treated sections were gently washed three times in cold PBS, and fixed in 4% paraformaldehyde fixative for 15 min, followed by another three washes in PBS. Washed sections were then subject to a sensitive immunoperoxidase staining protocol, using the primary rabbit monoclonal antibody against VCP antibody (EPR3307(2)) (1:10,000; ab109240, Abcam) and rabbit polyclonal antibody against NPLOC4 (1:500; NBPI-82166, Novus Biologicals) and Vectastain Elite kit as secondary reagents (Vector Laboratories, USA), followed by a nickel-sulfate-enhanced diaminobenzidine reaction without nuclear counterstaining, mounted and microscopically evaluated and representative images documented by an experienced oncopathologist.

**Isothermal titration calorimetry (ITC).** Experiments were performed at 25°C with a Nano ITC Low Volume (TA Instruments) and analysed by Nano Analyze Software v.2.3.6. During all measurements, injections of 2.5 μl of ligand (16 μM) were titrated into 250 μl protein (2 μM) with time intervals of 300 s, a stirring speed of 250 r.p.m. All ITC experiments were conducted with degassed buffered solutions 20 mM HEPES buffer pH 7.3, in the presence of 1% DMSO. Purified GST-NPL4(WT) and GST-NPL4(MUT) proteins were used in ITC experiment.

**Drug affinity responsive target stability (DARTS).** DARTS was performed according to a modified published protocol<sup>38</sup>. Purified GST-NPL4(WT) and GST-NPL4(MUT) proteins were diluted by 100 mM phosphate buffer, pH 7.4 to final concentration of 0.03 μg μl<sup>-1</sup>. The proteins were treated with CuET (final concentration of 5 μM; dissolved in DMSO) for 1 h and equal amounts of DMSO were added to the solutions, which served as control samples. Pronase (Sigma-Aldrich) was dissolved in TNC buffer (50 mM Tris-Cl, 50 mM NaCl, 10 mM CaCl<sub>2</sub>, pH 7.5). The 0.025 μg of pronase was added to 50 μl of protein solution and incubated for 1 h at 37°C. Samples without pronase served as the non-digested controls. The pronase reaction was stopped by addition of 5 × SDS loading buffer; the samples were boiled at 95°C for 15 min and loaded on SDS-PAGE gels. After SDS-PAGE, gels were silver-stained and scanned on a GS-800 Calibrated Densitometer (Bio-Rad) or used for western blot analysis.

**20S proteasome activity.** To measure proteasome activity in cell extracts, cell lines were seeded in 100-mm Petri dishes at a density of 3 × 10<sup>6</sup> cells per dish. After 24 h, cells were washed twice with 2 ml of ice-cold PBS and scraped in to 1,000 μl ice-cold PBS. The cells were then isolated and suspended in buffer (50 mM HEPES (pH 7.5), 150 mM NaCl, 1% Triton X-100 and 0.1 μM PMSF) and then centrifuged at 15,000 r.p.m. for 15 min at 4°C. The cell lysates (10 μg) were incubated with 20 μM of substrates for measurement of chymotrypsin-like, trypsin-like and caspase-like activities (Suc-LLVT-AMC, Ac-RLR-AMC and Z-LLE-AMC (Boston Biochem)) in 90 μl of assay buffer (30 mM Tris-HCl, 0.035% sodium dodecylsulfate (pH 7.4)) in the presence CuET (1 μM and 5 μM) and BTZ (1 μM) for the investigation of proteasome inhibition; BTZ or an equivalent volume of solvent (DMSO) was used as a control. After 2 h of incubation at 37°C, inhibition of proteasome activity was measured by the release of hydrolysed free AMC groups by fluorimeter at

380/460 nm (TECAN, Infinite M200PRO). To measure proteasome activity in live cells, the cells were seeded in 24-well plate at a density of 0.2 × 10<sup>6</sup> cells per well. Cell lines were treated with CuET (1 μM and 5 μM), vehicle control or 1 μM BTZ for 1 h. After incubation, cells were twice washed with 0.5 ml of 1 × ice-cold PBS and scraped into 100 μl ice-cold lysis buffer and then centrifuged at 15,000 r.p.m. for 15 min at 4°C. Subsequently, the cell extract (10 μg) was incubated with 20 μM substrates to measure chymotrypsin-like, trypsin-like and caspase-like activities in assay buffer (30 mM Tris-HCl (pH 7.4)). After 2 h of incubation at 37°C, inhibition of proteasome enzymatic activities was measured by the release of hydrolysed free AMC as described above.

**Ub(G76V)-GFP degradation.** HeLa Ub(G76V)-GFP-ODD-Luc cells expressing Ub(G76V)-GFP were seeded at a density of 10<sup>4</sup> cells per well in 96-well plates. The next day, cells were treated with 4 μM MG132 for 3 h. After that, the medium was discarded and cells were washed twice with PBS and then incubated with the tested compound in the presence of 30 μg ml<sup>-1</sup> cycloheximide for another 3 h. The GFP signal was acquired using an ImageXpress automated microscope. For each well, four images were taken (corresponding to 200–250 cells). Cells were analysed every 30 min during 3 h of treatment. Normalized GFP signal intensity was calculated using the following formula: (test compound – background)/(basal GFP signal intensity × background) where 'test compound' is defined as the mean GFP signal intensity of Ub(G76V)-GFP-expressing cells treated with the test compound. 'Background' is defined as the background GFP signal intensity of HeLa cells. 'Basal GFP signal intensity' is defined as mean GFP signal intensity of Ub(G76V)-GFP-expressing cells treated with DMSO. The degradation rate constant (*k*) was obtained from the slope of the linear range of plotting ln(normalized GFP signal intensity) versus time ranging from 90 to 180 min. The percentage of remaining *k* for each compound is calculated using the following formula (test compound/DMSO control) × 100.

**p97 ATPase activity assay.** P97 ATPase assay was performed as described previously<sup>28</sup>. A total of 250 nM of p97 protein was diluted in assay buffer (50 mM Tris-HCl pH 7.4, 20 mM MgCl<sub>2</sub>, 0.5 mM DTT). Test compounds were added in DMSO (final concentration of DMSO was 5%). After 10 min of incubation, the reaction was started with ATP (100 μM final concentration) followed by a 1-h incubation at room temperature. The reaction was stopped by adding Bioluminescence solution (Enzo) and free phosphate was measured according to the manufacturer's instructions. Results are expressed as the percentage of activity of the control (a well containing only DMSO).

**26S proteasome activity.** The RPN11 assay is described in PubChem (AID588493). In brief, a synthetic fluorescently labelled substrate, Ub4pepOG, was used to measure RPN11 activity. Fluorescence polarization assay was performed in a low-volume 384-well solid black plate in the presence of (i) 5 μl of the compound 1,10-phenanthroline or CuEt in 3% DMSO or 3% DMSO control; (ii) 5 μl of BioMol 26S proteasome; and (iii) 5 μl of substrate (15 nM Ub4pepOG). Fluorescence polarization is measured using a plate reader with excitation of 480 nm and emission of 520 nm filter set. The activity was normalized to DMSO control and fit to a dose-response curve.

**Protein expression and purification.** All proteins were expressed in *E. coli* BL21 (DE3) cells (Novagen). p97-His (pET28a vector) and Ufd1-His (pET28a vector) expression were induced by 1 mM IPTG (Life Technologies) at an OD<sub>600</sub> of 0.6 for 10 h at 22°C. NPL4(WT) and NPL4(MUT) (pGEX-2TK) were induced by 0.4 mM IPTG at an OD<sub>600</sub> of 0.8 overnight at 16°C. For p97 and UFD1, the bacterial pellet was suspended in buffer (50 mM Tris-HCl pH 8.0, 300 mM NaCl, 2.5 mM MgCl<sub>2</sub>, 20 mM imidazole, 5% glycerol) and lysed by sonication and centrifuged (14,000g for 20 min). Proteins were purified by Ni-NTA chromatography (Qiagen) according to the manufacturer's instructions. For p97, the protein was further purified by gel filtration (Superdex 200, GE Healthcare). For GST-NPL4(WT) and GST-NPL4(MUT), the bacterial pellet was suspended in phosphate buffer (PBS, 0.1% Triton X-100, 300 mM NaCl) and lysed by sonication and centrifuged (14,000g for 10 min). Proteins were purified by glutathione sepharose 4B (Life Technologies) according to the manufacturer's protocol. The proteins were further purified by gel filtration (Superdex 200, GE Healthcare).

**Chemicals.** CuET was prepared by direct synthesis from water solutions of diethyldithiocarbamate sodium salt and copper(II) chloride as described previously<sup>53</sup>. CuET for *in vivo* experiments was prepared equally with a slight modification. The reaction between diethyldithiocarbamate sodium salt and copper(II) chloride was performed in a sterile 1% aqueous solution of bovine serum albumin. The resulting solution was used directly. The following chemicals were purchased from commercial vendors: tetraethylthiuram disulfide (disulfiram, DSF) (Sigma-Aldrich), sodium diethyldithiocarbamate trihydrate (Sigma-Aldrich), copper D-gluconate (Sigma-Aldrich), BTZ (Velcade, Janssen-Cilag International N.V.), MG132 (Sigma-Aldrich), DBE-Q (Sigma-Aldrich), NMS873 (Abmole), cycloheximide (Sigma-Aldrich), dicoumarol (Sigma-Aldrich), 1,10-phenanthroline (Sigma) and MLN7243 (Active Biochem).

**Statistical analyses and reproducibility.** For the epidemiological study, we calculated hazard ratios and 95% confidence intervals estimating cancer-specific mortality, based on a Cox model regressing of both propensity scores and disulfiram use, balancing baseline characteristics of previous and continuing users of DSF and adjusting estimated hazard ratios of cancer-specific mortality associated with DSF use<sup>51</sup>. The propensity score estimates were conditional on multiple covariates, based on using logistic regression (see 'Epidemiological analyses and access to health registers' for specifics of cohorts and covariates). In the Cox model, the propensity score is further included as a restricted cubic spline to model possible nonlinearities, in addition to the categorical disulfiram use as the variable of interest. Statistical significance of DSF use was evaluated by likelihood ratio tests, using the software R for statistical computing<sup>52</sup>.

For evaluation of the animal studies, STATISTICA software, v.12 (StatSoft) was used to estimate sample size. For a power of 80%, the level of significance set at 5%, 4 groups and RMSSE = 0.8, seven mice per group were estimated. For usage of non-parametrical statistical methods, the number of eight mice per group was finally planned. The differences between tumour volumes were statistically analysed by non-parametrical Kruskal–Wallis test, not requiring any assumptions of normality and homoscedascity. To test the effect of CuET treatment on survival of AMO-1-xenografted mice, a Kaplan–Meier graph and log-rank statistical test were

used. For other experiments, the statistics, such as number of repetitions, centre value and error bars, are specified in figure legends.

**Data availability.** Most data generated or analysed during this study are included in the article and its Supplementary Information. Uncropped images of all gels and blots can be found in Supplementary Fig. 1. Source Data for all graphs are provided in the online version of the paper. Additional datasets generated during and/or analysed during the current study and relevant information are available from the corresponding authors upon reasonable request.

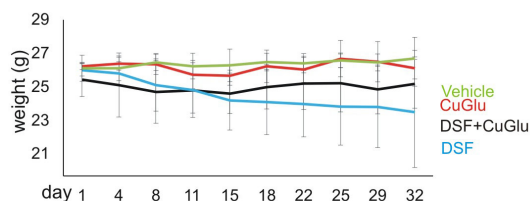
50. Thygesen, L. C., Daasnes, C., Thaulow, I. & Brønnum-Hansen, H. Introduction to Danish (nationwide) registers on health and social issues: structure, access, legislation, and archiving. *Scand. J. Public Health* **39** (Suppl), 12–16 (2011).
51. Rosenbaum, P. R. & Rubin, D. B. The central role of the propensity score in observational studies for causal effects. *Biometrika* **70**, 41–55 (1983).
52. R Core Team. *R: A language and environment for statistical computing*. R Foundation for Statistical Computing <https://www.R-project.org/> R v.3.2.3 (2015-12-10) (R Foundation for Statistical Computing, 2016).
53. Cvek, B., Milacic, V., Taraba, J. & Dou, Q. P. Ni(II), Cu(II), and Zn(II) diethyldithiocarbamate complexes show various activities against the proteasome in breast cancer cells. *J. Med. Chem.* **51**, 6256–6258 (2008).

a

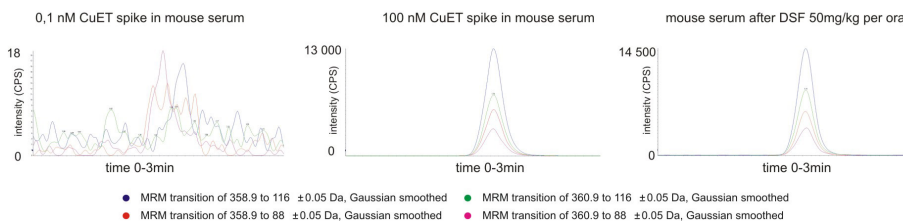
Cancer type	Overall			
	No <sup>a</sup>	HR	95 CI	p-value
<b>Colon cancer</b>				
Previous users	326	1.00		
Continuing users	103	0.75	0.66-0.85	0.000
No prescriptions	31,812	0.84	0.79-0.91	0.000
<b>Prostate cancer</b>				
Previous users	377	1.00		
Continuing users	175	0.81	0.66-0.98	0.029
No prescriptions	36,338	0.86	0.75-0.98	0.021
<b>Breast cancer</b>				
Previous users	408	1.00		
Continuing users	192	0.75	0.50-1.12	0.163
No prescriptions	48,106	0.62	0.49-0.78	0.000

<sup>a</sup> number of patients included

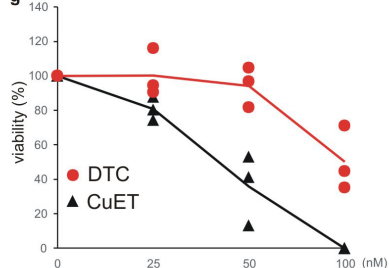
c



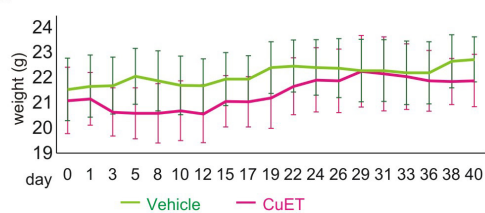
e



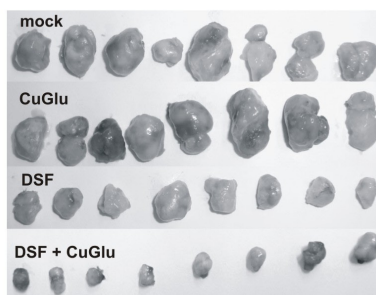
g



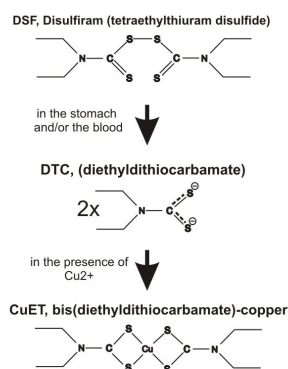
h



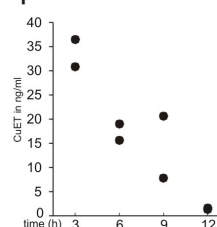
b



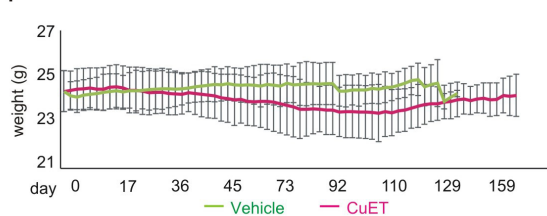
d



f



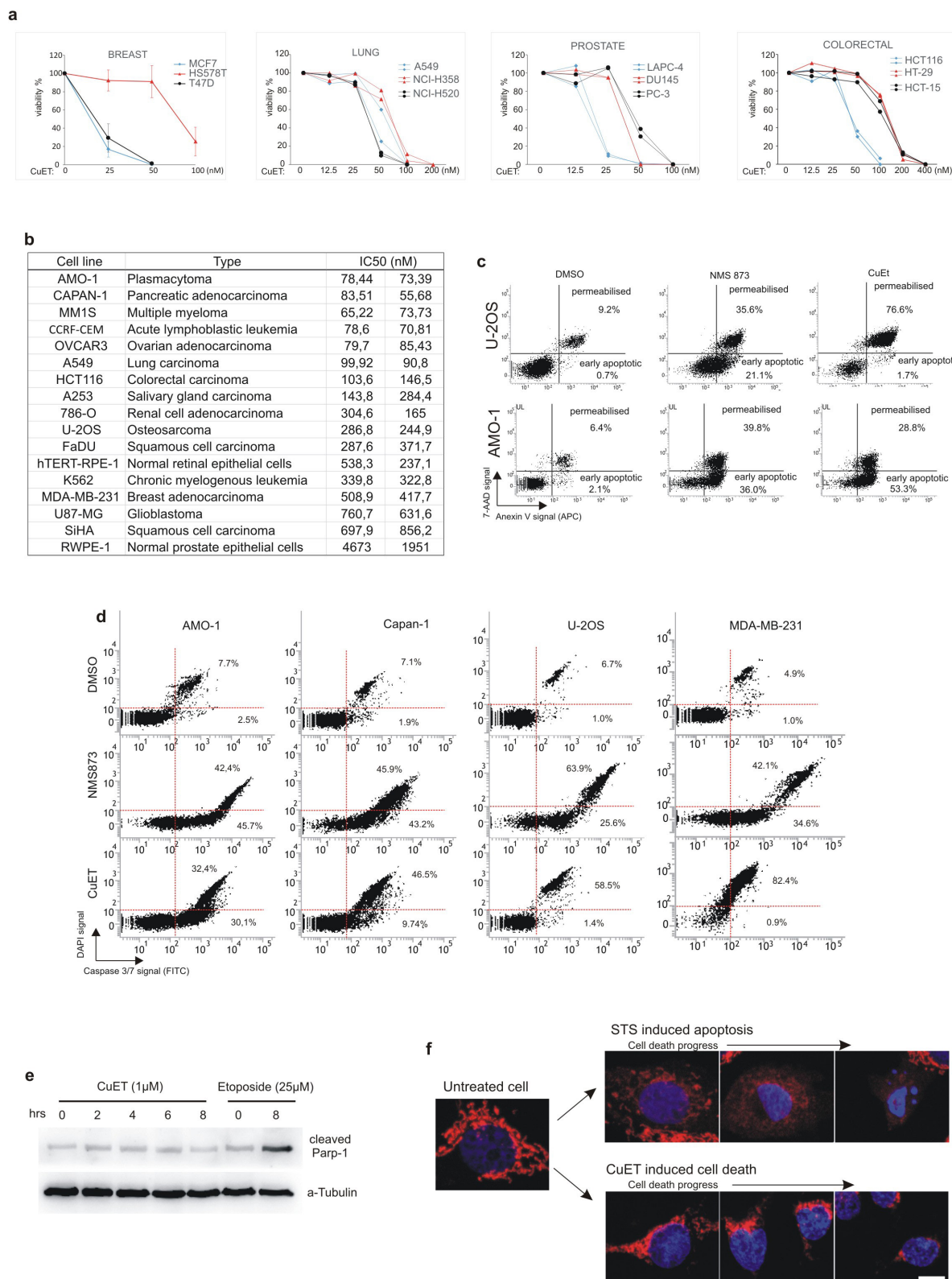
i



**Extended Data Figure 1 | Epidemiological and pre-clinical data of the anti-cancer effects of DSF.** a, Summary of hazard ratios (HR) and 95% confidence intervals (CI) for cancer-specific mortality among Danish patients with cancer, comparing continuing and previous users of DSF for selected types of cancer (for statistical analysis and definitions of DSF exposure categories, see Methods). b, Photographs of subcutaneously growing human MDA-MB-231 tumours extracted from mice at day 32. c, Time-course diagram of mouse weight. *n* = 8 animals per group. d, Model of CuET formation during metabolic processing of orally administered DSF in the human body. e, Examples of mass-spectrometry spectra of

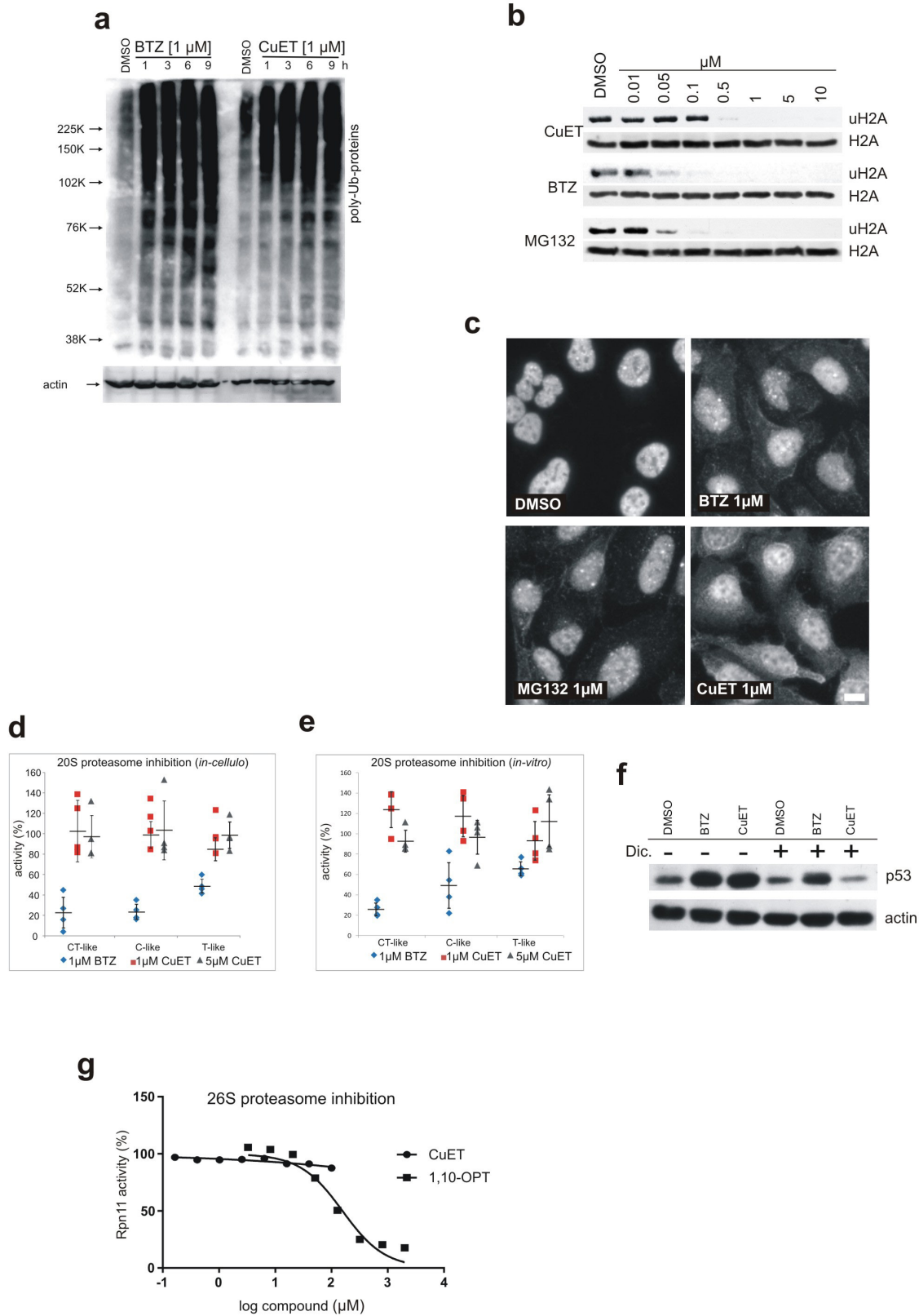
CuET expressed as peaks of 4 MRM transitions in mouse serum after CuET spikes, compared to orally applied DSF (50 mg kg<sup>-1</sup>). Data are representative of two independent experiments. f, Pharmacokinetic analysis of CuET levels in mouse serum after orally applied DSF (50 mg kg<sup>-1</sup>). *n* = 2 animals per time point. g, Effect of DTC and CuET on MDA-MB-231 cells analysed by colony formation assay. *n* = 3 independent experiments. h, Time-course diagram of weight in CuET- and vehicle-treated mice. *n* = 10 animals per group. i, Extended time-course diagram of weight in CuET- and vehicle-treated mice. *n* = 10 animals per group. Data are mean ± s.d. (c, h, i) or linked means (g).





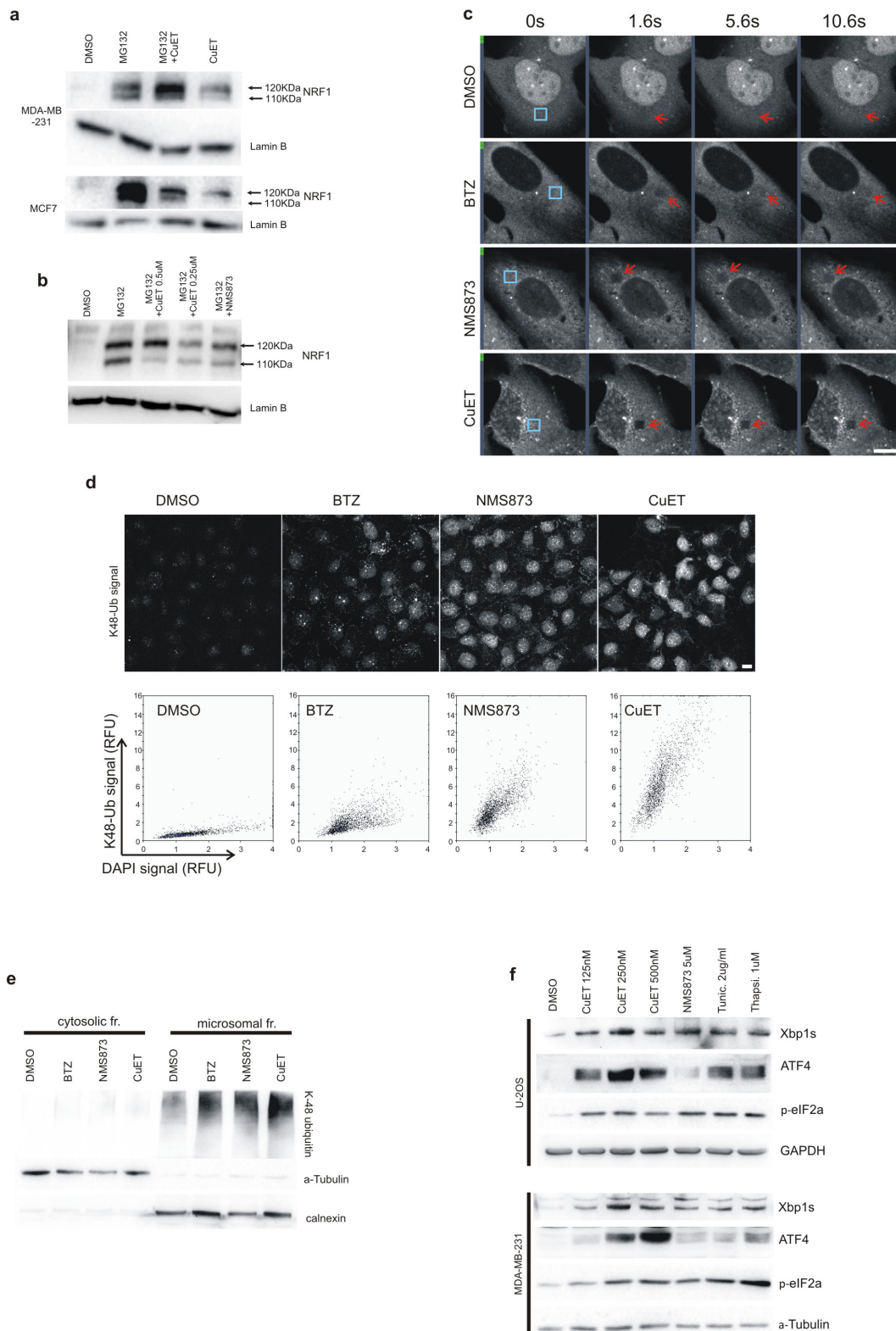
**Extended Data Figure 2 | CuET is the major anti-cancer metabolite of DSF.** **a**, CuET cytotoxicity measured by a colony-formation assay in human cell lines derived from breast, lung, colon and prostate carcinomas. Data are mean  $\pm$  s.d. of three independent experiments (breast) or presented individually for two independent biological experiments for each cell line (lung, colon and prostate). **b**, IC<sub>50</sub> values from two independent biological experiments documenting differential CuET-induced cytotoxicity across a panel of cancer and non-cancerous cell lines (48 h treatment). **c**, Analysis of annexin V signal in AMO-1 cells exposed to toxic doses of NMS873 (5  $\mu$ M, 16 h) or CuET (100 nM, 16 h) and in U2OS cell exposed to toxic doses of NMS873 (10  $\mu$ M, 16 h) or CuET

(1  $\mu$ M, 16 h). **d**, Analysis of caspase 3/7 activity in selected cell lines after apoptosis induction by NMS873 (AMO-1: 6 h, 5  $\mu$ M; Capan1: 16 h, 10  $\mu$ M; U2OS: 16 h, 10  $\mu$ M; MDA-MB-231: 24 h, 10  $\mu$ M) or CuET (AMO-1: 16 h, 100 nM; Capan1: 16 h, 250 nM; U2OS: 16 h, 1  $\mu$ M; MDA-MB-231: 24 h, 1  $\mu$ M). **e**, Absence of cleaved PARP1 after a toxic dose of CuET in U2OS cells, compared to etoposide treatment as a positive control. **f**, Analysis of cytochrome c (in red) release from mitochondria in U2OS cells during cell death induced by the positive control staurosporin (STS, 1  $\mu$ M) compared to cell death induced by CuET (1  $\mu$ M). Blue, DAPI. Scale bar, 10  $\mu$ m. **c-f**, Data are representative of two independent biological experiments.



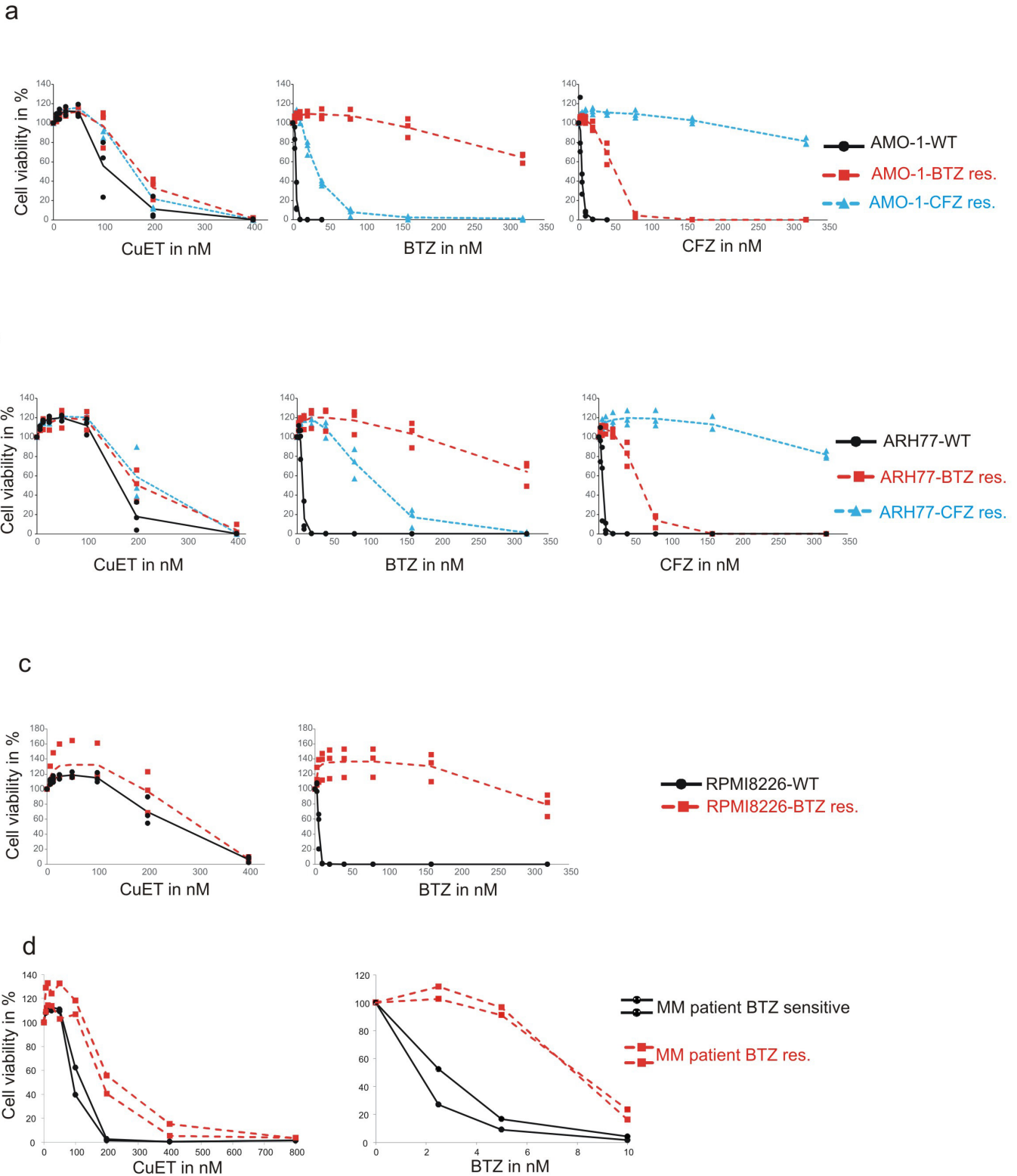
**Extended Data Figure 3 | CuET-induced proteasome inhibition-like response is not due to proteasome inhibition.** **a**, Kinetics of poly-Ub protein accumulation in U2OS cells treated with CuET or the proteasome inhibitor BTZ. **b**, CuET treatment (1.5 h) induces rapid deubiquitylation of ubiquitylated histone H2A (uH2A) similarly to proteasome inhibitors BTZ or MG132 in U2OS cells. **c**, CuET treatment (1.5 h) induces rapid cytoplasmic accumulation of poly-ubiquitylated proteins (FK2 antibody staining) in U2OS cells, similar to BTZ and MG132 treatment.

Scale bar, 10  $\mu$ m. **d**, **e**, 20S proteasome activity is not inhibited by CuET as examined in live MDA-MB-231 cells (**d**) or in lysates from MDA-MB-231 cells (**e**). Data are mean  $\pm$  s.d. of four independent experiments. **f**, CuET treatment (1  $\mu$ M, 6 h) does not cause accumulation of p53 in the presence of dicoumarol (300  $\mu$ M) in MCF7 cells. **g**, *In vitro* 26S proteasome function measured as RPN11 deubiquitylation activity, is not inhibited by CuET; 1,10-phenanthroline (1,10-OPT) served as a positive control. Data are representative of two (**a-c**, **f**) or three (**g**) independent experiments.



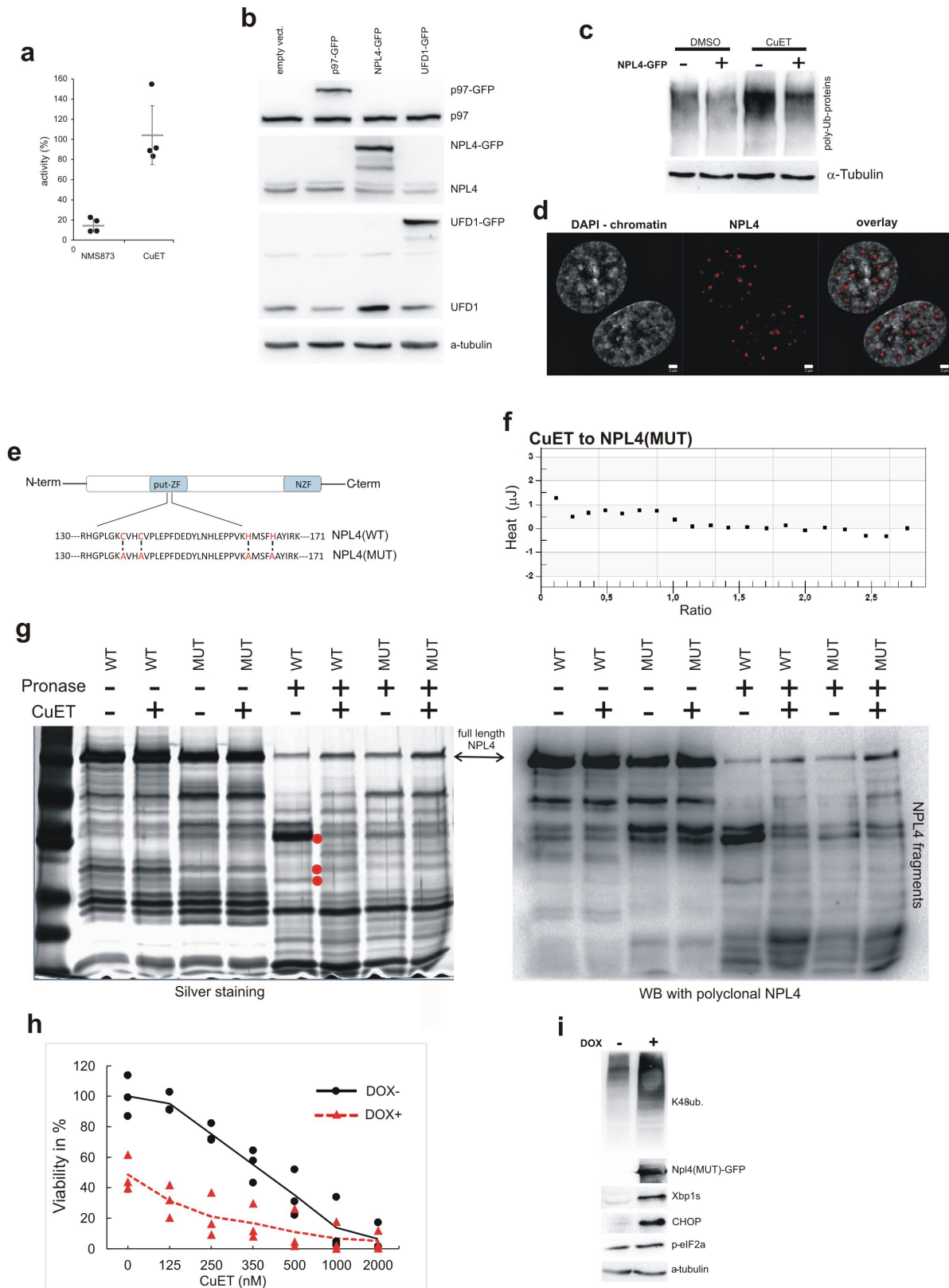
**Extended Data Figure 4 | CuET inhibits the p97 pathway and induces cellular UPR.** **a**, MG132-treated cells (5  $\mu$ M, 6 h) accumulate both forms of NRF1 (120-kDa and 110-kDa bands, top and bottom arrows, respectively), whereas CuET-treated cells (1  $\mu$ M, 6 h) accumulate only the non-cleaved 120-kDa form. **b**, Inhibition of the NRF1 cleavage process (appearance of the lower band) by CuET and NMS873 (a p97 inhibitor; 5  $\mu$ M) in mouse NIH3T3 cells co-treated with the proteasome inhibitor MG132 (5  $\mu$ M for 6 h). **c**, Time-course example images from a FRAP experiment, for which the quantitative analysis is shown in Fig. 2g (U2OS cells, blue boxes mark areas before bleaching, arrows after bleaching). **d**, U2OS cells pre-extracted with Triton X-100 and stained for poly-Ub(K48). The antibody

signal intensities for cells treated with DMSO, BTZ (1  $\mu$ M), NMS873 (10  $\mu$ M) and CuET (1  $\mu$ M) are analysed by microscopy-based cytometry and plotted below. **e**, Western blot analysis of accumulated poly-Ub proteins in the ultracentrifugation-separated microsomal fraction from U2OS cells treated with mock, CuET (1  $\mu$ M), NMS873 (10  $\mu$ M) or BTZ (1  $\mu$ M) for 3 h. **f**, UPR in U2OS and MDA-MB-231 cell lines induced by 6-h treatment with CuET (various concentrations) or positive controls (5  $\mu$ M NMS873, 2  $\mu$ g ml<sup>-1</sup> tunicamycin, 1  $\mu$ M thapsigargin) is shown by increased levels of XBP1s, ATF4 and p-eIF2 $\alpha$ . **a–f**, Data are representative of two independent experiments. All scale bars, 10  $\mu$ m.



**Extended Data Figure 5 | CuET kills BTZ-resistant cells. a**, BTZ-adapted (BTZres), CFZ-adapted (CFZres) and non-adapted AMO-1 human myeloma cells are equally sensitive to treatment with CuET. **b**, BTZ-adapted, CFZ-adapted and non-adapted ARH77 human plasmocytoma cells are equally sensitive to treatment with CuET. **c**, BTZ-adapted and non-adapted RPMI8226 human myeloma cells are equally sensitive to

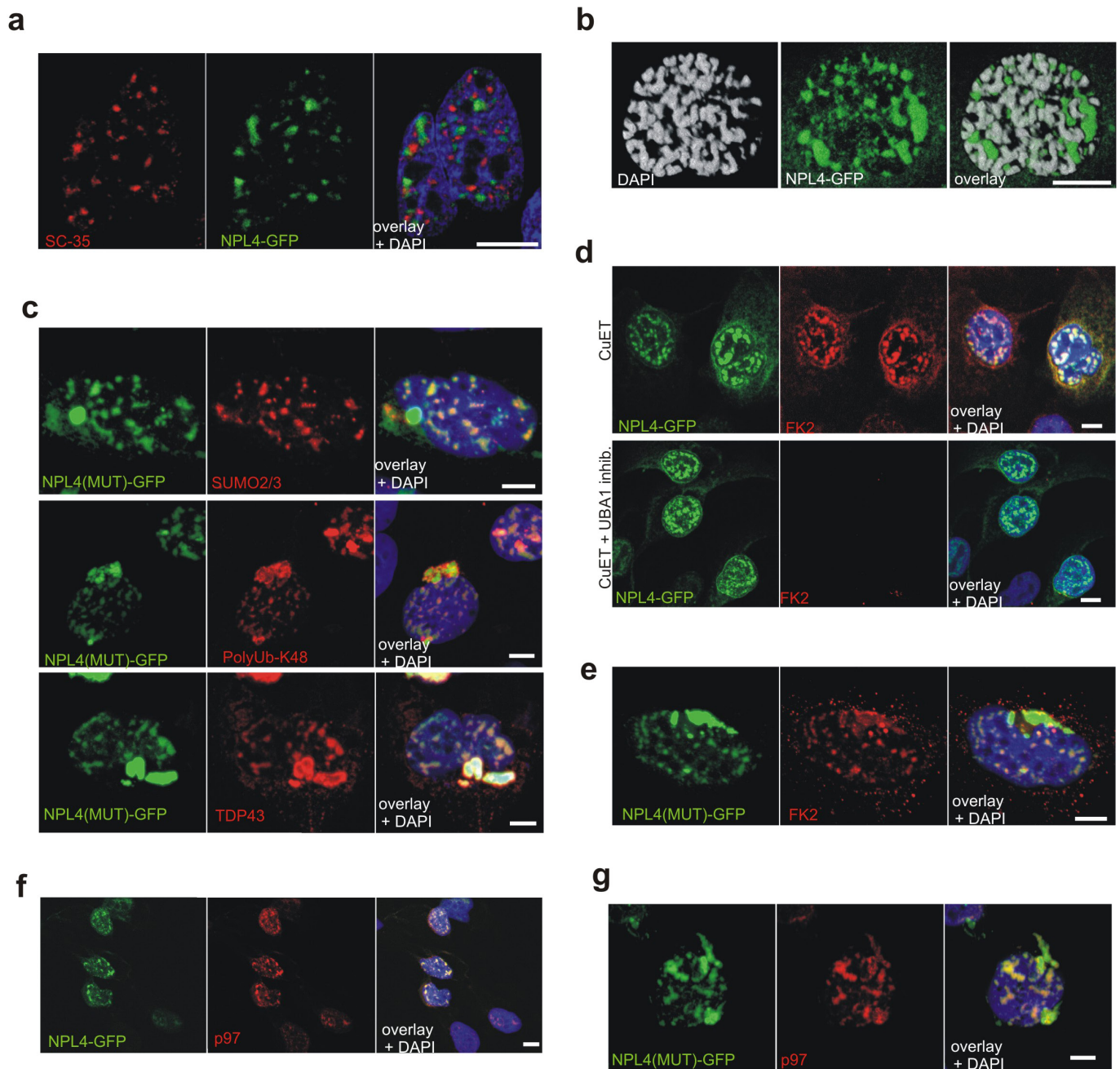
treatment with CuET. **d**, Human myeloma cells derived from a patient with BTZ-resistant myeloma show CuET sensitivity comparable to myeloma cells derived from a patient with BTZ-sensitive myeloma. Data are means linked of three independent experiments (a–c) or data are from two independent experiments (d).



Extended Data Figure 6 | See next page for caption.

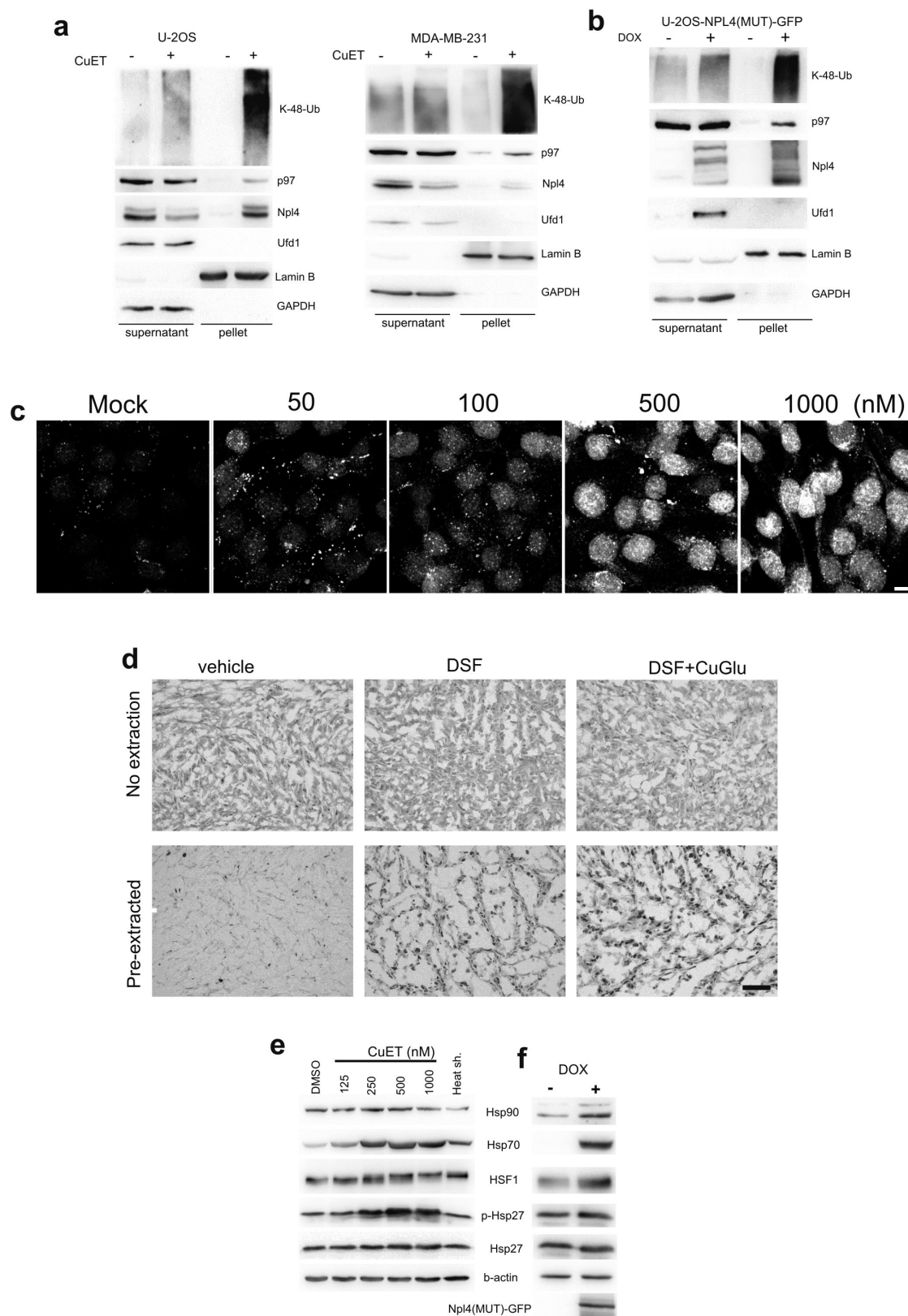
**Extended Data Figure 6 | CuET targets NPL4, causing immobilization and nuclear clustering of NPL4.** **a**, CuET (1  $\mu$ M) does not inhibit ATPase activity of p97. NMS873 (5  $\mu$ M) was used as a positive control. Data are mean  $\pm$  s.d. from four independent experiments. **b**, Western blotting analysis showing levels of ectopic p97-GFP, NPL4-GFP and UFD1-GFP in stable U2OS-derived cell lines used for the CuET-treatment rescue and cluster formation experiments. **c**, Ectopic expression of NPL4-GFP alleviates CuET-induced (125 nM, 4 h) accumulation of poly-Ub proteins in U2OS cells. **d**, Distribution of NPL4 nuclear clusters relative to chromatin in cells treated with CuET (1  $\mu$ M, 2 h). Scale bars, 2  $\mu$ m. **e**, Schematic representation of site-directed mutagenesis within the amino acid sequence of the putative zinc finger domain of NPL4.

**f**, ITC curve showing the lack of CuET binding to purified NPL4(MUT) protein. **g**, DARTS analysis of recombinant NPL4 proteins shows that differential pronase-mediated proteolysis after CuET addition is apparent for NPL4(WT) but not for NPL4(MUT); detected by either silver-stained SDS-PAGE (the most prominent differential bands are marked by red dots) or by blotting with an anti-NPL4 polyclonal antibody. **h**, Viability of cells expressing doxycycline-inducible NPL4(MUT)-GFP, treated with CuET for 48 h. Data are from three independent experiments, means are linked. **i**, Accumulation of K48-ubiquitinated proteins and activation of UPR in cells expressing the doxycycline-inducible NPL4(MUT)-GFP. **b-d, f, g, i**, Data are representative of two independent experiments.



**Extended Data Figure 7 | Immobilized NPL4 forms insoluble protein aggregates.** **a**, NPL4-GFP aggregates induced by CuET treatment (1  $\mu$ M, 3 h) do not co-localize with nuclear speckles (stained by SC-35 antibody) or nucleoli (visible as a DAPI<sup>-</sup> nuclear signal). **b**, NPL4-GFP nuclear aggregates induced by CuET (1  $\mu$ M, 3 h) are excluded from chromatin in early prometaphase U2OS cells. **c**, Co-localization of spontaneous NPL4(MUT)-GFP aggregates with SUMO2/3, poly-UB(K48) and TDP43 in pre-extracted U2OS cells. **d**, NPL4-GFP aggregates are formed independently of ubiquitylation, as shown in CuET-treated (1  $\mu$ M, 3 h)

cells pre-treated with a chemical UBA1 inhibitor (MLN7243, 10  $\mu$ M, 1 h). The lack of cellular FK2 staining of ubiquitylated proteins validates the efficacy of the MLN7243 inhibitor. **e**, Co-localization of FK2 signal with the spontaneous NPL4(MUT)-GFP aggregates in pre-extracted U2OS cells. **f**, Analysis of p97 in CuET-induced (1  $\mu$ M, 3 h) NPL4-GFP aggregates in pre-extracted U2OS cells. **g**, Analysis of p97 in spontaneous NPL4(MUT)-GFP aggregates in pre-extracted U2OS cells. **a-g**, Data are representative of two independent biological experiments. All scale bars, 10  $\mu$ m.



**Extended Data Figure 8 | NPL4 aggregation immobilizes the p97 binding partner and induces a global cellular HSR.** **a**, Immobilization of selected proteins in Triton X-100-resistant pellet fractions of CuET-treated (1  $\mu$ M, 3 h) U2OS cells. **b**, Immobilization of selected proteins in Triton X-100-resistant pellet fractions from U2OS cells expressing doxycycline-inducible NPL4(MUT)-GFP (48 h after induction). **c**, CuET dose-dependent immobilization of p97 in Triton X-100 pre-extracted MDA-MB-231 cells (3 h). Scale bar, 10  $\mu$ m. **d**, Immunohistochemical

staining showing non-extractable p97 in MDA-MB-231 xenografts from mice treated with DSF or DSF and CuGlu, compared to vehicle. Scale bar, 50  $\mu$ m. **e**, HSR after CuET (8 h treatment) is shown by various HSR markers detected by western blotting of U2OS cell extracts. **f**, HSR markers in U2OS cells expressing doxycycline-inducible NPL4(MUT)-GFP (24 h after induction). **a–f**, Data are representative of two independent biological experiments.



## Life Sciences Reporting Summary

Nature Research wishes to improve the reproducibility of the work that we publish. This form is intended for publication with all accepted life science papers and provides structure for consistency and transparency in reporting. Every life science submission will use this form; some list items might not apply to an individual manuscript, but all fields must be completed for clarity.

For further information on the points included in this form, see [Reporting Life Sciences Research](#). For further information on Nature Research policies, including our [data availability policy](#), see [Authors & Referees](#) and the [Editorial Policy Checklist](#).

### ► Experimental design

#### 1. Sample size

Describe how sample size was determined.

STATISTICA software, ver. 12 (StatSoft Inc., USA) was used to estimate the sample size. For the power of 80%, the level of significance set at 5%, 4 groups and RMSSE = 0.8, 7 mice in each group was estimated. For usage of non-parametrical statistical methods, the number of 8 (and 10) mice in each group was finally planned.

#### 2. Data exclusions

Describe any data exclusions.

No data were excluded.

#### 3. Replication

Describe whether the experimental findings were reliably reproduced.

All experiments were reproduced to reliably support conclusions stated in the manuscript.

#### 4. Randomization

Describe how samples/organisms/participants were allocated into experimental groups.

Animals were randomly divided into experimental groups.

#### 5. Blinding

Describe whether the investigators were blinded to group allocation during data collection and/or analysis.

Administration of compounds was carried out as a blinded experiment (all information about the expected outputs and the nature of used compounds were kept from the animal-technicians).

Note: all studies involving animals and/or human research participants must disclose whether blinding and randomization were used.

#### 6. Statistical parameters

For all figures and tables that use statistical methods, confirm that the following items are present in relevant figure legends (or in the Methods section if additional space is needed).

- | n/a                                 | Confirmed   |
|-------------------------------------|---|
| <input type="checkbox"/>            | <input checked="" type="checkbox"/> The <u>exact sample size</u> ( $n$ ) for each experimental group/condition, given as a discrete number and unit of measurement (animals, litters, cultures, etc.)                         |
| <input type="checkbox"/>            | <input checked="" type="checkbox"/> A description of how samples were collected, noting whether measurements were taken from distinct samples or whether the same sample was measured repeatedly                              |
| <input type="checkbox"/>            | <input checked="" type="checkbox"/> A statement indicating how many times each experiment was replicated  |
| <input checked="" type="checkbox"/> | <input type="checkbox"/> The statistical test(s) used and whether they are one- or two-sided (note: only common tests should be described solely by name; more complex techniques should be described in the Methods section) |
| <input checked="" type="checkbox"/> | <input type="checkbox"/> A description of any assumptions or corrections, such as an adjustment for multiple comparisons  |
| <input type="checkbox"/>            | <input checked="" type="checkbox"/> The test results (e.g. $P$ values) given as exact values whenever possible and with confidence intervals noted  |
| <input type="checkbox"/>            | <input checked="" type="checkbox"/> A clear description of statistics including <u>central tendency</u> (e.g. median, mean) and <u>variation</u> (e.g. standard deviation, interquartile range)                               |
| <input type="checkbox"/>            | <input checked="" type="checkbox"/> Clearly defined error bars  |

See the web collection on [statistics for biologists](#) for further resources and guidance.

## ► Software

Policy information about [availability of computer code](#)

### 7. Software

Describe the software used to analyze the data in this study.

The data were analyzed using Microsoft Excel 2016, STATISTICA 12, Graphpad Prism 4, PeakView 1.2, Image Lab 4.1, Carl Zeiss Zen 2011 SP6 (black), Nano Analyze Software 2.3.6, Olympus ScanR Analysis 1.3.0.3.

For manuscripts utilizing custom algorithms or software that are central to the paper but not yet described in the published literature, software must be made available to editors and reviewers upon request. We strongly encourage code deposition in a community repository (e.g. GitHub). *Nature Methods* [guidance for providing algorithms and software for publication](#) provides further information on this topic.

## ► Materials and reagents

Policy information about [availability of materials](#)

### 8. Materials availability

Indicate whether there are restrictions on availability of unique materials or if these materials are only available for distribution by a for-profit company.

All materials used is fully available from commercial sources with the exception of LAPC4 cell line, that we obtained from Zoran Culig, University of Innsbruck.

### 9. Antibodies

Describe the antibodies used and how they were validated for use in the system under study (i.e. assay and species).

anti-ubiquitin (Cell Signaling, cat.n.:3933; lot 4), anti-H2A, acidic patch (Merck Millipore, cat. n.: 07-146; lot 2880748), anti-monoubiquityl-H2A ( Merck Millipore, clone E6C5; lot 2239798), anti-Ik $\beta$  ( Santa Cruz Biotechnology, cat. n.: sc-371), anti-phospho(Ser32/36)-Ik $\beta$  ( Cell Signaling, clone 5A5), anti-p53 (1:500; Santa Cruz Biotechnology, clone DO-1; D0915), anti-HIF1 $\alpha$  ( BD Biosciences, cat. n.: 610958; lot 47858), anti-Cdc25A (Santa Cruz Biotechnology, clone DCS-120; our own clone commercially available by Santa Cruz), anti-NRF1 ( Cell Signaling, clone D5B10; lot 1), anti-VCP ( Abcam, cat. n.: ab11433; lot GR298429-3), anti-VCP ( Novus Bio, cat. n.: NBP100-1557; lot A1), anti-NPLOC4 ( Novus Bio, cat. n.: NBP1-82166; lot A96635), anti-ubiquitin lys48-specific ( Merck Millipore, clone Apu2; lot 2724416), anti- $\beta$ -actin ( Santa Cruz Biotechnology, cat. n.: sc-1616; lot B2206), anti- $\beta$ -actin ( Santa Cruz Biotechnology, C4, cat. n.: sc-47778; lot C0916), anti-GAPDH (GeneTex, clone 1D4; lot 821603479), anti-Lamin B ( Santa Cruz Biotechnology, M20, cat. n.: sc-6217; lot J2313), anti-calnexin ( Santa Cruz Biotechnology, H70, cat. n.: sc-11397; lot C1214), anti- $\alpha$ -Tubulin ( Santa Cruz Biotechnology, B7, cat. n.: sc-5286; lot C1313), anti-Xbp1 ( Santa Cruz Biotechnology, M-186, cat. n.: sc-7160; lot A2314), CHOP ( Cell Signaling, L63F7, cat. n.: 2895; lot 10), Ufd1 ( Abcam, cat. n.: ab155003; lot GR119674-2), cleaved PARP1 ( Cell Signaling, cat. n.: 9544; lot 4), p-eIF2 $\alpha$  ( Cell Signaling, cat. n.: 3597; lot 9), ATF4 ( Merck Millipore, cat. n.: ABE387 lot 2736396), HSP90 ( Enzo, cat. n.: ADI-SPA-810; lot 05051501), TDP-43 ( Proteintech, cat. n.: 10782-2-AP; lot number not provided by manufacturer), HSP70 ( Enzo, cat. n.: ADI-SPA-830; lot 05021648), HSF1( Cell Signaling, cat. n.: 4356; lot 2, pHSP27 ( Abcam, cat. n.: 155987; lot GR117377), HSP27 (Abcam, cat. n.: 109376; lot GR61497-8). FK2 antibody ( Enzo, cat. n.: BML-PW8810), Sumo2/3 ( Abcam, cat. n.: ab3742; lot GR8249-1), Cytochrome c Alexa Fluor 555 conjugated (BD Pharmingen, cat. n.: 558700). Secondary antibodies: goat-anti mouse IgG-HRP (GE Healthcare), goat-anti rabbit (GE Healthcare), donkey-anti goat IgG-HRP (Santa Cruz Biotechnology, sc-2020), Alexa Fluor 488 and Alexa Fluor 568 (Invitrogen, 1:1000). Antibodies critical for novel conclusions were validated by elimination of signals upon KD experiments and/or by functional assays. All antibodies were used in the system under study (assay and species) according to the profile of manufacturer.

## 10. Eukaryotic cell lines

a. State the source of each eukaryotic cell line used.

HCT116 (ATCC), DU145 (ECACC), PC3 (ECACC), T47D (NCI60), HS578T (NCI60), MCF7 (ECACC), MDA-MB-231 (ATCC), U-2-OS (ECACC), HeLa (ATCC), NIH-3T3 (ATCC), CAPAN-1 (ATCC), A253 (ATCC), FaDu (ATCC), h-TERT-RPE1 (ATCC), NCI-H358 (ATCC), NCI-H52 (ATCC), HCT-15 (ATCC), AMO-1 (ATCC), MM-1S (ATCC), ARH77 (ATCC), RPMI8226 (ATCC), OVCAR-3 (NCI60), CCRF-CEM (ATCC), K562 (ATCC), 786-0 (NCI60), U87-MG (ATCC), SiHA (ATCC), A549 (ATCC), HT29 (ATCC), LAPC4 (kindly provided by prof. Zoran Culig, University of Innsbruck). RWPE-1 (ATCC)

b. Describe the method of cell line authentication used.

All cell lines authenticated by STR method.

c. Report whether the cell lines were tested for mycoplasma contamination.

All cell lines were tested for mycoplasma contamination.

d. If any of the cell lines used are listed in the database of commonly misidentified cell lines maintained by [ICLAC](#), provide a scientific rationale for their use.

None of the used cell lines is listed in ICLAC database.

## ► Animals and human research participants

Policy information about [studies involving animals](#); when reporting animal research, follow the [ARRIVE guidelines](#)

## 11. Description of research animals

Provide details on animals and/or animal-derived materials used in the study.

In this study were used athymic nu/nu female mice (AnLab Ltd.) median age 13 weeks (+/- 1 week) and SCID female mice (ENVIGO, NL) median age 10 weeks (+/- 2 weeks).

Policy information about [studies involving human research participants](#)

## 12. Description of human research participants

Describe the covariate-relevant population characteristics of the human research participants.

Human participants were 4 males (age of 34, 38, 41, 60 years) and 5 females (age of 37, 56, 46, 59, 63 years). All freshly diagnosed for alcohol use disorder and dedicated for Antabuse therapy. Blood samples were collected before and after first application of Antabuse.

## Flow Cytometry Reporting Summary

Form fields will expand as needed. Please do not leave fields blank.

### ► Data presentation

For all flow cytometry data, confirm that:

- 1. The axis labels state the marker and fluorochrome used (e.g. CD4-FITC).
- 2. The axis scales are clearly visible. Include numbers along axes only for bottom left plot of group (a 'group' is an analysis of identical markers).
- 3. All plots are contour plots with outliers or pseudocolor plots.
- 4. A numerical value for number of cells or percentage (with statistics) is provided.

### ► Methodological details

5. Describe the sample preparation.

Cell cultures were treated as indicated and harvested by trypsinization. Initial culture medium and wash buffer were collected to include detached cells. Cells were centrifuged (250g, 5min) and resuspended in staining buffer (140 mM NaCl, 4 mM KCl, 0.75 mM MgCl<sub>2</sub>, 10 mM HEPES). Then cell number was determined and after centrifugation, cells were resuspended in appropriate amount of staining buffer to get concentration of 1million cells per 900 microliters. For annexinV analysis, 1x10<sup>5</sup> cells was incubated in 100 microliters of staining buffer containing 2.5 mM CaCl<sub>2</sub>, Annexin V-APC (1:20, BD Biosciences) and 2.5 µg/ml 7-AAD (BD Biosciences) for 15 minutes on ice in the dark. For caspases 3/7 activity assay 1x10<sup>5</sup> cells was incubated in 100 microliters of staining buffer supplemented with 2% FBS, 0.5 µM CellEvent™ Caspase-3/7 Green Detection Reagent (ThermoFisher Scientific) for 45 minutes at room temperature in the dark. Subsequently, 0.5 µg/mL DAPI was added before analysis by flow cytometry. Samples were analyzed by flow cytometry using BD FACSVersé (BD Biosciences), at least 10.000 events were acquired per sample . Collected data were processed by BD FACSSuite (BD Biosciences).

6. Identify the instrument used for data collection.

BD FACSVersé (BD Biosciences) equipped with 405nm,488nm and 640nm lasers, manufactured in october 2012.

7. Describe the software used to collect and analyze the flow cytometry data.

BD FACSSuite (BD Biosciences)

8. Describe the abundance of the relevant cell populations within post-sort fractions.

cell sorting not employed

9. Describe the gating strategy used.

Using the FSC/SSC gating, debris was removed by gating on the main cell population. Positivity threshold for each cell line was defined on the basis of mock-treated (DMSO) sample. Identical positivity threshold was applied to all samples within cell line.

Tick this box to confirm that a figure exemplifying the gating strategy is provided in the Supplementary Information.

#### 8.3.4. Appendix D

**Turi, Z.;** Lacey, M.; Mistrik, M; Moudry, P. Impaired ribosome biogenesis: mechanisms and relevance to cancer and aging. *Aging*. In press (**2019**). IF (2019) not defined yet

# Impaired ribosome biogenesis: mechanisms and relevance to cancer and aging

Zsofia Turi<sup>1</sup>, Matthew Lacey<sup>1</sup>, Martin Mistrik<sup>1</sup>, Pavel Moudry<sup>1</sup>

<sup>1</sup>Institute of Molecular and Translational Medicine, Faculty of Medicine and Dentistry, Palacky University, 779 00 Olomouc, Czech Republic

**Correspondence to:** Pavel Moudry; email: [pavel.moudry@upol.cz](mailto:pavel.moudry@upol.cz)

**Keywords:** ribosome biogenesis, ribosomopathy, aging, cancer, p53

**Received:** December 11, 2018

**Accepted:** April 4, 2019

**Published:** April 26, 2019

**Copyright:** Turi et al. This is an open-access article distributed under the terms of the Creative Commons Attribution License (CC BY 3.0), which permits unrestricted use, distribution, and reproduction in any medium, provided the original author and source are credited.

## ABSTRACT

The biosynthesis of ribosomes is a complex process that requires the coordinated action of many factors and a huge energy investment from the cell. Ribosomes are essential for protein production, and thus for cellular survival, growth and proliferation. Ribosome biogenesis is initiated in the nucleolus and includes: the synthesis and processing of ribosomal RNAs, assembly of ribosomal proteins, transport to the cytoplasm and association of ribosomal subunits. The disruption of ribosome biogenesis at various steps, with either increased or decreased expression of different ribosomal components, can promote cell cycle arrest, senescence or apoptosis. Additionally, interference with ribosomal biogenesis is often associated with cancer, aging and age-related degenerative diseases. Here, we review current knowledge on impaired ribosome biogenesis, discuss the main factors involved in stress responses under such circumstances and focus on examples with clinical relevance.

## INTRODUCTION

The nucleolus has gained prominent attention in molecular research over the past two decades, due to its emerging role in various cellular processes. Among them, the production of ribosomes is seemingly the most important, as it controls translation of all proteins in the cell and thus governs cell growth and proliferation [1]. The nucleolus is a subnuclear, membrane-less organelle, formed in early G1 phase of the cell cycle around the short arms of acrocentric chromosomes (chromosome 13, 14, 15, 21 and 22), in nucleolar organizer regions (NORs). These NORs contain the ribosomal DNA (rDNA) genes, arranged in tandem repeats and transcribed by RNA Polymerase I (Pol I) [2]. The resulting single polycistronic transcript, known as 47S pre-rRNA, is further modified in the nucleolus. The maturation of the primary transcript is initiated co-transcriptionally and the main processing steps involve endo- and exonucleolytic cleavages,

pseudouridylation and 2'-O-methylation which lead to the emergence of three ribosomal RNA (rRNA) species: 18S, 5.8S and 28S rRNAs. While 18S rRNA is incorporated into the small ribosomal subunit (SSU), 5.8S and 28S rRNAs, along with 5S rRNA, are members of the large ribosomal subunit (LSU) [3]. The gene encoding 5S rRNA is an exception when compared to other rRNA genes as it is located on chromosome 1 and transcribed by RNA Polymerase III (Pol III) in the nucleus [4, 5]. The protein components of the ribosome are 80 ribosomal proteins (RPs), which are transcribed in the nucleus by RNA Polymerase II (Pol II) and translated in the cytoplasm. However, both the 5S rRNA and the RPs need to be imported into the nucleolus in order to be incorporated into the ribosome [6]. During late ribosome maturation, the forming subunits are first moved into the nucleus, followed by transport to the cytoplasm where ribosomes can fully assemble and assume their protein-translation function [3].

It can be readily accepted that ribosome biosynthesis consumes most of the cell's energy, particularly when compared to other biological processes, as it requires the synthesis of the most abundant RNA and protein species in the cell. This not only includes the concerted action of all three RNA polymerases and the cell's translation apparatus, but also the activity of more than 200 non-ribosomal factors within the nucleolus [7, 8]. Therefore, it is not surprising that cellular signaling networks which sense the nutrient status, growth factors, extra- and intracellular stress levels affect the rate of ribosome biogenesis, mainly by altering the activity of Pol I [9, 10]. Disruption of ribosome biogenesis also promotes signaling pathways that lead to cell cycle arrest and cellular senescence or apoptosis [8, 11]. The earliest observation that impaired ribosome biogenesis halts cell cycle progression comes from a study by Volarevic et al., where they described that the conditional knockout of ribosomal protein *RPS6* (*eS6*) causes cell cycle arrest in mouse liver cells [12]. Since then, a number of studies have demonstrated that the disruption of virtually any step in ribosome biogenesis can result in cell cycle arrest, primarily through activation of the tumor suppressor protein p53. This particular process was recently termed as the Impaired Ribosome Biogenesis Checkpoint (IRBC) [13].

Impaired ribosome biogenesis is usually best visible as structural alterations of the nucleolus which can be seen also in various human diseases [14-17]. Importantly, increased size of nucleoli usually reflects intense ribosome biogenesis and has been recognized by physicians for a long time as a hallmark of many tumor types [18]. Interestingly, despite excessive ribosome biogenesis being believed to drive the fast proliferation of cancer cells, some of the most rapidly dividing tumor cells do not display this phenotype [19]. Moreover, patients with another group of human diseases called ribosomopathies, are prone to developing various kinds of tumors. Ribosomopathies are characterized by mutations in RPs or ribosome biogenesis factors, showing a decreased rate of ribosome biosynthesis due to deficiencies of these components required in the ribosome biogenesis pathway. Symptoms of these disorders arise from tissue specific growth arrest and/or incompetent translation. There is a wide spectrum of phenotypes displayed by ribosomopathy patients and affected tissues frequently show upregulation of p53 as a consequence of IRBC [20, 21]. Altered ribosome biogenesis was also connected to aging and it is also relevant in neurodegenerative disorders such as: Alzheimer, Parkinson, Huntington and other advanced age-related diseases (for more details on this topic see the following reviews [16, 17]). However, the exact contribution of IRBC to these complex disorders and aging remains an intriguing question open to further research.

In this review, we summarize the most important steps of ribosome biogenesis, focusing mainly on human cell culture studies. Furthermore, we describe the main effectors of IRBC and review studies that provide evidence for the existence of this pathway as well as examining the clinical relevance of IRBC in aging and age-related diseases.

## Ribosome biogenesis

Ribosome biogenesis begins with rRNA synthesis in the nucleolus. As a first step a pre-initiation complex (PIC) is formed around the rDNA promoter region. The PIC itself consists of the upstream binding factor (UBF), selectivity factor (SL1 also known as TIF1-B), transcription initiation factor 1A (TIF1-A or hRRN3) and Pol I. UBF marks the promoter regions by binding as a homodimer to the core promoter surrounding the transcription start site and to the upstream core element (UCE), thereby creating a DNA loop structure. Next, SL1 is recruited to the promoter: binding to both UBF and the rDNA. The interaction of TIF1-A with Pol I is essential for its recruitment to the promoter and formation of the complete PIC. Promoter opening and escape is also stimulated by UBF and is accompanied by the release of TIF1-A from the Pol I complex [22, 23]. Surprisingly, UBF was shown to bind the whole length of rDNA transcript units, and it has been suggested that it is involved in the control of elongation process as well [24]. Transcription termination occurs when Pol I encounters transcription termination factor 1 (TTF-1)-bound terminator elements, the stalled Pol I is subsequently removed by the polymerase I and transcript release factor (PTRF) [25].

In contrast to the synthesis of 47S rRNA, the precursor of 5S rRNA is transcribed by Pol III in the nucleoplasm. The main factors involved in this process are the transcription factors IIIA, IIIB and IIIC (TFIIIA, TFIIIB and TFIIIC), which are responsible for labeling of the promoter region and the recruitment of Pol III [5, 26].

The rate of ribosome production is regulated mainly on the level of rRNA synthesis. This is carried out by a number of factors and signaling pathways which are dependent on various cellular needs, such as the availability of nutrients, and the presence of mitogenic or stress signaling [10]. Mitogenic stimuli activate several, typically oncogenic pathways which upregulate rDNA transcription. For example, MAPK/ERK pathway phosphorylates UBF, TIF1-A and TFIIIB to stimulate Pol I and Pol III mediated rRNA transcription, respectively [27-30]. Moreover, both MAPK/ERK and PI3K/AKT signaling activate the expression of c-Myc [31, 32], which can boost ribosome biogenesis at multiple levels. It stimulates the formation of PIC by

recruiting SL1 to the rDNA promoter, increasing the activity of Pol II to drive transcription of RP genes while simultaneously upregulating Pol III transcription by activating TFIIB [33-35]. Furthermore, growth factors also activate the mammalian target of rapamycin (mTOR) signaling network which contributes to the activation of UBF, TIF1-A and Pol III associated transcription factors TFIIB and TFIIC [36-38]. Additionally, p53 is also involved, both directly and indirectly, in the control of Pol I transcription. It interacts with SL1 to prevent its recruitment to rDNA promoters, thus inhibiting Pol I transcription [39], and also limits Pol III activity via the direct binding of TFIIB [40]. One of the main transcriptional targets of p53 is p21, which is able to activate the retinoblastoma protein (pRb) through the inhibition of CDKs [41, 42]. Besides its well-known role in cell cycle regulation, pRb is able to bind to several ribosome biogenesis factors, like UBF and TFIIB to suppress rRNA transcription [43-45].

Transcription of rDNA results in the emergence of a single polycistronic primary transcript, known as the 47S rRNA. This transcript contains 18S, 5.8S and 28S rRNAs separated by internal transcribed spacers (ITS1 and ITS2) and flanked by external transcribed spacers (5'-ETS and 3'-ETS). Over the course of rRNA maturation, the ITSs and ETSs are removed by the combined action of endo- and exonucleases. The processing of the 47S pre-rRNA is initiated co-transcriptionally by the formation of the so-called small subunit (SSU) processome [3]. The recruitment of the transcriptional U three protein (t-UTP) complex to the 5' end of the 47S pre-rRNA belongs among the earliest steps of SSU processome formation. t-UTPs strictly colocalize with the Pol I transcription machinery; forming bead-like structures during active transcription in the nucleolus [46]. Subsequently, t-UTPs and other SSU processome factors initiate the early processing steps of 18S rRNA [46]. Importantly, a cleavage in the ITS1 region separates the processing pathways of the two subunits (for more information on the topic of rRNA processing refer to one of the following reviews [3, 47]).

The maturation of rRNA is coordinated mainly by box C/D and box H/ACA small nucleolar ribonucleoprotein complexes (snoRNPs), named after a specific motif of the RNA component, which catalyze site-specific 2'-O-methylation and pseudouridylation of rRNA species respectively. Box C/D snoRNPs are composed of the methyltransferase fibrillarin (FBL), accessory proteins Nop56, Nop58, and 15.5K/NHPX along with the snoRNA component. The snoRNA hybridizes to the pre-rRNA to bring it into the proper conformation to be accessible for methylation by FBL. Furthermore, FBL's

function is not limited to the methylation of pre-rRNA, when it forms a complex with e.g. U3, U8 or U14 box C/D snoRNAs, it is also involved in chaperoning and directing the pre-rRNA for endo- and exonucleolytic cleavages [48]. Box H/ACA snoRNPs consist of the pseudouridine synthase dyskerin, the accessory proteins Nhp2, Nop10, Gar1 and the H/ACA snoRNA component [48]. Box H/ACA snoRNPs operate similarly to box C/D snoRNPs, besides their function in site-specific pseudouridylation and cleavage of rRNA, box H/ACA RNPs are also involved in other cellular processes such as: mRNA splicing, production of miRNAs and telomere maintenance [48, 49].

In addition to snoRNPs, numerous other proteins (e.g. ATPases, GTPases, RNA helicases) are also implicated in rRNA processing. By chaperoning rRNA to facilitate proper folding, or by the removal of processing factors from the rRNA, these factors allow subsequent rRNA maturation steps and the assembly of RPs onto the rRNA to proceed [3]. An example of this is the multifunctional protein nucleolin (NCL), which is involved in multiple stages of ribosome biogenesis. NCL is recruited to the rRNA genes and interacts with both the promoter and the coding regions to facilitate transcription elongation by Pol I [50]. Furthermore, as a histone chaperone, NCL can bind to H2A-H2B dimers to promote their dissociation from the nucleosome and stimulate chromatin remodelers, like SWI/SNF and ACF, thereby increasing the rate of transcription [51]. NCL is also involved in rRNA maturation, as it binds to a specific site in the 5'-ETS region of the pre-rRNA and has a role in the cleavage of this site possibly by facilitating the action of its interaction partner, U3 snoRNA [52, 53]. Moreover, NCL was demonstrated to interact with a subset of RPs and have an important function in the pre-ribosome assembly [54, 55].

Nucleophosmin (NPM) is another multifunctional protein that is involved in ribosome biogenesis at multiple levels. Similarly to NCL, NPM is a histone chaperone, with the ability to stimulate rRNA transcription [56]. The requirement of NPM for rRNA processing was first described by Savkur and Olson in 1998. This study demonstrated that NPM is involved in the cleavage of pre-rRNA in the ITS2 region to promote the release of 28S rRNA [57]. These results were confirmed later on, as downregulation of NPM led to the impairment of this processing step [58]. Furthermore, NPM has been demonstrated to have a role in the nuclear export of RPL5 (uL18) and the pre-ribosomal subunits [59, 60]. Additionally, NPM has been implicated in numerous other cellular processes such as: centrosome duplication, regulation of cell cycle and maintenance of genome stability [61].



In parallel with the rRNA processing the newly synthesized RPs are imported into the nucleus and assemble onto the pre-ribosomal subunits [3]. Since nascent RPs in the cytoplasm are readily degraded by the proteasome, their nuclear import has to occur immediately following their synthesis [62, 63]. The nuclear import of RPs is an active, energy-dependent process facilitated by several proteins of the  $\beta$ -karyopherin family. Importin- $\beta$ , transportin, RanBP5 and RanBP7 have been reported to promote the nuclear import of RPL23A (uL23), RPS7 (eS7) and RPL5 [64], while importin-11 was suggested to be a mediator of RPL12 (uL11) transport [65]. Furthermore, importin-7 was shown to participate in the nuclear import of several RPs, such as RPL4 (uL4), RPL6 (eL6) and RPL23A [66]. Once in the nucleus or nucleolus, RPs are believed to be actively involved in rRNA maturation presumably by stabilizing the secondary structure of the pre-rRNA. The incorporation of RPs into the pre-ribosome occurs in a highly hierarchical order, which correlates to the level of rRNA processing they are involved in, during either the early or late phases of maturation [3].

In addition to its synthesis, the maturation and assembly of 5S rRNA into the LSU is also exceptional. The pre-

cursor of the 5S rRNA is matured in the nucleus and is assembled shortly after maturation; adding two LSU RPs, RPL5 and RPL11 (uL5) to the structure. As a ternary complex, the 5S RNP is incorporated into the pre-60S subunit [67, 68].

Similar to the nuclear import of RPs, the export of the pre-40S and pre-60S particles occurs through an energy-dependent process, which is also facilitated by  $\beta$ -karyopherins. Most importantly, exportin-1 is involved in the export of both of the pre-ribosomal subunits [69]. After their transport into the cytoplasm, pre-40S and pre-60S ribosomal subunits undergo the final maturation steps which include the dissociation of the remaining non-ribosomal proteins and the association of last RPs into their subunits [70]. Finally, the mature SSU and LSU particles can be joined together during translation initiation to fulfil their protein production function [71].

### Impaired ribosome biogenesis

Ribosome biogenesis is an extremely energy-demanding process, which cells utilize for their growth and proliferation. In the case of impaired ribosome biogenesis, cells must immediately shut down their cell

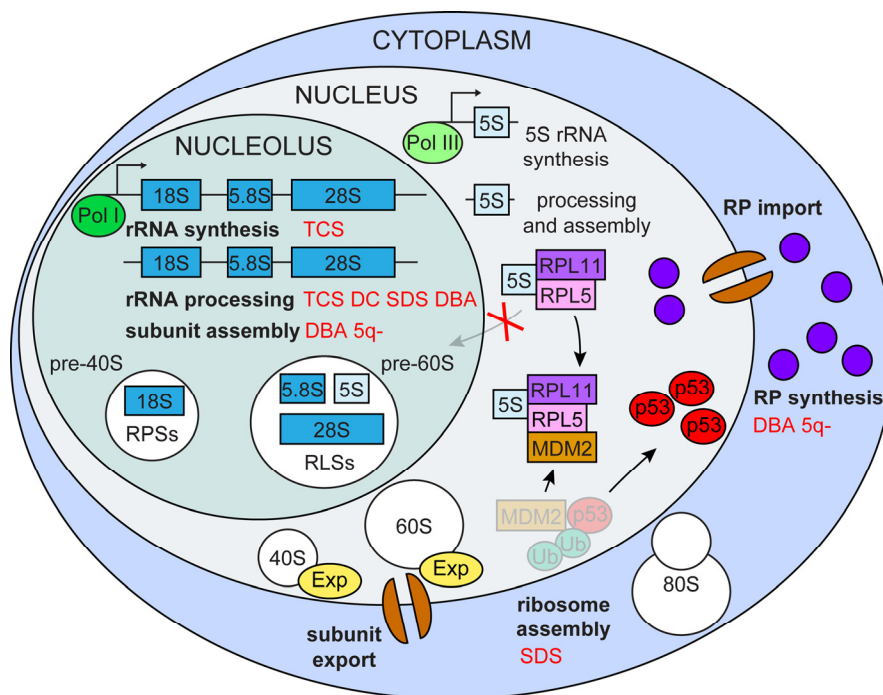


**Figure 1. Impaired ribosome biogenesis.** Impairment of multiple ribosome biogenesis stages (in bold black) activate p53 via the RPL5/RPL11/5S rRNA/Mdm2 pathway and is associated with various ribosomopathies (in red) TCS (Treacher Collins syndrome), DC (dyskeratosis congenital), SDS (Shwachman-Diamond syndrome), DBA (Diamond-Blackfan anemia) 5q- (5q- syndrome).

cycle to avoid incomplete growth and unprepared division. The central player in this control is the tumor suppressor protein p53 (Figure 1).

### Activation of p53 by impaired ribosome biogenesis

Under normal conditions the level of p53 in cells is kept low, despite the fact that it is continuously expressed. Downregulation of p53 is ensured post-translationally by Mdm2, an E3 ubiquitin ligase [72-74]. Mdm2 forms a heterodimer with its inactive paralogue MdmX and their interaction is required for the stability of the complex [75]. Ubiquitylation of p53 by Mdm2 stimulates the nuclear export of p53 and its degradation by the 26S proteasome [76]. In addition, the interaction between Mdm2 and p53 counteracts p53's transactivating activity; the ability to trigger the expression of its target genes [77]. Once stabilized, p53 is also responsible for the transactivation of Mdm2, providing a negative feedback loop to quench its own activity after the activating stress has been overcome [78, 79].

Perturbation of ribosome biogenesis promotes the recruitment and binding of a group of RPs and nucleolar factors to the Mdm2 central acidic domain, thereby disrupting its interaction with p53 which is then no longer degraded and thus becomes activated [8, 80]. Although Mdm2 binding activity, and thus the ability to induce p53 was shown for multiple RPs, it is generally accepted that RPL5 and RPL11 have major roles in p53 activation in response to ribosomal stress. This effect is best illustrated when Pol I is inhibited by, for example, a low dose of actinomycin D (ActD) treatment, which normally induces a p53 response. In the absence of RPL5 and/or RPL11 ActD induced p53 stabilization is largely inhibited. Interestingly, depletion of other RPs cannot abolish p53 activation in this manner [81, 82]. While most RPs are still synthesized during impaired ribosome biogenesis, they are rapidly degraded by the proteasome [63, 82, 83]. However, under these conditions RPL5 and RPL11 are able to accumulate in a ribosome free fraction, as a result of their mutual protection from proteasomal degradation, further supporting the central function of these proteins in IRBC [82]. Moreover, the assembly of RPL5 and RPL11 into the 5S RNP complex is continued even when ribosome biogenesis is impaired; the formation of this particle is essential for the binding of Mdm2 by these RPs [84]. Furthermore, the association of such a complex might render RPL5 and RPL11 more resistant to degradation when compared to other RPs.

The source of the Mdm2 binding RPs that are involved in IRBC is an intriguing question. In most cases, impairment of ribosome biogenesis leads to the disintegration of the nucleolar structure leading to

spontaneous release of RPs and other nucleolar proteins into the nucleoplasm. Thus, disruption of the nucleoli seems to be an important prerequisite for p53 activation [85]. However, this logical proposal was questioned by Fumagalli et al. who demonstrated that RPS6 silencing, which inhibits SSU biogenesis, does not disrupt nucleolar structure, while p53 still accumulates via IRBC. It turned out that under these conditions translation of 5' terminal oligopyrimidin tract containing messenger RNAs (5'-TOP mRNAs), including RPL11 and RPL5 mRNA, is upregulated [81, 86]. The newly synthesized RPs are then actively imported into the nucleus to promote a p53-dependent response while nucleolar structure stays intact [8, 87]. Furthermore, it has been also demonstrated that even when disintegration of the nucleoli occurs upon impaired ribosome biogenesis, the induction of p53 relies on the presence of nascent RPL5 and RPL11 proteins [82]. Thus, while disruption of the nucleolus might be only a consequence of perturbed ribosome biogenesis, the conditions and mechanisms which induce such morphological changes remain unclear.

Besides RPL5 and RPL11, there is another nucleolar factor, called alternative reading frame protein (ARF), which is capable of binding to Mdm2 and thereby promotes the activation of p53 [88]. ARF is a tumor suppressor protein encoded by the *INK4A* locus, which also encodes a cyclin-dependent kinase (CDK) inhibitor termed p16 using alternative reading frame of the same genetic locus [88, 89]. Under normal conditions, ARF is expressed at low levels and sequestered into the nucleolus by NPM [90]. ARF is typically activated by oncogenes, which overstimulate ribosome biogenesis to gain excessive growth potential. Under such stimuli, ARF is released to the nucleoplasm where, similarly to RPs, it interacts with the central acidic domain of Mdm2 and indirectly promotes the stabilization of p53 [88, 91, 92]. Consequently, it was demonstrated that the absence of NPM triggers p53-mediated apoptosis through the activation of ARF [93]. Additionally, excessive quantities of ARF was shown to promote the degradation of NPM and therefore inhibit ribosome biogenesis [58]. This was suggested to induce 5S RNP mediated IRBC, implicating an interplay between the two pathways [87]. Moreover, ARF has a direct inhibitory effect on ribosome biogenesis; by suppressing the phosphorylation of UBF and the nucleolar import of TTF-1 it is able to shutdown rRNA synthesis, which triggers IRBC [87, 94, 95]. Surprisingly, one study demonstrated that overexpression of NPM also promotes the upregulation of p53, since NPM is also capable of interacting directly with Mdm2 to prevent p53's degradation [96]. Overexpression of NPM also inhibits the translocation of p53 from the nucleus to mitochondria, which prevents the activation of the so

called intrinsic apoptotic pathway [97]. However, upon apoptotic stimuli, NPM display pro-apoptotic activity as it translocates to the cytoplasm, where NPM binds the pro-apoptotic BAX protein, triggering cytochrome-c release from the mitochondria [98]. This dual function of NPM in the apoptotic process depicts the numerous functions of NPM in cells, which often differ depending on the conditions.

It is also worth mentioning that several studies have uncovered that activated IRBC also promotes cell cycle arrest through p53-independent pathways. For instance, RPL11 is capable of promoting the degradation of E2F-1 by binding to Mdm2 [99, 100]; E2F-1 is a transcription factor that is required for cell cycle progression [101]. Since nearly half of human cancers have inactivated p53 [102], discovering p53-independent pathways of IRBC, makes ribosome biogenesis relevant therapeutic target in cancer research (for more detailed reviews see [11, 87, 103, 104]).

### Impaired rRNA synthesis

Perturbation of rRNA synthesis at multiple levels was shown to activate IRBC. It has been demonstrated by numerous studies that the induction of IRBC and the stabilization of p53 can be achieved by different conditions of inhibited Pol I transcription, including: the silencing of *POLR1A*, a gene encoding the catalytic subunit of Pol I [105]; knockout of the *TIF1-A* gene [106]; or inactivation of UBF by a monoclonal antibody [85]. Impairment of the Pol I transcription machinery can also be accomplished by using several small molecule inhibitors. For instance, the DNA intercalating agent ActD is a very potent inhibitor of rRNA synthesis; it intercalates into the DNA at guanosine-cytosine (GC) rich regions which are mainly present in rDNA genes. Therefore, at lower concentrations it preferentially inhibits transcription by Pol I [107, 108]. Several studies showed that ActD causes severe stress through this mechanism, disrupts the nucleolar structure and strongly induces p53 [11, 85, 104]. BMH-21, a newly identified drug has a similar mechanism of action, as it also intercalates into the GC-rich rDNA. Besides its incorporation into the rDNA, BMH-21 also promotes the proteasomal degradation of Pol I [109, 110]. Other chemical compounds employ different mechanisms to suppress rRNA synthesis. CX-3543 (quarfloxin) inhibits transcription elongation by disrupting the interaction of NCL with rDNA [111], and CX-5461 prevents the recruitment of SL1 to rDNA promoters [112]. Both drugs are potent inducers of the IRBC response. Furthermore, CX-5461 showed a preferential toxicity in some cancer cells compared to normal primary cells, causing p53-dependent apoptosis in E $\mu$ -*Myc* lymphoma cells [113], as well as inducing

p53-independent senescence and autophagy in solid tumor cell lines [112]. CX-5461 quickly advanced to phase I clinical trials [113-115], representing an example of therapeutic potential in targeting ribosome biogenesis. Of note, a recent study showed that in addition to their inhibitory effect on rDNA transcription, both CX-5461 and CX-3543 elicit cytotoxicity through induction of DNA damage [116]. Mechanistically, these drugs bind to and stabilize the four stranded DNA structures, G-quadruplexes (G4), thereby causing replication-dependent DNA damage [111, 116]. Elimination of G4 structures is carried out mainly by the homologous recombination (HR) machinery, therefore cancer cells deficient in HR components are particularly sensitive to these drugs [116]. Thus, besides the activation of IRBC, DNA damage induction also contributes to the increased sensitivity of cancer cells towards CX-5461 and CX-3543.

Impairment of the Pol III transcription machinery was also investigated by several research groups. Depletion of the *POLR3A* gene, which encodes the catalytic subunit of Pol III, impairs 5S rRNA biosynthesis and leads to cell cycle arrest in a p53-independent manner [117]. Since 5S rRNA is the essential component of 5S RNP, formed during both intact and impaired ribosome biogenesis, perturbation of its biosynthesis diminishes the formation of the ternary RNP complex which is involved in p53 stabilization. This may explain the lack of p53 induction in Pol III depleted cells [84]. Furthermore, deficiency of TFIIIA, which is involved exclusively in 5S rRNA transcription [118, 119], also led to p53-independent cell cycle arrest and could reverse the activation of p53 induced by Pol I depletion, supporting the hypothesis that 5S rRNA is essential for the induction of p53 in IRBC [68, 84, 117, 120].

Consequences of impaired rRNA synthesis and activated IRBC are well represented by patients suffering from Treacher Collins syndrome (TCS). TCS is a severe craniofacial disease with symptoms including: micrognathia, retrognathia, coloboma of the lower eyelids, loss of medial eyelashes, external ear aplasia or microtia, a large or protruding nose and zygomatic bone hypoplasia [121, 122]. TCS is an autosomal dominant disorder mainly caused by mutations in the *TCOF1* gene. A minority of TCS cases (~8%) are associated with mutations in the *POLR1C* and *POLR1D* genes, which encode the RPAC1 and RPAC2 proteins, respectively. Both RPAC1 and RPAC2 proteins are parts of the RNA polymerase I and III complexes [123, 124]. The *TCOF1* gene encodes a protein named Treacle, which has a prominent role in both rRNA synthesis and the early processing steps [125, 126]. Haploinsufficiency of Treacle disrupts ribosome bio-

genesis, leading to the activation of IRBC and the initiation of p53-mediated apoptosis specific to the neural crest cells during early embryogenesis. The affected stem cell population is responsible for the formation of the bone, cartilage and connective tissue of the head [127, 128]. The strong connection of IRBC and p53-induced neural crest cell apoptosis with the pathogenesis of TCS was shown in the mouse model of the disease. Similarly to TCS patients, Treacle haploinsufficient mice display severe craniofacial abnormalities. Importantly, this phenotype can be reversed either by the chemical inhibition or genetic inactivation of p53 [129]. Recent findings suggest that TCOF1 is involved in the DNA damage response (DDR) and this might also contribute to TCS pathology. It was shown by several groups that upon DNA damage DDR protein NBS1 is relocated to the nucleolus, where it interacts with TCOF1 in a CK2- and ATM-dependent manner in order to suppress rRNA transcription [130, 131]. Interestingly, neuroepithelial cells, including progenitors of neural crest cells, have been reported to exhibit increased amount of DNA damage in a *Tcof1*<sup>+/-</sup> background. The accumulation of DNA damage has been suggested to be a consequence of the higher level of reactive oxygen species (ROS) produced in this tissue [132]. Since ROS are potent inducers of DNA damage [133, 134], proficient expression of TCOF1 in neural crest cells is essential. Indeed, the administration of the antioxidant N-acetyl-cysteine partially reduced craniofacial malformations in *Tcof1*<sup>+/-</sup> mouse embryos and accumulation of p53 [132], indicating that both DNA damage and the IRBC contribute to TCS pathology. Additionally, a recent study provides insight into pathogenesis and tissue-specificity of TCS. Calo et al. reported that upon TCOF1 depletion the nucleolar RNA helicase DDX21 redistributes to the nucleoplasm, leading to the inhibition of ribosome biogenesis [135]. Interestingly, such disruptions in the localization of DDX21 seem to be specific for cranial neural crest cells and depletion of DDX21 alone has been presented to induce craniofacial malformations [135]. The authors suggest that rDNA damage that occurs as a consequence of impaired Pol I transcription machinery induces p53 activation and DDX21 relocation, followed by apoptosis in tissues, which are hypersensitive to elevated levels of p53 [135]. These findings add novel layers to the research of ribosomopathies and offer new therapeutic avenues for the small group of TCS patients.

### Impaired rRNA maturation

rRNA processing is initiated co-transcriptionally and early processing factors, such as the t-UTP complex and Treacle, have been shown to have an important role in facilitating both rRNA synthesis and maturation.

Therefore, perturbation of ribosome biogenesis due to the absence of these early processing factors leads to a drop in rRNA synthesis and impaired rRNA processing as well [46, 125, 126]. We have recently demonstrated that the depletion of one such early factor, HEAT repeat containing 1 (HEATR1) activates IRBC. Impaired expression of HEATR1 strongly induced p53 and p53-dependent cell cycle arrest. In this scenario activation of p53 was triggered by IRBC, evidenced by the robust disruption of the nucleolar structure and the emergence of Mdm2-RPL5 interaction. Furthermore, under these conditions p53 induction can be reversed by concomitant depletion of RPL5 or RPL11 [136]. UTP10, the yeast homolog of HEATR1 is a member of the t-UTP complex and has been demonstrated to have a role in rRNA synthesis as well as in early steps of pre-rRNA processing [137-139]. Correspondingly, we and others have demonstrated that human HEATR1 positively regulates rRNA synthesis and co-localizes with the Pol I transcription machinery regardless of active transcription [46, 136]. Upon impaired rRNA synthesis, HEATR1, along with other Pol I associated factors, is redistributed to the periphery of the nucleolus to form so-called nucleolar caps; structures characteristic for impaired rDNA transcription [46, 136, 140]. Moreover, this localization appears to be solely dependent on UBF [46]. In addition, similarly to UTP10, HEATR1 has also been shown to be involved in the early 18 S rRNA maturation [46]. The exact function of HEATR1 in rRNA synthesis and processing remains largely unknown. However, as it possesses a C-terminal HEAT repeat, a motif suggested to mediate protein-protein interactions, HEATR1 might promote connections between the Pol I transcription machinery and rRNA processing factors. Analogous results, i.e. repressed transcription and processing of rRNA and IRBC activation, were obtained for other yeast t-UTP homologs, such as: 1A6/DRIM [141], WDR43 [142] and NOL11 [143].

Depletion, mutation or overexpression of numerous subsequent processing factors have been shown to impair rRNA maturation and induce IRBC [144-147]. Downregulation of the box C/D snoRNP component FBL is one such an example; it has been shown to impair rRNA processing and activate the IRBC pathway which leads to p53-mediated apoptosis in embryonic stem cells [148]. Similarly, depletion of box C/D snoRNAs, such as U3 and U8 has been proposed to induce IRBC, resulting in a very potent induction of p53 [149]. Both, FBL and U3 or U8 expression has been shown to be upregulated in several cancer types, indicating their potential involvement in tumorigenesis [149-153]. High FBL expression led to the alteration of the 2'-O-methylation pattern of rRNA and translational infidelity. Moreover, the altered methylation of the

rRNA also promoted the internal ribosome entry site (IRES)-dependent translation of proto-oncogenic mRNAs, such as IGF1R, MYC, FGF1/2 and VEGFA [154]. An abnormal rRNA methylation pattern has been observed in aggressive breast cancer, where it induces a decrease in the IRES-dependent translation of p53, which contributes to tumor progression [153]. Additionally, opposing these effects, p53 was demonstrated to counteract such harmful methylation pattern by directly inhibiting the expression of FBL [154]. Consistently, recent study by Sharma et al. showed that p53 depletion results in a robust increase in the level of FBL and introduces alterations in the methylation pattern of rRNAs. In addition, FBL ablation promotes the loss of mainly peripheral 2-O-methylated sites [155].

Mutations of the box H/ACA snoRNP component dyskerin encoding gene *DKC1* is associated with a rare genetic condition known as X-linked form of dyskeratosis congenita (X-DC). Dyskeratosis congenita (DC) is a premature aging syndrome characterized by the classical triad of mucocutaneous symptoms: abnormal pigmentation of the skin, nail dystrophy and leukoplakia of the oral mucosa. The most common cause of death is bone marrow failure, but further symptoms may also include: pulmonary fibrosis, increased risk for various malignancies, mental retardation, ophthalmic, skeletal, gastrointestinal and genitourinary abnormalities [156, 157]. The pathogenesis of DC was originally thought to be a consequence of impaired rRNA processing, caused by mutations of dyskerin [49]. However, dyskerin is also a component of the telomerase complex, formed from the box H/ACA telomerase RNA component (TERC), telomerase reverse transcriptase (TERT) and the box H/ACA snoRNA associated proteins [49, 156]. Patients with X-DC show accelerated telomere shortening, which mainly affects the rapidly dividing stem and progenitor cell populations. The possibility that DC is actually a telomerase dysfunction disorder is supported by the occurrence of DC due to mutations of TERT and TERC in the autosomal dominant form of the disease [49, 156, 158]. Furthermore, while depletion of dyskerin in human fibroblasts leads to early activation of p53, presumably through the IRBC pathway, similar upregulation of p53 was only observed later in the fibroblasts of patients with X-DC or autosomal dominant DC [159]. However, in the latter case p53 activation is actually the result of DNA damage arisen from telomere attrition after cells go through several cycles of population doubling [158, 159]. In agreement with this, most of the mutations in *DKC1* gene affect the RNA binding domain, which is involved in association with TERC, rather than affecting catalytic activity or the expression level of dyskerin in X-DC

cases [156, 160]. *DKC1* mutations also seem to cause altered rRNA pseudouridylation, which impairs the IRES-dependent translation of a specific group of tumor suppressor mRNAs, including: p53, the CDK inhibitor p27 and the anti-apoptotic proteins XIAP and BCL-X<sub>L</sub>. Thus, impaired rRNA processing might contribute to the cancer susceptibility observed in X-DC patients [161, 162]. In addition, similarly to FBL, the overexpression of dyskerin has also been associated with cancer [163, 164], likely contributing via the dysregulated rRNA pseudouridylation, but precise mechanism is not known.

Due to their importance in ribosome biogenesis, depletion of the multifunctional proteins NCL or NPM impairs this process at multiple levels; in the case of NCL, it has been demonstrated to result in the activation of p53, presumably via IRBC [51, 165]. Importantly, overexpression of NCL has been documented in many types of cancer [166]. This upregulation of NCL might promote tumorigenesis by increasing the rate of rRNA transcription and thus enhance ribosome production [167-169]. Apart from that, NCL was shown to also be involved in other cellular processes such as: chromatin organization, DNA and RNA metabolism, angiogenesis, cytokinesis, telomere maintenance, cell growth and proliferation, all of which can contribute to the tumorigenic potential of upregulated NCL [166, 167, 170]. Due to its high expression level NCL represents an interesting target for cancer therapy [167]. Indeed, aptameric compound AS1411, a G-rich oligonucleotide which binds to NCL with high affinity, counteracts NCL's RNA binding activity and induces apoptosis in various cancer cells [171, 172]. The therapeutic potential of AS1411 was already presented in a phase I trial for patients with different kinds of advanced cancer [173, 174] and phase II trials for patients with advanced renal cell carcinoma and acute myeloid leukemia (AML) [175, 176].

In contrast to other nucleolar processing factors, by binding to Mdm2, NPM has been shown to be actively involved in IRBC [96]. While another study reported that ablation of NPM also induces the upregulation of p53 through the activation of ARF [93]. Consistent with these rather conflicting results, NPM has been demonstrated to display both pro-oncogenic and tumor suppressive functions during tumorigenesis [61, 177, 178]. Overexpression of NPM has in fact been reported in many types of solid tumors [179-189]. Its role in tumorigenesis is commonly linked to its function in ribosome biogenesis. Interestingly, low levels of NPM have also been reported for certain cancers; such as gastric or breast cancer [190, 191]. Furthermore, mutations and rearrangements of the *NPM1* gene are often seen in numerous hematological malignancies

[177, 192, 193]. The involvement and importance of NPM in tumorigenesis, particularly in cases when it is upregulated, makes it an attractive target for cancer therapy. Indeed, several small molecule inhibitors of NPM have been tested in preclinical studies and clinical trials [194]. One such promising compound is NSC348884 which, by binding to NPM, is able to dissociate ARF from the complex with NPM; thereby inducing the upregulation of p53, which subsequently triggers apoptosis [195]. Furthermore, this compound has been shown to efficiently induce cytotoxicity in preclinical studies involving solid and hematological cancers [195, 196], however clinical trials of NSC348884 has not been initiated to date.

### RP imbalance and impaired pre-ribosome assembly

The activation of p53 via the downregulation of both SSU and LSU RPs has been consistently demonstrated by multiple studies [81, 82, 86, 197-204]. Phenotypic consequences of the RP deficiency are well represented by a rare autosomal dominant disorder called Diamond Blackfan anemia (DBA), which is a bone marrow failure syndrome due to elevated apoptosis of the erythroid progenitor cells [202, 205, 206]. Patients suffering from DBA often show other symptoms as well, including: short stature, craniofacial, cardiac or genitourinary abnormalities and predisposition to cancer [157, 206]. Mutations in a subset of both 40S and 60S RP genes are observed in approximately 50% of DBA cases; the molecular background of the remaining cases is unknown [206-208]. In the most cases of DBA, disruption of the *RPS19* (*eS19*) gene is observed, however several patients show mutations of: *RPL5*, *RPL11*, *RPL15* (*eL15*), *RPL36* (*eL36*), *RPL35A* (*eL33*), *RPS7*, *RPS10* (*eS10*), *RPS17* (*eS17*), *RPS24* (*eS24*), *RPS26* (*eS26*) or *RPS27A* (*eS31*) genes. These mutations cause the haploinsufficiency of the certain RP and most likely impair the global translational capacity of the cells [205, 207]. In erythroid progenitors such insufficiency reduces the production of hemoglobin, leading to increased amount of free heme which has strong pro-oxidative potential. Elevated oxidative stress then leads to p53-independent apoptosis of these cells [209, 210]. This theory was well supported by a mouse model where the gene for Feline Leukemia Virus Subgroup Receptor 1 (FLVCR1), a heme exporter protein, was deleted. FLVCR1-null mice exhibit increased intracellular heme and show a phenotype resembling DBA [211]. Since the RPs which are commonly mutated in DBA patients are involved also in several diverse steps of ribosome biogenesis, their reduced expression also activates the IRBC and subsequent p53-dependent apoptosis [21, 210]. Such IRBC activation is indeed detectable as accumulation of p53 has been shown in DBA-patients' bone marrow

samples [202]. Similarly, some mouse and zebrafish models of DBA, which show a similar, but not completely overlapping phenotype with impaired erythropoiesis, also have upregulated p53 [212-215]. The contribution of IRBC- and heme-induced apoptosis to the resulting DBA phenotype was studied by p53 inactivation in various models. While in zebrafish p53 inactivation only rescued developmental abnormalities, but did not affect the observed defective erythropoiesis, in mouse models inactivation of p53 reversed the apoptosis of erythroid progenitors [212, 214, 215].

Another ribosomopathy characterized by the reduced expression of an RP is 5q<sup>-</sup> syndrome, which is often referred to as a somatically acquired form of DBA. The 5q<sup>-</sup> syndrome is a myelodysplastic disease, which is predominantly present in women of advanced age and is caused by the deletion of the long arm of chromosome 5. Similarly to DBA, it is also characterized by disrupted erythropoiesis in the bone marrow, causing macrocytic anemia and a predisposition to AML. Although the extensive deletion of chromosome 5 q arm results in the loss of about 40 genes, *RPS14* (*uS11*) seems to be particularly important for the pathogenesis of the disease [205, 216-219]. This is illustrated by mouse models with haploinsufficiency of *RPS14* which recapitulate the human phenotype and also show upregulation of p53. In these mouse models, genetic inactivation of p53 was sufficient to rescue apoptosis of bone marrow progenitors [219]. Additionally, an increased level of p53 was also represented in hematopoietic cells of 5q<sup>-</sup> patients [202, 217].

Overall, due to the involvement of RPs in ribosome biogenesis a decrease in their expression leads to the initiation of the IRBC pathway. The subsequent stabilization and activation of p53 resulting in p53-dependent apoptosis seems to be the main cause of the pathogenesis of these diseases. However, active IRBC alone does not explain the tissue-specific effects of defective RPs in either of the aforementioned diseases. The sensitivity of erythroid progenitors is explained by an increased dependence on ribosome biogenesis due to rapid cell division combined with additional oxidative stress caused by the heme overload [21, 209]. The relative contribution of IRBC *versus* oxidative stress to the apoptosis of erythroid progenitors remains an unanswered question.

In contrast to the decreased expression of RPs, the selective overexpression of certain RPs has been observed in multiple types of cancer, suggesting an active role in tumorigenesis [6]. For instance, *RPS13* (*uS15*) and *RPL23* (*uL14*) were shown to be up-

regulated in gastric cancer contributing to the multidrug resistance of these cells [220].

### **Impaired RP import and pre-ribosome export**

Golomb et al. demonstrated that depletion of  $\beta$ -karyopherin importin-7, not only disrupts the nuclear import of some RPs, but also causes the disruption of the nucleolar structure and activates IRBC, leading to p53 stabilization and activation [221]. In addition to  $\beta$ -karyopherins, other transport adaptor proteins might also be involved in the nuclear import of RPs. Lately, symportin-1 was identified as a crucial protein required for the co-import of RPL5 and RPL11 in yeast [222]. Furthermore, symportin-1 in *Chaetomium thermophilum* might also serve as a molecular chaperon for the assembly of RPL5 and RPL11 with 5S rRNA, to form the 5S RNP complex, which is able to subsequently incorporate into the LSU [223]. Whether human homolog of symportin-1, HEAT repeat containing protein 3 (HEATR3), has analogous functions remains to be investigated. Since 5S RNP is the main mediator of IRBC (as discussed above), impairment of the chaperoning of this complex might counteract the activation of the IRBC pathway and as a consequence could potentially lead to tumorigenesis.

Depletion or leptomycin-B-mediated pharmacological inhibition of exportin-1 inhibits the nuclear export of the premature subunits, induces morphological alterations of the nucleolus and activates p53 through IRBC [221]. Therefore, the disruption of either the import of RPs or the export of the pre-ribosomal particles is able to elicit the IRBC response.

As with the other steps of ribosome biogenesis, the transport of RPs and pre-ribosomal subunits also appears to be upregulated in cancer. For instance, the nuclear import of RPs was reported to be upregulated by the mTOR and c-Myc oncogenic pathways [221, 224]. Moreover, c-Myc is also required for the upregulation of exportin-1 expression [221]. Thus, targeting  $\beta$ -karyopherins involved in ribosome biogenesis might be an appealing approach for cancer therapy; although, it is important to bear in mind that these transport adaptor proteins have a large subset of cargo proteins which are involved in other cellular processes as well.

### **Impaired assembly of ribosomal subunits**

One of the most important steps to initiate the subunit assembly is the release of the eukaryotic translation initiation factor 6 (eIF6) from the LSU, which is promoted by the GTPase activity of elongation factor

like-1 (EFL1). Interestingly, ribosome maturation is abrogated at this step in a human autosomal recessive disorder, called Shwachman-Diamond syndrome (SDS) [225-227]. SDS is another bone marrow failure syndrome, with additional symptoms, including: exocrine pancreatic insufficiency, gastrointestinal, skeletal, immune system abnormalities and predisposition to AML [208, 228, 229]. Biallelic mutations in the *SBDS* gene is present in 90% of SDS cases. Ribosome maturation protein SBDS is required for the EFL1-promoted removal of eIF6 from the 60S ribosomal subunit, thus governing the final assembly of the ribosome [225-227]. Furthermore, SBDS was also reported to localize into the nucleolus [230], where it interacts with the 28S rRNA and NPM, which implies that it might have additional functions in the earlier steps of ribosome biogenesis as well [231]. The involvement of SBDS in both early and late steps of ribosome biogenesis is consistent with the observation of upregulated p53 in SDS patient-derived samples, presumably a consequence of active IRBC [232, 233]. However, concomitant depletion of p53 in zebrafish and mouse models of SDS only partially rescues the pathologic phenotype; indicating that insufficient translation, alongside with activated IRBC and up-regulated p53, has a prominent role in the pathogenesis of the disease [234, 235].

### **Aberrant ribosome biogenesis and aging**

Numerous studies presented a direct connection between dysregulated ribosome biogenesis and aging. For instance, the downregulation of ribosome biogenesis components or nutrient sensing pathways, which stimulate ribosome production, have been shown to increase the lifespan of multiple organisms including *C. elegans*, *D. melanogaster*, yeast, mice and human [236-249]. Therefore, enhanced ribosome biogenesis, visualized by enlarged nucleoli, is believed to accelerate aging. Indeed, consistent with this idea, the size of the nucleoli and the amount of rRNA increases during aging in human primary fibroblasts and a single, large nucleolus is often observed in senescent cells [250, 251]. Furthermore, fibroblasts isolated from patients suffering from the premature aging disease Hutchinson-Gilford progeria, have enlarged nucleoli and upregulated ribosome biogenesis [251]. Since the rate of protein translation is proportional to the rate of ribosome biogenesis [22, 252] it was suggested that upregulation of protein synthesis and disruption of global proteostasis is the mechanism through which ribosome biogenesis promotes aging [253]. This theory is supported by studies showing that reduction in the rate of translation can increase lifespan, and furthermore that altered proteostasis is a hallmark of aging [238, 254-258]. Additionally, caloric restriction that has been

shown to promote longevity [259-261], leads to the downregulation of ribosome biogenesis by several mechanisms [262-264]. Under such dietary conditions, deacetylase SIRT1 is induced [265, 266]. SIRT1, as a component of the energy dependent nucleolar silencing complex (eNoSC), is responsible for the epigenetic silencing of rDNA gene expression [264] and its overexpression can extend the lifespan [267]. Furthermore, a higher rate of metabolism and reduced amount of the tumor suppressors p53 and ARF might also contribute to aging [268, 269].

### **Accumulation of DNA damage in rDNA**

Besides direct changes in rDNA expression level and/or rate of ribosome biogenesis, another theory relates to the accumulation of rDNA damage for aging. The repetitive nature of rDNA and the high rate of rRNA synthesis cause the rDNA repeats to be subject to recombination events and DNA damage, possibly due to collisions between the replication and transcription machineries and R-loop formations [270-274]. As a result, DNA damage can accumulate in rDNA, this in turn can lead to genome instability, which has also been implicated in cellular aging [258, 275]. Indeed, it has been recently demonstrated that hematopoietic stem cells, which are highly proliferative, and thus have upregulated ribosome biogenesis, accumulate DNA damage in their rDNA genes during aging [276]. Moreover, premature aging diseases, such as Bloom and Werner syndromes are associated with increased rDNA instability [277-279]. BLM and WRN helicases, that are mutated in Bloom and Werner syndromes, respectively have been shown to associate with the Pol I transcription machinery and promote rRNA synthesis [280, 281]. These findings indicate that rDNA instability in these diseases can be attributed to disrupted rRNA transcription and consequent accumulation of rDNA damage due to unresolved rDNA structures.

### **Deregulation of ribosome biogenesis in aging**

Several studies have reported the downregulation of ribosome biogenesis in aged tissues. A progressive decrease in the expression of RPs or rRNA has been observed during the aging process [282, 283], inefficient ribosome biogenesis has been accounted for age-related cataract [284] and diminished skeletal muscle hypertrophy [285]. On the other hand, it has been suggested that such decrease of ribosome biosynthesis may be a compensatory mechanism in aged tissues to prolong lifespan [283].

Being an age-related disease, upregulation of ribosome biogenesis and increased size of the nucleoli have been observed in various types of cancer cells [18].

Numerous reports suggests that rather than being a passive consequence of tumorigenesis, upregulation of ribosome biogenesis is a key step to promote this process [113, 162, 286]. The increase in the rate of ribosome biogenesis drives translation, excess growth and proliferation [287] and the selective upregulation of certain ribosome biogenesis components in many cases contributes to tumorigenesis. For instance, overexpression of key rRNA processing factors, such as FBL or dyskerin has been reported in various cancers [150-153, 163, 164]. Upregulation of FBL or dyskerin alters the posttranscriptional modification of the rRNAs, thus changes the structure of the ribosomes. These altered ribosomes presumably do not change the amount of total protein production, however they affect the quality of translation [288]. Marcel et al. designated these altered complexes ‘cancer ribosomes’ in FBL upregulated cells, because of their active involvement in tumorigenesis due to preference for IRES-dependent translation of oncogene mRNAs [154]. Moreover, FBL overexpression has been observed in aged mice [289] and lower expression of it seems to be associated with increased lifespan in humans [262]. Additionally, similarly to FBL and dyskerin, selective overexpression of certain RPs has been reported to promote tumorigenesis [220, 290, 291]. Changes in the balance of the RPs might change the structure of the ribosome; however, since many of these RPs possess extra-ribosomal functions, these cannot be excluded from contribution to tumorigenesis.

A high rate of ribosome biogenesis and enlarged nucleoli are the main characteristics of stem cells as well as cancer cells. Similarly to cancer cells, stem cells rely on ribosome biogenesis for their growth and proliferation and it also ensures pluripotency [148, 292-294]. During differentiation these cells lose high expression of ribosome biogenesis factors and obtain shrunken nucleoli [295]. Several studies have demonstrated that partial depletion of certain nucleolar factors involved in ribosome biosynthesis induces differentiation of pluripotent stem cells [148, 292, 294, 296, 297]. Furthermore, complete loss of some ribosome biogenesis components affects stem cells more drastically, when compared to differentiated cells [148, 297]. Consistently, decreased expression of ribosome biosynthesis factors observed in ribosomopathies induces growth arrest and apoptosis in hematopoietic or other stem cell types, while differentiated cells remain mostly unaffected. Furthermore, although upregulation of ribosome biogenesis is traditionally associated with aging and cancer, downregulation of this process can also promote tumorigenesis, as patients with ribosomopathies are predisposed to development of certain cancer types [20, 205, 208]. This can be explained as a result of a lower amount of available



mature ribosomes introducing competition between various mRNAs. Thus tumor suppressors encoding mRNAs with lower affinity to the ribosome may lose their translational capacity [287]. High and stable expression of p53 can decrease lifespan in mice and humans [298-300], therefore it is possible that upregulated p53 usually observed in ribosomopathies can also contribute to accelerated aging of those patients. Indeed, one of the ribosomopathies, dyskeratosis congenita has been associated with premature aging. Whether this is a more general feature that is also shared by other ribosomopathies needs further investigation. Although, both upregulation and downregulation of ribosome biogenesis can accelerate aging process, timing of the downregulation of the ribosome biogenesis is important factor that must be considered. While numerous studies show that an overall decrease in ribosome biogenesis promotes longevity, it must occur in the post-developmental phase. When it is downregulated early in life, as in the case of ribosomopathies, it has more severe consequences, which reduce lifespan [301].

Although differentiated, non-dividing cells usually display shrunken nucleoli and reduced rate of ribosome biogenesis, prominent nucleoli can be observed in terminally differentiated neurons [17]. It has been demonstrated that during development, post-mitotic neurons rely on increased ribosome biogenesis for their somatoneuritic growth [302, 303]. Specifically, neurotrophics, such as the brain-derived neurotrophic factor (BDNF) stimulate ribosome biosynthesis, through the ERK1/2 signaling cascade [302]. Consequently, upregulated ribosome biogenesis supply developing neurites with a sufficient number of ribosomes for the increased local protein synthesis to promote morphogenesis of the neurons [17, 302]. Furthermore, it has been also suggested that neurite outgrowth, which is promoted in mature neurons during regeneration of the nerves following injury, depends on the upregulation of ribosome biogenesis [304, 305].

### **Ribosome biogenesis and neurodegenerative diseases**

The importance of active ribosome biogenesis in mature neurons is further supported by the observation that it is frequently impaired in neurodegenerative diseases. For instance, Alzheimer's disease (AD) has been reported to associate with reduced number of the ribosomes [306], which may be the linked to the increased oxidation of rRNA [307, 308] and/or epigenetic silencing of rDNA, seen in AD patient's brains [309, 310]. Furthermore, aberrant NORs have been also observed in AD patients [311]. Additionally, the microtubule-associated protein, tau, whose function is severely impaired in AD, has been reported to localize to the nucleolus, where it

interacts with several nucleolar proteins and may have a role in several nucleolus-associated functions under normal conditions [312-315]. Downregulation of ribosome biogenesis has also been documented in Parkinson's disease (PD), which is often accompanied with disrupted nucleolar structure of the affected dopaminergic neurons [316, 317]. This phenotype may be mediated by NCL, since its expression has been reported to be decreased in the *substantia nigra* of PD patients [318]. Furthermore, NCL has been also documented to interact with  $\alpha$ -synuclein and DJ-1, the two major proteins involved in the pathogenesis of familial PD [319]. Moreover, a mutation of DJ-1 has been presented to impair ribosome biogenesis by the exclusion of TNF receptor associated protein (TTRAP) from the nucleolus [320]. Whereas another study on PD has been reported that the overexpression of parkin associated substrate (PARIS) represses rRNA transcription by direct interaction with the Pol I transcription machinery [321]. Several factors perturbing ribosome biogenesis have been observed in Huntington's disease (HD) as well. For instance, the PIC component, UBF has been shown to be downregulated in HD patients [322]. UBF's function and thus rRNA synthesis has been also suggested to be inhibited via the decreased acetylation and/or increased methylation of UBF, both mediated by the mutant huntingtin protein [322, 323]. Furthermore, it has been also suggested that the CAG triplet expansion containing transcripts, characteristic of HD, are able to associate with NCL and this interaction leads to the reduced recruitment and binding of NCL to the rDNA promoter, followed by promoter hypermethylation and results in the rRNA synthesis suppression [324]. Overall, numerous studies indicate that impaired ribosome biogenesis is a key feature of neurodegeneration. The diversity and complexity of mechanisms that perturb this process indicate the existence of more factors capable of impairing ribosome biogenesis in these syndromes with a rather heterogeneous genetic background. Additionally, since the accumulation of p53 has been reported in AD, PD and HD [325-327], the activation of IRBC is evident and may be fundamental for the pathology of these diseases.

Although the complex relationship between aging, age-related diseases and ribosome biogenesis and the regulation thereof is just being elucidated, the importance of the tight regulation of these processes is evident from these examples.

### **CONCLUSION**

In the past decades, a tremendous effort was made to explore the various steps of ribosome biogenesis and the regulation of this process. It has long been acknowledged that due to its complexity, ribosome biogenesis

requires a huge energy investment from cells. Therefore, it is regulated by numerous complex pathways. The impairment of ribosome biogenesis, at any step from rRNA synthesis to ribosome assembly, has been demonstrated to result in severe consequences such as: cell cycle arrest, senescence or apoptosis mainly through the RPL5/RPL11/5S rRNA/Mdm2/p53 axis. Although the process of IRBC is well-established and widely accepted, further research is ongoing. For instance, it is not fully understood how the defects in various steps of ribosome biogenesis are sensed and transduced to uniformly induce IRBC.

The dependence of ribosome biogenesis on the nutrient and energy status of cells renders the entire process highly vulnerable to internal and external stress stimuli. Indeed, multiple studies have reported that a number of typical cellular stressors, such as: DNA damaging agents (UV- and  $\gamma$ -irradiation, genotoxic chemotherapeutics); hypoxia, nutrient and growth factor deprivation; heat shock and oncogene activation induce alterations in ribosome biogenesis and ultimately activate the IRBC [328]. Consistently, a report from Burger and colleagues showed that a diverse group of commonly used chemotherapeutic drugs (e.g. alkylating agents, antimetabolites, mitosis inhibitors, kinase inhibitors, translation inhibitors, etc.), are all capable of perturbing ribosome biogenesis [108]. Interestingly, the stage of ribosome biogenesis inhibition differed between these compounds; some of them suppressed the process earlier while others inhibited later steps [108]. These results suggest that chemotherapeutic agents induce IRBC, which might contribute to their cytotoxicity. IRBC-induced apoptosis or senescence might be beneficial for cancer therapeutics, since cancer cells highly rely on ribosome production for their growth and proliferation. However, traditional chemotherapeutic drugs possess other cytotoxic effects such as: genotoxicity, nucleotide deprivation, inhibition of signal transduction, and others which poison non-cancerous cells as well. Therefore, it might be more favorable to take advantage of those compounds, which are rather specific and exclusively inhibit ribosome biogenesis. However, these agents must still be treated with caution, as other populations of rapidly dividing cells, such as stem cells might be sensitive to the perturbation of ribosome biogenesis. Other therapeutic approaches, targeting the various steps of ribosome biogenesis may be a valid therapeutic strategy, as selective upregulation of some ribosome biosynthesis factors is observed in various cancers.

## CONFLICTS OF INTEREST

The authors declare no conflicts of interest.

## FUNDING

The work was supported by the Grant Agency of the Czech Republic (17-14743S and 17-25976S), the Internal Grant of Palacky University (IGA-LF-2019-026) and the European Regional Development Fund - Project ENOCH (No. CZ.02.1.01/0.0/0.0/16\_019/0000868

## REFERENCES

1. Rudra D, Warner JR. What better measure than ribosome synthesis? *Genes Dev.* 2004; 18:2431–36. <https://doi.org/10.1101/gad.1256704>
2. McStay B. Nucleolar organizer regions: genomic ‘dark matter’ requiring illumination. *Genes Dev.* 2016; 30:1598–610. <https://doi.org/10.1101/gad.283838.116>
3. Henras AK, Plisson-Chastang C, O’Donohue MF, Chakraborty A, Gleizes PE. An overview of pre-ribosomal RNA processing in eukaryotes. *Wiley Interdiscip Rev RNA.* 2015; 6:225–42. <https://doi.org/10.1002/wrna.1269>
4. Sørensen PD, Frederiksen S. Characterization of human 5S rRNA genes. *Nucleic Acids Res.* 1991; 19:4147–51. <https://doi.org/10.1093/nar/19.15.4147>
5. Paule MR, White RJ. Survey and summary: transcription by RNA polymerases I and III. *Nucleic Acids Res.* 2000; 28:1283–98. <https://doi.org/10.1093/nar/28.6.1283>
6. Wang W, Nag S, Zhang X, Wang MH, Wang H, Zhou J, Zhang R. Ribosomal proteins and human diseases: pathogenesis, molecular mechanisms, and therapeutic implications. *Med Res Rev.* 2015; 35:225–85. <https://doi.org/10.1002/med.21327>
7. Fromont-Racine M, Senger B, Saveanu C, Fasiolo F. Ribosome assembly in eukaryotes. *Gene.* 2003; 313:17–42. [https://doi.org/10.1016/S0378-1119\(03\)00629-2](https://doi.org/10.1016/S0378-1119(03)00629-2)
8. Golomb L, Volarevic S, Oren M. p53 and ribosome biogenesis stress: the essentials. *FEBS Lett.* 2014; 588:2571–79. <https://doi.org/10.1016/j.febslet.2014.04.014>
9. Grummt I. Life on a planet of its own: regulation of RNA polymerase I transcription in the nucleolus. *Genes Dev.* 2003; 17:1691–702. <https://doi.org/10.1101/gad.1098503R>
10. Grummt I. Wisely chosen paths--regulation of rRNA synthesis: delivered on 30 June 2010 at the 35th FEBS Congress in Gothenburg, Sweden. *FEBS J.* 2010; 277:4626–39.

<https://doi.org/10.1111/j.1742-4658.2010.07892.x>

11. James A, Wang Y, Raje H, Rosby R, DiMario P. Nucleolar stress with and without p53. *Nucleus*. 2014; 5:402–26. <https://doi.org/10.4161/nucl.32235>
12. Volarević S, Stewart MJ, Ledermann B, Zilberman F, Terracciano L, Montini E, Grompe M, Kozma SC, Thomas G. Proliferation, but not growth, blocked by conditional deletion of 40S ribosomal protein S6. *Science*. 2000; 288:2045–47. <https://doi.org/10.1126/science.288.5473.2045>
13. Gentilella A, Morón-Duran FD, Fuentes P, Zweig-Rocha G, Riaño-Canalias F, Pelletier J, Ruiz M, Turón G, Castaño J, Tauler A, Bueno C, Menéndez P, Kozma SC, Thomas G. Autogenous Control of 5'TOP mRNA Stability by 40S Ribosomes. *Mol Cell*. 2017; 67:55–70.e4. <https://doi.org/10.1016/j.molcel.2017.06.005>
14. Hariharan N, Sussman MA. Stressing on the nucleolus in cardiovascular disease. *Biochim Biophys Acta*. 2014; 1842:798–801. <https://doi.org/10.1016/j.bbadis.2013.09.016>
15. Salvetti A, Greco A. Viruses and the nucleolus: the fatal attraction. *Biochim Biophys Acta*. 2014; 1842:840–47. <https://doi.org/10.1016/j.bbadis.2013.12.010>
16. Parlato R, Liss B. How Parkinson's disease meets nucleolar stress. *Biochim Biophys Acta*. 2014; 1842:791–97. <https://doi.org/10.1016/j.bbadis.2013.12.014>
17. Hetman M, Pietrzak M. Emerging roles of the neuronal nucleolus. *Trends Neurosci*. 2012; 35:305–14. <https://doi.org/10.1016/j.tins.2012.01.002>
18. Montanaro L, Treré D, Derenzini M. Nucleolus, ribosomes, and cancer. *Am J Pathol*. 2008; 173:301–10. <https://doi.org/10.2353/ajpath.2008.070752>
19. Zink D, Fischer AH, Nickerson JA. Nuclear structure in cancer cells. *Nat Rev Cancer*. 2004; 4:677–87. <https://doi.org/10.1038/nrc1430>
20. Armistead J, Triggs-Raine B. Diverse diseases from a ubiquitous process: the ribosomopathy paradox. *FEBS Lett*. 2014; 588:1491–500. <https://doi.org/10.1016/j.febslet.2014.03.024>
21. Danilova N, Gazda HT. Ribosomopathies: how a common root can cause a tree of pathologies. *Dis Model Mech*. 2015; 8:1013–26. <https://doi.org/10.1242/dmm.020529>
22. Russell J, Zomerdijk JC. RNA-polymerase-I-directed rDNA transcription, life and works. *Trends Biochem Sci*. 2005; 30:87–96. <https://doi.org/10.1016/j.tibs.2004.12.008>
23. Albert B, Perez-Fernandez J, Léger-Silvestre I, Gadal O. Regulation of ribosomal RNA production by RNA polymerase I: does elongation come first? *Genet Res Int*. 2012; 2012:276948. <https://doi.org/10.1155/2012/276948>
24. O'Sullivan AC, Sullivan GJ, McStay B. UBF binding in vivo is not restricted to regulatory sequences within the vertebrate ribosomal DNA repeat. *Mol Cell Biol*. 2002; 22:657–68. <https://doi.org/10.1128/MCB.22.2.657-668.2002>
25. Jansa P, Grummt I. Mechanism of transcription termination: PTRF interacts with the largest subunit of RNA polymerase I and dissociates paused transcription complexes from yeast and mouse. *Mol Gen Genet*. 1999; 262:508–14. <https://doi.org/10.1007/s004380051112>
26. Ciganda M, Williams N. Eukaryotic 5S rRNA biogenesis. *Wiley Interdiscip Rev RNA*. 2011; 2:523–33. <https://doi.org/10.1002/wrna.74>
27. Stefanovsky V, Langlois F, Gagnon-Kugler T, Rothblum LI, Moss T. Growth factor signaling regulates elongation of RNA polymerase I transcription in mammals via UBF phosphorylation and r-chromatin remodeling. *Mol Cell*. 2006; 21:629–39. <https://doi.org/10.1016/j.molcel.2006.01.023>
28. Stefanovsky VY, Moss T. The splice variants of UBF differentially regulate RNA polymerase I transcription elongation in response to ERK phosphorylation. *Nucleic Acids Res*. 2008; 36:5093–101. <https://doi.org/10.1093/nar/gkn484>
29. Zhao J, Yuan X, Frödin M, Grummt I. ERK-dependent phosphorylation of the transcription initiation factor TIF-IA is required for RNA polymerase I transcription and cell growth. *Mol Cell*. 2003; 11:405–13. [https://doi.org/10.1016/S1097-2765\(03\)00036-4](https://doi.org/10.1016/S1097-2765(03)00036-4)
30. Felton-Edkins ZA, Fairley JA, Graham EL, Johnston IM, White RJ, Scott PH. The mitogen-activated protein (MAP) kinase ERK induces tRNA synthesis by phosphorylating TFIIB. *EMBO J*. 2003; 22:2422–32. <https://doi.org/10.1093/emboj/cdg240>
31. Zhu J, Blenis J, Yuan J. Activation of PI3K/Akt and MAPK pathways regulates Myc-mediated transcription by phosphorylating and promoting the degradation of Mad1. *Proc Natl Acad Sci USA*. 2008; 105:6584–89. <https://doi.org/10.1073/pnas.0802785105>
32. Mendoza MC, Er EE, Blenis J. The Ras-ERK and PI3K-mTOR pathways: cross-talk and compensation. *Trends Biochem Sci*. 2011; 36:320–28. <https://doi.org/10.1016/j.tibs.2011.03.006>

33. Gomez-Roman N, Felton-Edkins ZA, Kenneth NS, Goodfellow SJ, Athineos D, Zhang J, Ramsbottom BA, Innes F, Kantidakis T, Kerr ER, Brodie J, Grandori C, White RJ. Activation by c-Myc of transcription by RNA polymerases I, II and III. *Biochem Soc Symp.* 2006; 73:141–54. <https://doi.org/10.1042/bss0730141>
34. van Riggelen J, Yetil A, Felsher DW. MYC as a regulator of ribosome biogenesis and protein synthesis. *Nat Rev Cancer.* 2010; 10:301–09. <https://doi.org/10.1038/nrc2819>
35. White RJ. RNA polymerases I and III, growth control and cancer. *Nat Rev Mol Cell Biol.* 2005; 6:69–78. <https://doi.org/10.1038/nrm1551>
36. Mayer C, Grummt I. Ribosome biogenesis and cell growth: mTOR coordinates transcription by all three classes of nuclear RNA polymerases. *Oncogene.* 2006; 25:6384–91. <https://doi.org/10.1038/sj.onc.1209883>
37. Woiwode A, Johnson SA, Zhong S, Zhang C, Roeder RG, Teichmann M, Johnson DL. PTEN represses RNA polymerase III-dependent transcription by targeting the TFIIIB complex. *Mol Cell Biol.* 2008; 28:4204–14. <https://doi.org/10.1128/MCB.01912-07>
38. Kantidakis T, Ramsbottom BA, Birch JL, Dowding SN, White RJ. mTOR associates with TFIIIC, is found at tRNA and 5S rRNA genes, and targets their repressor Maf1. *Proc Natl Acad Sci USA.* 2010; 107:11823–28. <https://doi.org/10.1073/pnas.1005188107>
39. Zhai W, Comai L. Repression of RNA polymerase I transcription by the tumor suppressor p53. *Mol Cell Biol.* 2000; 20:5930–38. <https://doi.org/10.1128/MCB.20.16.5930-5938.2000>
40. Crighton D, Woiwode A, Zhang C, Mandavia N, Morton JP, Warnock LJ, Milner J, White RJ, Johnson DL. p53 represses RNA polymerase III transcription by targeting TBP and inhibiting promoter occupancy by TFIIIB. *EMBO J.* 2003; 22:2810–20. <https://doi.org/10.1093/emboj/cdg265>
41. Gartel AL, Tyner AL. Transcriptional regulation of the p21((WAF1/CIP1)) gene. *Exp Cell Res.* 1999; 246:280–89. <https://doi.org/10.1006/excr.1998.4319>
42. Harper JW, Elledge SJ, Keyomarsi K, Dynlacht B, Tsai LH, Zhang P, Dobrowski S, Bai C, Connell-Crowley L, Swindell E. Inhibition of cyclin-dependent kinases by p21. *Mol Biol Cell.* 1995; 6:387–400. <https://doi.org/10.1091/mbc.6.4.387>
43. Cavanaugh AH, Hempel WM, Taylor LJ, Rogalsky V, Todorov G, Rothblum LI. Activity of RNA polymerase I transcription factor UBF blocked by Rb gene product. *Nature.* 1995; 374:177–80. <https://doi.org/10.1038/374177a0>
44. Hannan KM, Hannan RD, Smith SD, Jefferson LS, Lun M, Rothblum LI. Rb and p130 regulate RNA polymerase I transcription: rb disrupts the interaction between UBF and SL-1. *Oncogene.* 2000; 19:4988–99. <https://doi.org/10.1038/sj.onc.1203875>
45. Scott PH, Cairns CA, Sutcliffe JE, Alzuherri HM, McLees A, Winter AG, White RJ. Regulation of RNA polymerase III transcription during cell cycle entry. *J Biol Chem.* 2001; 276:1005–14. <https://doi.org/10.1074/jbc.M005417200>
46. Prieto JL, McStay B. Recruitment of factors linking transcription and processing of pre-rRNA to NOR chromatin is UBF-dependent and occurs independent of transcription in human cells. *Genes Dev.* 2007; 21:2041–54. <https://doi.org/10.1101/gad.436707>
47. Mullineux ST, Lafontaine DL. Mapping the cleavage sites on mammalian pre-rRNAs: where do we stand? *Biochimie.* 2012; 94:1521–32. <https://doi.org/10.1016/j.biochi.2012.02.001>
48. Watkins NJ, Bohnsack MT. The box C/D and H/ACA snoRNPs: key players in the modification, processing and the dynamic folding of ribosomal RNA. *Wiley Interdiscip Rev RNA.* 2012; 3:397–414. <https://doi.org/10.1002/wrna.117>
49. Angrisani A, Vicidomini R, Turano M, Furia M. Human dyskerin: beyond telomeres. *Biol Chem.* 2014; 395:593–610. <https://doi.org/10.1515/hsz-2013-0287>
50. Cong R, Das S, Ugrinova I, Kumar S, Mongelard F, Wong J, Bouvet P. Interaction of nucleolin with ribosomal RNA genes and its role in RNA polymerase I transcription. *Nucleic Acids Res.* 2012; 40:9441–54. <https://doi.org/10.1093/nar/gks720>
51. Angelov D, Bondarenko VA, Almagro S, Menoni H, Mongelard F, Hans F, Miettton F, Studitsky VM, Hamiche A, Dimitrov S, Bouvet P. Nucleolin is a histone chaperone with FACT-like activity and assists remodeling of nucleosomes. *EMBO J.* 2006; 25:1669–79. <https://doi.org/10.1038/sj.emboj.7601046>
52. Ginisty H, Amalric F, Bouvet P. Nucleolin functions in the first step of ribosomal RNA processing. *EMBO J.* 1998; 17:1476–86. <https://doi.org/10.1093/emboj/17.5.1476>
53. Ginisty H, Serin G, Ghisolfi-Nieto L, Roger B, Libante V, Amalric F, Bouvet P. Interaction of nucleolin with an evolutionarily conserved pre-ribosomal RNA sequence is required for the assembly of the primary processing complex. *J Biol Chem.* 2000; 275:18845–50. <https://doi.org/10.1074/jbc.M002350200>
54. Bouvet P, Diaz JJ, Kindbeiter K, Madjar JJ, Amalric F. Nucleolin interacts with several ribosomal proteins through its RGG domain. *J Biol Chem.* 1998; 273:19025–29.

- <https://doi.org/10.1074/jbc.273.30.19025>
55. Roger B, Moisan A, Amalric F, Bouvet P. Nucleolin provides a link between RNA polymerase I transcription and pre-ribosome assembly. *Chromosoma*. 2003; 111:399–407. <https://doi.org/10.1007/s00412-002-0221-5>
  56. Murano K, Okuwaki M, Hisaoka M, Nagata K. Transcription regulation of the rRNA gene by a multifunctional nucleolar protein, B23/nucleophosmin, through its histone chaperone activity. *Mol Cell Biol*. 2008; 28:3114–26. <https://doi.org/10.1128/MCB.02078-07>
  57. Savkur RS, Olson MO. Preferential cleavage in pre-ribosomal RNA by protein B23 endoribonuclease. *Nucleic Acids Res*. 1998; 26:4508–15. <https://doi.org/10.1093/nar/26.19.4508>
  58. Itahana K, Bhat KP, Jin A, Itahana Y, Hawke D, Kobayashi R, Zhang Y. Tumor suppressor ARF degrades B23, a nucleolar protein involved in ribosome biogenesis and cell proliferation. *Mol Cell*. 2003; 12:1151–64. [https://doi.org/10.1016/S1097-2765\(03\)00431-3](https://doi.org/10.1016/S1097-2765(03)00431-3)
  59. Yu Y, Maggi LB Jr, Brady SN, Apicelli AJ, Dai MS, Lu H, Weber JD. Nucleophosmin is essential for ribosomal protein L5 nuclear export. *Mol Cell Biol*. 2006; 26:3798–809. <https://doi.org/10.1128/MCB.26.10.3798-3809.2006>
  60. Maggi LB Jr, Kuchenruether M, Dadey DY, Schwoppe RM, Grisendi S, Townsend RR, Pandolfi PP, Weber JD. Nucleophosmin serves as a rate-limiting nuclear export chaperone for the mammalian ribosome. *Mol Cell Biol*. 2008; 28:7050–65. <https://doi.org/10.1128/MCB.01548-07>
  61. Box JK, Paquet N, Adams MN, Boucher D, Bolderson E, O’Byrne KJ, Richard DJ. Nucleophosmin: from structure and function to disease development. *BMC Mol Biol*. 2016; 17:19. <https://doi.org/10.1186/s12867-016-0073-9>
  62. Warner JR, Mitra G, Schwindinger WF, Studeny M, Fried HM. *Saccharomyces cerevisiae* coordinates accumulation of yeast ribosomal proteins by modulating mRNA splicing, translational initiation, and protein turnover. *Mol Cell Biol*. 1985; 5:1512–21. <https://doi.org/10.1128/MCB.5.6.1512>
  63. Lam YW, Lamond AI, Mann M, Andersen JS. Analysis of nucleolar protein dynamics reveals the nuclear degradation of ribosomal proteins. *Curr Biol*. 2007; 17:749–60. <https://doi.org/10.1016/j.cub.2007.03.064>
  64. Jäkel S, Görlich D. Importin beta, transportin, RanBP5 and RanBP7 mediate nuclear import of ribosomal proteins in mammalian cells. *EMBO J*. 1998; 17:4491–502. <https://doi.org/10.1093/emboj/17.15.4491>
  65. Plafker SM, Macara IG. Ribosomal protein L12 uses a distinct nuclear import pathway mediated by importin 11. *Mol Cell Biol*. 2002; 22:1266–75. <https://doi.org/10.1128/MCB.22.4.1266-1275.2002>
  66. Jäkel S, Mingot JM, Schwarzmaier P, Hartmann E, Görlich D. Importins fulfil a dual function as nuclear import receptors and cytoplasmic chaperones for exposed basic domains. *EMBO J*. 2002; 21:377–86. <https://doi.org/10.1093/emboj/21.3.377>
  67. Zhang J, Harnpicharnchai P, Jakovljevic J, Tang L, Guo Y, Oeffinger M, Rout MP, Hiley SL, Hughes T, Woolford JL Jr. Assembly factors Rpf2 and Rrs1 recruit 5S rRNA and ribosomal proteins rpL5 and rpL11 into nascent ribosomes. *Genes Dev*. 2007; 21:2580–92. <https://doi.org/10.1101/gad.1569307>
  68. Sloan KE, Bohnsack MT, Watkins NJ. The 5S RNP couples p53 homeostasis to ribosome biogenesis and nucleolar stress. *Cell Reports*. 2013; 5:237–47. <https://doi.org/10.1016/j.celrep.2013.08.049>
  69. Thomas F, Kutay U. Biogenesis and nuclear export of ribosomal subunits in higher eukaryotes depend on the CRM1 export pathway. *J Cell Sci*. 2003; 116:2409–19. <https://doi.org/10.1242/jcs.00464>
  70. Henras AK, Soudet J, Gêrus M, Lebaron S, Caizergues-Ferrer M, Mougin A, Henry Y. The post-transcriptional steps of eukaryotic ribosome biogenesis. *Cell Mol Life Sci*. 2008; 65:2334–59. <https://doi.org/10.1007/s00018-008-8027-0>
  71. Jackson RJ, Hellen CU, Pestova TV. The mechanism of eukaryotic translation initiation and principles of its regulation. *Nat Rev Mol Cell Biol*. 2010; 11:113–27. <https://doi.org/10.1038/nrm2838>
  72. Honda R, Tanaka H, Yasuda H. Oncoprotein MDM2 is a ubiquitin ligase E3 for tumor suppressor p53. *FEBS Lett*. 1997; 420:25–27. [https://doi.org/10.1016/S0014-5793\(97\)01480-4](https://doi.org/10.1016/S0014-5793(97)01480-4)
  73. Michael D, Oren M. The p53-Mdm2 module and the ubiquitin system. *Semin Cancer Biol*. 2003; 13:49–58. [https://doi.org/10.1016/S1044-579X\(02\)00099-8](https://doi.org/10.1016/S1044-579X(02)00099-8)
  74. Haupt Y, Maya R, Kazanietz A, Oren M. Mdm2 promotes the rapid degradation of p53. *Nature*. 1997; 387:296–99. <https://doi.org/10.1038/387296a0>
  75. Gu J, Kawai H, Nie L, Kitao H, Wiederschain D, Jochemsen AG, Parant J, Lozano G, Yuan ZM. Mutual dependence of MDM2 and MDMX in their functional inactivation of p53. *J Biol Chem*. 2002; 277:19251–54. <https://doi.org/10.1074/jbc.C200150200>
  76. Hock AK, Vousden KH. The role of ubiquitin modifica-

- tion in the regulation of p53. *Biochim Biophys Acta*. 2014; 1843:137–49. <https://doi.org/10.1016/j.bbamcr.2013.05.022>
77. Toledo F, Wahl GM. Regulating the p53 pathway: in vitro hypotheses, in vivo veritas. *Nat Rev Cancer*. 2006; 6:909–23. <https://doi.org/10.1038/nrc2012>
  78. Picksley SM, Lane DP. The p53-mdm2 autoregulatory feedback loop: a paradigm for the regulation of growth control by p53? *BioEssays*. 1993; 15:689–90. <https://doi.org/10.1002/bies.950151008>
  79. Murray-Zmijewski F, Slee EA, Lu X. A complex barcode underlies the heterogeneous response of p53 to stress. *Nat Rev Mol Cell Biol*. 2008; 9:702–12. <https://doi.org/10.1038/nrm2451>
  80. Zhang Y, Lu H. Signaling to p53: ribosomal proteins find their way. *Cancer Cell*. 2009; 16:369–77. <https://doi.org/10.1016/j.ccr.2009.09.024>
  81. Fumagalli S, Ivanenkov VV, Teng T, Thomas G. Suprainduction of p53 by disruption of 40S and 60S ribosome biogenesis leads to the activation of a novel G2/M checkpoint. *Genes Dev*. 2012; 26:1028–40. <https://doi.org/10.1101/gad.189951.112>
  82. Bursać S, Brdovčak MC, Pfannkuchen M, Orsolić I, Golomb L, Zhu Y, Katz C, Daftuar L, Grabušić K, Vukelić I, Filić V, Oren M, Prives C, Volarevic S. Mutual protection of ribosomal proteins L5 and L11 from degradation is essential for p53 activation upon ribosomal biogenesis stress. *Proc Natl Acad Sci USA*. 2012; 109:20467–72. <https://doi.org/10.1073/pnas.1218535109>
  83. Warner JR. In the absence of ribosomal RNA synthesis, the ribosomal proteins of HeLa cells are synthesized normally and degraded rapidly. *J Mol Biol*. 1977; 115:315–33. [https://doi.org/10.1016/0022-2836\(77\)90157-7](https://doi.org/10.1016/0022-2836(77)90157-7)
  84. Donati G, Peddigari S, Mercer CA, Thomas G. 5S ribosomal RNA is an essential component of a nascent ribosomal precursor complex that regulates the Hdm2-p53 checkpoint. *Cell Reports*. 2013; 4:87–98. <https://doi.org/10.1016/j.celrep.2013.05.045>
  85. Rubbi CP, Milner J. Disruption of the nucleolus mediates stabilization of p53 in response to DNA damage and other stresses. *EMBO J*. 2003; 22:6068–77. <https://doi.org/10.1093/emboj/cdg579>
  86. Fumagalli S, Di Cara A, Neb-Gulati A, Natt F, Schwemberger S, Hall J, Babcock GF, Bernardi R, Pandolfi PP, Thomas G. Absence of nucleolar disruption after impairment of 40S ribosome biogenesis reveals an rpl11-translation-dependent mechanism of p53 induction. *Nat Cell Biol*. 2009; 11:501–08. <https://doi.org/10.1038/ncb1858>
  87. Bursac S, Brdovcak MC, Donati G, Volarevic S. Activation of the tumor suppressor p53 upon impairment of ribosome biogenesis. *Biochim Biophys Acta*. 2014; 1842:817–30. <https://doi.org/10.1016/j.bbadis.2013.08.014>
  88. Sherr CJ. Divorcing ARF and p53: an unsettled case. *Nat Rev Cancer*. 2006; 6:663–73. <https://doi.org/10.1038/nrc1954>
  89. Quelle DE, Zindy F, Ashmun RA, Sherr CJ. Alternative reading frames of the INK4a tumor suppressor gene encode two unrelated proteins capable of inducing cell cycle arrest. *Cell*. 1995; 83:993–1000. [https://doi.org/10.1016/0092-8674\(95\)90214-7](https://doi.org/10.1016/0092-8674(95)90214-7)
  90. Korgaonkar C, Hagen J, Tompkins V, Frazier AA, Allamargot C, Quelle FW, Quelle DE. Nucleophosmin (B23) targets ARF to nucleoli and inhibits its function. *Mol Cell Biol*. 2005; 25:1258–71. <https://doi.org/10.1128/MCB.25.4.1258-1271.2005>
  91. Sherr CJ. Ink4-Arf locus in cancer and aging. *Wiley Interdiscip Rev Dev Biol*. 2012; 1:731–41. <https://doi.org/10.1002/wdev.40>
  92. Midgley CA, Desterro JM, Saville MK, Howard S, Sparks A, Hay RT, Lane DP. An N-terminal p14ARF peptide blocks Mdm2-dependent ubiquitination in vitro and can activate p53 in vivo. *Oncogene*. 2000; 19:2312–23. <https://doi.org/10.1038/sj.onc.1203593>
  93. Qin FX, Shao HY, Chen XC, Tan S, Zhang HJ, Miao ZY, Wang L, Hui-Chen, Zhang L. Knockdown of NPM1 by RNA interference inhibits cells proliferation and induces apoptosis in leukemic cell line. *Int J Med Sci*. 2011; 8:287–94. <https://doi.org/10.7150/ijms.8.287>
  94. Lessard F, Morin F, Ivanchuk S, Langlois F, Stefanovsky V, Rutka J, Moss T. The ARF tumor suppressor controls ribosome biogenesis by regulating the RNA polymerase I transcription factor TTF-I. *Mol Cell*. 2010; 38:539–50. <https://doi.org/10.1016/j.molcel.2010.03.015>
  95. Ayrault O, Andrique L, Fauvin D, Eymin B, Gazzeri S, Séité P. Human tumor suppressor p14ARF negatively regulates rRNA transcription and inhibits UBF1 transcription factor phosphorylation. *Oncogene*. 2006; 25:7577–86. <https://doi.org/10.1038/sj.onc.1209743>
  96. Kurki S, Peltonen K, Latonen L, Kiviharju TM, Ojala PM, Meek D, Laiho M. Nucleolar protein NPM interacts with HDM2 and protects tumor suppressor protein p53 from HDM2-mediated degradation. *Cancer Cell*. 2004; 5:465–75. [https://doi.org/10.1016/S1535-6108\(04\)00110-2](https://doi.org/10.1016/S1535-6108(04)00110-2)
  97. Dhar SK, St Clair DK. Nucleophosmin blocks mitochondrial localization of p53 and apoptosis. *J Biol Chem*.

- 2009; 284:16409–18.  
<https://doi.org/10.1074/jbc.M109.005736>
98. Kerr LE, Birse-Archbold JL, Short DM, McGregor AL, Heron I, Macdonald DC, Thompson J, Carlson GJ, Kelly JS, McCulloch J, Sharkey J. Nucleophosmin is a novel Bax chaperone that regulates apoptotic cell death. *Oncogene*. 2007; 26:2554–62.  
<https://doi.org/10.1038/sj.onc.1210044>
  99. Donati G, Brighenti E, Vici M, Mazzini G, Treré D, Montanaro L, Derenzini M. Selective inhibition of rRNA transcription downregulates E2F-1: a new p53-independent mechanism linking cell growth to cell proliferation. *J Cell Sci*. 2011; 124:3017–28.  
<https://doi.org/10.1242/jcs.086074>
  100. Zhang Z, Wang H, Li M, Rayburn ER, Agrawal S, Zhang R. Stabilization of E2F1 protein by MDM2 through the E2F1 ubiquitination pathway. *Oncogene*. 2005; 24:7238–47. <https://doi.org/10.1038/sj.onc.1208814>
  101. Crosby ME, Almasan A. Opposing roles of E2Fs in cell proliferation and death. *Cancer Biol Ther*. 2004; 3:1208–11. <https://doi.org/10.4161/cbt.3.12.1494>
  102. Hollstein M, Sidransky D, Vogelstein B, Harris CC. p53 mutations in human cancers. *Science*. 1991; 253:49–53. <https://doi.org/10.1126/science.1905840>
  103. Orsolic I, Jurada D, Pullen N, Oren M, Eliopoulos AG, Volarevic S. The relationship between the nucleolus and cancer: current evidence and emerging paradigms. *Semin Cancer Biol*. 2016; 37-38:36–50. <https://doi.org/10.1016/j.semcancer.2015.12.004>
  104. Holmberg Olausson K, Nistér M, Lindström MS. p53 - Dependent and -Independent Nucleolar Stress Responses. *Cells*. 2012; 1:774–98.  
<https://doi.org/10.3390/cells1040774>
  105. Donati G, Bertoni S, Brighenti E, Vici M, Treré D, Volarevic S, Montanaro L, Derenzini M. The balance between rRNA and ribosomal protein synthesis up- and downregulates the tumour suppressor p53 in mammalian cells. *Oncogene*. 2011; 30:3274–88. <https://doi.org/10.1038/onc.2011.48>
  106. Yuan X, Zhou Y, Casanova E, Chai M, Kiss E, Gröne HJ, Schütz G, Grummt I. Genetic inactivation of the transcription factor TIF-IA leads to nucleolar disruption, cell cycle arrest, and p53-mediated apoptosis. *Mol Cell*. 2005; 19:77–87.  
<https://doi.org/10.1016/j.molcel.2005.05.023>
  107. Hernandez-Verdun D, Roussel P, Thiry M, Sirri V, Lafontaine DL. The nucleolus: structure/function relationship in RNA metabolism. *Wiley Interdiscip Rev RNA*. 2010; 1:415–31.  
<https://doi.org/10.1002/wrna.39>
  108. Burger K, Mühl B, Harasim T, Rohrmoser M, Malamoussi A, Orban M, Kellner M, Gruber-Eber A, Kremmer E, Hölzel M, Eick D. Chemotherapeutic drugs inhibit ribosome biogenesis at various levels. *J Biol Chem*. 2010; 285:12416–25.  
<https://doi.org/10.1074/jbc.M109.074211>
  109. Peltonen K, Colis L, Liu H, Jäämaa S, Moore HM, Enbäck J, Laakkonen P, Vaahtokari A, Jones RJ, af Hällström TM, Laiho M. Identification of novel p53 pathway activating small-molecule compounds reveals unexpected similarities with known therapeutic agents. *PLoS One*. 2010; 5:e12996. <https://doi.org/10.1371/journal.pone.0012996>
  110. Peltonen K, Colis L, Liu H, Trivedi R, Moubarek MS, Moore HM, Bai B, Rudek MA, Bieberich CJ, Laiho M. A targeting modality for destruction of RNA polymerase I that possesses anticancer activity. *Cancer Cell*. 2014; 25:77–90. <https://doi.org/10.1016/j.ccr.2013.12.009>
  111. Drygin D, Siddiqui-Jain A, O'Brien S, Schwaebe M, Lin A, Bliesath J, Ho CB, Proffitt C, Trent K, Whitten JP, Lim JK, Von Hoff D, Anderes K, Rice WG. Anticancer activity of CX-3543: a direct inhibitor of rRNA biogenesis. *Cancer Res*. 2009; 69:7653–61. <https://doi.org/10.1158/0008-5472.CAN-09-1304>
  112. Drygin D, Lin A, Bliesath J, Ho CB, O'Brien SE, Proffitt C, Omori M, Haddach M, Schwaebe MK, Siddiqui-Jain A, Streiner N, Quin JE, Sanij E, et al. Targeting RNA polymerase I with an oral small molecule CX-5461 inhibits ribosomal RNA synthesis and solid tumor growth. *Cancer Res*. 2011; 71:1418–30. <https://doi.org/10.1158/0008-5472.CAN-10-1728>
  113. Bywater MJ, Poortinga G, Sanij E, Hein N, Peck A, Cullinane C, Wall M, Cluse L, Drygin D, Anderes K, Huser N, Proffitt C, Bliesath J, et al. Inhibition of RNA polymerase I as a therapeutic strategy to promote cancer-specific activation of p53. *Cancer Cell*. 2012; 22:51–65. <https://doi.org/10.1016/j.ccr.2012.05.019>
  114. National Health and Medical Research Council. (2013). A Phase 1, Open-Label, Dose Escalation, Safety, Pharmacokinetic, and Pharmacodynamic Study of Intravenously Administered CX-5461 in Patients with Advanced Haematologic Malignancies. <https://www.anzctr.org.au/Trial/Registration/TrialReview.aspx?id=364713> Registration number: ACTRN12613001061729. Australian New Zealand Clinical Trials Registry.
  115. Canadian Cancer Trials Group. (2016). A Phase I Study of CX5461. Available from: <https://ClinicalTrials.gov/show/NCT02719977>. NLM identifier: NCT02719977
  116. Xu H, Di Antonio M, McKinney S, Mathew V, Ho B, O'Neil NJ, Santos ND, Silvester J, Wei V, Garcia J, Kabeer F, Lai D, Soriano P, et al. CX-5461 is a DNA G-quadruplex stabilizer with selective lethality in

- BRCA1/2 deficient tumours. *Nat Commun.* 2017; 8:14432. <https://doi.org/10.1038/ncomms14432>
117. Onofrillo C. (2013). Ribosome Biogenesis and cell cycle regulation: Effect of RNA Polymerase III inhibition [dissertation]. *Oncologia e Patologia Sperimentale: Uniuniversità dii Bollogna.*
  118. Engelke DR, Ng SY, Shastry BS, Roeder RG. Specific interaction of a purified transcription factor with an internal control region of 5S RNA genes. *Cell.* 1980; 19:717–28. [https://doi.org/10.1016/S0092-8674\(80\)80048-1](https://doi.org/10.1016/S0092-8674(80)80048-1)
  119. Shastry BS, Honda BM, Roeder RG. Altered levels of a 5 S gene-specific transcription factor (TFIIIA) during oogenesis and embryonic development of *Xenopus laevis*. *J Biol Chem.* 1984; 259:11373–82.
  120. Nishimura K, Kumazawa T, Kuroda T, Katagiri N, Tsuchiya M, Goto N, Furumai R, Murayama A, Yanagisawa J, Kimura K. Perturbation of ribosome biogenesis drives cells into senescence through 5S RNP-mediated p53 activation. *Cell Reports.* 2015; 10:1310–23. <https://doi.org/10.1016/j.celrep.2015.01.055>
  121. Chang CC, Steinbacher DM. Treacher collins syndrome. *Semin Plast Surg.* 2012; 26:83–90. <https://doi.org/10.1055/s-0032-1320066>
  122. Posnick JC. 2013. Principles and Practice of Orthognathic Surgery. Elsevier Health Sciences. Chapter 4, Frequently Seen Malformations with Dentofacial Deformity. p. 1059-94.
  123. Kadakia S, Helman SN, Badhey AK, Saman M, Ducic Y. Treacher Collins Syndrome: the genetics of a craniofacial disease. *Int J Pediatr Otorhinolaryngol.* 2014; 78:893–98. <https://doi.org/10.1016/j.ijporl.2014.03.006>
  124. Ahmed MK, Ye X, Taub PJ. Review of the Genetic Basis of Jaw Malformations. *J Pediatr Genet.* 2016; 5:209–19. <https://doi.org/10.1055/s-0036-1593505>
  125. Valdez BC, Henning D, So RB, Dixon J, Dixon MJ. The Treacher Collins syndrome (TCOF1) gene product is involved in ribosomal DNA gene transcription by interacting with upstream binding factor. *Proc Natl Acad Sci USA.* 2004; 101:10709–14. <https://doi.org/10.1073/pnas.0402492101>
  126. Gonzales B, Henning D, So RB, Dixon J, Dixon MJ, Valdez BC. The Treacher Collins syndrome (TCOF1) gene product is involved in pre-rRNA methylation. *Hum Mol Genet.* 2005; 14:2035–43. <https://doi.org/10.1093/hmg/ddi208>
  127. Dixon J, Jones NC, Sandell LL, Jayasinghe SM, Crane J, Rey JP, Dixon MJ, Trainor PA. Tcof1/Treacle is required for neural crest cell formation and proliferation deficiencies that cause craniofacial abnormalities. *Proc Natl Acad Sci USA.* 2006; 103:13403–08. <https://doi.org/10.1073/pnas.0603730103>
  128. Graham A, Koentges G, Lumsden A. Neural Crest Apoptosis and the Establishment of Craniofacial Pattern: An Honorable Death. *Mol Cell Neurosci.* 1996; 8:76–83. <https://doi.org/10.1006/mcne.1996.0046>
  129. Jones NC, Lynn ML, Gaudenz K, Sakai D, Aoto K, Rey JP, Glynn EF, Ellington L, Du C, Dixon J, Dixon MJ, Trainor PA. Prevention of the neurocristopathy Treacher Collins syndrome through inhibition of p53 function. *Nat Med.* 2008; 14:125–33. <https://doi.org/10.1038/nm1725>
  130. Larsen DH, Hari F, Clapperton JA, Gwerder M, Gutsche K, Altmeyer M, Jungmichel S, Toledo LI, Fink D, Rask MB, Grøfte M, Lukas C, Nielsen ML, et al. The NBS1-Treacle complex controls ribosomal RNA transcription in response to DNA damage. *Nat Cell Biol.* 2014; 16:792–803. <https://doi.org/10.1038/ncb3007>
  131. Ciccia A, Huang JW, Izhar L, Sowa ME, Harper JW, Elledge SJ. Treacher Collins syndrome TCOF1 protein cooperates with NBS1 in the DNA damage response. *Proc Natl Acad Sci USA.* 2014; 111:18631–36. <https://doi.org/10.1073/pnas.1422488112>
  132. Sakai D, Dixon J, Achilleos A, Dixon M, Trainor PA. Prevention of Treacher Collins syndrome craniofacial anomalies in mouse models via maternal antioxidant supplementation. *Nat Commun.* 2016; 7:10328. <https://doi.org/10.1038/ncomms10328>
  133. Cadet J, Wagner JR. DNA base damage by reactive oxygen species, oxidizing agents, and UV radiation. *Cold Spring Harb Perspect Biol.* 2013; 5:a012559. <https://doi.org/10.1101/cshperspect.a012559>
  134. Jena NR. DNA damage by reactive species: Mechanisms, mutation and repair. *J Biosci.* 2012; 37:503–17. <https://doi.org/10.1007/s12038-012-9218-2>
  135. Calo E, Gu B, Bowen ME, Aryan F, Zalc A, Liang J, Flynn RA, Swigut T, Chang HY, Attardi LD, Wysocka J. Tissue-selective effects of nucleolar stress and rDNA damage in developmental disorders. *Nature.* 2018; 554:112–17. <https://doi.org/10.1038/nature25449>
  136. Turi Z, Senkyrikova M, Mistrik M, Bartek J, Moudry P. Perturbation of RNA Polymerase I transcription machinery by ablation of HEATR1 triggers the RPL5/RPL11-MDM2-p53 ribosome biogenesis stress checkpoint pathway in human cells. *Cell Cycle.* 2018; 17:92–101.



- <https://doi.org/10.1080/15384101.2017.1403685>
137. Gallagher JE, Dunbar DA, Granneman S, Mitchell BM, Osheim Y, Beyer AL, Baserga SJ. RNA polymerase I transcription and pre-rRNA processing are linked by specific SSU processome components. *Genes Dev.* 2004; 18:2506–17.  
<https://doi.org/10.1101/gad.1226604>
138. Dez C, Dlakić M, Tollervey D. Roles of the HEAT repeat proteins Utp10 and Utp20 in 40S ribosome maturation. *RNA.* 2007; 13:1516–27.  
<https://doi.org/10.1261/rna.609807>
139. Krogan NJ, Peng WT, Cagney G, Robinson MD, Haw R, Zhong G, Guo X, Zhang X, Canadien V, Richards DP, Beattie BK, Lalev A, Zhang W, et al. High-definition macromolecular composition of yeast RNA-processing complexes. *Mol Cell.* 2004; 13:225–39.  
[https://doi.org/10.1016/S1097-2765\(04\)00003-6](https://doi.org/10.1016/S1097-2765(04)00003-6)
140. Shav-Tal Y, Blechman J, Darzacq X, Montagna C, Dye BT, Patton JG, Singer RH, Zipori D. Dynamic sorting of nuclear components into distinct nucleolar caps during transcriptional inhibition. *Mol Biol Cell.* 2005; 16:2395–413. <https://doi.org/10.1091/mbc.e04-11-0992>
141. Peng Q, Wu J, Zhang Y, Liu Y, Kong R, Hu L, Du X, Ke Y. 1A6/DRIM, a novel t-UTP, activates RNA polymerase I transcription and promotes cell proliferation. *PLoS One.* 2010; 5:e14244.  
<https://doi.org/10.1371/journal.pone.0014244>
142. Zhao C, Andreeva V, Gibert Y, LaBonty M, Lattanzi V, Prabhudesai S, Zhou Y, Zon L, McCann KL, Baserga S, Yelick PC. Tissue specific roles for the ribosome biogenesis factor Wdr43 in zebrafish development. *PLoS Genet.* 2014; 10:e1004074.  
<https://doi.org/10.1371/journal.pgen.1004074>
143. Griffin JN, Sondalle SB, Del Viso F, Baserga SJ, Khokha MK. The ribosome biogenesis factor Nol11 is required for optimal rDNA transcription and craniofacial development in *Xenopus*. *PLoS Genet.* 2015; 11:e1005018.  
<https://doi.org/10.1371/journal.pgen.1005018>
144. Hölzel M, Rohrmoser M, Schlee M, Grimm T, Harasim T, Malamoussi A, Gruber-Eber A, Kremmer E, Hiddemann W, Bornkamm GW, Eick D. Mammalian WDR12 is a novel member of the Pes1-Bop1 complex and is required for ribosome biogenesis and cell proliferation. *J Cell Biol.* 2005; 170:367–78.  
<https://doi.org/10.1083/jcb.200501141>
145. Yu W, Qiu Z, Gao N, Wang L, Cui H, Qian Y, Jiang L, Luo J, Yi Z, Lu H, Li D, Liu M. PAK1IP1, a ribosomal stress-induced nucleolar protein, regulates cell proliferation via the p53-MDM2 loop. *Nucleic Acids Res.* 2011; 39:2234–48.  
<https://doi.org/10.1093/nar/gkq1117>
146. McMahon M, Ayllón V, Panov KI, O'Connor R. Ribosomal 18 S RNA processing by the IGF-I-responsive WDR3 protein is integrated with p53 function in cancer cell proliferation. *J Biol Chem.* 2010; 285:18309–18.  
<https://doi.org/10.1074/jbc.M110.108555>
147. Skarie JM, Link BA. The primary open-angle glaucoma gene WDR36 functions in ribosomal RNA processing and interacts with the p53 stress-response pathway. *Hum Mol Genet.* 2008; 17:2474–85.  
<https://doi.org/10.1093/hmg/ddn147>
148. Watanabe-Susaki K, Takada H, Enomoto K, Miwata K, Ishimine H, Intoh A, Ohtaka M, Nakanishi M, Sugino H, Asashima M, Kurisaki A. Biosynthesis of ribosomal RNA in nucleoli regulates pluripotency and differentiation ability of pluripotent stem cells. *Stem Cells.* 2014; 32:3099–111.  
<https://doi.org/10.1002/stem.1825>
149. Langhendries JL, Nicolas E, Doumont G, Goldman S, Lafontaine DL. The human box C/D snoRNAs U3 and U8 are required for pre-rRNA processing and tumorigenesis. *Oncotarget.* 2016; 7:59519–34.  
<https://doi.org/10.18632/oncotarget.11148>
150. Choi YW, Kim YW, Bae SM, Kwak SY, Chun HJ, Tong SY, Lee HN, Shin JC, Kim KT, Kim YJ, Ahn WS. Identification of differentially expressed genes using annealing control primer-based GeneFishing in human squamous cell cervical carcinoma. *Clin Oncol (R Coll Radiol).* 2007; 19:308–18.  
<https://doi.org/10.1016/j.clon.2007.02.010>
151. Koh CM, Gurel B, Sutcliffe S, Aryee MJ, Schultz D, Iwata T, Uemura M, Zeller KI, Anele U, Zheng Q, Hicks JL, Nelson WG, Dang CV, et al. Alterations in nucleolar structure and gene expression programs in prostatic neoplasia are driven by the MYC oncogene. *Am J Pathol.* 2011; 178:1824–34.  
<https://doi.org/10.1016/j.ajpath.2010.12.040>
152. Su H, Xu T, Ganapathy S, Shadfan M, Long M, Huang TH, Thompson I, Yuan ZM. Elevated snoRNA biogenesis is essential in breast cancer. *Oncogene.* 2014; 33:1348–58.  
<https://doi.org/10.1038/onc.2013.89>
153. Belin S, Beghin A, Solano-González E, Bezin L, Brunet-Manquat S, Textoris J, Prats AC, Mertani HC, Dumontet C, Diaz JJ. Dysregulation of ribosome biogenesis and translational capacity is associated with tumor progression of human breast cancer cells. *PLoS One.* 2009; 4:e7147.  
<https://doi.org/10.1371/journal.pone.0007147>
154. Marcel V, Ghayad SE, Belin S, Therizols G, Morel AP, Solano-González E, Vendrell JA, Hacot S, Mertani HC,

- Albaret MA, Bourdon JC, Jordan L, Thompson A, et al. p53 acts as a safeguard of translational control by regulating fibrillarin and rRNA methylation in cancer. *Cancer Cell*. 2013; 24:318–30. <https://doi.org/10.1016/j.ccr.2013.08.013>
155. Sharma S, Marchand V, Motorin Y, Lafontaine DL. Identification of sites of 2'-O-methylation vulnerability in human ribosomal RNAs by systematic mapping. *Sci Rep*. 2017; 7:11490. <https://doi.org/10.1038/s41598-017-09734-9>
156. Kirwan M, Dokal I. Dyskeratosis congenita: a genetic disorder of many faces. *Clin Genet*. 2008; 73:103–12. <https://doi.org/10.1111/j.1399-0004.2007.00923.x>
157. Wilson DB, Link DC, Mason PJ, Bessler M. Inherited bone marrow failure syndromes in adolescents and young adults. *Ann Med*. 2014; 46:353–63. <https://doi.org/10.3109/07853890.2014.915579>
158. Fok WC, Niero EL, Dege C, Brenner KA, Sturgeon CM, Batista LF. p53 Mediates Failure of Human Definitive Hematopoiesis in Dyskeratosis Congenita. *Stem Cell Reports*. 2017; 9:409–18. <https://doi.org/10.1016/j.stemcr.2017.06.015>
159. Carrillo J, González A, Manguán-García C, Pintado-Berninches L, Perona R. p53 pathway activation by telomere attrition in X-DC primary fibroblasts occurs in the absence of ribosome biogenesis failure and as a consequence of DNA damage. *Clin Transl Oncol*. 2014; 16:529–38. <https://doi.org/10.1007/s12094-013-1112-3>
160. Mason PJ, Bessler M. The genetics of dyskeratosis congenita. *Cancer Genet*. 2011; 204:635–45. <https://doi.org/10.1016/j.cancergen.2011.11.002>
161. Bellodi C, Kopmar N, Ruggero D. Deregulation of oncogene-induced senescence and p53 translational control in X-linked dyskeratosis congenita. *EMBO J*. 2010; 29:1865–76. <https://doi.org/10.1038/emboj.2010.83>
162. Yoon A, Peng G, Brandenburger Y, Zollo O, Xu W, Rego E, Ruggero D. Impaired control of IRES-mediated translation in X-linked dyskeratosis congenita. *Science*. 2006; 312:902–06. <https://doi.org/10.1126/science.1123835>
163. Liu B, Zhang J, Huang C, Liu H. Dyskerin overexpression in human hepatocellular carcinoma is associated with advanced clinical stage and poor patient prognosis. *PLoS One*. 2012; 7:e43147. <https://doi.org/10.1371/journal.pone.0043147>
164. Sieron P, Hader C, Hatina J, Engers R, Wlazlinski A, Müller M, Schulz WA. DKC1 overexpression associated with prostate cancer progression. *Br J Cancer*. 2009; 101:1410–16. <https://doi.org/10.1038/sj.bjc.6605299>
165. Takagi M, Absalon MJ, McLure KG, Kastan MB. Regulation of p53 translation and induction after DNA damage by ribosomal protein L26 and nucleolin. *Cell*. 2005; 123:49–63. <https://doi.org/10.1016/j.cell.2005.07.034>
166. Jia W, Yao Z, Zhao J, Guan Q, Gao L. New perspectives of physiological and pathological functions of nucleolin (NCL). *Life Sci*. 2017; 186:1–10. <https://doi.org/10.1016/j.lfs.2017.07.025>
167. Abdelmohsen K, Gorospe M. RNA-binding protein nucleolin in disease. *RNA Biol*. 2012; 9:799–808. <https://doi.org/10.4161/rna.19718>
168. Berger CM, Gaume X, Bouvet P. The roles of nucleolin subcellular localization in cancer. *Biochimie*. 2015; 113:78–85. <https://doi.org/10.1016/j.biochi.2015.03.023>
169. Farin K, Schokoroy S, Haklai R, Cohen-Or I, Elad-Sfadia G, Reyes-Reyes ME, Bates PJ, Cox AD, Kloog Y, Pinkas-Kramarski R. Oncogenic synergism between ErbB1, nucleolin, and mutant Ras. *Cancer Res*. 2011; 71:2140–51. <https://doi.org/10.1158/0008-5472.CAN-10-2887>
170. Tajrishi MM, Tuteja R, Tuteja N. Nucleolin: the most abundant multifunctional phosphoprotein of nucleolus. *Commun Integr Biol*. 2011; 4:267–75. <https://doi.org/10.4161/cib.4.3.14884>
171. Soundararajan S, Chen W, Spicer EK, Courtenay-Luck N, Fernandes DJ. The nucleolin targeting aptamer AS1411 destabilizes Bcl-2 messenger RNA in human breast cancer cells. *Cancer Res*. 2008; 68:2358–65. <https://doi.org/10.1158/0008-5472.CAN-07-5723>
172. Bates PJ, Laber DA, Miller DM, Thomas SD, Trent JO. Discovery and development of the G-rich oligonucleotide AS1411 as a novel treatment for cancer. *Exp Mol Pathol*. 2009; 86:151–64. <https://doi.org/10.1016/j.yexmp.2009.01.004>
173. Laber DA, Taft BS, Kloecker GH, Bates PJ, Trent JO, Miller DM. Extended phase I study of AS1411 in renal and non-small cell lung cancers. *J Clin Oncol*. 2006; 24:13098.
174. Laber DA, Choudry MA, Taft BS, Bhupalam L, Sharma VR, Hendler FJ, Barnhart KM. A phase I study of AGRO100 in advanced cancer. *J Clin Oncol*. 2004; 22:3112. [https://doi.org/10.1200/jco.2004.22.14\\_suppl.3112](https://doi.org/10.1200/jco.2004.22.14_suppl.3112)
175. Rosenberg JE, Bambury RM, Van Allen EM, Drabkin HA, Lara PN Jr, Harzstark AL, Wagle N, Figlin RA, Smith GW, Garraway LA, Choueiri T, Erlandsson F, Laber DA. A phase II trial of AS1411 (a novel nucleolin-targeted DNA aptamer) in metastatic renal cell carcinoma.

- Invest New Drugs. 2014; 32:178–87.  
<https://doi.org/10.1007/s10637-013-0045-6>
176. Stuart RK, Stockerl-Goldstein K, Cooper M, Devetten M, Herzig R, Medeiros B, Schiller G, Wei A, Acton G, Rizzieri D. Randomized phase II trial of the nucleolin targeting aptamer AS1411 combined with high-dose cytarabine in relapsed/refractory acute myeloid leukemia (AML). *J Clin Oncol*. 2009; 27:7019.
177. Colombo E, Alcalay M, Pelicci PG. Nucleophosmin and its complex network: a possible therapeutic target in hematological diseases. *Oncogene*. 2011; 30:2595–609. <https://doi.org/10.1038/onc.2010.646>
178. Lim MJ, Wang XW. Nucleophosmin and human cancer. *Cancer Detect Prev*. 2006; 30:481–90. <https://doi.org/10.1016/j.cdp.2006.10.008>
179. Holmberg Olausson K, Elsir T, Moazemi Goudarzi K, Nistér M, Lindström MS. NPM1 histone chaperone is upregulated in glioblastoma to promote cell survival and maintain nucleolar shape. *Sci Rep*. 2015; 5:16495. <https://doi.org/10.1038/srep16495>
180. Coutinho-Camillo CM, Lourenço SV, Nishimoto IN, Kowalski LP, Soares FA. Nucleophosmin, p53, and Ki-67 expression patterns on an oral squamous cell carcinoma tissue microarray. *Hum Pathol*. 2010; 41:1079–86. <https://doi.org/10.1016/j.humpath.2009.12.010>
181. Sekhar KR, Benamar M, Venkateswaran A, Sasi S, Penthala NR, Crooks PA, Hann SR, Geng L, Balusu R, Abbas T, Freeman ML. Targeting nucleophosmin 1 represents a rational strategy for radiation sensitization. *Int J Radiat Oncol Biol Phys*. 2014; 89:1106–14. <https://doi.org/10.1016/j.ijrobp.2014.04.012>
182. Liu X, Liu D, Qian D, Dai J, An Y, Jiang S, Stanley B, Yang J, Wang B, Liu X, Liu DX. Nucleophosmin (NPM1/B23) interacts with activating transcription factor 5 (ATF5) protein and promotes proteasome- and caspase-dependent ATF5 degradation in hepatocellular carcinoma cells. *J Biol Chem*. 2012; 287:19599–609. <https://doi.org/10.1074/jbc.M112.363622>
183. Kim KH, Yoo BC, Kim WK, Hong JP, Kim K, Song EY, Lee JY, Cho JY, Ku JL. CD133 and CD133-regulated nucleophosmin linked to 5-fluorouracil susceptibility in human colon cancer cell line SW620. *Electrophoresis*. 2014; 35:522–32. <https://doi.org/10.1002/elps.201300364>
184. Wong JC, Hasan MR, Rahman M, Yu AC, Chan SK, Schaeffer DF, Kennecke HF, Lim HJ, Owen D, Tai IT. Nucleophosmin 1, upregulated in adenomas and cancers of the colon, inhibits p53-mediated cellular senescence. *Int J Cancer*. 2013; 133:1567–77. <https://doi.org/10.1002/ijc.28180>
185. Kalra RS, Bapat SA. Enhanced levels of double-strand DNA break repair proteins protect ovarian cancer cells against genotoxic stress-induced apoptosis. *J Ovarian Res*. 2013; 6:66. <https://doi.org/10.1186/1757-2215-6-66>
186. Zhou Y, Shen J, Xia L, Wang Y. Estrogen mediated expression of nucleophosmin 1 in human endometrial carcinoma clinical stages through estrogen receptor- $\alpha$  signaling. *Cancer Cell Int*. 2014; 14:540. <https://doi.org/10.1186/s12935-014-0145-1>
187. Léotoing L, Meunier L, Manin M, Mauduit C, Decaussin M, Verrijdt G, Claessens F, Benahmed M, Veyssi re G, Morel L, Beaudoin C. Influence of nucleophosmin/B23 on DNA binding and transcriptional activity of the androgen receptor in prostate cancer cell. *Oncogene*. 2008; 27:2858–67. <https://doi.org/10.1038/sj.onc.1210942>
188. Tsui KH, Cheng AJ, Chang P, Pan TL, Yung BY. Association of nucleophosmin/B23 mRNA expression with clinical outcome in patients with bladder carcinoma. *Urology*. 2004; 64:839–44. <https://doi.org/10.1016/j.urology.2004.05.020>
189. Pianta A, Puppini C, Franzoni A, Fabbro D, Di Loreto C, Bulotta S, Deganuto M, Paron I, Tell G, Puxeddu E, Filetti S, Russo D, Damante G. Nucleophosmin is overexpressed in thyroid tumors. *Biochem Biophys Res Commun*. 2010; 397:499–504. <https://doi.org/10.1016/j.bbrc.2010.05.142>
190. Leal MF, Mazzotti TK, Calcagno DQ, Cirilo PD, Martinez MC, Demachki S, Assump o PP, Chammas R, Burbano RR, Smith MC. Deregulated expression of Nucleophosmin 1 in gastric cancer and its clinicopathological implications. *BMC Gastroenterol*. 2014; 14:9. <https://doi.org/10.1186/1471-230X-14-9>
191. Karhemo PR, Rivinoja A, Lundin J, Hyv nen M, Chernenko A, Lammi J, Sihto H, Lundin M, Heikkil  P, Joensuu H, Bono P, Laakkonen P. An extensive tumor array analysis supports tumor suppressive role for nucleophosmin in breast cancer. *Am J Pathol*. 2011; 179:1004–14. <https://doi.org/10.1016/j.ajpath.2011.04.009>
192. Falini B, Martelli MP, Bolli N, Sportoletti P, Liso A, Tiacci E, Haferlach T. Acute myeloid leukemia with mutated nucleophosmin (NPM1): is it a distinct entity? *Blood*. 2011; 117:1109–20. <https://doi.org/10.1182/blood-2010-08-299990>
193. Naoe T, Suzuki T, Kiyoi H, Urano T. Nucleophosmin: a versatile molecule associated with hematological malignancies. *Cancer Sci*. 2006; 97:963–69. <https://doi.org/10.1111/j.1349-7006.2006.00270.x>

194. Di Matteo A, Franceschini M, Chiarella S, Rocchio S, Travaglini-Allocatelli C, Federici L. Molecules that target nucleophosmin for cancer treatment: an update. *Oncotarget*. 2016; 7:44821–40. <https://doi.org/10.18632/oncotarget.8599>
195. Qi W, Shakalya K, Stejskal A, Goldman A, Beeck S, Cooke L, Mahadevan D. NSC348884, a nucleophosmin inhibitor disrupts oligomer formation and induces apoptosis in human cancer cells. *Oncogene*. 2008; 27:4210–20. <https://doi.org/10.1038/onc.2008.54>
196. Balusu R, Fiskus W, Rao R, Chong DG, Nalluri S, Mudunuru U, Ma H, Chen L, Venkannagari S, Ha K, Abhyankar S, Williams C, McGuirk J, et al. Targeting levels or oligomerization of nucleophosmin 1 induces differentiation and loss of survival of human AML cells with mutant NPM1. *Blood*. 2011; 118:3096–106. <https://doi.org/10.1182/blood-2010-09-309674>
197. Lindström MS, Nistér M. Silencing of ribosomal protein S9 elicits a multitude of cellular responses inhibiting the growth of cancer cells subsequent to p53 activation. *PLoS One*. 2010; 5:e9578. <https://doi.org/10.1371/journal.pone.0009578>
198. Jin A, Itahana K, O’Keefe K, Zhang Y. Inhibition of HDM2 and activation of p53 by ribosomal protein L23. *Mol Cell Biol*. 2004; 24:7669–80. <https://doi.org/10.1128/MCB.24.17.7669-7680.2004>
199. Barkić M, Crnomarković S, Grabusić K, Bogetić I, Panić L, Tamarut S, Cokarić M, Jerić I, Vidak S, Volarević S. The p53 tumor suppressor causes congenital malformations in Rpl24-deficient mice and promotes their survival. *Mol Cell Biol*. 2009; 29:2489–504. <https://doi.org/10.1128/MCB.01588-08>
200. Sun XX, Wang YG, Xirodimas DP, Dai MS. Perturbation of 60 S ribosomal biogenesis results in ribosomal protein L5- and L11-dependent p53 activation. *J Biol Chem*. 2010; 285:25812–21. <https://doi.org/10.1074/jbc.M109.098442>
201. Llanos S, Serrano M. Depletion of ribosomal protein L37 occurs in response to DNA damage and activates p53 through the L11/MDM2 pathway. *Cell Cycle*. 2010; 9:4005–12. <https://doi.org/10.4161/cc.9.19.13299>
202. Dutt S, Narla A, Lin K, Mullally A, Abayasekara N, Megerdichian C, Wilson FH, Currie T, Khanna-Gupta A, Berliner N, Kutok JL, Ebert BL. Haploinsufficiency for ribosomal protein genes causes selective activation of p53 in human erythroid progenitor cells. *Blood*. 2011; 117:2567–76. <https://doi.org/10.1182/blood-2010-07-295238>
203. Zhou X, Hao Q, Liao J, Zhang Q, Lu H. Ribosomal protein S14 unties the MDM2-p53 loop upon ribosomal stress. *Oncogene*. 2013; 32:388–96. <https://doi.org/10.1038/onc.2012.63>
204. Daftuar L, Zhu Y, Jacq X, Prives C. Ribosomal proteins RPL37, RPS15 and RPS20 regulate the Mdm2-p53-MdmX network. *PLoS One*. 2013; 8:e68667. <https://doi.org/10.1371/journal.pone.0068667>
205. Narla A, Ebert BL. Ribosomopathies: human disorders of ribosome dysfunction. *Blood*. 2010; 115:3196–205. <https://doi.org/10.1182/blood-2009-10-178129>
206. Lipton JM, Ellis SR. Diamond-Blackfan anemia: diagnosis, treatment, and molecular pathogenesis. *Hematol Oncol Clin North Am*. 2009; 23:261–82. <https://doi.org/10.1016/j.hoc.2009.01.004>
207. Ellis SR, Gleizes PE. Diamond Blackfan anemia: ribosomal proteins going rogue. *Semin Hematol*. 2011; 48:89–96. <https://doi.org/10.1053/j.seminhematol.2011.02.005>
208. Nakhoul H, Ke J, Zhou X, Liao W, Zeng SX, Lu H. Ribosomopathies: mechanisms of disease. *Clin Med Insights Blood Disord*. 2014; 7:7–16. <https://doi.org/10.4137/CMBD.S16952>
209. Chiabrando D, Tolosano E. Diamond Blackfan Anemia at the Crossroad between Ribosome Biogenesis and Heme Metabolism. *Adv Hematol*. 2010; 2010:790632. <https://doi.org/10.1155/2010/790632>
210. Ellis SR. Nucleolar stress in Diamond Blackfan anemia pathophysiology. *Biochim Biophys Acta*. 2014; 1842:765–68. <https://doi.org/10.1016/j.bbadis.2013.12.013>
211. Keel SB, Doty RT, Yang Z, Quigley JG, Chen J, Knoblauch S, Kingsley PD, De Domenico I, Vaughn MB, Kaplan J, Palis J, Abkowitz JL. A heme export protein is required for red blood cell differentiation and iron homeostasis. *Science*. 2008; 319:825–28. <https://doi.org/10.1126/science.1151133>
212. McGowan KA, Li JZ, Park CY, Beaudry V, Tabor HK, Sabnis AJ, Zhang W, Fuchs H, de Angelis MH, Myers RM, Attardi LD, Barsh GS. Ribosomal mutations cause p53-mediated dark skin and pleiotropic effects. *Nat Genet*. 2008; 40:963–70. <https://doi.org/10.1038/ng.188>
213. Jaako P, Flygare J, Olsson K, Quere R, Ehinger M, Henson A, Ellis S, Schambach A, Baum C, Richter J, Larsson J, Bryder D, Karlsson S. Mice with ribosomal protein S19 deficiency develop bone marrow failure and symptoms like patients with Diamond-Blackfan anemia. *Blood*. 2011; 118:6087–96. <https://doi.org/10.1182/blood-2011-08-371963>
214. Danilova N, Sakamoto KM, Lin S. Ribosomal protein S19 deficiency in zebrafish leads to developmental abnormalities and defective erythropoiesis through

- activation of p53 protein family. *Blood*. 2008; 112:5228–37. <https://doi.org/10.1182/blood-2008-01-132290>
215. Torihara H, Uechi T, Chakraborty A, Shinya M, Sakai N, Kenmochi N. Erythropoiesis failure due to RPS19 deficiency is independent of an activated Tp53 response in a zebrafish model of Diamond-Blackfan anaemia. *Br J Haematol*. 2011; 152:648–54. <https://doi.org/10.1111/j.1365-2141.2010.08535.x>
216. Padron E, Komrokji R, List AF. Biology and treatment of the 5q- syndrome. *Expert Rev Hematol*. 2011; 4:61–69. <https://doi.org/10.1586/ehm.11.2>
217. Pellagatti A, Boultonwood J. Recent Advances in the 5q-Syndrome. *Mediterr J Hematol Infect Dis*. 2015; 7:e2015037. <https://doi.org/10.4084/mjhid.2015.037>
218. Ebert BL, Pretz J, Bosco J, Chang CY, Tamayo P, Galili N, Raza A, Root DE, Attar E, Ellis SR, Golub TR. Identification of RPS14 as a 5q- syndrome gene by RNA interference screen. *Nature*. 2008; 451:335–39. <https://doi.org/10.1038/nature06494>
219. Barlow JL, Drynan LF, Hewett DR, Holmes LR, Lorenzo-Abalde S, Lane AL, Jolin HE, Pannell R, Middleton AJ, Wong SH, Warren AJ, Wainscoat JS, Boultonwood J, McKenzie AN. A p53-dependent mechanism underlies macrocytic anemia in a mouse model of human 5q-syndrome. *Nat Med*. 2010; 16:59–66. <https://doi.org/10.1038/nm.2063>
220. Shi Y, Zhai H, Wang X, Han Z, Liu C, Lan M, Du J, Guo C, Zhang Y, Wu K, Fan D. Ribosomal proteins S13 and L23 promote multidrug resistance in gastric cancer cells by suppressing drug-induced apoptosis. *Exp Cell Res*. 2004; 296:337–46. <https://doi.org/10.1016/j.yexcr.2004.02.009>
221. Golomb L, Bublik DR, Wilder S, Nevo R, Kiss V, Grabusic K, Volarevic S, Oren M. Importin 7 and exportin 1 link c-Myc and p53 to regulation of ribosomal biogenesis. *Mol Cell*. 2012; 45:222–32. <https://doi.org/10.1016/j.molcel.2011.11.022>
222. Kressler D, Bange G, Ogawa Y, Stjepanovic G, Bradatsch B, Pratte D, Amlacher S, Strauß D, Yoneda Y, Katahira J, Sinning I, Hurt E. Synchronizing nuclear import of ribosomal proteins with ribosome assembly. *Science*. 2012; 338:666–71. <https://doi.org/10.1126/science.1226960>
223. Calviño FR, Kharde S, Ori A, Hendricks A, Wild K, Kressler D, Bange G, Hurt E, Beck M, Sinning I. Symportin 1 chaperones 5S RNP assembly during ribosome biogenesis by occupying an essential rRNA-binding site. *Nat Commun*. 2015; 6:6510. <https://doi.org/10.1038/ncomms7510>
224. Kazyken D, Kaz Y, Kiyan V, Zhykibayev AA, Chen CH, Agarwal NK, Sarbassov D. The nuclear import of ribosomal proteins is regulated by mTOR. *Oncotarget*. 2014; 5:9577–93. <https://doi.org/10.18632/oncotarget.2473>
225. Finch AJ, Hilcenko C, Basse N, Drynan LF, Goyenechea B, Menne TF, González Fernández A, Simpson P, D’Santos CS, Arends MJ, Donadieu J, Bellanné-Chantelot C, Costanzo M, et al. Uncoupling of GTP hydrolysis from eIF6 release on the ribosome causes Shwachman-Diamond syndrome. *Genes Dev*. 2011; 25:917–29. <https://doi.org/10.1101/gad.623011>
226. Wong CC, Traynor D, Basse N, Kay RR, Warren AJ. Defective ribosome assembly in Shwachman-Diamond syndrome. *Blood*. 2011; 118:4305–12. <https://doi.org/10.1182/blood-2011-06-353938>
227. Burwick N, Coats SA, Nakamura T, Shimamura A. Impaired ribosomal subunit association in Shwachman-Diamond syndrome. *Blood*. 2012; 120:5143–52. <https://doi.org/10.1182/blood-2012-04-420166>
228. Burroughs L, Woolfrey A, Shimamura A. Shwachman-Diamond syndrome: a review of the clinical presentation, molecular pathogenesis, diagnosis, and treatment. *Hematol Oncol Clin North Am*. 2009; 23:233–48. <https://doi.org/10.1016/j.hoc.2009.01.007>
229. Nelson AS, Myers KC. Diagnosis, Treatment, and Molecular Pathology of Shwachman-Diamond Syndrome. *Hematol Oncol Clin North Am*. 2018; 32:687–700. <https://doi.org/10.1016/j.hoc.2018.04.006>
230. Austin KM, Leary RJ, Shimamura A. The Shwachman-Diamond SBDS protein localizes to the nucleolus. *Blood*. 2005; 106:1253–58. <https://doi.org/10.1182/blood-2005-02-0807>
231. Ganapathi KA, Austin KM, Lee CS, Dias A, Malsch MM, Reed R, Shimamura A. The human Shwachman-Diamond syndrome protein, SBDS, associates with ribosomal RNA. *Blood*. 2007; 110:1458–65. <https://doi.org/10.1182/blood-2007-02-075184>
232. Elghetany MT, Alter BP. p53 protein overexpression in bone marrow biopsies of patients with Shwachman-Diamond syndrome has a prevalence similar to that of patients with refractory anemia. *Arch Pathol Lab Med*. 2002; 126:452–55.
233. Dror Y. P53 protein overexpression in Shwachman-Diamond syndrome. *Arch Pathol Lab Med*. 2002; 126:1157–58.
234. Provost E, Wehner KA, Zhong X, Ashar F, Nguyen E, Green R, Parsons MJ, Leach SD. Ribosomal biogenesis genes play an essential and p53-independent role in

- zebrafish pancreas development. *Development*. 2012; 139:3232–41.  
<https://doi.org/10.1242/dev.077107>
235. Tourlakis ME, Zhang S, Ball HL, Gandhi R, Liu H, Zhong J, Yuan JS, Guidos CJ, Durie PR, Rommens JM. In Vivo Senescence in the Sbds-Deficient Murine Pancreas: Cell-Type Specific Consequences of Translation Insufficiency. *PLoS Genet*. 2015; 11:e1005288.  
<https://doi.org/10.1371/journal.pgen.1005288>
236. Evans DS, Kapahi P, Hsueh WC, Kockel L. TOR signaling never gets old: aging, longevity and TORC1 activity. *Ageing Res Rev*. 2011; 10:225–37.  
<https://doi.org/10.1016/j.arr.2010.04.001>
237. Steffen KK, MacKay VL, Kerr EO, Tsuchiya M, Hu D, Fox LA, Dang N, Johnston ED, Oakes JA, Tchao BN, Pak DN, Fields S, Kennedy BK, Kaerberlein M. Yeast life span extension by depletion of 60s ribosomal subunits is mediated by Gcn4. *Cell*. 2008; 133:292–302. <https://doi.org/10.1016/j.cell.2008.02.037>
238. Hansen M, Taubert S, Crawford D, Libina N, Lee SJ, Kenyon C. Lifespan extension by conditions that inhibit translation in *Caenorhabditis elegans*. *Aging Cell*. 2007; 6:95–110. <https://doi.org/10.1111/j.1474-9726.2006.00267.x>
239. Chen D, Pan KZ, Palter JE, Kapahi P. Longevity determined by developmental arrest genes in *Caenorhabditis elegans*. *Aging Cell*. 2007; 6:525–33. <https://doi.org/10.1111/j.1474-9726.2007.00305.x>
240. Chiocchetti A, Zhou J, Zhu H, Karl T, Haubenreisser O, Rinnerthaler M, Heeren G, Oender K, Bauer J, Hintner H, Breitenbach M, Breitenbach-Koller L. Ribosomal proteins Rpl10 and Rps6 are potent regulators of yeast replicative life span. *Exp Gerontol*. 2007; 42:275–86.  
<https://doi.org/10.1016/j.exger.2006.11.002>
241. Curran SP, Ruvkun G. Lifespan regulation by evolutionarily conserved genes essential for viability. *PLoS Genet*. 2007; 3:e56.  
<https://doi.org/10.1371/journal.pgen.0030056>
242. Kaerberlein M, Powers RW 3rd, Steffen KK, Westman EA, Hu D, Dang N, Kerr EO, Kirkland KT, Fields S, Kennedy BK. Regulation of yeast replicative life span by TOR and Sch9 in response to nutrients. *Science*. 2005; 310:1193–96.  
<https://doi.org/10.1126/science.1115535>
243. Powers RW 3rd, Kaerberlein M, Caldwell SD, Kennedy BK, Fields S. Extension of chronological life span in yeast by decreased TOR pathway signaling. *Genes Dev*. 2006; 20:174–84.  
<https://doi.org/10.1101/gad.1381406>
244. Kapahi P, Zid BM, Harper T, Koslover D, Sapin V, Benzer S. Regulation of lifespan in *Drosophila* by modulation of genes in the TOR signaling pathway. *Curr Biol*. 2004; 14:885–90.  
<https://doi.org/10.1016/j.cub.2004.03.059>
245. Harrison DE, Strong R, Sharp ZD, Nelson JF, Astle CM, Flurkey K, Nadon NL, Wilkinson JE, Frenkel K, Carter CS, Pahor M, Javors MA, Fernandez E, Miller RA. Rapamycin fed late in life extends lifespan in genetically heterogeneous mice. *Nature*. 2009; 460:392–95. <https://doi.org/10.1038/nature08221>
246. Passtoors WM, Beekman M, Deelen J, van der Breggen R, Maier AB, Guigas B, Derhovanessian E, van Heemst D, de Craen AJ, Gunn DA, Pawelec G, Slagboom PE. Gene expression analysis of mTOR pathway: association with human longevity. *Aging Cell*. 2013; 12:24–31.  
<https://doi.org/10.1111/ace1.12015>
247. Miller RA, Harrison DE, Astle CM, Baur JA, Boyd AR, de Cabo R, Fernandez E, Flurkey K, Javors MA, Nelson JF, Orihuela CJ, Pletcher S, Sharp ZD, et al. Rapamycin, but not resveratrol or simvastatin, extends life span of genetically heterogeneous mice. *J Gerontol A Biol Sci Med Sci*. 2011; 66:191–201.  
<https://doi.org/10.1093/gerona/g1q178>
248. Hofmann JW, Zhao X, De Cecco M, Peterson AL, Pagliaroli L, Manivannan J, Hubbard GB, Ikeno Y, Zhang Y, Feng B, Li X, Serre T, Qi W, et al. Reduced expression of MYC increases longevity and enhances healthspan. *Cell*. 2015; 160:477–88.  
<https://doi.org/10.1016/j.cell.2014.12.016>
249. Schosserer M, Minois N, Angerer TB, Amring M, Dellago H, Harreither E, Calle-Perez A, Pircher A, Gerstl MP, Pfeifenberger S, Brandl C, Sonntagbauer M, Kriegner A, et al. Methylation of ribosomal RNA by NSUN5 is a conserved mechanism modulating organismal lifespan. *Nat Commun*. 2015; 6:6158.  
<https://doi.org/10.1038/ncomms7158>
250. Bemiller PM, Lee LH. Nucleolar changes in senescing WI-38 cells. *Mech Ageing Dev*. 1978; 8:417–27.  
[https://doi.org/10.1016/0047-6374\(78\)90041-6](https://doi.org/10.1016/0047-6374(78)90041-6)
251. Buchwalter A, Hetzer MW. Nucleolar expansion and elevated protein translation in premature aging. *Nat Commun*. 2017; 8:328.  
<https://doi.org/10.1038/s41467-017-00322-z>
252. Ruggero D, Pandolfi PP. Does the ribosome translate cancer? *Nat Rev Cancer*. 2003; 3:179–92.  
<https://doi.org/10.1038/nrc1015>
253. Tiku V, Antebi A. Nucleolar Function in Lifespan Regulation. *Trends Cell Biol*. 2018; 28:662–72.  
<https://doi.org/10.1016/j.tcb.2018.03.007>
254. Syntichaki P, Troulinaki K, Tavernarakis N. Protein

- synthesis is a novel determinant of aging in *Caenorhabditis elegans*. *Ann N Y Acad Sci*. 2007; 1119:289–95.  
<https://doi.org/10.1196/annals.1404.001>
255. Syntichaki P, Troulinaki K, Tavernarakis N. eIF4E function in somatic cells modulates ageing in *Caenorhabditis elegans*. *Nature*. 2007; 445:922–26.  
<https://doi.org/10.1038/nature05603>
  256. Kaushik S, Cuervo AM. Proteostasis and aging. *Nat Med*. 2015; 21:1406–15.  
<https://doi.org/10.1038/nm.4001>
  257. Pan KZ, Palter JE, Rogers AN, Olsen A, Chen D, Lithgow GJ, Kapahi P. Inhibition of mRNA translation extends lifespan in *Caenorhabditis elegans*. *Aging Cell*. 2007; 6:111–19. <https://doi.org/10.1111/j.1474-9726.2006.00266.x>
  258. López-Otín C, Blasco MA, Partridge L, Serrano M, Kroemer G. The hallmarks of aging. *Cell*. 2013; 153:1194–217.  
<https://doi.org/10.1016/j.cell.2013.05.039>
  259. McCay C, Crowell M, Maynard LA. The effect of retarded growth upon the length of life span and upon the ultimate body size. *J Nutr*. 1935; 10:63–79.  
<https://doi.org/10.1093/jn/10.1.63>
  260. Al-Regaiey KA. The effects of calorie restriction on aging: a brief review. *Eur Rev Med Pharmacol Sci*. 2016; 20:2468–73.
  261. Heilbronn LK, Ravussin E. Calorie restriction and aging: review of the literature and implications for studies in humans. *Am J Clin Nutr*. 2003; 78:361–69.  
<https://doi.org/10.1093/ajcn/78.3.361>
  262. Tiku V, Jain C, Raz Y, Nakamura S, Heestand B, Liu W, Späth M, Suchiman HE, Müller RU, Slagboom PE, Partridge L, Antebi A. Small nucleoli are a cellular hallmark of longevity. *Nat Commun*. 2017; 8:16083.  
<https://doi.org/10.1038/ncomms16083>
  263. Jack CV, Cruz C, Hull RM, Keller MA, Ralser M, Houseley J. Regulation of ribosomal DNA amplification by the TOR pathway. *Proc Natl Acad Sci USA*. 2015; 112:9674–79.  
<https://doi.org/10.1073/pnas.1505015112>
  264. Murayama A, Ohmori K, Fujimura A, Minami H, Yasuzawa-Tanaka K, Kuroda T, Oie S, Daitoku H, Okuwaki M, Nagata K, Fukamizu A, Kimura K, Shimizu T, Yanagisawa J. Epigenetic control of rDNA loci in response to intracellular energy status. *Cell*. 2008; 133:627–39.  
<https://doi.org/10.1016/j.cell.2008.03.030>
  265. Cohen HY, Miller C, Bitterman KJ, Wall NR, Hekking B, Kessler B, Howitz KT, Gorospe M, de Cabo R, Sinclair DA. Calorie restriction promotes mammalian cell survival by inducing the SIRT1 deacetylase. *Science*. 2004; 305:390–92.  
<https://doi.org/10.1126/science.1099196>
  266. Nemoto S, Fergusson MM, Finkel T. Nutrient availability regulates SIRT1 through a forkhead-dependent pathway. *Science*. 2004; 306:2105–08.  
<https://doi.org/10.1126/science.1101731>
  267. Satoh A, Brace CS, Rensing N, Cliften P, Wozniak DF, Herzog ED, Yamada KA, Imai S. Sirt1 extends life span and delays aging in mice through the regulation of Nk2 homeobox 1 in the DMH and LH. *Cell Metab*. 2013; 18:416–30.  
<https://doi.org/10.1016/j.cmet.2013.07.013>
  268. Matheu A, Maraver A, Klatt P, Flores I, Garcia-Cao I, Borrás C, Flores JM, Viña J, Blasco MA, Serrano M. Delayed ageing through damage protection by the Arf/p53 pathway. *Nature*. 2007; 448:375–79.  
<https://doi.org/10.1038/nature05949>
  269. Hulbert AJ, Pamplona R, Buffenstein R, Buttemer WA. Life and death: metabolic rate, membrane composition, and life span of animals. *Physiol Rev*. 2007; 87:1175–213.  
<https://doi.org/10.1152/physrev.00047.2006>
  270. Takeuchi Y, Horiuchi T, Kobayashi T. Transcription-dependent recombination and the role of fork collision in yeast rDNA. *Genes Dev*. 2003; 17:1497–506. <https://doi.org/10.1101/gad.1085403>
  271. Ginno PA, Lott PL, Christensen HC, Korf I, Chédin F. R-loop formation is a distinctive characteristic of unmethylated human CpG island promoters. *Mol Cell*. 2012; 45:814–25.  
<https://doi.org/10.1016/j.molcel.2012.01.017>
  272. Helmrich A, Ballarino M, Tora L. Collisions between replication and transcription complexes cause common fragile site instability at the longest human genes. *Mol Cell*. 2011; 44:966–77.  
<https://doi.org/10.1016/j.molcel.2011.10.013>
  273. El Hage A, French SL, Beyer AL, Tollervey D. Loss of Topoisomerase I leads to R-loop-mediated transcriptional blocks during ribosomal RNA synthesis. *Genes Dev*. 2010; 24:1546–58.  
<https://doi.org/10.1101/gad.573310>
  274. Wahba L, Costantino L, Tan FJ, Zimmer A, Koshland D. S1-DRIP-seq identifies high expression and polyA tracts as major contributors to R-loop formation. *Genes Dev*. 2016; 30:1327–38.  
<https://doi.org/10.1101/gad.280834.116>
  275. Vijg J, Suh Y. Genome instability and aging. *Annu Rev Physiol*. 2013; 75:645–68.  
<https://doi.org/10.1146/annurev-physiol-030212-183715>

276. Flach J, Bakker ST, Mohrin M, Conroy PC, Pietras EM, Reynaud D, Alvarez S, Diolaiti ME, Ugarte F, Forsberg EC, Le Beau MM, Stohr BA, Méndez J, et al. Replication stress is a potent driver of functional decline in ageing haematopoietic stem cells. *Nature*. 2014; 512:198–202. <https://doi.org/10.1038/nature13619>
277. Schawalder J, Paric E, Neff NF. Telomere and ribosomal DNA repeats are chromosomal targets of the bloom syndrome DNA helicase. *BMC Cell Biol*. 2003; 4:15. <https://doi.org/10.1186/1471-2121-4-15>
278. Sinclair DA, Mills K, Guarente L. Accelerated aging and nucleolar fragmentation in yeast *sgs1* mutants. *Science*. 1997; 277:1313–16. <https://doi.org/10.1126/science.277.5330.1313>
279. Sinclair DA, Guarente L. Extrachromosomal rDNA circles—a cause of aging in yeast. *Cell*. 1997; 91:1033–42. [https://doi.org/10.1016/S0092-8674\(00\)80493-6](https://doi.org/10.1016/S0092-8674(00)80493-6)
280. Grierson PM, Lillard K, Behbehani GK, Combs KA, Bhattacharyya S, Acharya S, Groden J. BLM helicase facilitates RNA polymerase I-mediated ribosomal RNA transcription. *Hum Mol Genet*. 2012; 21:1172–83. <https://doi.org/10.1093/hmg/ddr545>
281. Shiratori M, Suzuki T, Itoh C, Goto M, Furuichi Y, Matsumoto T. WRN helicase accelerates the transcription of ribosomal RNA as a component of an RNA polymerase I-associated complex. *Oncogene*. 2002; 21:2447–54. <https://doi.org/10.1038/sj.onc.1205334>
282. D'Aquila P, Montesanto A, Mandalà M, Garasto S, Mari V, Corsonello A, Bellizzi D, Passarino G. Methylation of the ribosomal RNA gene promoter is associated with aging and age-related decline. *Aging Cell*. 2017; 16:966–75. <https://doi.org/10.1111/accel.12603>
283. Jung M, Jin SG, Zhang X, Xiong W, Gogoshin G, Rodin AS, Pfeifer GP. Longitudinal epigenetic and gene expression profiles analyzed by three-component analysis reveal down-regulation of genes involved in protein translation in human aging. *Nucleic Acids Res*. 2015; 43:e100. <https://doi.org/10.1093/nar/gkv473>
284. Zhang W, Hawse J, Huang Q, Sheets N, Miller KM, Horwitz J, Kantorow M. Decreased expression of ribosomal proteins in human age-related cataract. *Invest Ophthalmol Vis Sci*. 2002; 43:198–204.
285. Kirby TJ, Lee JD, England JH, Chaillou T, Esser KA, McCarthy JJ. Blunted hypertrophic response in aged skeletal muscle is associated with decreased ribosome biogenesis. *J Appl Physiol* (1985). 2015; 119:321–27. <https://doi.org/10.1152/jappphysiol.00296.2015>
286. Barna M, Pusic A, Zollo O, Costa M, Kondrashov N, Rego E, Rao PH, Ruggero D. Suppression of Myc oncogenic activity by ribosomal protein haploinsufficiency. *Nature*. 2008; 456:971–75. <https://doi.org/10.1038/nature07449>
287. Ruggero D. Translational control in cancer etiology. *Cold Spring Harb Perspect Biol*. 2013; 5:5. <https://doi.org/10.1101/cshperspect.a012336>
288. Xue S, Barna M. Specialized ribosomes: a new frontier in gene regulation and organismal biology. *Nat Rev Mol Cell Biol*. 2012; 13:355–69. <https://doi.org/10.1038/nrm3359>
289. Duncan FE, Jasti S, Paulson A, Kelsh JM, Fegley B, Gerton JL. Age-associated dysregulation of protein metabolism in the mammalian oocyte. *Aging Cell*. 2017; 16:1381–93. <https://doi.org/10.1111/accel.12676>
290. Guo X, Shi Y, Gou Y, Li J, Han S, Zhang Y, Huo J, Ning X, Sun L, Chen Y, Sun S, Fan D. Human ribosomal protein S13 promotes gastric cancer growth through down-regulating p27(Kip1). *J Cell Mol Med*. 2011; 15:296–306. <https://doi.org/10.1111/j.1582-4934.2009.00969.x>
291. Du J, Shi Y, Pan Y, Jin X, Liu C, Liu N, Han Q, Lu Y, Qiao T, Fan D. Regulation of multidrug resistance by ribosomal protein l6 in gastric cancer cells. *Cancer Biol Ther*. 2005; 4:242–47. <https://doi.org/10.4161/cbt.4.2.1477>
292. Qu J, Bishop JM. Nucleostemin maintains self-renewal of embryonic stem cells and promotes reprogramming of somatic cells to pluripotency. *J Cell Biol*. 2012; 197:731–45. <https://doi.org/10.1083/jcb.201103071>
293. Le Bouteiller M, Souilhol C, Beck-Cormier S, Stedman A, Burlen-Defranoux O, Vandormael-Pournin S, Bernex F, Cumano A, Cohen-Tannoudji M. Notchless-dependent ribosome synthesis is required for the maintenance of adult hematopoietic stem cells. *J Exp Med*. 2013; 210:2351–69. <https://doi.org/10.1084/jem.20122019>
294. Yang A, Shi G, Zhou C, Lu R, Li H, Sun L, Jin Y. Nucleolin maintains embryonic stem cell self-renewal by suppression of p53 protein-dependent pathway. *J Biol Chem*. 2011; 286:43370–82. <https://doi.org/10.1074/jbc.M111.225185>
295. Meshorer E, Misteli T. Chromatin in pluripotent embryonic stem cells and differentiation. *Nat Rev Mol Cell Biol*. 2006; 7:540–46. <https://doi.org/10.1038/nrm1938>
296. Hayashi Y, Kuroda T, Kishimoto H, Wang C, Iwama A, Kimura K. Downregulation of rRNA transcription



- triggers cell differentiation. *PLoS One*. 2014; 9:e98586.  
<https://doi.org/10.1371/journal.pone.0098586>
297. Stedman A, Beck-Cormier S, Le Bouteiller M, Raveux A, Vandormael-Pournin S, Coqueran S, Lejour V, Jarzebowski L, Toledo F, Robine S, Cohen-Tannoudji M. Ribosome biogenesis dysfunction leads to p53-mediated apoptosis and goblet cell differentiation of mouse intestinal stem/progenitor cells. *Cell Death Differ*. 2015; 22:1865–76.  
<https://doi.org/10.1038/cdd.2015.57>
  298. Tyner SD, Venkatachalam S, Choi J, Jones S, Ghebranious N, Igelmann H, Lu X, Soron G, Cooper B, Brayton C, Park SH, Thompson T, Karsenty G, et al. p53 mutant mice that display early ageing-associated phenotypes. *Nature*. 2002; 415:45–53.  
<https://doi.org/10.1038/415045a>
  299. Maier B, Gluba W, Bernier B, Turner T, Mohammad K, Guise T, Sutherland A, Thorner M, Scrabble H. Modulation of mammalian life span by the short isoform of p53. *Genes Dev*. 2004; 18:306–19.  
<https://doi.org/10.1101/gad.1162404>
  300. van Heemst D, Mooijaart SP, Beekman M, Schreuder J, de Craen AJ, Brandt BW, Slagboom PE, Westendorp RG, and Long Life study group. Variation in the human TP53 gene affects old age survival and cancer mortality. *Exp Gerontol*. 2005; 40:11–15.  
<https://doi.org/10.1016/j.exger.2004.10.001>
  301. Steffen KK, Dillin A. A Ribosomal Perspective on Proteostasis and Aging. *Cell Metab*. 2016; 23:1004–12. <https://doi.org/10.1016/j.cmet.2016.05.013>
  302. Gomes C, Smith SC, Youssef MN, Zheng JJ, Hagg T, Hetman M. RNA polymerase 1-driven transcription as a mediator of BDNF-induced neurite outgrowth. *J Biol Chem*. 2011; 286:4357–63.  
<https://doi.org/10.1074/jbc.M110.170134>
  303. Slomnicki LP, Pietrzak M, Vashishta A, Jones J, Lynch N, Elliot S, Poulos E, Malicote D, Morris BE, Hallgren J, Hetman M. Requirement of Neuronal Ribosome Synthesis for Growth and Maintenance of the Dendritic Tree. *J Biol Chem*. 2016; 291:5721–39.  
<https://doi.org/10.1074/jbc.M115.682161>
  304. Kinderman NB, Harrington CA, Drengler SM, Jones KJ. Ribosomal RNA transcriptional activation and processing in hamster facial motoneurons: effects of axotomy with or without exposure to testosterone. *J Comp Neurol*. 1998; 401:205–16.  
[https://doi.org/10.1002/\(SICI\)1096-9861\(19981116\)401:2<205::AID-CNE4>3.0.CO;2-4](https://doi.org/10.1002/(SICI)1096-9861(19981116)401:2<205::AID-CNE4>3.0.CO;2-4)
  305. Storer PD, Jones KJ. Ribosomal RNA transcriptional activation and processing in hamster rubrospinal motoneurons: effects of axotomy and testosterone treatment. *J Comp Neurol*. 2003; 458:326–33.  
<https://doi.org/10.1002/cne.10623>
  306. Ding Q, Markesbery WR, Chen Q, Li F, Keller JN. Ribosome dysfunction is an early event in Alzheimer's disease. *J Neurosci*. 2005; 25:9171–75.  
<https://doi.org/10.1523/JNEUROSCI.3040-05.2005>
  307. Honda K, Smith MA, Zhu X, Baus D, Merrick WC, Tartakoff AM, Hattier T, Harris PL, Siedlak SL, Fujioka H, Liu Q, Moreira PI, Miller FP, et al. Ribosomal RNA in Alzheimer disease is oxidized by bound redox-active iron. *J Biol Chem*. 2005; 280:20978–86.  
<https://doi.org/10.1074/jbc.M500526200>
  308. Ding Q, Markesbery WR, Cecarini V, Keller JN. Decreased RNA, and increased RNA oxidation, in ribosomes from early Alzheimer's disease. *Neurochem Res*. 2006; 31:705–10.  
<https://doi.org/10.1007/s11064-006-9071-5>
  309. Pietrzak M, Rempala G, Nelson PT, Zheng JJ, Hetman M. Epigenetic silencing of nucleolar rRNA genes in Alzheimer's disease. *PLoS One*. 2011; 6:e22585.  
<https://doi.org/10.1371/journal.pone.0022585>
  310. Zeng J, Libien J, Shaik F, Wolk J, Hernández AI. Nucleolar PARP-1 Expression Is Decreased in Alzheimer's Disease: Consequences for Epigenetic Regulation of rDNA and Cognition. *Neural Plast*. 2016; 2016:8987928.  
<https://doi.org/10.1155/2016/8987928>
  311. Dönmez-Altuntaş H, Akalin H, Karaman Y, Demirtaş H, Imamoğlu N, Özkul Y. Evaluation of the nucleolar organizer regions in Alzheimer's disease. *Gerontology*. 2005; 51:297–301.  
<https://doi.org/10.1159/000086365>
  312. Bou Samra E, Buhagiar-Labarchède G, Machon C, Guitton J, Onclercq-Delic R, Green MR, Alibert O, Gazin C, Veaute X, Amor-Guéret M. A role for Tau protein in maintaining ribosomal DNA stability and cytidine deaminase-deficient cell survival. *Nat Commun*. 2017; 8:693.  
<https://doi.org/10.1038/s41467-017-00633-1>
  313. Sjöberg MK, Shestakova E, Mansuroglu Z, Maccioni RB, Bonnefoy E. Tau protein binds to pericentromeric DNA: a putative role for nuclear tau in nucleolar organization. *J Cell Sci*. 2006; 119:2025–34.  
<https://doi.org/10.1242/jcs.02907>
  314. Vanderweyde T, Apicco DJ, Youmans-Kidder K, Ash PE, Cook C, Lummertz da Rocha E, Jansen-West K, Frame AA, Citro A, Leszyk JD, Ivanov P, Abisambra JF, Steffen M, et al. Interaction of tau with the RNA-Binding Protein TIA1 Regulates tau Pathophysiology and Toxicity. *Cell Reports*. 2016; 15:1455–66.  
<https://doi.org/10.1016/j.celrep.2016.04.045>

315. Maina MB, Bailey LJ, Wagih S, Biasetti L, Pollack SJ, Quinn JP, Thorpe JR, Doherty AJ, Serpell LC. The involvement of tau in nucleolar transcription and the stress response. *Acta Neuropathol Commun.* 2018; 6:70. <https://doi.org/10.1186/s40478-018-0565-6>
316. Rieker C, Engblom D, Kreiner G, Domanskyi A, Schober A, Stotz S, Neumann M, Yuan X, Grummt I, Schütz G, Parlato R. Nucleolar disruption in dopaminergic neurons leads to oxidative damage and parkinsonism through repression of mammalian target of rapamycin signaling. *J Neurosci.* 2011; 31:453–60. <https://doi.org/10.1523/JNEUROSCI.0590-10.2011>
317. Healy-Stoffel M, Ahmad SO, Stanford JA, Levant B. Altered nucleolar morphology in substantia nigra dopamine neurons following 6-hydroxydopamine lesion in rats. *Neurosci Lett.* 2013; 546:26–30. <https://doi.org/10.1016/j.neulet.2013.04.033>
318. Caudle WM, Kitsou E, Li J, Bradner J, Zhang J. A role for a novel protein, nucleolin, in Parkinson's disease. *Neurosci Lett.* 2009; 459:11–15. <https://doi.org/10.1016/j.neulet.2009.04.060>
319. Jin J, Li GJ, Davis J, Zhu D, Wang Y, Pan C, Zhang J. Identification of novel proteins associated with both  $\alpha$ -synuclein and DJ-1. *Mol Cell Proteomics.* 2007; 6:845–59. <https://doi.org/10.1074/mcp.M600182-MCP200>
320. Vilotti S, Codrich M, Dal Ferro M, Pinto M, Ferrer I, Collavin L, Gustincich S, Zucchelli S. Parkinson's disease DJ-1 L166P alters rRNA biogenesis by exclusion of TTRAP from the nucleolus and sequestration into cytoplasmic aggregates via TRAF6. *PLoS One.* 2012; 7:e35051. <https://doi.org/10.1371/journal.pone.0035051>
321. Kang H, Shin JH. Repression of rRNA transcription by PARIS contributes to Parkinson's disease. *Neurobiol Dis.* 2015; 73:220–28. <https://doi.org/10.1016/j.nbd.2014.10.003>
322. Lee J, Hwang YJ, Boo JH, Han D, Kwon OK, Todorova K, Kowall NW, Kim Y, Ryu H. Dysregulation of upstream binding factor-1 acetylation at K352 is linked to impaired ribosomal DNA transcription in Huntington's disease. *Cell Death Differ.* 2011; 18:1726–35. <https://doi.org/10.1038/cdd.2011.38>
323. Lee J, Hwang YJ, Ryu H, Kowall NW, Ryu H. Nucleolar dysfunction in Huntington's disease. *Biochim Biophys Acta.* 2014; 1842:785–90. <https://doi.org/10.1016/j.bbadis.2013.09.017>
324. Tsoi H, Lau TC, Tsang SY, Lau KF, Chan HY. CAG expansion induces nucleolar stress in polyglutamine diseases. *Proc Natl Acad Sci USA.* 2012; 109:13428–
33. <https://doi.org/10.1073/pnas.1204089109>
325. Bae BI, Xu H, Igarashi S, Fujimuro M, Agrawal N, Taya Y, Hayward SD, Moran TH, Montell C, Ross CA, Snyder SH, Sawa A. p53 mediates cellular dysfunction and behavioral abnormalities in Huntington's disease. *Neuron.* 2005; 47:29–41. <https://doi.org/10.1016/j.neuron.2005.06.005>
326. Kitamura Y, Shimohama S, Kamoshima W, Matsuoka Y, Nomura Y, Taniguchi T. Changes of p53 in the brains of patients with Alzheimer's disease. *Biochem Biophys Res Commun.* 1997; 232:418–21. <https://doi.org/10.1006/bbrc.1997.6301>
327. Nair VD, McNaught KS, González-Maeso J, Sealton SC, Olanow CW. p53 mediates nontranscriptional cell death in dopaminergic cells in response to proteasome inhibition. *J Biol Chem.* 2006; 281:39550–60. <https://doi.org/10.1074/jbc.M603950200>
328. Boulon S, Westman BJ, Hutten S, Boisvert FM, Lamond AI. The nucleolus under stress. *Mol Cell.* 2010; 40:216–27. <https://doi.org/10.1016/j.molcel.2010.09.024>